

**THE RELATIONSHIP BETWEEN *IN-VITRO*
ENDOTHELIAL PERMEABILITY AND
MOLECULES OF THE INTERCELLULAR
JUNCTION.**



By

Rachel Ann Budworth, BSc (Hons)

Thesis submitted to the University of Nottingham for the
Degree of Doctor of Philosophy

February 2003

TABLE OF CONTENTS

Table of Contents	i
Acknowledgements	ix
Abstract	x
Abbreviations	xi

CHAPTER 1: GENERAL INTRODUCTION.

1.1 THE ENDOTHELIUM	1
1.2 CAPILLARIES	2
1.3 STRUCTURE OF HUMAN SKIN	2
1.4 MECHANISMS OF SKIN IRRITATION AND INTERACTION WITH THE ENDOTHELIUM	4
1.4.1 Role of the Endothelium in Inflammation	4
1.5 PRINCIPAL PATHWAYS IN VASCULAR PERMEABILITY	5
1.6 ENDOTHELIAL CELL-CELL JUNCTIONS	9
1.6.1 The Adherens Junction	11
1.6.2 Cadherins	11
1.6.2.1 Vascular-Endothelial Cadherin	12
1.6.2.2 The Catenins	14
1.6.2.3 F-actin	16
1.6.3 The Tight Junction	17
1.7 INVOLVEMENT OF JUNCTIONAL COMPONENTS IN OTHER PHYSIOLOGICAL PROCESSES	18
1.8 USE OF ENDOTHELIAL CELLS <i>IN-VITRO</i>	19
1.8.1 Drawbacks of <i>In-Vitro</i> Studies	20
1.9 DEVELOPMENT OF <i>IN-VITRO</i> APPROACHES TO	

	TOXICOLOGY	21
1.10	HYPOTHESIS AND AIMS OF THIS THESIS	22

CHAPTER 2: EVALUATION OF POTENTIAL ENDOTHELIAL CELL-LINES FOR STUDYING VASCULAR PERMEABILITY IN-VITRO.

2.1	INTRODUCTION	24
2.2	MATERIALS AND METHODS	28
2.2.1	Materials	28
2.2.1.1	Chemicals and Reagents	28
2.2.1.2	Antibodies	29
2.2.1.3	Immortalised Cell-lines	29
2.2.1.4	Consumerables	30
2.2.1.5	DNA Profile	30
2.2.2	Methods	31
2.2.2.1	Preparation of Solutions and Cell Culture Media	31
2.2.2.2	Treatment of Tissue Culture Plastic and CM Inserts with Extracellular Matrix Proteins	32
2.2.2.3	Subculture of Endothelial Cells	33
2.2.2.4	Cryopreservation of Endothelial Cells	33
2.2.2.5	Determination of the growth rate of HMEC-1 and ECV304 cells	34
2.2.2.6	Determination of Monolayer Permeability in Endothelial Cells	35
2.2.2.7	Isolation of Human Umbilical Vein Endothelial Cells (HUVEC)	37
2.2.2.8	Detection of von Willebrand Factor (vWF), Platelet-Endothelial Cell Adhesion Molecule (PECAM-1) and Vascular-Endothelial Cadherin (VE-Cadherin)	38

2.2.2.9	Short Tandem Repeat (STR) profiling of HMEC-1 and HUVEC cells	39
2.2.2.10	Analysis of Results	40
2.3	RESULTS	41
2.3.1	Determination of the Growth Rate of HMEC-1 and ECV304 Cells	41
2.3.2	Determination of the Optimum Seeding Density to measure 70-kDa Dextran Flux – the ECV304 cell-line	42
2.3.3	Permeability of the ECV304 Cell-line to Known Vasoactive Agents which Act via a Variety of Mechanisms	44
2.3.3.1	Effect of IL-1 α on the Permeability of ECV304 Cells to FD70	45
2.3.3.2	Effect of A23187, a Calcium Ionophore, on the Permeability of ECV304 Cells to FD70	46
2.3.3.3	Effect of TNF α on the Permeability of ECV304 Cells to FD70	48
2.3.3.4	Effect of Phorbol Myristate-13-Acetyester (PMA) on the Permeability of ECV304 Cells to FD70	49
2.3.4	Ability of Endothelial Cells to Form Stable Barriers to FD70 when Grown on CM Inserts Coated with Extracellular Matrix (ECM) Proteins	51
2.3.4.1	Ability of ECM-Coated CM Inserts to Support Growth of a Stable Monolayer of ECV304 Cells	52
2.3.4.2	Determination of Optimum Seeding Density and Ability of Collagen-Coated CM Inserts to Support Growth of the HMEC-1 Cell-line	56
2.3.5	Analysis of the Intercellular Junctions of the HMEC-1 and ECV304 Cell-lines by Immunofluorescence	60
2.3.6	STR Profiling of Cultured Cell Samples	65
2.4	DISCUSSION	67

CHAPTER 3: EVALUATION OF METHODS FOR STUDYING ENDOTHELIAL PERMEABILITY IN-VITRO.

3.1	INTRODUCTION	72
3.1.1	Factors Affecting Capillary Permeability	73
3.1.1.1	General Factors	73
3.1.1.2	Hydrostatic and Osmotic Pressure across a Capillary Wall	74
3.1.2	The Use of <i>In-Vitro</i> Techniques to Study Endothelial Permeability	76
3.1.3	Variations in the <i>In-Vitro</i> METHOD	79
3.2	MATERIAL AND METHODS	82
3.2.1	Materials	82
3.2.1.1	Chemical Reagents	82
3.2.2	Methods	82
3.2.2.1	Effect of Hydrostatic Pressure on the Flux of 70kDa-dextran	82
3.2.2.2	Effect of Osmotic Pressure on the Flux of 70kDa-dextran	83
3.2.2.3	Effect of removal of a small volume of liquid from the Abluminal Compartment on the Flux of 70kDa-dextran	83
3.2.2.4	Effect of medium used in Permeability Assay on the Flux of 70kDa-dextran	83
3.2.2.5	Assessment of measuring the Flux of two dextrans of differing molecular weights simultaneously	83
3.3	RESULTS	85
3.3.1	Effect of Hydrostatic Pressure on the Flux of 70-kDa Dextran	85
3.3.2	Effect of Osmotic Pressure on the Flux of 70-kDa-dextran	87
3.3.3	Effect of removal of a small volume of liquid from the Abluminal Compartment on the Flux of 70-kDa-dextran	88
3.3.4	Effect of medium used in Permeability Assay on the Flux of 70-kDa-dextran	90

3.3.5	Assessment of measuring the Flux of two dextrans of differing molecular weights simultaneously	91
3.4	DISCUSSION	95

CHAPTER 4: MODULATION OF PERMEABILITY AND MOLECULES OF THE INTERCELLULAR JUNCTIONS IN THE HMEC-1 CELL-LINE

4.1	INTRODUCTION	97
4.2	MATERIALS and METHODS	100
4.2.1	Materials	100
4.2.1.1	Chemicals and Reagents	100
4.2.1.2	Antibodies	100
4.2.2	Methods	101
4.2.2.1	Leakage of macromolecules through HMEC-1 monolayers	101
4.2.2.2	Alamar Blue [™] / Resazurin assay	102
4.2.2.3	Treatment of confluent HMEC-1 monolayers with chemicals	103
4.2.2.4	Immunocytochemistry for VE-cadherin, Occludin and ZO-1	104
4.2.2.5	Phalloidin staining for F-actin	105
4.2.2.6	Transmission Electron Microscopy	105
4.3	RESULTS	108
4.3.1	Observation of Junction Ultrastructure and Molecules in HMEC-1 Cultures on Collagen-coated CM Inserts	108
4.3.1.1	Ultrastructure of HMEC-1 Paracellular Cleft	108
4.3.1.2	The detection of Tight Junction Molecules in the HMEC-1 Cell-Line	110
4.3.1.3	Permeability of HMEC-1 Cell-Line to Dextrans of 40, 70 & 150-kDa	112
4.3.2	Permeability of the HMEC-1 Cell-Line to known Vaso-active agents which act via a variety of mechanisms	118

4.3.3.1	Effect of EGTA on the Permeability and Adherens Junction Molecules of HMEC-1 Cells	118
4.3.3.2	Effects of A23187 on the Permeability and Adherens Junction Molecules of HMEC-1 Cells	124
4.3.3.3	Effects of Cocamido-Propylbetaine (CAPB) on the Permeability and Adherens Junction Molecules of HMEC-1 Cells	129
4.3.3.4	Effects of Phorbol Myristate-13-Acetyler (PMA) on the Permeability and Adherens Junction Molecules of HMEC-1 Cells	134
4.3.3.5	Conclusion of the Permeability Studies	139
4.4	DISCUSSION	142

CHAPTER 5: ACTION OF HISTAMINE PERMEABILITY AND ADHERENS JUNCTION COMPONENTS OF THE HMEC-1 CELL-LINE.

5.1	INTRODUCTION	149
5.1.1	Histamine	149
5.1.2	Histamine Receptors	150
5.1.3	Action of Histamine on the Endothelium	152
5.2	MATERIALS & METHODS	154
5.2.1	Materials	154
5.2.1.1	Chemicals and Reagents	154
5.2.2	Methods	154
5.2.2.1	Histamine Exposure – Original Permeability Method	154
5.2.2.2	Method Variations to Measure the Effect of Histamine on HMEC-1 Monolayer Permeability	155
5.2.2.2.1	<i>'Above and Below' Permeability Method</i>	155
5.2.2.2.2	<i>'Bolus' Permeability Method</i>	155
5.2.2.3	Histamine Exposure for Immunofluorescence Studies	156

5.2.2.4	Reversal of Histamine Effects for F-actin Studies	157
5.2.2.5	Counting Method for Quantifying the Number of Rounded Cells	157
5.2.2.6	Counting Method for Quantifying VE-Cadherin Immunolabelling	158
5.2.2.7	Neutral Red Uptake (NRU) Assay	159
5.3	RESULTS	160
6.3.2	Effect of Histamine of 40, 70 AND 150-kDa Dextran Leakage Original Method	160
6.3.2	Effect of Histamine on FD70 Leakage 'Above and Below Method	160
5.3.3	Effect of Histamine on FD70 Leakage – 'Bolus' Method	161
5.3.4	Effect of Histamine on HMEC-1 Morphology and F-actin Distribution	165
5.3.5	Toxicity of Histamine	167
5.3.6	Recovery of HMEC-1 F-actin Arrangement following Histamine Exposure	168
5.3.7	Effect of Histamine on the Expression and Localisation of VE-cadherin	171
5.3.8	Quantitation of VE-cadherin Localisation	171
5.4	DISCUSSION	177
 CHAPTER 6: EFFECT OF CYCLIC AMP ON THE EXPRESSION AND LOCALISATION OF JUNCTIONAL MOLECULES AND PERMEABILITY OF HMEC-1 CELLS		
6.1	INTRODUCTION	181
6.1.1	Role of Cyclic AMP in Cell-Cell Adhesion	182
6.1.2	Aims	183
6.2	MATERIALS & METHODS	184
6.2.1	Materials	184
6.2.1.1	Chemicals and Reagents	184

6.2.1.2	Antibodies	184
6.2.1.3	Preparation of Solution and Cell Culture Media	185
6.2.2	Methods	185
6.2.2.1	Cyclic AMP Treatment	185
6.2.2.2	Leakage of Macromolecules and Sodium Fluorescein through HMEC-1 monolayers	186
6.2.2.3	Measurement of Triton-Soluble and Triton-Insoluble α -Catenin by Western Blot	186
6.3	RESULTS	188
6.3.2	Effect of Cyclic AMP Media on Leakage of FD40, 70 and Sodium Fluorescein through the HMEC-1 monolayer	188
6.3.2	Effect of Cyclic AMP Media on Morphology and Junction Components of the HMEC-1 Cell-line	190
6.3.3	Effect of Cyclic AMP Media on the Levels of α -Catenin Protein in Triton-Soluble and –Insoluble Cell Fractions	195
6.3.4	Effect of Cyclic AMP on HMEC-1 Permeability Response to Histamine	196
6.4	DISCUSSION	198
CHAPTER 7:	GENERAL DISCUSSION	200
CHAPTER 8:	REFERENCES	215

ACKNOWLEDGEMENTS

I would like to thank the people who have helped make the undertaking of this research interesting and enjoyable.

Firstly I would like to thank my supervisors Dr Richard Clothier and Dr Lopa Leach for their support, patience and encouragement throughout this research project. They have always given so much more of themselves and their time than I could have ever asked.

I received help and guidance from many of the technical and research staff during the course of this work and I would like to thank Dr Susan Anderson for all help and advice on imaging queries, Barry Shaw for his patience while cutting ultrathin section of my samples. Dr Peter Jones and his group helped with the western blotting, giving of their expertise and equipment. Also Professor Mayhew for his invaluable advice on quantifying the immunofluorescence images.

I would also like to give a huge thank you to everyone in the FRAME laboratories and the other PhD students for making this a lively place to conduct research and form good friendships, especially Pete Wilkinson for his expert proof reading skills. Thanks to Dr Carol Barker, Anthony Tromans, Linda Noble, Dr Nancy Khammo, Dr Jane Oglivie, Tamsin Ford and all my other friends and colleagues.

Finally, I would like to thank my partner Justin, my daughters Maddy and Belle and my parents Madeline and David and my sister Catherine for their support, love and tolerance while I persevered with this work. Their ability to make any cloud have a silver lining kept me sane and enabled me to write this thesis.

ABSTRACT

Changes in endothelial permeability are known to contribute to many pathologies, including inflammation seen in skin irritation. The regulation of permeability has been linked to inter-endothelial junctions, specifically the tight and adherens junctions (TJ and AJ). The functional state of the junction is thought to be associated with numerous factors including cytoskeletal changes and the interactions between junctional components. How these factors interact and respond to inflammatory stimuli is still not fully understood.

This project examined two human endothelial cell-lines for use in *in-vitro* permeability studies, ECV304 and HMEC-1. Changes in permeability along with arrangement of the F-actin cytoskeleton and the adherens junction molecule VE-cadherin were studied in response to a variety of compounds. Macromolecular permeability was assessed by measuring the leakage of fluorescently labelled dextrans of varying molecular weights. The F-actin and VE-cadherin were visualised using immunocytochemical techniques. TEM was undertaken to examine the ultrastructure of the junctions

The ECV304 cells, whilst showing an increased permeability to a variety to vaso-active mediators, did not express some of the pertinent junctional molecules of the endothelium and thus are not recommended for use. The basal permeability of the HMEC-1 cell-line was shown to act in predictable fashion, giving comparable permeability coefficients to other endothelial cells. The increase in permeability following exposure to A23187, CAPB, EGTA and PMA was shown to correlate to an altered expression of VE-cadherin and F-actin. These observations were furthered using histamine, where a quantifiable change in the levels of continuous and stitch VE-cadherin staining was demonstrated. The permeability response to histamine occurred much later than the VE-cadherin and F-actin changes. This could be due to methodology and/or the cells lack of TJs. The apparent lack of mature AJs was approached by exposing the cultures to cAMP-raising media. This significantly reduced the basal permeability and increased the expression of AJ components, apart from β -catenin, at the cell-cell contacts. Indeed α -catenin was redistributed from the triton-soluble fraction of the cells to the triton-insoluble fraction, which is proposed to contain the junctional components.

These results demonstrate additional information on the role that the adherens junction molecules play in endothelial permeability and characterise the HMEC-1 cell-line for further use in this field.

LIST OF ABBREVIATIONS

α-Catenin	alpha-catenin
β-Catenin	beta-catenin
γ-Catenin	gamma catenin
A23187	calcium ionophore
AJ	adherens junction
AP-1	activator protein-1
AMG	loci used in the STR DNA profile
ANOVA	analysis of variance
BSA	bovine serum albumin
Ca²⁺	calcium ions
CaM	calmodulin
cAMP	cyclic adenosine 3', 5'-monophosphate
CO₂	carbon dioxide
CREB	cAMP responsive element binding protein
DAG	diacylglycerol
dH₂O	distilled water
DMEM	Dulbecco's modified eagles medium
DMEM/FCS	Dulbecco's modified eagles medium containing 10% foetal calf serum
DMSO	dimethhysulphoxide
DPB	dense peripheral band
EB	extraction buffer
EC	endothelial cells
ECACC	European Collection of Animal Cell Cultures

ECGS	endothelial cell growth supplement
ECM	extracellular matrix
EDTA	ethylene diamine tetra-acetic acid
EGF	epidermal growth factor
EGTA	ethylene glycol-bis(beta-aminoethyl ether)-N, N, N', N'-tetraacetic acid
ECVAM	European Centre for the Validation of Alternative Methods
ENOS	endothelial nitric oxide synthase
EU	European Union
F-actin	filamentous actin
FCS	foetal calf serum
FD70	FITC-labelled 70kDa dextran
FITC	fluorescein isothiocyanate
fov	field/s of view
FU	fluorescence units
GLP	good laboratory practise
HBSS	Hank's balanced salt solution
HMEC-1	human dermal microvascular endothelial cells (cell line)
HUVEC	human umbilical vein endothelial cells
IBMX	isobutyl methylxanthine
IgG	immunoglobulin G
IGF-1	insulin-like growth factor 1
IL-1α	interleukin-1 α
kDa	kilo Dalton

KSFM	keratinocyte serum free media
LGR	company used to give DNA profile of HMEC-1 cells
M199	Medium 199
MES	morpholinoethanesulfuric acid
min	minute
NaFl	sodium fluorescein
N-cadherin	Neural-cadherin
nm	nanometre
NO	nitric oxide
OsO4	osmium tetroxide
PBS	phosphate buffered saline
PBS/BSA	PBS containing 0.1% (w/v) bovine serum albumin
PC	permeability coefficients
P-cadherin	Placental-cadherin
PCR	polymerase chain reaction
PECAM-1	platelet-endothelial cell adhesion molecule
PKC	protein kinase C
PMA	phorbol 12-myristate 13-acetate
RT	room temperature
SAL/AB	0.9% saline solution with 200IU ml ⁻¹ penicillin and 200µg ml ⁻¹ streptomycin
SDS	sodium dodecyl sulphate
SEM	standard error of the mean
STR	short tandem repeat
TEM	transmission electron microscope/microscopy

TGF-β1	transforming growth factor- β 1
TJ	tight junction
TNF-α	tumour necrosis factor- α
TRITC	rhodamine B isothiocyanate
Trypsin/	trypsin (0.05%w/v) with ethylene diamine tetra-acetic acid
EDTA	(EDTA) disodium salt (0.02% w/v) in PBS
VE-cadherin	vascular endothelial-cadherin
VEGF	vascular endothelial growth factor
VVOs	vesiculo-vacuolar organelles
vWF	von Willebrand factor
w/v	weight per volume
ZO	zonula occludens

CHAPTER 1

GENERAL INTRODUCTION.

CHAPTER 1

GENERAL INTRODUCTION

1.1

THE ENDOTHELIUM

The endothelium has been calculated to cover an area of 7000 m², consisting of approximately 6 x 10¹³ cells, and to weigh nearly 1kg (Simionescu, 1988; Wolinsky, 1980). Our perception of the endothelium has changed drastically over the past two decades. Historically this large organ was predominantly considered as an inert lining of blood vessels.

Permselective Barrier
Metabolic synthesis and secretion
Vascular tone regulation
Vascular growth regulation
Hormone target and source
Integration and transduction of blood borne signals
Immune function
Inflammatory response

Table 1.1: Examples of functions and properties of endothelial tissue. Adapted from Gimbrone, 1986.

However the endothelium has become increasingly recognised as an active participant in the regulation and maintenance of vascular functions (Table 1).

The discovery of the endothelium's potential has led to an improved understanding of the physiology and pharmacology of this tissue. Detailed studies of endothelial cell function became feasible with the advent of cell culture techniques in the 1970s.

1.2

CAPILLARIES

Capillaries of the body vary depending on several factors such as localisation, tissues being served and metabolic needs of the tissues and organs. There are 3 main types:

- | | |
|--------------------------------------|--|
| Type I / Continuous capillaries | – e.g. as found mainly in skin and muscle. |
| Type II / Fenestrated capillaries | – e.g. as found in the kidney and gastrointestinal tract. |
| Type III / Discontinuous capillaries | - found in highly metabolic organs such as the liver and spleen. |

1.3

STRUCTURE OF HUMAN SKIN

Skin is the largest organ in the body, having a surface area of approximately 2m^2 , and is made up of 3 layers: i) the epidermis, ii) the dermis and iii) the hypodermis (figure 1.1).

This is composed of an epidermis, 80-90% of the cells being keratinocytes (Holbrook, 1994). Within the epidermis the keratinocytes migrate upwards from the basal proliferative layer towards the outer surface of the skin.

Different layers are formed as they migrate and through programmed cell death become the stratum corneum at the surface. There are three other identifiable layers, the strata spinosum, granulosum and lucidum (Stevens and Lowe, 1999).

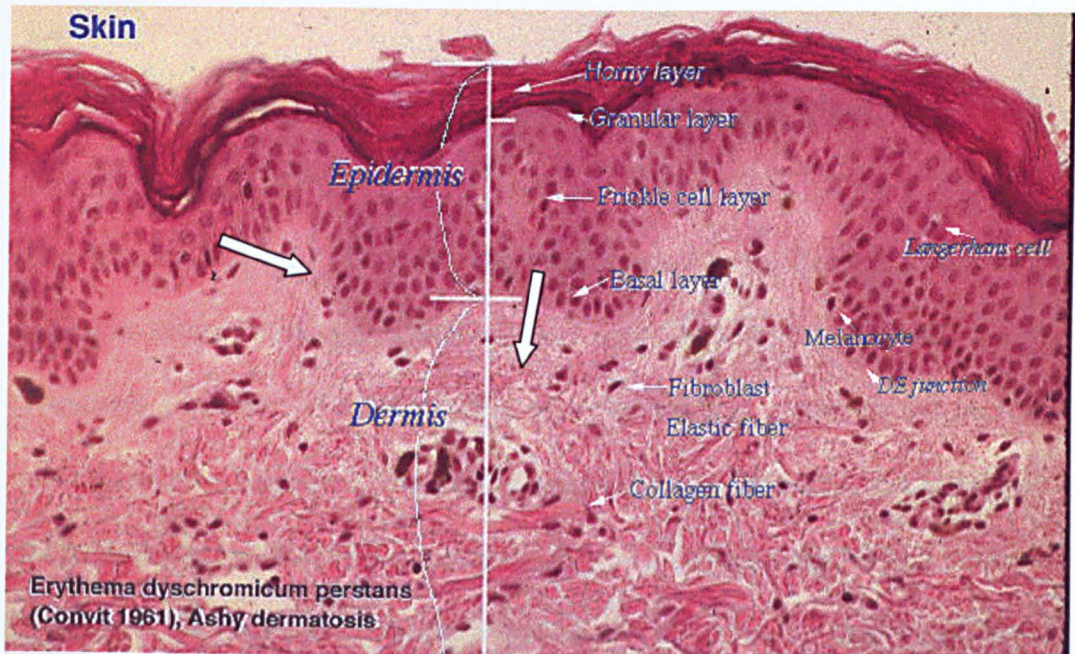


Figure 1.1: Histology of human skin showing the epithelium and dermal layers. Endothelial cells forming large and small vessels can be seen in the dermis (arrows).

The dermis underlies the epidermis and is composed of fibroelastic connective tissue made up of collagen and elastin fibres with a gel matrix of water, salts and glycosaminoglycans (Odland, 1983). There is a thick connective tissue layer just under the epidermis, that contains branches of the microvasculature, the main connective tissue layer with blood vessels and nerve supply, and the hypodermis that also includes the glands and adipose tissue (Stevens & Lowe, 1999).

The blood vessels of the skin are located in the dermis and are of the continuous type. The capillaries are lined with squamous endothelial cells,

0.2 - 0.3 μm thick, that curve to make a lumen with a diameter of 7-9 μm . The endothelial cells secrete a basal lamina, mainly consisting of collagen microfibrils, that is 20 - 50nm thick (Tu, 1992).

1.4

MECHANISMS OF SKIN IRRITATION AND INTERACTION WITH THE ENDOTHELIUM

The skin, in response to topical chemical exposure, mechanical damage or radiation-induced damage, releases factors from the epidermal keratinocytes. These are a mixture of cytokines that result in oedema, erythema and pain, a typical irritation response. The factors released by the keratinocytes influence the endothelial cells of the microvasculature. In allergic and irritant contact dermatitis, keratinocytes are major target cells that can be activated to take part in local reactions by secreting soluble mediators. Among the factors produced are vascular endothelial growth factor (VEGF) and histamine, powerful inducers of permeability in endothelial cells (Bates *et al.*, 1999; Koizumi and Ohkawara, 1999).

1.4.1

ROLE OF THE ENDOTHELIUM IN INFLAMMATION

The role of the dermal microvascular endothelium is key to controlling the passage of blood borne chemicals and dermal tissue factors between blood and tissue. The permeability of the endothelium acts as a responsive system, capable of modulation dependent upon the skins requirements. The passage of blood borne nutrients and substances into the surrounding tissues is regulated

by the proteins that together compose the adhesion molecules that span and define the size of the intercellular space between the endothelial cells. The endothelial cells are also responsive to the signalling chemicals released from the keratinocytes in the epidermis and nerve cells located in the dermis. Hence, once an irritant has penetrated the epidermal stratum corneal barrier, a cascade of events occurs that results in a typical irritant response. The endothelium is metabolically active, and this activity can also affect vascular homeostasis. During inflammation, the endothelium responds to the mediators from the damaged keratinocytes. This leads to an increased permeability, notably to the large molecules that would normally remain in the vascular compartment.

As part of an approach to evaluate, *in vitro*, the potential of chemicals to cause irritancy, it is important to ensure that the endothelial models correspond in barrier function with those *in vivo*. *In vivo* endothelial cells, derived from different tissues have differing barrier functions dependent upon permeability requirements. For example the microvascular endothelium from the brain has a specifically tight barrier function (Rubin, 1992). The placenta has to protect the developing fetus and thus the placental vessels appear less sensitive to inflammatory mediators such as TNF α (Dye *et al.*, 2001).

1.5

PRINCIPAL PATHWAYS IN VASCULAR PERMEABILITY

The vascular endothelium acts as a selective barrier to the passage of macromolecules between the blood plasma in the vascular lumen and the interstitial fluid in the perivascular spaces. In inflammatory situations this

barrier becomes more permeable to certain molecules leading to the physiological observations linked with various disease states and acute irritant or allergic response.

The studies of vascular permeability *in vivo*, apply modifications of the classical Miles and Miles (1952) permeability assay. Vascular leakage of an intra-venous injected marker from the plasma into the skin of challenged areas is measured. Other *in-vivo/ex-vivo* systems use the mesenteric or hamster cheek pouch microcirculation (Rumbaut *et al.*, 1999). With the development of techniques to isolate and culture endothelial cells *in vitro*, more direct methods have been introduced to study vascular permeability. A commonly used system employs endothelial cells grown to confluence on a porous surface, an insert with particular pore sizes. The surface separates two compartments and allows measurement of macromolecule permeation (e.g., labelled albumin, dextran or enzymes, such as horseradish peroxidase) from one compartment to the other. The confluent monolayer of endothelial cells acts to restrict the flux of these macromolecules until stimulated with compounds that affect the barrier function of the endothelial monolayer. The primary forces producing movement of water and solutes across the capillary wall are diffusion, solvent drag, filtration, osmosis, active transport, and the processes of exocytosis and endocytosis. It should be noted that next to biologic membranes *in vivo* there is a layer of relatively unstirred fluid. Solutes cross this unstirred layer by diffusion.

In-vivo the selective permeability property of many vessels to water and solutes, ranging in size from electrolytes to plasma proteins, has been described as consisting of 3 pathways:

- i) an exclusive water pathway,
- ii) a population of small pores with a radius of 4-5nm,
- iii) a population of larger pores of 20-30nm radiuses.

Pappenheimer *et al.*, (1951), estimated that the fractional area of the small pores was <1% of the total surface area and suggested that the small pore system lay within the intercellular 'cement' that was assumed to be present in the intercellular junction. This has now been postulated as a fibre matrix within part of the cleft upon with the fibre matrix theory of Curry and Michel (1980) was based.

Specifically the molecular filter is assumed to be a fibre matrix associated with the endothelial cell glycocalyx and possibly extending into the intercellular cleft. Evidence indicates that the glycocalyx extends approximately 60nm from the luminal surface of the endothelium and that this can absorb plasma proteins (Adamson and Clough, 1992; Schneeberger and Hamelin, 1984). Adamson (1990) demonstrated that enzymatic removal of the glycocalyx with pronase increased the hydraulic conductivity of frog mesenteric capillaries by 2.5-fold. This gave rise to the theory that the glycocalyx acts as a substantial resistance in series to transendothelial transport.

The present theory of capillary permeability is a combination of the fibre matrix and small pore theory. It suggests that although the endothelial glycocalyx is the primary molecular sieve, the size and frequency of porous pathways determines the effective area for exchange of water and solutes across the endothelial barrier. The porous pathways may or may not contain a second molecular sieve (Michel and Curry, 1999) which could be breaks in

junctional strands (regulated by cell-cell contact mechanisms), but may also include fenestrations, transcellular breaks or vesicles fused to both luminal and abluminal membrane.

Two putative systems for trans-endothelial transport have been suggested (McDonald *et al.*, 1999; Renkin, 1994):

The inter-endothelial or paracellular system. Evidence to support this theory was first provided by the pioneering work of Majno and Palade (1961), which linked permeability increases with the formation of gaps between the endothelial cells. Several studies with endothelial cells have shown that the increase in permeability caused by inflammatory mediators is virtually always accompanied by changes in the cell cytoskeleton which are thought to be linked with the production of macro and/or microscopic gaps between the cells (Budworth *et al.*, 1999; Esser *et al.*, 1998; Leach *et al.*, 1995; McDonald *et al.*, 1999; Shasby *et al.*, 1982). These gaps are proposed to be the conduit for the passage of hydrophilic solutes and water (Clough, 1991).

The trans-endothelial vesicular system. At around the same time as Majno and Palade (1961) showed the importance of intercellular gaps in the endothelium, Palade (1960) demonstrated that certain types of transendothelial transport could be linked to the 'shuttling' back and forth with endothelial cells of vesicles. Dvorak *et al.* (1996) has shown that the fusion of vesicles and vacuoles near endothelial cell membranes to form VVO's (Vesiculo-Vacuolar Organelles) are part of the vessels response to inflammatory agents. This hypothesis has been chased by Michel and Neal (1999) who via the use of serial sectioning in TEM have demonstrated that the majority of openings

across the endothelium, following permeability increase to specific stimuli, are transcellular, not intercellular in nature.

Although there is clearly some degree of disagreement in the involvement of the two systems described above it is likely that they would act together to regulate permeability. It has been suggested that the transcellular system transport may be sustained for a longer period than that of the intercellular junctions, which have been shown to act briefly (within 1 minute) after inflammatory stimuli (Niimi *et al.*, 1992). However more recent studies have shown VEGF causes changes in permeability, postulated to be via the paracellular cleft, 4hr after administration (Esser *et al.*, 1998).

1.6

ENDOTHELIAL CELL-CELL JUNCTIONS

There is a general consensus of opinion that in continuous endothelium the major transit pathway for fluid and macromolecules and for diapedesis of blood cells is by way of the interendothelial cell junctions. These junctions are dynamically organised structures that vary in composition and function according to their position in the vascular tree (Simionescu and Simionescu, 1991). They are complex integral membrane structures that associate with the network of cytoplasmic filaments, i.e. the cytoskeleton (Haselton, 1992). During the regulation of vascular permeability, endothelial intercellular junctions need to be dynamically managed in concert with the functional requirements of the system. Currently there are thought to be 3 types of vascular inter-endothelial junction that may infer an effect on permeability

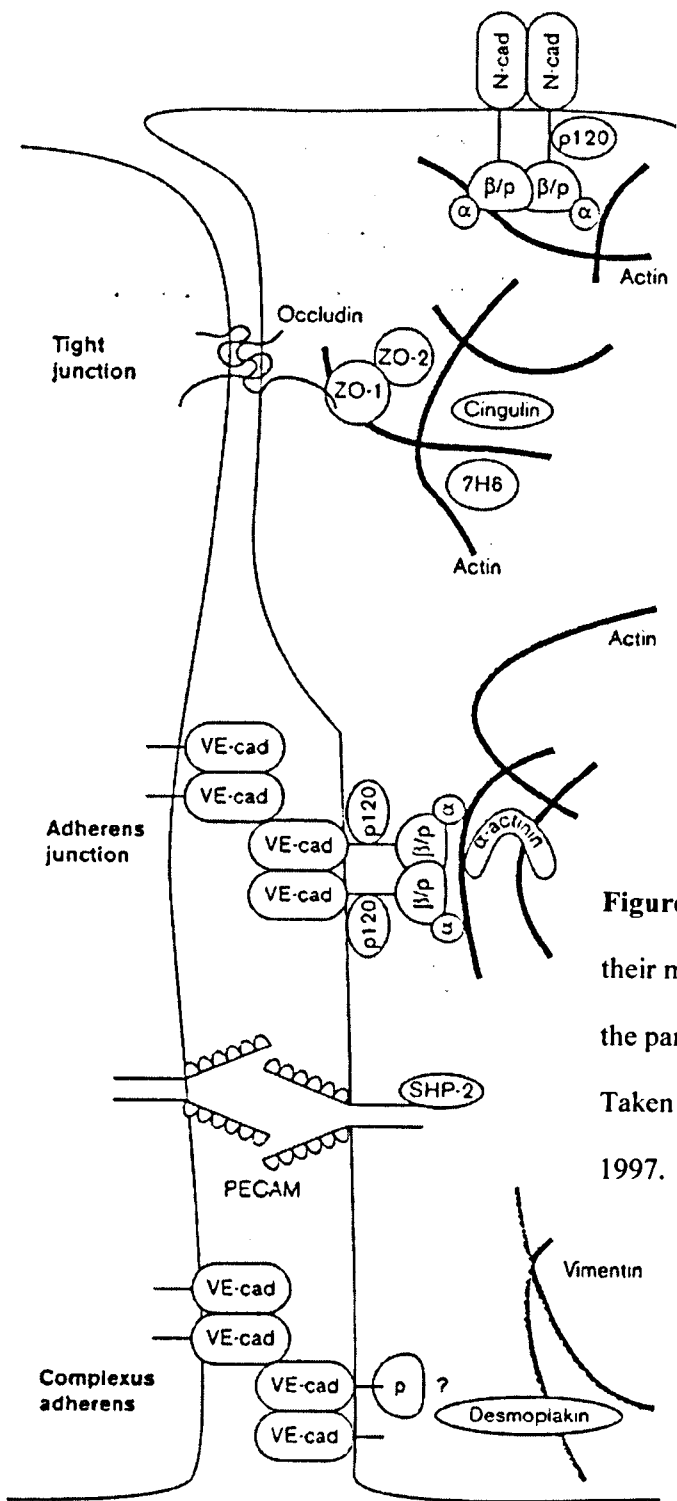


Figure 1.2: Junctional structures and their molecular composition found within the paracellular clefts of the endothelium. Taken from Lampugnani and Dejana, 1997.

© 1997 Current Opinion in Cell Biology

(figure 1.2), the adherens junction and the tight junction. Complexus adhaerentes are junctions of variable size and shape that occur in lymphatic endothelia (Franke *et al.*, 1994).

1.6.1

THE ADHERENS JUNCTION

The adherens junction (AJ) was first described in mammalian blood vessels by Franke *et al.*, (1988). AJs are a family of transmembranous, multimolecular complexes in which the actin cytoskeleton is linked to the plasma membrane through a specialised sub-membrane plaque containing cadherins and a variety of associated proteins (Geiger and Ginsburg, 1991; Shasby and Shasby, 1986; Tsukita *et al.*, 1992). AJs are virtually ubiquitous along the vascular tree and are essential for tight and gap junction assembly (Dejana *et al.*, 1995).

1.6.2

CADHERINS

The cadherins represent a family of tissue-specific cell adhesion molecules, which are essential for morphogenic processes and establishing and maintaining cell polarity (Rimm and Morrow, 1994; Takeichi, 1991). Cadherins are single chain transmembrane proteins comprised of a highly conserved cytoplasmic region and an extracellular domain containing Ca^{2+} binding motifs. Cadherins promote homophilic, Ca^{2+} -dependent cell-to-cell recognition (Kemler, 1993). Endothelial cells have been shown to express both specific and non-specific cadherins. The specific cadherin expressed at the interendothelial junctions is Vascular Endothelial Cadherin (VE- cadherin).

VE-cadherin shows moderate homology with other cadherin family members, but stark differences are evident in both the cytoplasmic and extracellular domains (Suzuki *et al.*, 1991), suggesting a specific behaviour for this molecule in cell-cell adhesion and cytoskeletal protein interactions.

N-cadherin, also found in nervous and muscular cells, has been detected in the endothelium. However, it is distributed in a non-junctional manner, remaining diffuse on the cell membrane (Salomon *et al.*, 1992). The presence of P-cadherin has been shown in low levels (Liaw *et al.*, 1990). E-cadherin has been detected, but only in the tighter endothelium of the brain (Rubin, 1992). The basic cell-cell adhesion complex is thought to be composed of four cadherin molecules. Two cadherins from each cell surface seem to interact and cooperate to form the basic cell-cell adhesion complex (Tomschy *et al.*, 1996). The cadherins forms complexes with the catenins, α - β - and γ -catenin (homologous with plakoglobin). These molecules in collaboration with a variety of other molecules, some to be identified, link to actin microfilaments to stabilise and strengthen the junctions (Tsukita *et al.*, 1992).

1.6.2.1

VASCULAR ENDOTHELIAL CADHERIN

Vascular Endothelial Cadherin (VE-cadherin) was first described by Lampugnani *et al.* in 1992 as the major cadherin expressed in inter-endothelial cell clefts. The structure of VE-cadherin as indicated by its homology to other members of the cadherin group has been put forward as confirmation that it is involved with cell-cell adhesion and cytoskeletal interactions (Dejana *et al.*, 1995). It has a large extracellular domain, consisting of five homologous

repeats (figure 1.3) which have been suggested as Ca^{2+} binding regions (Dejana, 1996). It acts as a classic cadherin since it causes cells to adhere to each other in a calcium-dependent, homophilic manner (Ali *et al.*, 1997). Various vasoactive mediators including thrombin, elastase, inflammatory cytokines, histamine and VEGF have been shown to change VE-cadherin distribution at junctions in parallel with increased permeability (Andriopoulou *et al.*, 1999; Esser *et al.*, 1998; Lampugnani *et al.*, 1992; Leach *et al.*, 1995). Intravenous injection of a monoclonal antibody against VE-cadherin in mice increases permeability (Corada, 1999; Gao, 2000) indicating that VE-cadherin is involved in the regulation of endothelial barrier function *in-vivo*.

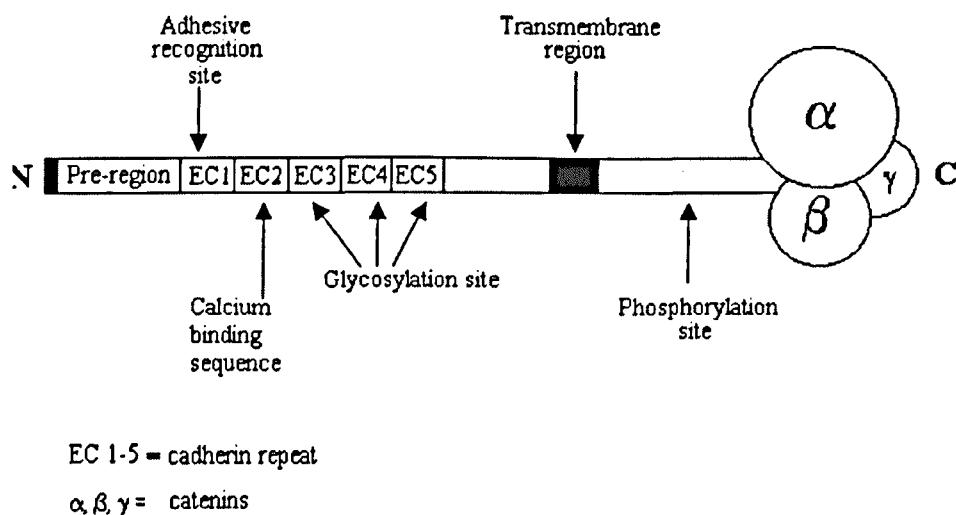


Figure 1.3: Cadherin structure.

1.6.2.2

THE CATENINS

The catenin family of armadillo proteins is made up of 3 major isoforms, α -, β - and γ -catenin. β - and γ -catenin bind directly to the C-terminal domain of the cadherin molecule, while α -catenin attaches via the β/γ complex. It is suggested that α -catenin links α -actinin to microfilaments (Janssens *et al.*, 2001; Kemler, 1993; Knudsen *et al.*, 1995; Lampugnani *et al.*, 1995). In human umbilical vein endothelial cells (HUVEC), during the establishment of confluency, first VE-cadherin with α - and β - catenin is organised at junctions without apparent linkage with the actin cytoskeleton. Only at later stages do plakoglobin and actin microfilaments get associated to these structures (Lampugnani *et al.*, 1995). Another member of the catenin family is p120 that binds to the juxtamembrane portions of cadherins, influencing clustering and the adhesive strength (Yap *et al.*, 1998). Hence, while cadherins are the major adhesion proteins in cell-cell interactions, it is the cadherin/catenin cytoplasmic complex that binds to the actin cytoskeleton that determines the strength of the intercellular adhesion. In addition to β -catenin's role in the cadherin-catenin complex, it is a key component in the signalling processes involved in embryonic development and a central player in the wnt/wingless signal transduction cascade (Stockinger *et al.*, 2001). The involvement of α -catenin in the cadherin/catenin complex is essential for strong cell-cell adhesion (Hirano *et al.*, 1992; Torres *et al.*, 1997). Indeed, in tumour progression its expression is often reduced (Hirohashi 1998). Reintroduction into cell-lines that lack α -catenin reduces cell growth and promotes cell-cell adhesion (Watabe *et al.*, 1994).

There is accumulating evidence that junctional integrity is regulated by tyrosine phosphorylation of specific components. The catenins are targets of such tyrosine phosphorylation. Hoschuetzky *et al.*, (1994) showed that epidermal growth factor (EGF) caused cell rounding in epithelial cells concomitantly with phosphorylation of tyrosine residues on β -catenin and plakoglobin. Conversely p120 is dephosphorylated by a variety of growth factors (Ratcliffe *et al.*, 1999; Wong *et al.*, 2000). In the endothelium Lampugnani *et al.*, (1997) illustrated that the levels of phosphorylation of junctional molecules differed markedly between loosely and tightly confluent endothelial cell monolayers. Other evidence includes the association between loss of intercellular contact and increased tyrosine phosphorylation in AJ (Esser *et al.*, 1998) and the lowering of adhesion between cells upon exposure to phosphatase inhibitors along with increased permeability (Collarex-Buzato *et al.*, 1998; Volberg *et al.*, 1992). Ratcliffe *et al.*, (1999) have shown that dephosphorylation of p120/100 occurs after exposure to histamine leading to a feasible suggestion that there is a delicate balance between dephosphorylative and phosphorylative components of the junction (Gulino *et al.*, 1998). Attention has focused on the assembly of cadherin-catenin-actin complexes and the role they play in cell-cell adhesion. Understanding the dynamics of cadherin-catenin-actin complex assembly and the significance of these interactions in stabilizing cell-cell contacts are crucial for defining mechanisms by which tissue integrity is established and maintained and, in the context of the endothelium regulated.

1.6.2.3

F-ACTIN

The actin cytoskeleton is a highly dynamic network, changing structure during the cell cycle and in response to extra- and intracellular signals (Hall, 1994). It is involved in the formation and maintenance of adherens junctions, which are fundamental to the correct functioning of cell monolayers (Tsukita *et al.*, 1992). Many physiological agents, which alter endothelial monolayer permeability in-vitro, have been strongly linked with a modification in the F-actin cytoskeleton (Haselton 1992; Yu and Gotlieb, 1992). Cytoskeletal filaments are structurally regulated through signals transmitted via receptors and second messengers (Haselton 1992). Endothelial cell contraction is directly associated with phosphorylation of myosin light chains (MLC) by the Ca^{2+} /Calmodulin (CaM)-dependent myosin light chain kinases (MLCK) (Garcia *et al.*, 1995; Patterson *et al.*, 1994; Wysolmerski and Lagunoff, 1990). MLCK activation has been shown to be strongly linked to permeability increase (Garcia *et al.*, 1995). Verin *et al.*, 1995, used calyculin to inhibit serine/threonine phosphatases which lead to an accumulation of phosphorylated MLC and an increase in albumin permeability. Gilbert-McClain *et al.*, (1998) showed that vanadate increased albumin permeability in bovine pulmonary endothelial cells concomitant with an increase in MLC phosphorylation.

1.6.3

THE TIGHT JUNCTION

Tight junctions (TJ) regulate the passage of materials through the paracellular cleft between one cell and the next (Balda *et al.*, 1996). In contradiction to the epithelial tight junction, within the endothelium they are not a continuous seal around the apical surface of the cells. Rather, they have discontinuities that can be actively regulated to achieve selective barrier function (Leach and Firth, 1995). One molecule that is important in the functionality of TJs is the transmembrane molecule occludin (Balda *et al.*, 1996; Furuse *et al.*, 1993). Associated with occludin is the MAGUK family member, ZO-1 (Kimura *et al.*, 1996), ZO-2 and cingulin (Anderson *et al.*, 1993). Occludin has four transmembrane domains and spans the intercellular junction (Furuse *et al.*, 1994). *In vitro* it has been shown that the occludin transmembrane domain is a fusion protein with glutathione-S-transferase and this specifically binds to both ZO-1 and ZO-2 (Furuse *et al.*, 1994). The correct assembly of the tight junctions has been shown to be dependent of protein kinase C (PKC) (Stuart & Nigam, 1995). The work with protein kinase C inhibitor Calphostin C also demonstrated that while occludin was affected at certain concentrations, the desmosomes and adherens junctions were not. Stuart and Nigam, (1995) also suggested that ZO-1 might be a direct target of PKC. Tight junctions are most abundant in large vessels where strict control of permeability is needed and least abundant in smaller vessels where efficient exchange is necessary (Simionescu and Simionescu, 1991). Occludin itself has been shown to have differential expression dependent on the function of vessels (Leach *et al.*, 2000).

1.7

INVOLVEMENT OF JUNCTIONAL COMPONENTS IN OTHER
PHYSIOLOGICAL PROCESSES

In addition to the role of the endothelial cell-cell junctions in the regulation of vascular permeability they appear to be important players in other physiological processes. Carmeliet *et al.* (1999) showed, in transgenic mice, that inactivation or truncation of VE-cadherin induced apoptosis in the developing blood vessels. These mutations also stopped the transmission of the VEGF-A induced endothelial survival signal by preventing the formation of a complex consisting of VE-cadherin, VEGFR receptor-2, β -catenin and phosphoinositide-3-OH kinase. Thus VE-cadherin is proposed to act as part of an antiapoptotic pathway in endothelial cells. The involvement of cadherins in apoptosis is supported by Weiske *et al.* (2001). They showed that the desmosomal cadherin-catenin complex is targeted by caspases during the induction of apoptosis, releasing the extracellular domains from the cell surface.

From studies with proximal tubule epithelial cells it has also been shown that inducible nitric oxide can also cause a dispersal of basolateral integrins (p1) and E-cadherin. Hence, during an inflammatory response where NOS is up-regulated E-cadherin can be affected and even interaction of the epithelial cells with the laminin of the basal membrane (Glynne *et al.*, 2001). Coronary endothelial cells have been shown to express VE-cadherin and endothelial type nitric oxide synthase (eNOS) (Li *et al.*, 2001). Stimulation of the E-cadherin mediated cell-cell adhesion can be obtained in primary breast cancer cells that are sensitive to insulin-like growth factor 1 via IGF-R1, which is associated

with the ZO-1 and E-cadherin complex. The up-regulation in adhesion appears to be associated with increase in ZO-1 and IGF-IR (α -catenin) ZO-1 binding. This enhances the ZO-1/actin association leading to a stronger connection between E-cadherin complex and the active cytoskeleton (Mauro *et al.*, 2001). However, in the MCR-10ATG3B breast epithelial cells, the cell-cell and cell-extra cellular matrix interactions can be disrupted with Kepone treatment. The Kepone results in a decrease in E-cadherin and β -catenin, but not in desmoglein, α -and γ -catenin (Starcevic *et al.*, 2001).

In mobile cells *in vitro*, the accumulation of E-cadherin and β -catenin is decreased at cell-to-cell adhesion sites in MDCK cells (Kodama *et al.*, 2001).

Evidence from precision cut liver slices has shown that of the four distinct cell-cell adhesion complexes, namely, E-cadherin/ β -catenin/ α -catenin; E-cadherin/ γ -catenin/ γ -catenin; N-cadherin/ β -catenin/ α -catenin and N-cadherin/ γ -catenin/ α -catenin, it is E-cadherin/ β -catenin complex that is sensitive to oxidative stress (Schmelz *et al.*, 2001). Hence oxidative stress could play a role in vascular endothelial permeability.

1.8

USE OF ENDOTHELIAL CELLS *IN-VITRO*

Methods for the isolation and culture of micro- and macro-vascular endothelial cells from several species, including human sources, have been developed, whereby junctional complexes are retained. Human umbilical vein endothelial cells (HUVEC) have been extensively used to study endothelial cell physiology, including the regulation of permeability. Immortalised human endothelial cell-lines are available, including the ECV-304 from the European

and American tissue culture collections and the HMEC-1 cell line. The full consequences of the immortalisation process on the normal functioning of the adhesion molecules and the barrier function are not fully appreciated. Evaluation of a set of parameters pertinent to the cell functions being studied is a prudent expedient prior to the routine use of a cell-line in an *in-vitro* model.

1.8.1

DRAWBACKS OF *IN-VITRO* STUDIES

Limitations of *in-vitro* studies of endothelial cell function are that cell culture perturbs the cells from a quiescent *in-vivo* state (0.1% replications per day) to an activated phenotype (1 - 10% replications per day) with the loss of specialised functions associated with diverse vessels and organ systems. The potential interaction between tissues is also lost, unless other tissue components are included, e.g. in skin models including both dermal and epidermal components. It is also difficult to reproduce precisely the basal membrane upon which the cells are normally constructed *in vivo* and to reproduce the blood flow through the vascular tubes and the production of such tubes.

Despite these differences and drawbacks, the endothelial cell model systems can be employed to demonstrate the effects of individual chemicals, endogenous and exogenous, on the barrier function of the microvascular endothelium.

1.9

DEVELOPMENT OF *IN-VITRO* APPROACHES TO TOXICOLOGY

Part of this project was to define a model of endothelial permeability that could potentially be used, in a battery of tests, as an alternative to using animals in research and regulatory toxicology testing.

In 1995, ECVAM, the European Centre for the Validation of Alternative Methods, produced a report on the Validation of Alternative Test Methods (Balls & Karcher, 1995). This laid down the important steps that need to be followed when developing *in vitro* assay systems that are designed to replace, or investigate specific effects *in vivo*. Prior to the progression to full validation, a pre-validation step is recommended (Curren *et al.*, 1995). To progress to pre-validation, phase I of a three-phase process needs to be satisfied. Phase I includes, creation of a workable, GLP-compliant protocol for the procedure; production of accompanying SOPs; determination of the intra-laboratory reproducibility of the method; Evaluation of its suitability for progression to phase II “Protocol Transfer” (Curren *et al.*, 1995). Hence, in the development of the assay system outlined in this thesis, it was recognized that the assay to be developed should ideally be validated via the strict criteria applied at present only to *in vitro* assays. In addition to the above a prediction model for interpretation of the results obtained is required.

The publication of the EU white paper “Strategy for a future chemicals policy” (Worth and Balls, 2001) has promoted the need for full data on the potential toxic effects of chemicals. The main points of this document is to ensure safety data required for new chemicals since 1981 is also available for existing chemicals.

It is recognized that such a proposal would require additional information concerning potential effects including specifically skin irritation potential. It also promotes the use of *in vitro* methods where possible to provide such data. This increased requirement for information is not just a European pre-occupation; in the US similar concerns are being raised in connection with High Production Volume chemicals. In response to this the National Institute of Health instigated an expert meeting and reports to address the issue of The Interagency Coordination of Validation of Alternative Methods on *In Vitro* methods for assessing acute systemic toxicity, in October 2000. The report has been issued and contains recommendations based on validation of alternative methods.

1.10

HYPOTHESIS AND AIMS OF THIS THESIS.

The vascular endothelium provides the permeability barrier between blood-borne substrates and the underlying matrix. Increased vascular leakage is a complication found in many pathologies, linked with the inflammatory process. The adherens junction has been implicated in maintaining the endothelial barrier and regulating permeability. Indeed, *in-vitro*, the focal loss of adherens junction molecules, concomitant with increased permeability, has been induced by a variety of inflammatory mediators. In parallel, the increased demand for reliable, defined *in-vitro* models of endothelia has encouraged the development of immortalised cell-lines. However, the junctional phenotype of these cells is often overlooked. Therefore the working hypothesis of this project was:

In two defined endothelial cell-lines; HMEC-1 and ECV304, alteration in the expression of adherens junction proteins correlates to changes in macromolecule permeability.

Based on this hypothesis, the specific aims were as follows:

- Establish HMEC-1 and ECV304 as suitable models to assess the effects of inflammatory mediators on endothelial permeability.
- Refine the *in-vitro* method for measuring permeability.
- Analyse VE-cadherin distribution in confluent monolayers upon exposure to a variety of vasoactive agents, including calcium chelator, calcium ionophore, PKC activator, amphoteric surfactant and cAMP promoter.
- Analyse the effects of histamine on VE-cadherin and F-actin distribution and correlate with permeability to tracers of known sizes.
- Elucidate the role of the cytoplasmic linking molecules, specifically α -catenin, in establishing restrictive junctions.

CHAPTER 2

EVALUATION OF POTENTIAL
ENDOTHELIAL CELL-LINES FOR
STUDYING VASCULAR PERMEABILITY
IN-VITRO.

CHAPTER 2**EVALUATION OF POTENTIAL ENDOTHELIAL CELL-LINES FOR
STUDYING VASCULAR PERMEABILITY IN-VITRO.****2.1****INTRODUCTION**

Methods for the isolation and culture of micro- and macro-vascular endothelial cells from several species, including human, has enabled investigators to gain insight into the physiology and pathophysiology of the endothelial cell (Cines *et al.*, 1998; Davies and Hagen, 1993; Jaffe, 1987; Pearson, 1991). Altered endothelial cell functions play a central role in regulating vascular permeability, as a result of alterations in local tissues. Most of the pioneer work on elucidating the control of permeability was originally conducted on hamster cheek pouch (Svensjo *et al.*, 1978). Later the human umbilical vein endothelial cells (HUVEC) were isolated and employed (Carson *et al.*, 1989; Killackey *et al.*, 1984; Lampugnani *et al.*, 1991; Lum & Malik 1996). This research has lead to defining the specific growth and functional properties of endothelial cells in general. However, the endothelium is a highly heterogeneous tissue, being morphologically and functionally different, in part related to its location in the body (Swerlick and Lawley, 1993). Auerbach *et al.* (1985) showed that mouse capillary endothelial cells from different organs expressed a unique array of cell surface-associated molecules.

Another example of heterogeneity is the endothelium's response to various drugs and compounds; the immunosuppressant cyclosporin can affect the release of prostacyclin dependent upon the type of endothelium studied

(Table 2.1). Brown *et al.*, (1987) saw a decrease in prostacyclin release upon exposure to cyclosporin in HUVEC cells, whilst microvascular endothelial cells from rat fat tissue showed an increase in prostacyclin release in response to a concentration range of cyclosporin which overlapped the range used for the HUVEC cells (Lau *et al.*, 1989). These differences could reflect not only the type of endothelial cell used but also the species variation in response to cyclosporin.

ENDOTHELIAL CELL TYPE	ENDOTHELIAL CELL ORIGIN	CYCLOSPORIN DOSE	EFFECT OF CYCLOSPORIN
Microvascular (Lau <i>et al.</i> , 1989)	Rat Perirenal Fat	0.01 – 1µg ml ⁻¹	Dose dependent increase in prostacyclin release
Vein (HUVEC) (Brown <i>et al.</i> , 1987)	Human Umbilical	0.1-100µg ml ⁻¹	Dose dependent decrease in prostacyclin release

Table 2.1: Effect of cyclosporin on prostacyclin release from endothelial cells originating from different anatomical sites and species.

The advantages of using HUVEC are that umbilical cords tend to be readily available; however, they also have several disadvantages. The life span of these cells was relatively short, hence they were used up to and including passage 3. Later passages begin to lose their differentiated functions, for example prostacyclin production and the post-transcriptional regulation of

Interleukin-1 α (IL-1 α) (Introna *et al.*, 1994). This, along with their long population doubling time of approximately 90hrs (Takahashi *et al.*, 1990) and the donor variations highlights potential problems with the routine use of these cells. Researchers have pooled cells from different cords in order to limit the potential high degree of variability found between cells from different donors. In a study by Casnocha *et al.* (1989) variation in permeability coefficients to albumin, ranged from $4.8 \times 10^{-6} \text{ cm s}^{-1}$ to $5.5 \times 10^{-7} \text{ cm s}^{-1}$. HUVECs represent endothelial cells that are at the end of their normal *in-vivo* life span as, following the birth of a child; the umbilical cord is expelled from the body, serving no more purpose. Based on the heterogeneity observed between various endothelial cells, cells derived from human dermal component of skin were preferential in the study reported here since this endothelium is important in the dermal response to irritants and/or injury. Therefore, the immortalised human dermal microvascular endothelial cell-line, HMEC-1 was evaluated. However, as HUVEC are used extensively in permeability research we utilised the ECV304 cell-line which was reported to be spontaneously immortalised from HUVEC (Takahashi *et al.*, 1990). The permeability of these cell-lines grown on porous membrane supports was investigated, following exposure to a variety of vaso-active chemicals. The method used was derived from Hashida (1986) employing a fluorescein-isothiocyanate (FITC)-labelled 70kDa dextran (FD70) as the tracer. Additionally the morphology of the cell cultures was observed using phase-contrast microscopy at various time points. Evidence suggests that both tight and adherens inter-endothelial junctions govern the regulation of vascular permeability (Braverman and Keh-Yen, 1986; Gotlieb *et al.*, 1991; Niimi *et al.*, 1992). Therefore, immunocytochemistry studies are

included to establish the basal expression and localisation of the important endothelial proteins; VE-cadherin and PECAM-1 which are normally expressed and located at cell-cell contacts *in-vivo* and *in-vitro* (Albelda *et al.*, 1991; Lampugnani *et al.*, 1992; Muller *et al.*, 1989), and von Willebrand Factor, a marker for the verification of the cells' endothelial origin. In addition, for the HMEC-1 cells, a DNA profile was obtained from LGC, an independent chemical analysis laboratory, to ensure the identity of this cell line.

2.2

MATERIALS AND METHODS

2.2.1

MATERIALS

2.2.1.1

Chemicals and Reagents

Phosphate buffered saline (PBS) (calcium- and magnesium- free) was purchased from Oxoid Ltd, Basingstoke, UK. Medium 199; MCB D 131 medium; DMEM (phenol red-free); Hanks Balanced Salt Solution (HBSS); amphotericin B; L-glutamine; and trypsin (0.05%w/v) with ethylene diamine tetra-acetic acid (EDTA) disodium salt (0.02% w/v) in PBS (trypsin/EDTA) were purchased from Life Technologies, Paisley, UK. Foetal Calf Serum (FCS) was purchased from Autogen Bioclear UK Ltd., Wiltshire, UK. Hyclone FCS was purchased from Pierce and Warriner (UK) Ltd., Chester, UK. Hydrocortisone; epidermal growth factor (EGF); dimethylsulphoxide (DMSO); penicillin-streptomycin; fibronectin from human plasma; FITC-labelled 70-kDa dextran (FD70); gelatine; collagenase type II; Triton-X-100; paraformaldehyde; heparin; IL-1 α ; TNF α ; A23187; phorbol 12-myristate 13-acetate (PMA); normal goat serum; bovine serum albumin were purchased from Sigma, Poole, UK. Endothelial cell growth supplement (ECGS) was purchased from First Link, Brierley Hill, UK. Vectorshield was purchased from Vector Laboratories, Peterborough, UK. Laminin and Cellagen-PC3 (acidified type I bovine collagen, 0.3%w/v) was purchased from ICN

Pharmaceutical Ltd., Basingstoke, UK. Sodium chloride solution (0.9% w/v) was purchased from Baxter Healthcare Ltd., Thetford, UK. TrigeneTM was obtained from Scientific Laboratory Supplies Ltd., Nottingham, UK.

2.2.1.2

Antibodies

Rabbit polyclonal anti-human von Willebrand Factor (vWF) antibody was purchased from Sigma-Aldrich, Poole, UK. Mouse monoclonal anti-human PECAM-1 was purchased from R&D Systems, Oxon, UK. Mouse monoclonal anti-human VE-Cadherin was purchased from Cambio, Cambridge, UK. Upon arrival anti-PECAM-1 antibody was diluted to 1mg ml⁻¹ in sterile water. Both anti-PECAM-1 and anti-vWF were dispensed into aliquots and stored at -80°C. VE-Cadherin antibody was stored at 4°C. FITC-conjugated goat anti-mouse or goat anti-rabbit immunoglobulin G (whole molecule) was purchased from Sigma-Aldrich, Poole, UK, and was stored protected from light at 4°C.

2.2.1.3

Immortalised Cell-lines

The ECV304 cell-line was purchased from the European Collection of Animal Cell Cultures (ECACC), N° 92091712. The HMEC-1 cell-line was a gift from Dr. Ades, Department of Dermatology, Emory University School of Medicine, Atlanta, Georgia. USA.

2.2.1.4

Consumables

Nunc™ tissue culture flasks; plates; chamberslides and 0.2µM Anopore inserts were purchased from Life Technologies, Paisley, UK. Costar tissue culture plates were purchased from Corning Costar, Fisher Scientific UK, Loughborough, UK. CM Inserts and the Cytofluor fluorescent plate reader were purchased from Millipore Ltd., Watford, UK. Cryopreservation tubes (1ml) were purchased from Sarstedt, Leicester, UK. 25ml Universal tubes were purchased from Bibby Sterilin Ltd, Staffordshire, UK. Mr Frosty™ cryopreservation container; container used to incubate umbilical cord and steel trays were purchased from Jencons-PLS, Leighton Buzzard, UK. 3-way stopcock was purchased from Vygon UK Ltd., Gloucestershire, UK. Suture was purchased from Davies and Geck Gosport, UK.

2.2.1.5

DNA Profile

The DNA profile of the cells used in this study was obtained from LGC, Middlesex, UK

2.2.2

METHODS

2.2.2.1

Preparation of Solutions and Cell Culture Media

PBS was prepared from pre-weighed tablets in distilled water, autoclaved and stored at room temperature. 1% (w/v) gelatine was prepared in sterile water, autoclaved and stored at 4°C.

For ECV304 cells, Medium 199 was supplemented with 10% (v/v) foetal calf serum (FCS) L-glutamine (2mM); penicillin (100 Units ml⁻¹) streptomycin (100µg ml⁻¹) and amphotericin B (2µg ml⁻¹).

For HMEC-1 cells, MCDB 131 medium was supplemented with 10% (v/v) FCS, EGF (10ng ml⁻¹), hydrocortisone (1µg ml⁻¹), L-glutamine (2mM); penicillin (100 Units ml⁻¹), streptomycin (100µg ml⁻¹) and amphotericin B (1µg ml⁻¹).

For HUVEC cells Medium 199 was supplemented with 20% (v/v) Hyclone FCS, ECGS (30µg ml⁻¹), heparin (90µg ml⁻¹), L-glutamine (2mM); penicillin (100 Units ml⁻¹), streptomycin (100µg ml⁻¹) and amphotericin B (0.2µg ml⁻¹).

All medium was stored at 4°C and used within 4 weeks. The following supplements were prepared in advance for preparation of the HMEC-1 medium; these solutions were filter-sterilised immediately following preparation. Hydrocortisone was stored at -20°C as a 500µg ml⁻¹ solution in MCDB 131 medium. EGF was stored at -20°C as a 1µg ml⁻¹ solution in PBS containing 0.1% (w/v) bovine serum albumin (PBS/BSA). L-glutamine was stored at -20°C as a 200mM solution in sterile water. All media were checked

for sterility by incubation of 2ml medium in a 25cm² cell culture flask for 48 hours at 37°C, 5% (v/v) carbon dioxide (CO₂) in air, prior to use.

2.2.2.2

Treatment of Tissue Culture Plastic and CM Inserts with Extracellular Matrix Proteins

For gelatine-coated tissue culture flasks 2ml of 1% sterile gelatine in water (37°C) was added to a 25cm² flask, or 5ml added to a 75cm² flask. Flasks were incubated at 37°C, 5% (v/v) CO₂ in air for 30 minutes. The gelatine was then removed and the flasks allowed to air-dry in the laminar flow hood under sterile conditions. The same procedure was used to gelatine-coat the 8-well chamberslides except 200µl of gelatine was added to each well pre-incubation. For coating of the CM inserts: Collagen type I solution was diluted to 0.075% w/v in 60% ethanol, 100µl was introduced into the insert. Fibronectin was diluted to 100µg ml⁻¹ in MCDB 131 medium, 150µl added to each insert. Laminin was diluted to 120µg ml⁻¹ in MCDB 131 medium, 100µl added to the insert. The inserts were then allowed to air dry in the laminar flow hood under sterile conditions. The matrix proteins were prepared in advance, aliquoted and stored as outlined below. Collagen type I was stored at 4°C. Fibronectin was reconstituted in distilled water to 1mg ml⁻¹ and stored at -20°C for up to 6 months. Laminin was diluted to 1µg ml⁻¹ in distilled water and stored at -20°C.

2.2.2.3

Subculture of Endothelial Cells

Endothelial cells were cultured in 75cm² culture flasks and subcultured at approximately 80% confluence. Medium was aspirated and the cells were washed with calcium- and magnesium-free PBS (pre-warmed to 37°C). Cultures were then incubated with 2ml trypsin/EDTA at 37°C, 5% (v/v) CO₂ in air for approximately 5 minutes. Cells were detached by tapping the flask. The appropriate medium containing FCS, to inhibit the action of the trypsin/EDTA, was added and the cell suspension was transferred to a 25ml universal tube. Following centrifugation at 100g for 5 minutes (at room temperature), the cell pellet was resuspended in 5ml medium. Cells were seeded into 75cm² culture flasks at a split ratio of approximately 1:10 (maximum 1:20). Medium was added to give a final volume of 20ml. Cultures were maintained at 37°C, 5% (v/v) CO₂ in air, and re-fed with fresh medium every 72 hours.

2.2.2.4

Cryopreservation of Endothelial Cell-lines

Endothelial cells were harvested during the exponential growth phase, as described in section 2.2.2.3. Cells were counted using a haemocytometer, and following centrifugation for 5 minutes at 100g, were resuspended to give a density of 3x10⁶ ml⁻¹ in sterile FCS, containing 10% (v/v) dimethylsulphoxide (DMSO) as a cryoprotectant. Endothelial cells were dispensed into 1ml sterile cryopreservation tubes and cooled at a rate of 1°C per minute to -80°C using Mr Frosty™, a thermal container with isopropanol. The tubes were then

transferred to liquid nitrogen for long-term storage. When required, cells were thawed rapidly, and following careful dilution in culture medium and centrifugation for 5 minutes at 100g, were resuspended in fresh culture medium and seeded into culture flasks.

2.2.2.5

Determination of the growth rate of HMEC-1 and ECV304 cells

Human endothelial cells, ECV304 and HMEC-1 were seeded into 25cm² flasks at a density of 5×10^4 cells per flask in 5ml of medium. Triplicate flasks were set up for each time point. Cultures were maintained at 37°C, 5% (v/v) CO₂ in air and re-fed with fresh medium every 48 hours. Endothelial cells were harvested as in 2.2.2.3 from 3 flasks after 24-hours of growth and subsequently every 24 hours. Total cell number was determined using a haemocytometer. The number of population doublings per day was then calculated as follows:

$$\left(\sqrt[3]{\frac{\text{total cell number at 96hrs}}{\text{total cell number at 24hrs}}} \right) - 1$$

Equation 2.1: Population doublings

2.2.2.6

Determination of Monolayer Permeability in Endothelial Cells.

Human endothelial cells were seeded into Anopore inserts at 5×10^5 cells ml^{-1} in 500 μl of medium. Three inserts received 500 μl of medium alone and were referred to as the no-cell inserts. The inserts were placed into 24-well culture plates with a further 500 μl of medium in the wells (figure 2.1). Cultures were maintained at 37°C, 5% (v/v) CO_2 in air. A confluent monolayer usually formed within 48hrs and was checked visually. At all times the inserts were handled with sterile forceps. After 72 hours in culture the leakage of FD70 was determined. The cells were washed with 500 μl of HBSS and the inserts transferred into fresh wells containing 500 μl media DMEM (phenol red-free) with 10% FCS (DMEM/FCS).

$$\left[\frac{\text{FU that crossed the monolayer and insert at time t.}}{\text{FU that crossed the no-cell insert alone at time t.}} \right] \times 100$$

Equation 2.2: Percentage leakage formula

500 μl of 50 μM FD70 was applied to the luminal compartment, above the cells. Plates were incubated at room temperature on an orbital shaker for 2hr, to allow adequate leakage of FD70 across the endothelial cell monolayer. The inserts were removed and the amount of fluorescence in the wells (the abluminal compartment) was measured on the Cytofluor fluorescent plate

reader at an excitation wavelength of 485/20nm and an emission wavelength of 530/25nm. These arbitrary fluorescent units (FU) relate to the amount of FITC-labelled 70kDa dextran (FD70) that had crossed the endothelial monolayer and the insert membrane over a 2hr period. The effect of various compounds, including agonists, on endothelial permeability was assessed by exposing the confluent monolayer to the compound of choice prior to, but not during the above assay. The amount of FD70 that had crossed the monolayer in relation to that which crossed an insert with no cells on could be calculated (equation 2.2). This was expressed as percent leakage of the dextran, the percentage across the no cell insert being set at 100%.

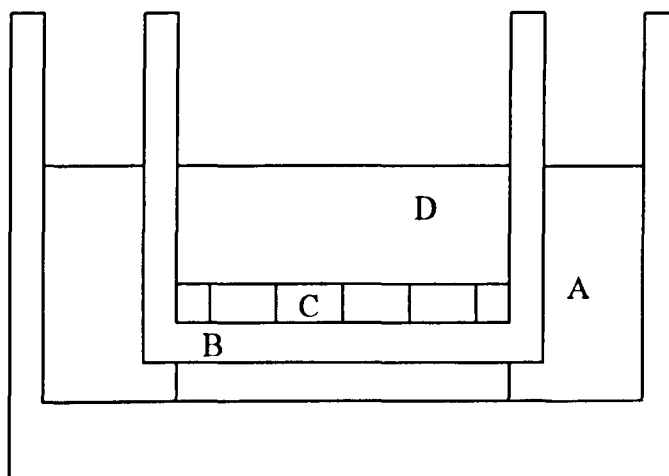


Figure 2.1: Schematic of the experimental apparatus used for determining endothelial permeability. A) abluminal chamber; B) aluminium oxide membrane; C) endothelial cell monolayer and D) luminal chamber.

2.2.2.7

Isolation of Human Umbilical Vein Endothelial Cells (HUVEC)

HUVEC were isolated based on the method by Jaffe *et al.*, 1973. Umbilical cords were obtained as waste tissue following normal delivery from Queen's Medical Centre, Nottingham. Immediately after clinical inspection of the placenta and umbilical cord, the cord was transferred to 0.9% saline solution containing 200IU ml⁻¹ penicillin and 200µg ml⁻¹ streptomycin (Sal/AB). Tissue was transported to the laboratory in a sterile container and stored at 4°C for up to 24 hours prior to use. Handling of the cord was done in a class two laminar flow hood vented to the outside, and all surfaces and equipment that came into contact with the tissue was decontaminated in TrigeneTM as a precaution against the potential infectious element of human tissue. The cord was inspected for damage that may affect the endothelium of the umbilical vein; e.g. clamp marks, or that may cause difficulty with the method; e.g. needle holes. The ends of the cord were blotted onto paper towelling and the vein teased open with round-ended forceps. Cannulation of the vein at both ends was achieved using 3-way stopcocks, tying securely with suture. The vein was then flushed through with Sal/AB to remove blood proteins and cells and then refilled until turgid to ensure that there are no punctures in the vein wall. The Sal/AB was removed and one of the stopcocks closed. A 0.5mg ml⁻¹ solution of collagenase type II in Medium 199 (M199) containing 100IU ml⁻¹ penicillin, 100µg ml⁻¹ streptomycin and 0.5µg ml⁻¹ amphotericin B was then introduced into the vein until turgid and the second stopcock closed. The umbilical cord was incubated in a water bath at 37°C for 10 minutes. Using two syringes, attached to the stopcocks at each end, the collagenase solution

was agitated back and forth through the vein to ensure all the endothelial cells had been removed from the vessel wall. The cell suspension was transferred from the syringe into serum containing M199 and centrifuged at 100g for 5 minutes at room temperature. The cell pellet was resuspended into 5ml of M199, supplemented as described in section 2.2.2.1, and seeded onto a gelatine coated 25cm² flask and incubated at 37°C, 5% CO₂ in air. After 2 hours, unattached cells were removed and the attached cells re-feeding with fresh medium. HUVECs were refed again following a further 24hr.in culture. Cultures were maintained at 37°C, 5% (v/v) CO₂ in air, and re-fed every 2-3 days with fresh medium. Cells were subcultured when they reached 90% confluent as in section 2.2.2.3.

2.2.2.8

Detection of von Willebrand Factor (vWF), Platelet-Endothelial Cell Adhesion Molecule (PECAM-1) and Vascular-Endothelial Cadherin (VE-Cadherin)

ECV304, HMEC-1 and HUVEC, were seeded onto gelatine-coated chamber slides (section 2.2.2.2), at a density of 1.5×10^5 cells per well, in 300µl of medium. Cultures were allowed to attach and grow to confluence at 37°C, 5% (v/v) CO₂ in air for 72hr after which time they were fixed in 300µl of 1% paraformaldehyde at room temperature for 30 minutes. The cells were washed once (10 min.) with 300µl of 0.1%BSA in PBS (PBS/BSA) and blocked in 5% goat serum in PBS for 30 min at RT. 200µl of anti-human vWF, anti-human PECAM-1 or anti-human VE-Cadherin diluted in PBS/BSA were exposed to the cells overnight at 4°C in a humidified environment. Anti-vWF was used at 100µg ml⁻¹ and anti-PECAM-1 and anti-VE-Cadherin were used at 10µg ml⁻¹.

Cultures were washed three times, 10 minutes each time, with 300µl of PBS/BSA. Cells were then exposed to 200µl of the appropriate FITC-tagged secondary antibody for 1hr at RT in the dark. Anti-mouse IgG was used for the PECAM-1 and VE-Cadherin exposed cultures, whilst anti-rabbit IgG was used for the vWF exposed cells. Secondary antibody was used at 5µg ml⁻¹. These optimal concentrations of antibodies were determined initially. The wells and glue were removed from the chamberslides leaving normal glass slides that were mounted using Vectorshield to preserve the fluorescence of the secondary antibody. The cells were examined using a Nikon fluorescence microscope, with a fluorescence filter of 490nm excitation / 550nm emission to visualise FITC.

2.2.2.9

Short Tandem Repeat (STR) profiling of HMEC-1 and HUVEC cells

A STR DNA profile is constructed by measuring the length of DNA at specific sites in the genome. These lengths differ by virtue of the number of repeat sequences at that site. The profiling was carried out by LGC, an independent UK chemical analysis laboratory. DNA was extracted under LGC protocols using the Qiagen extraction kit method. STR profiling was carried out with the SGMplus STR multiplex system, which consists of the loci HUMAMGX/Y, D16S539, D18S51, D19S433, D21S11, D3S1358, D8S1179, HUMFIBRA (FGA), HUMTH01 and HUMVWFA31/A.

2.2.2.10**Analysis of Results**

All experiments were performed at least in triplicate, with intra-experimental replicates performed for each experiment. For the experiments using immortalised endothelial cell lines, each repeat was performed on cells of different passage number. Primary HUVEC cells were used between passage 1 and 3 only. Where appropriate statistical analyses of the data were performed using one-way analysis of variance (ANOVA) or paired t-test. This was followed by an appropriate post-test. Differences were considered significant when $p < 0.05$. For these statistical tests the n number used was the sample number, not the number of replicates.

2.3

RESULTS

2.3.1

DETERMINATION OF THE GROWTH RATE OF HMEC-1 AND ECV304 CELLS

ECV304 and HMEC-1 cells were seeded at 5×10^4 cells ml^{-1} (section 2.2.2.5) and counted at 24-hr intervals up to 96 hours post seeding. Cells were taken from different passage numbers, to account for potential changes in cell cycle times.

At 24 hrs post seeding the cell number in the flasks had not changed from the initial number seeded (figure 2.2), indicating a possible lack of attachment of cells and/or more likely, a low rate of proliferation (i.e. an initial lag recovery phase post seeding) in this first 24 hours. After 48 hrs the cell number increased, but not significantly, when compared to 24hrs post seeding. However for every 24 hours following, a significant difference in cell number was observed in both HMEC-1 and ECV304 cell lines compared to 24hr post seeding. The number of population doublings per 24 hrs was determined (equation 2.1) as 1.0 ± 0.07 for HMEC-1 and 1.1 ± 0.03 for ECV304. No significant difference was observed between the doubling times of the two cell lines.

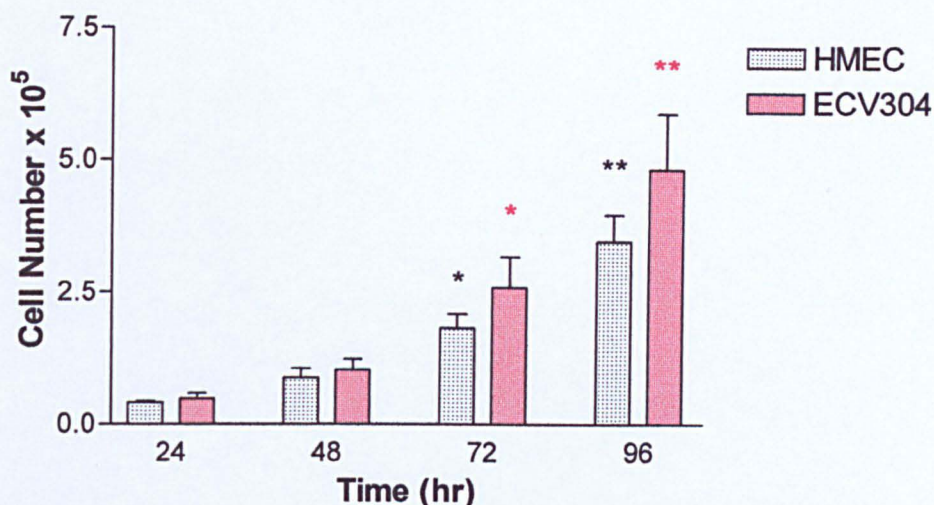


Figure 2.2: Growth curves of the ECV304 and HMEC-1 cell-lines over 96 hours in culture. Number of cells increased significantly over time (*/* = $p < 0.05$, **/** = $p < 0.01$ with respect to 24hr cultures, for HMEC-1 and ECV304 cultures respectively). Mean \pm SEM from triplicate 25cm² flasks for each time point, (n=3).

2.3.2

DETERMINATION OF THE OPTIMUM SEEDING DENSITY TO MEASURE 70-kDa DEXTRAN FLUX - THE ECV304 CELL-LINE

To assess the effects of seeding density on the flux of FD70 cells were seeded at 1×10^4 , 5×10^4 , 1×10^5 , 5×10^5 , 1×10^6 and 5×10^6 cells ml⁻¹ into 0.2 μ m Anopore inserts in 500 μ l of medium. The inserts were placed into 24-well culture plates with a further 500 μ l of medium added into the wells. Cultures were maintained at 37°C, 5% (v/v) CO₂ in air. After 72 hours in culture the leakage of FD70 was determined (section 2.2.2.6).

The basal permeability expressed here as FU, decreased proportionally with increasing seeding density (figure 2.3). Upon visual inspection, seeding at both 1×10^4 and 5×10^4 cells ml⁻¹ did not result in a confluent cell layer by 72hr. Seeding at 1×10^4 cells ml⁻¹ did not significantly alter the flux of the FD70

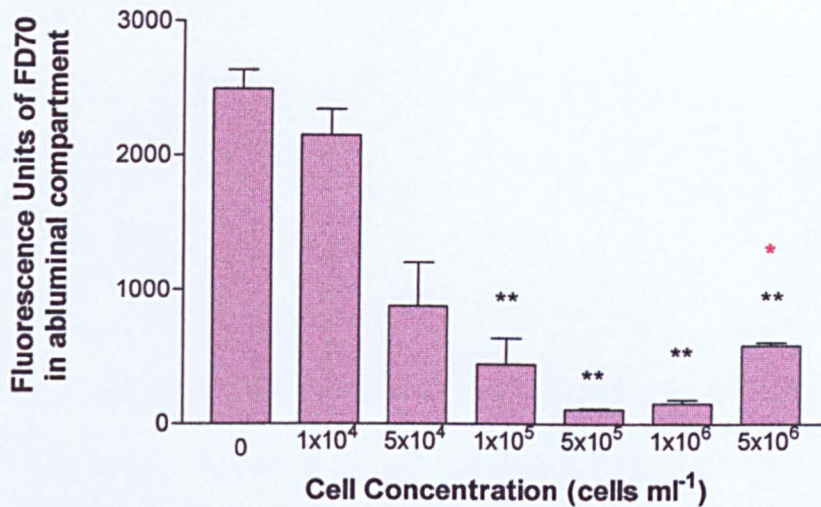


Figure 2.3: Effect of seeding density on FD70 flux across an ECV304 monolayer. A confluent monolayer was not formed in cultures seeded at 1 and 5 x 10⁴ cells ml⁻¹. Monolayers formed from seeding densities over 5 x 10⁴ cells ml⁻¹ significantly decreased the flux of FD70 (**, p<0.01 compared to insert alone). Seeding at 5 x 10⁵ cells ml⁻¹ gave the lowest flux of FD70; however 1 x 10⁵ and 1 x 10⁶ cells ml⁻¹ were not significantly different from that. At 5 x 10⁶ cells ml⁻¹ the flux significantly raised (* = p<0.05 compared to 5 x 10⁵ cells ml⁻¹). Mean ± SEM from triplicate inserts for each seeding density, (n=3).

compared to the insert alone. However the presence of the subconfluent cells on the insert seeded at 5 x 10⁴ cells ml⁻¹ caused a significant reduction in the flux by 65% respectively (**, p<0.01 compared to no cell control). The lowest flux (117 ± 5 FU) was observed at the seeding density 5 x 10⁵ cells ml⁻¹ (figure 2.3). This, when expressed as percentage leakage of FD70 (equation 2.2), was 4.7 ± 0.17 % of the total possible in the absence of cells. This flux was significantly different from that which occurred across monolayers seeded at 5 x 10⁶ cells ml⁻¹ (P<0.05), but not to those seeded at either 1 x 10⁵ or 1 x 10⁶ cells ml⁻¹.

2.3.3

PERMEABILITY OF THE ECV304 CELL-LINE TO KNOWN VASO-ACTIVE AGENTS WHICH ACT VIA A VARIETY OF MECHANISMS

Studies using whole blood vessels, both *in vivo* and *ex-vivo* have demonstrated that the endothelium comprises a major permeability barrier of the vessel wall. The integrity of this endothelial wall has an essential role in regulating vascular permeability. However, these approaches describe modulation of vascular permeability in which other cell types of the vessel wall, apart from the endothelial cells, may contribute to the barrier or mediate permeability changes. *In-vitro* systems have allowed the direct study of endothelium permeability responses alone to a variety of vaso-active agonists and other compounds (Cohen *et al.*, 1999; Hordijk *et al.*, 1999; Mehta *et al.*, 2001; Park *et al.*, 1999).

The permeability response of the ECV304 cell-line was investigated to examine its usefulness in permeability regulation studies. The vaso-active agents used here were chosen to represent a variety of signaling pathways known to be involved in the regulation of endothelial permeability.

For the following experiments, ECV304 cells were seeded and grown to confluence over 72 hrs. as in section 2.2.2.6. The compound of interest was then exposed to the cells for the required time and the leakage of FD70 was determined (section 2.2.2.6)

2.3.3.1

EFFECT OF IL-1 α ON THE PERMEABILITY OF ECV304 CELLS TO FD70

Interleukin-1 α (IL-1 α) is a potent regulator of inflammatory and immune responses, activating, via its receptor, specific protein kinases that modulate a number of transcription factors including NF κ B, AP1 and CREB (Stylianou and Saklatvala, 1998). These factors regulate a plethora of immediate early genes central to the inflammatory response. The effects of IL-1 α on the vascular endothelium have been extensively analysed including alteration of functional properties such as; vascular permeability, arachidonate metabolism, thrombogenic properties, leukocyte recruitment and cytokine production (Mantovani and Dejana, 1989).

IL-1 α was diluted in Keratinocyte Serum-free Medium (KSFM) to 2, 1, 0.5 and 0.1ng ml⁻¹. The initial decision to use KSFM as the diluent was based on possible future work where the effects of mediators released from keratinocytes were to be examined. Following 72 hr. in culture the media was aspirated from the luminal compartment and control cells and inserts with no cells were treated with 500 μ l of either KSFM alone, or with KSFM containing IL-1 α . After 4hrs at 37⁰C, 5% (v/v) CO₂ in air, the leakage of FD70 was determined. IL-1 α caused a dose dependent increase in the flux of FD70 across the ECV304 monolayer (figure 2.4). A significant decrease in the barrier function of the monolayer was seen at and above 0.5ng ml⁻¹.

2.3.3.2

EFFECT OF A23187, THE CALCIUM IONOPHORE, ON THE PERMEABILITY OF ECV304 CELLS TO FD70

Ionophores are small hydrophobic molecules that dissolve in the lipid bilayer of cell membranes, increasing their ion permeability. A23187 is a mobile ion carrier, shielding the charge of the transported ion so that it can traverse the cell membrane (Alberts *et al.*, 1989). It is commonly used to increase intracellular calcium levels in intact cells. Many well-known vaso-active mediators regulate endothelial permeability by increasing intracellular calcium levels, e.g. histamine, bradykinin and thrombin (Curry, 1992). There is also some evidence that the ionophore may work by promoting the release of nitric oxide (NO) from the endothelial cells (Boulanger *et al.*, 1990). A23187 has been shown to act both *in-vivo* (Neal and Michel, 1995) and *in-vitro* (Haselton *et al.*, 1992) to increase vascular and endothelial permeability respectively.

A23187 was diluted in KSFM to 1, 10, 100 and 1000 $\mu\text{g ml}^{-1}$. Following 72 hr. in culture the medium was aspirated from the luminal compartment of the control cells and inserts with no cells and 500 μl of either KSFM alone, or A23187 was added. A solvent control was also used as A23187 was initially dissolved in DMSO at 10 mg ml^{-1} . Therefore, extra inserts were used that received dilutions of DMSO in KSFM (1:10, 1:100 and 1:1000) to assess the solvent's direct affect on endothelial permeability. After 15 minutes at 37°C, 5% (v/v) CO₂ in air, the leakage of FD70 was determined. Any effect of the solvent was subtracted from the A23187 result. A23187 caused a dose dependent increase

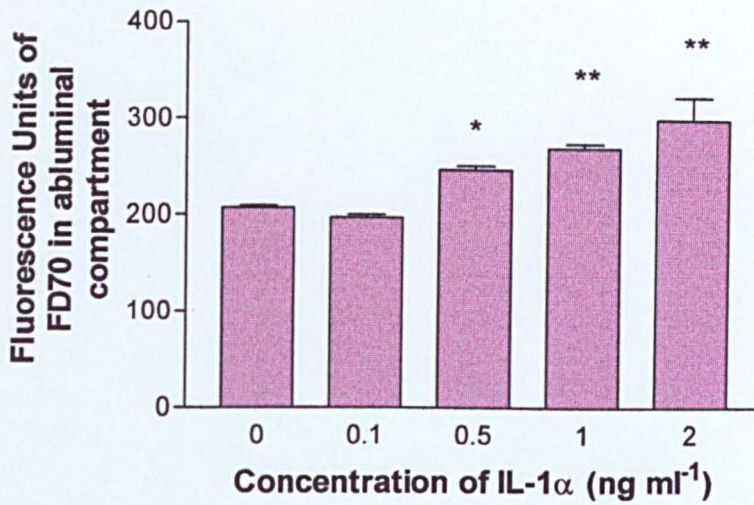


Figure 2.4: Effect of IL-1 α on the monolayer permeability of ECV304 cells (FD70). IL-1 α significantly increased FD70 leakage at 0.5ng ml⁻¹ and above (* = $p < 0.05$, ** = $p < 0.01$ with respect to control cultures). Mean \pm SEM from triplicate inserts for each concentration, (n=3).

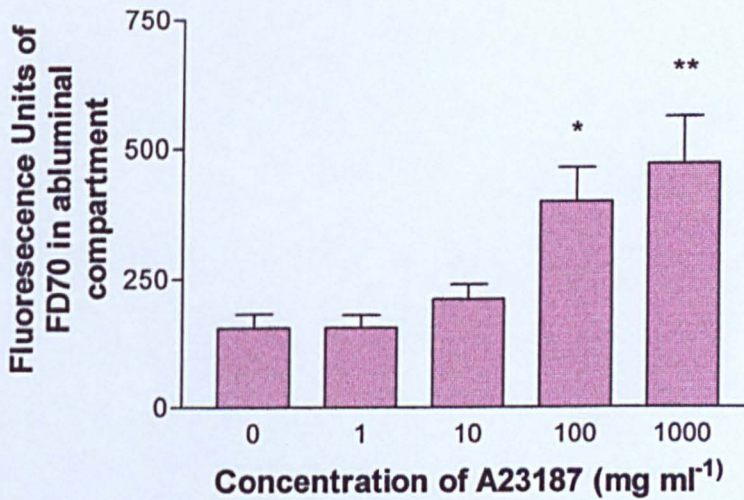


Figure 2.5: Effect of A23187 on monolayer permeability of ECV304 cells (FD70). A23187 significantly increased FD70 leakage at 100 and 1000mg ml⁻¹ (* = $p < 0.05$, ** = $p < 0.01$). Mean \pm SEM from triplicate inserts for each concentration, (n=3).

in the flux of FD70 across the ECV304 monolayer (figure 2.5). A significant increase in ECV304 monolayer permeability was seen at 100 and 1000mg ml⁻¹. An effect due to the DMSO was only observed at 1:10, and was subtracted from the data at 1000mg ml⁻¹.

2.3.3.3

EFFECT OF TNF- α ON THE PERMEABILITY OF ECV304 CELLS TO FD70

Tumour Necrosis Factor alpha (TNF- α) is mainly produced by activated macrophages and monocytes and exerts several effects on the growth and behaviour of endothelial cells. It induces expression of several adhesion molecules that promote leukocyte binding, enhances procoagulant activity and increases vascular permeability (Simionescu and Simionescu, 1988). In a similar fashion to IL-1 α , following receptor binding, TNF- α stimulates transcription and the subsequent expression of gene products that are involved in the inflammatory process. At the signaling level it induces several responses including; the activation of phosphatidylcholine-specific phospholipase C, phospholipase A₂ and sphingomyelinases which in turn stimulates the second messengers, diacylglycerol (DAG) and ceramide (Wójciak-Stothard *et al.*, 1998). Along with the action of TNF α on the endothelial cells themselves, there is evidence that it may alter permeability through alteration of the extracellular matrix (ECM) by inducing the endothelial cells to release metoalloproteinases (Partridge *et al.*, 1992).

TNF- α was diluted in KSFM between 5 and 1000U ml⁻¹. Following 72 hr. in culture the media was aspirated from the luminal compartment of control cells

and inserts with no cells, 500µl of either KSFM alone, or TNF-α was added. After 24hrs at 37°C, 5% (v/v) CO₂ in air, the leakage of FD70 was determined. TNF-α caused a dose dependent increase in the flux of FD70 across the ECV304 monolayer (figure 2.6). A significant increase in ECV304 monolayer permeability was seen at and above 10U ml⁻¹.

2.3.3.4

EFFECT OF PHORBOL MYRISATE-13-ACETYLESTER (PMA) ON THE PERMEABILITY OF ECV304 CELLS TO FD70

Tumour-promoting phorbol-esters such as PMA are often used to stimulate the DAG branch of the phosphoinositide-signaling pathway and activate protein kinase C (PKC). PKC is a calcium- and phospholipid-dependent protein kinase that plays a major role in transduction of many extracellular signals into a cellular response (Yu and Gotlieb, 1992). Studies have demonstrated that certain inflammatory mediators, such as bradykinin and hydrogen peroxide (H₂O₂), which increase endothelial permeability, also activate PKC (Nagpala *et al.*, 1996). PMA, like TNFα, can also induce remodelling of the ECM through the release of serine proteases and metalloproteinases. (Partridge *et al.*, 1992). PMA was diluted in ECV304 medium to give dilutions ranging from 1ng ml⁻¹ to 100µg ml⁻¹. Following 72 hr. in culture the media was aspirated from the luminal compartment of control cells and inserts with no cells and 500µl of either KSFM alone, or PMA was added. After a further 72hrs at 37°C, 5% (v/v) CO₂ in air, the leakage of FD70 was determined.

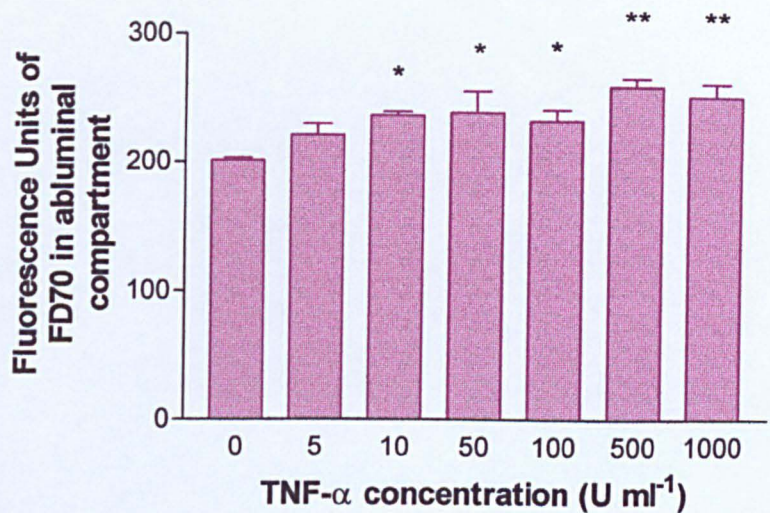


Figure 2.6: Effect of TNF-α on the monolayer permeability of ECV304 cells (FD70). TNF-α significantly increased FD70 leakage at and above 10U ml⁻¹ (* = p<0.05, ** = p<0.01). Mean ± SEM from triplicate inserts for each concentration, (n=3).

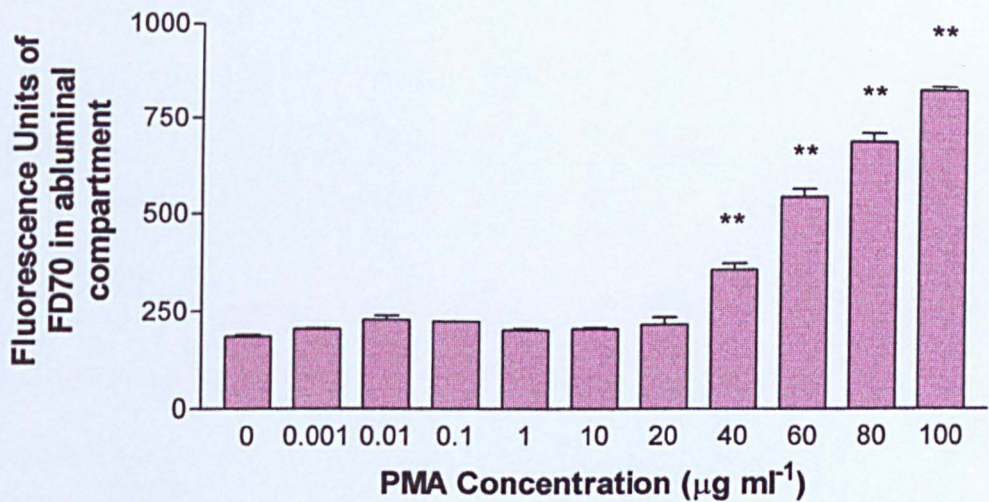


Figure 2.7: Effect of PMA on the monolayer permeability of ECV304 cells (FD70). PMA significantly increased FD70 leakage at and above 40μg ml⁻¹ (** = p<0.01 compared to control cultures). Mean ± SEM from triplicate inserts for each concentration, (n=3).

PMA caused a significant increase in monolayer permeability of the ECV304 cells at $40\mu\text{g ml}^{-1}$ and above. As with A23187, PMA was initially dissolved in DMSO. Hence, solvent controls were added and taken into account, as above.

2.3.4

ABILITY OF ENDOTHELIAL CELLS TO FORM STABLE BARRIERS TO FD70 WHEN GROWN ON CM INSERTS COATED WITH EXTRACELLULAR MATRIX PROTEINS

Since the permeability of the ECV304 cell-line could be modulated by a variety of vasoactive compounds, it was also possible that the nature of the surface upon which the cells were grown could affect permeability. Indeed components of the ECM are known to greatly affect endothelial cell morphology and function (Grant *et al.*, 1995; Lawley and Kubota, 1989; Madri *et al.*, 1983). Also evaluation of cells grown on different insert membranes, in this laboratory, indicated that there was a differential response to surfactant challenge (Ward *et al.*, 1996b; Ward *et al.*, 1997). The Anopore membranes initially chosen to grow the cells on were made of aluminium oxide and as such were too hard to be cut for transmission electron microscopy (TEM). Visualisation of the monolayer using TEM was deemed necessary so that the morphology of the interendothelial junctions could be studied. Inserts that could be cut with a diamond knife for TEM analysis were required. As such the CM inserts, which were made of cellulose, were examined. These required coating with basement membrane proteins to allow cell attachment and growth and could be processed for TEM investigation. ECV304 and HMEC-1 cell-line were grown on these inserts and checked for their ability to form stable,

confluent barrier monolayers on CM inserts. Inserts coated with either collagen type I, fibronectin or laminin, (section 2.2.2.2) were compared. The basal permeability to FD70 was measured and the fragility of the monolayer during the assay, via phase contrast microscopy, was recorded.

2.3.4.1

ABILITY OF ECM-COATED CM INSERTS TO SUPPORT GROWTH OF A STABLE MONOLAYER OF ECV304 CELLS.

ECV304 cells were seeded at 5×10^5 cells ml^{-1} (500 μl) into duplicate inserts for each ECM protein to be tested, and uncoated Anopore inserts as a control. This seeding density was used as it was ideal for the Anopore inserts and the CM inserts were of a similar surface area. The respective 'No Cell' controls received 500 μl of medium only. After 72hrs growth at 37°C, 5% (v/v) CO₂ in air, the leakage of FD70 was determined and the morphology of the cells was observed. Coating of the CM inserts with collagen enabled the ECV304 cells to grow to confluence (figure 2.8b), and form a barrier to the flux of FD70 (figure 2.9), equivalent to 8 ± 0.7 percent leakage; (figure 2.10). The laminin-coating (figure 2.8d) however, gave high variability in the resistance of the monolayer to disruption during the mechanics of the permeability assay (figure 2.9). Fibronectin allowed the cells to grow, but they did not form a confluent layer after 72hrs in culture (figure 2.8c) and these cells lifted off the insert during the permeability assay, providing no barrier to the FD70 flux (figure 2.9). Although the quality of this image is poor, the gap in the monolayer can clearly be seen (figure 2.8c, arrow). The ECV304s grew to confluence on the Anopore inserts (figure 2.8a) and behaved in the expected manner giving a flux

of 143 ± 12 FU or $7 \pm 0.6\%$ (figures 2.9 and 2.10). Note that the actual coating of the insert affected the flux of FD70 (figure 2.9), however displaying the data as percentage leakage corrects for this (figure 2.10).

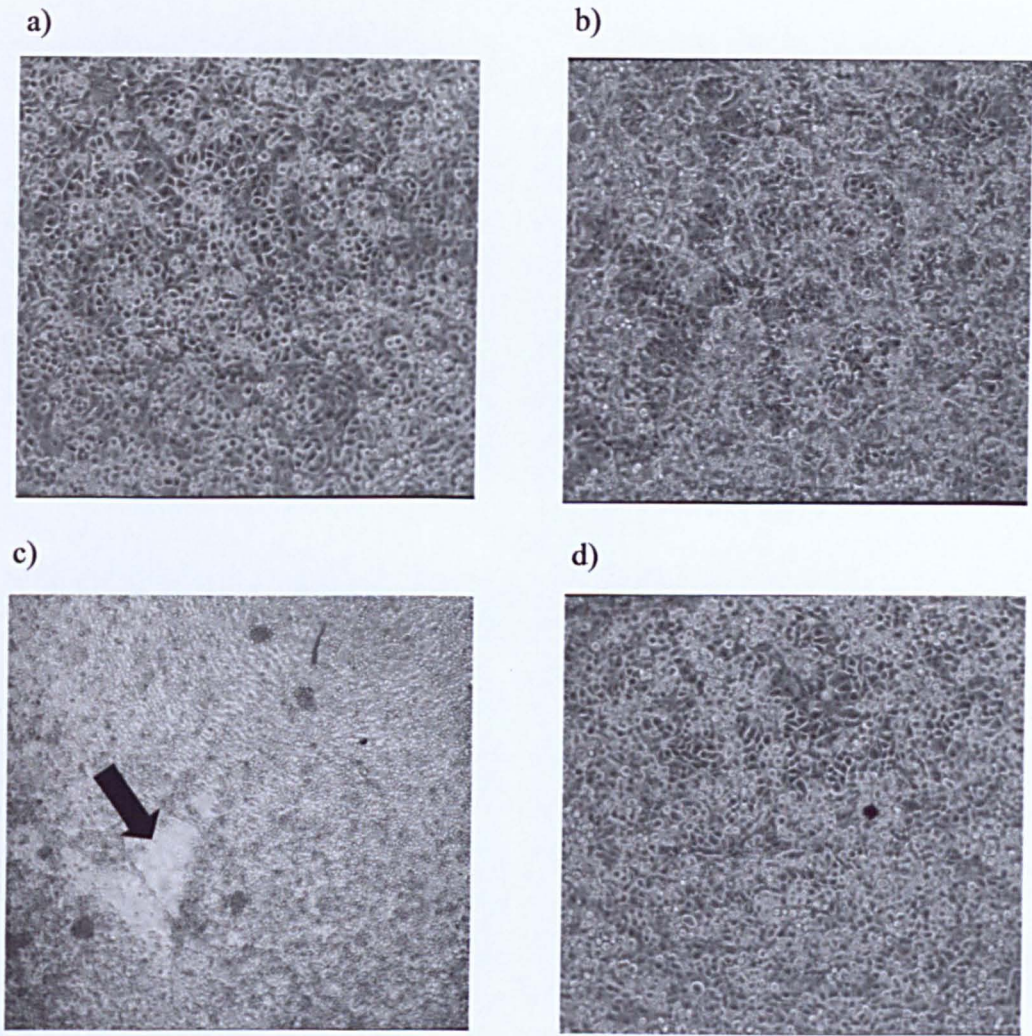


Figure 2.8: ECV304 cells grown to confluent monolayers on a) Anopore inserts, or CM inserts coated with b) collagen type I, c) fibronectin and d) laminin. A stable monolayer was formed on both Anopore (a) and collagen-coated CM inserts (b). However, fibronectin-coated CM inserts did not support the growth of the ECV304 cells to confluence (c, arrow shows gap in monolayer) and whilst laminin-coated CM inserts allowed for the growth of a confluent monolayer (d), this was easily disrupted with washing of the monolayer. Magnification x 43.

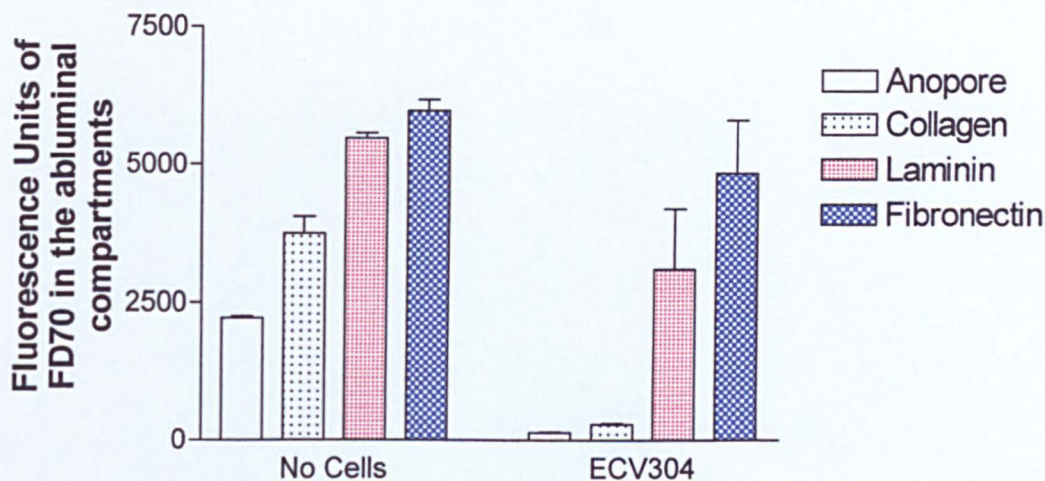


Figure 2.9: Effects of ECM coating of CM inserts on the monolayer permeability of ECV304 cells to FD70. Growth of cells on Anopore or collagen-coated CM insert gave the lowest FD70 flux. Mean \pm SEM from duplicate inserts for each coating protein and the Anopore insert, (n=3).

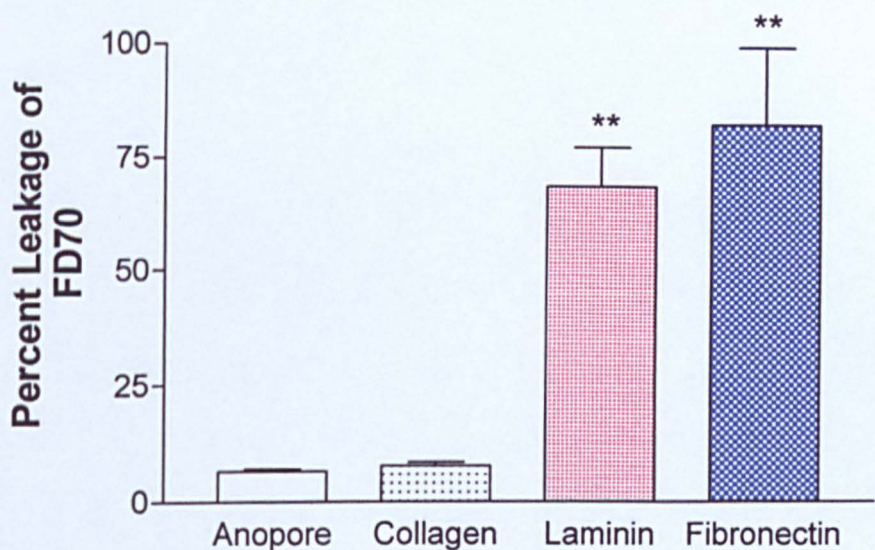


Figure 2.10: Effects of coating of CM inserts on the percentage leakage of FD70 in ECV304 cells. The percentage leakage through the monolayers grown on laminin- and fibronectin-coated CM inserts was significantly increased (** = $p < 0.01$ compared to monolayers grown on the Anopore inserts). Mean \pm SEM from duplicate inserts for each coating protein and the Anopore inserts, (n=3).

2.3.4.2

DETERMINATION OF THE OPTIMUM SEEDING DENSITY AND ABILITY OF COLLAGEN COATED CM-INSERTS TO SUPPORT GROWTH OF THE HMEC-1 CELL-LINE

The ideal seeding density for the ECV304 cells was determined to be 5×10^5 cells ml^{-1} . At this concentration they formed a stable monolayer with a low permeability barrier to FD70 when grown on both Anopore and collagen-coated CM inserts. These same experiments were carried out using the HMEC-1 cell-line.

As the CM insert was deduced as being the most versatile from studies with the ECV304 cells, HMEC-1 cells were seeded at 5×10^5 cells ml^{-1} (500 μl) into inserts as in section 2.3.4.1. After 72hrs growth at 37°C, 5% (v/v) CO₂ in air, the leakage of FD70 was determined and the morphology of the cells was observed.

Coating of the CM inserts with collagen or laminin enabled the HMEC-1 cells to grow to confluence (figures 2.11a and b), and form a barrier to the flux of FD70 (11 ± 1.7 and 7 ± 0.2 percent leakage respectively (figure 2.13). Fibronectin, however, allowed the cells to grow, but they did not form a confluent layer after 72hrs in culture (figure 2.11c) and these cells lifted off the insert during the permeability assay, providing no barrier to the FD70 flux (figure 2.12). In a similar manner HMEC-1 cells did not form a barrier on the Anopore inserts (figure 2.12) but in this case, a confluent monolayer was formed (figure 2.11d) but detached during the permeability assay. As there was no significant difference between the fluxes across the collagen- or laminin-coated inserts, it was decided to use collagen to allow direct comparisons with the ECV304 cell-line.

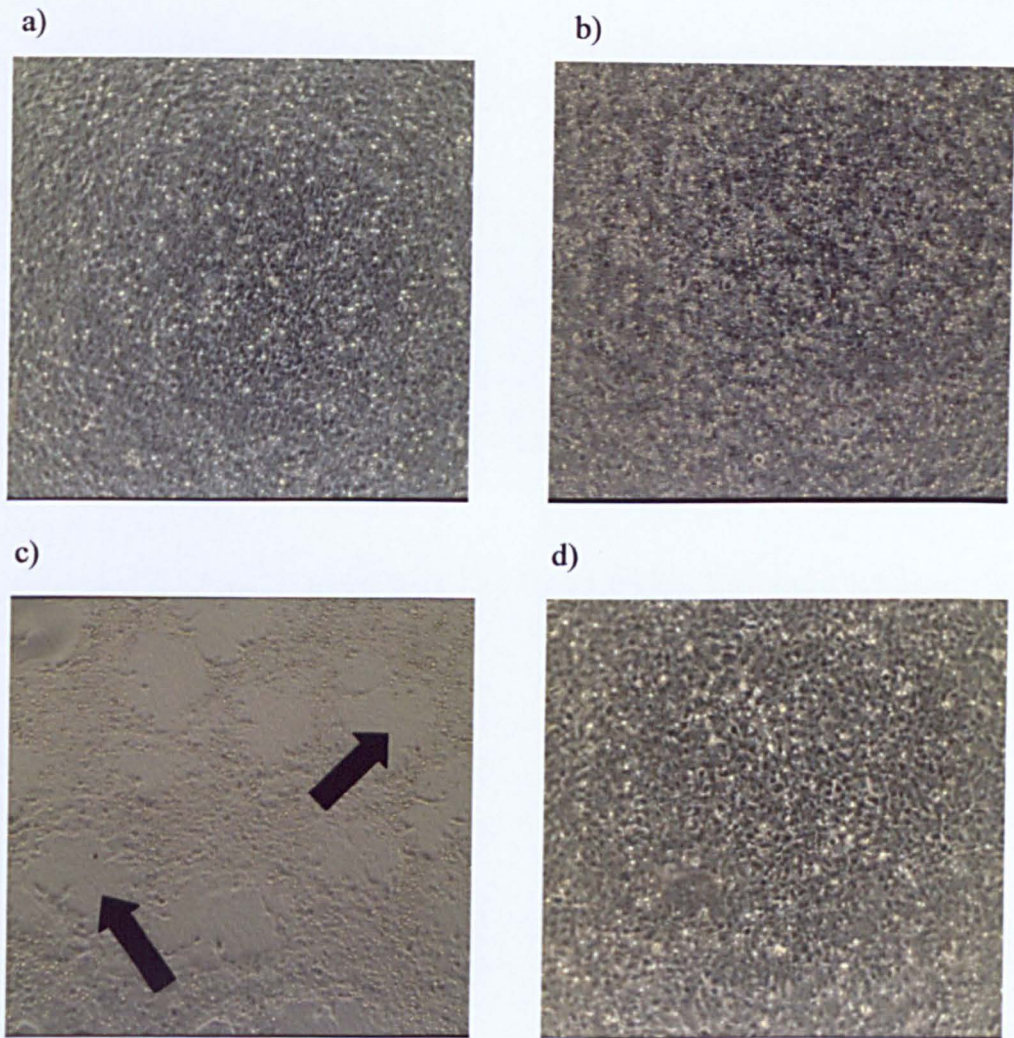


Figure 2.11: HMEC-1 cells grown to confluent monolayers on CM inserts coated with a) collagen type I, b) laminin, c) fibronectin and Anopore inserts. A stable monolayer was formed on both collagen- (a) and laminin-coated CM inserts (b). However, fibronectin-coated CM inserts did not support the growth of the HMEC-1 cells to confluence (c, arrows shows gaps in monolayer) and whilst Anopore inserts allowed for the growth of a confluent monolayer (d), this was easily disrupted with washing of the monolayer. Magnification x 43.

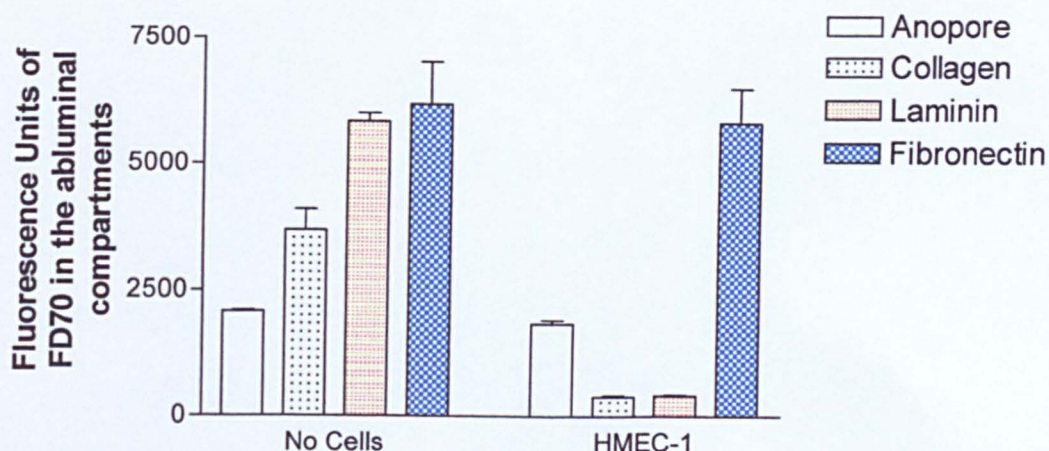


Figure 2.12: Effect of ECM coating on CM inserts on the monolayer permeability of HMEC-1 cells to FD70. Growth of cells on collagen- or laminin-coated CM insert gave the lowest FD70 flux. Mean \pm SEM from duplicate inserts for each coating protein and the Anopore insert, (n=3).

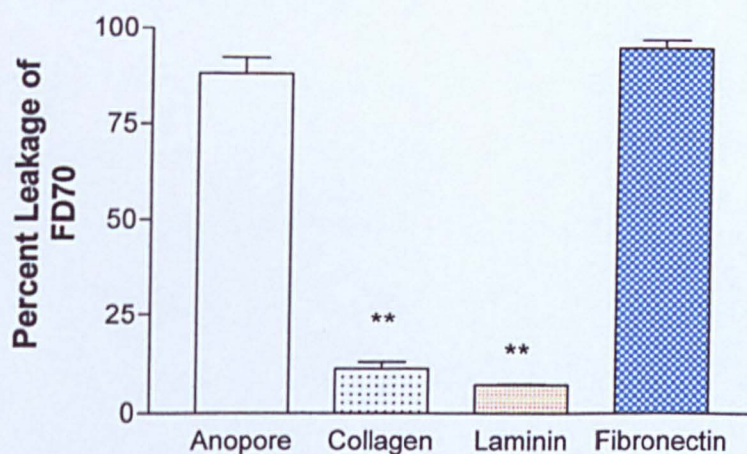


Figure 2.13: Effect of coating of CM inserts on the percentage leakage of FD70 in HMEC-1 cells. The percentage leakage through the monolayers grown on laminin- and collagen-coated CM inserts was significantly decreased (** = $p < 0.01$ compared to monolayers grown on the Anopore inserts. Mean \pm SEM from duplicate inserts for each coating protein and the Anopore inserts, (n=3).

To ensure that the seeding density used above was optimum for the HMEC-1 cells they were seeded at 1×10^4 , 5×10^4 , 1×10^5 , 5×10^5 and 1×10^6 cells ml^{-1} onto collagen-coated CM inserts in 500 μl of medium. The inserts were placed into 24-well culture plates with a further 500 μl of medium in the wells. Cultures were maintained at 37°C, 5% (v/v) CO_2 in air. After 72 hours in culture the leakage of FD70 was determined (section 2.2.2.6).

A confluent monolayer of HMEC-1 cells was only formed when seeded at 5×10^5 and 1×10^6 cells ml^{-1} . As such the permeability (FU) at these two seeding densities was significantly different ($P < 0.001$) to all of the lower seeding densities (figure 2.14). However in contrast to the ECV304 cultures on the Anopore insert, the presence of small populations of cells on the collagen-coated CM inserts did not significantly affect the flux of the FD70 compared to inserts with no cells. This could be a property of either the membrane being used (aluminium oxide versus cellulose) or the cell-line. There were no significant differences between the fluxes across monolayers seeded at either 5×10^5 cells ml^{-1} or 1×10^6 cells ml^{-1} , therefore, 5×10^5 cells ml^{-1} was chosen as the optimum seeding density, enabling fewer cells to be used per assay.

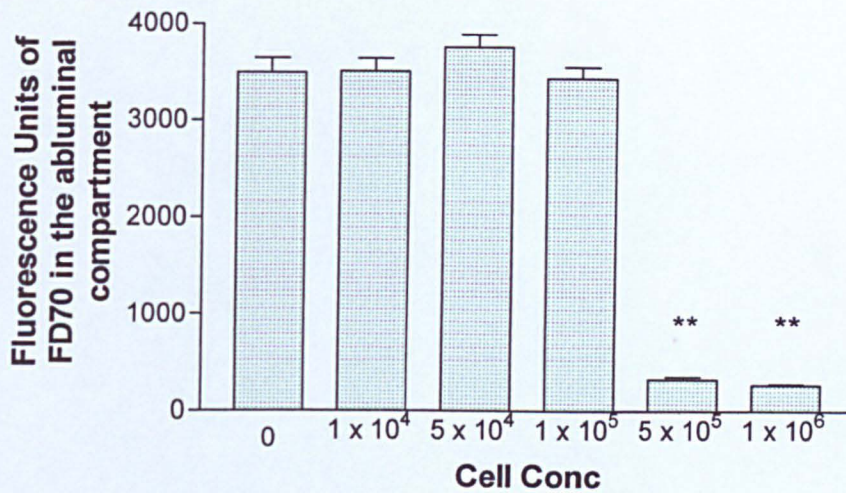


Figure 2.14: Effect of HMEC-1 seeding density on the flux of 70-kDa dextran across the monolayer. A confluent monolayer was not formed in cultures seeded at 1 , 5×10^4 or 1×10^5 cells ml^{-1} . Monolayers formed from seeding densities over 1×10^5 cells ml^{-1} significantly decreased the flux of FD70 (**, $p < 0.01$ compared to insert alone). Seeding at 5×10^5 cells ml^{-1} gave the lowest flux of FD70; 1×10^6 cells ml^{-1} was not significantly different from that. Mean \pm SEM from triplicate inserts for each seeding density, ($n=3$).

2.3.5

ANALYSIS OF THE INTERCELLULAR JUNCTIONS OF THE HMEC-1 AND ECV304 CELL-LINES BY IMMUNOFUORESCENCE

The regulation of permeability is thought to be reliant on the correct formation of interendothelial junctions. The molecular structure of these junctions is still under investigation. The adherens junction (as described in Chapter 1) is composed of VE-Cadherin, a calcium-dependent transmembrane glycoprotein linked to a plethora of intracellular molecules and the cells' cytoskeleton. Another important molecule found within the paracellular cleft, but located distinct from junctional regions, is PECAM-1. Changes in permeability are linked to an altered distribution of VE-cadherin and PECAM-1 (Heimark *et al.*, 1990; Lampugnani *et al.*, 1992; Leach *et al.*, 1995). The expression of these

pertinent molecules in the two cell-lines proposed for this research was investigated. Thus far the *in-vitro* research undertaken upon the molecular components of inter-endothelial junctions has mainly used HUVECs; therefore, they were used as a control culture in these experiments.

ECV304, HMEC-1 and HUVEC cultures were seeded and processed as described in section 2.2.2.8, to preserve the antigens; VE-Cadherin, PECAM-1 and vWF, a marker of endothelial heritage. Immuno-reactivity against these proteins revealed differences between all cell types. The HMEC-1 cell-line positively expressed VE-cadherin and PECAM-1 (figure 2.14b, and 2.15b) with distribution localised to cell-cell borders in a similar distribution to that observed in HUVEC cultures (figure 2.14a and 2.15a). However the band appeared wider and less dense with VE-cadherin and PECAM-1 expression was heterogeneous, with PECAM-1 staining at some cell-cell contacts stronger than others. The immuno-localisation of PECAM-1 in HUVEC cultures revealed a lack of staining at free cell edges (figure 2.15a, arrow). ECV304 cells, showed no immuno-reactivity towards either PECAM-1 or VE-cadherin (figure 2.14c and 2.15c). Expression of vWF, the general marker of endothelial phenotype, was punctate and localised in the cytoplasm of HUVECs (figure 2.16a). Positive fluorescence was seen in HMEC-1 cultures (figure 2.16b) but was not localised to cytoplasmic granules, whilst ECV304 cultures showed no reactivity (figure 2.16c).

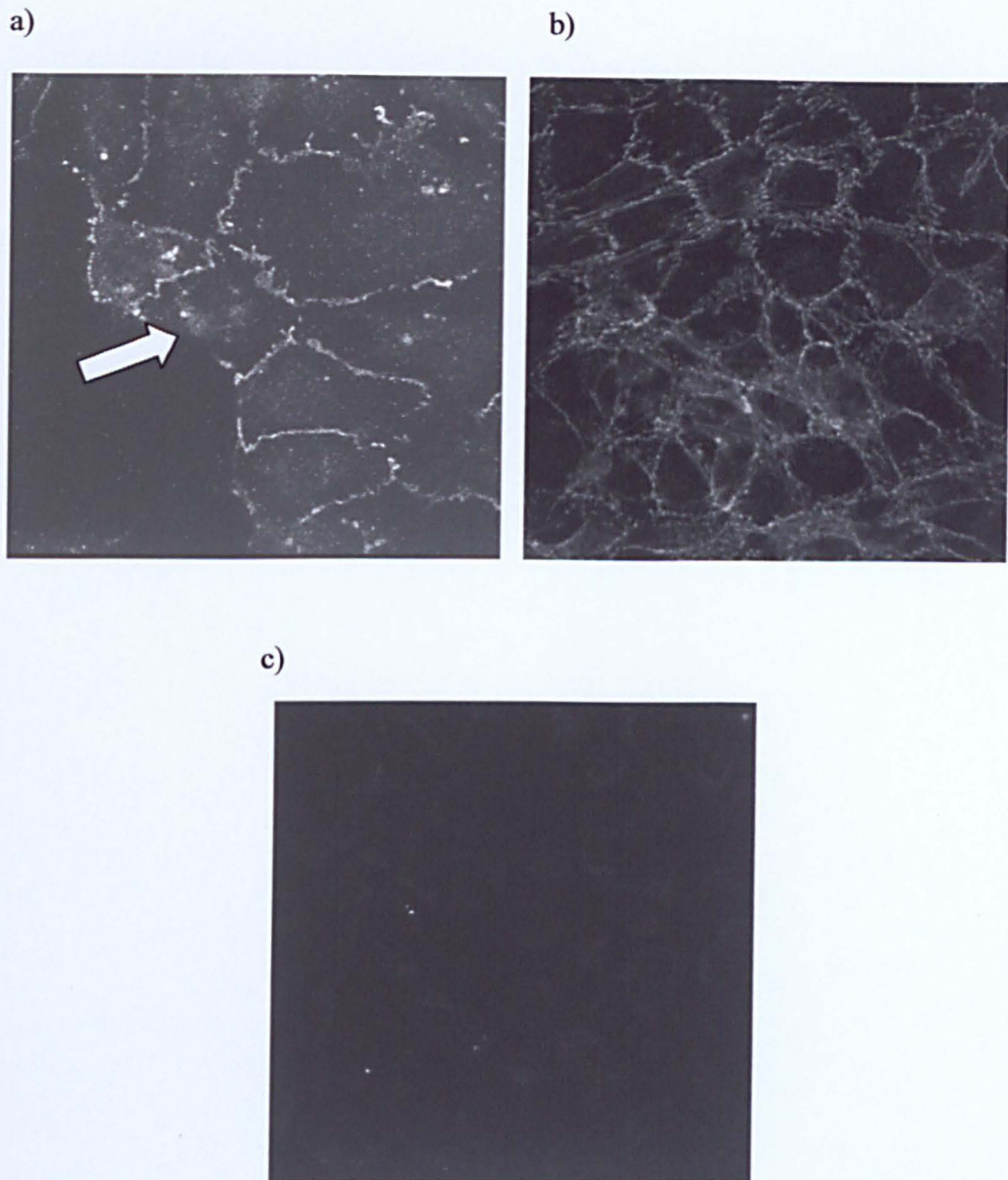


Figure 2.14: Immuno-reactivity against VE-cadherin in a) HUVEC, b) HMEC-1 and c) ECV304. Controls (figure 2.17) received PBS instead of primary antibody in i) HUVEC, ii) HMEC-1 and iii) ECV304. HUVEC positively expressed VE-cadherin at cell-cell contacts with a no immuno-reactivity at free cell edges (a, arrow). In HMEC-1 cultures the cadherin was also observed at cell-cell edges; however the band appeared wider, and less dense (b). No immuno-reactivity was observed in ECV304 cultures (c). Figure shows representative images. Magnification x 850.

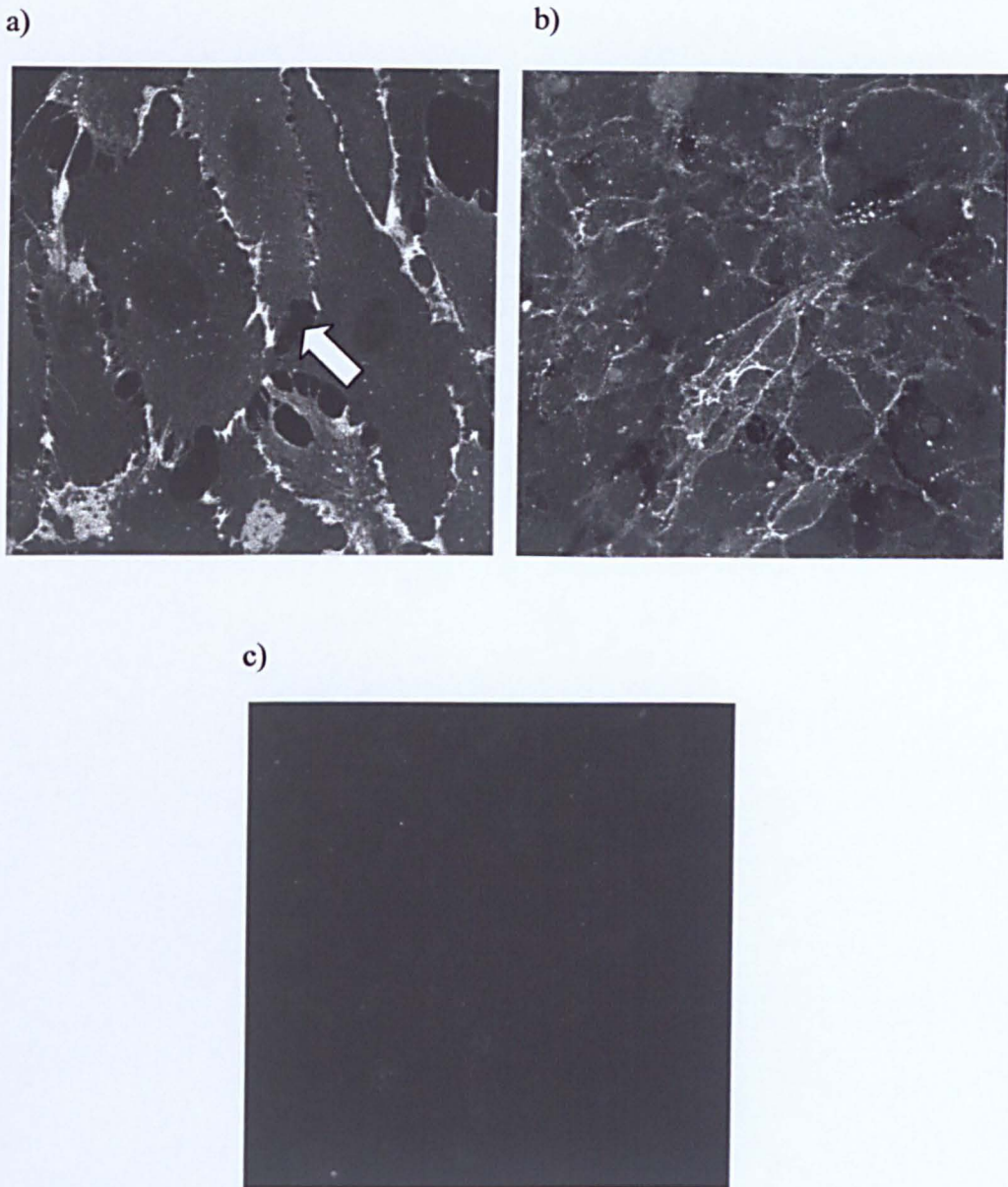


Figure 2.15: Immuno-reactivity against PECAM-1 in a) HUVEC, b) HMEC-1 and c) ECV304. Controls (figure 2.17) received PBS instead of primary antibody in i) HUVEC, ii) HMEC-1 and iii) ECV304. HUVEC positively expressed PECAM-1 at cell-cell contacts with a no immuno-reactivity at free cell edges (a, arrow). In HMEC-1 cultures PECAM-1 was also observed at cell-cell edges; however the expression was heterogeneous with some cell-cell contacts reacting more strongly than others (b). No immuno-reactivity was observed in ECV304 cultures (c). Figure shows representative images. Magnification x 850.

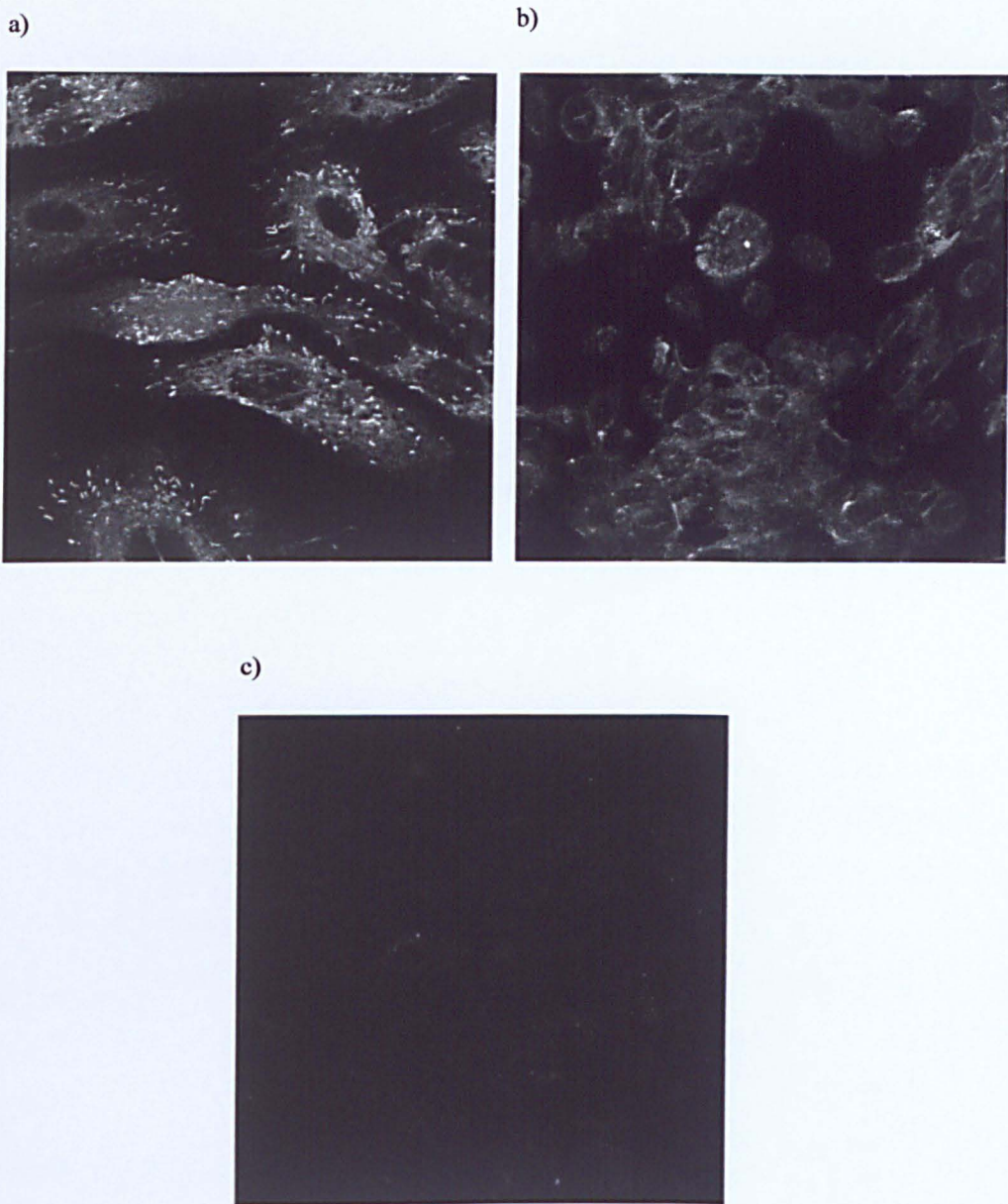


Figure 2.16: Immuno-reactivity against vWF in a) HUVEC, b) HMEC-1 and c) ECV304. Controls (figure 2.17) received PBS instead of primary antibody in i) HUVEC, ii) HMEC-1 and iii) ECV304. HUVEC positively expressed vWF in a punctate manner (a, arrow). In HMEC-1 cultures expression of vWF was detected, however the distinct punctate expression seen in HUVEC cultures was not mimicked (b). No immuno-reactivity was observed in ECV304 cultures (c). Figure shows representative images. Magnification x 850.

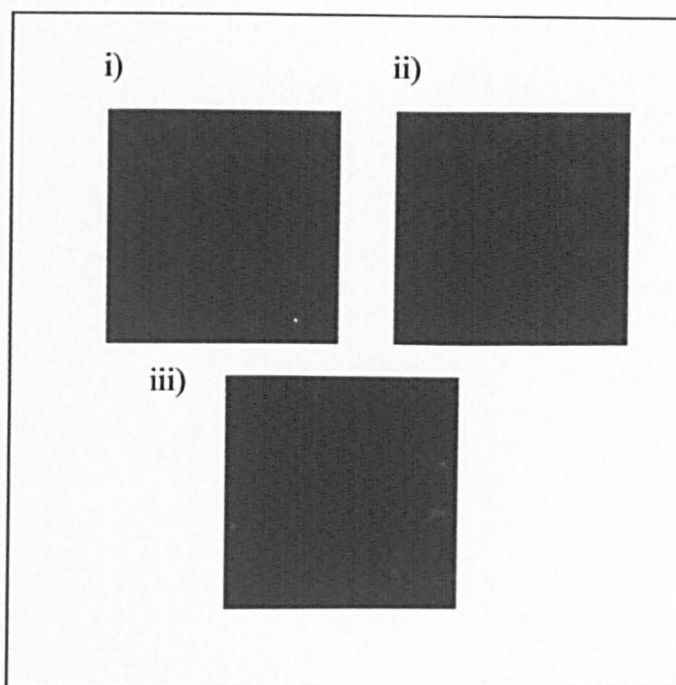


Figure 2.17: Controls cultures for immunofluorescence studies. Cells received PBS instead of primary antibody in i) HUVEC, ii) HMEC-1 and iii) ECV304. No fluorescence was observed in any culture. Figures show representative images. Magnification x 425.

2.3.6

STR PROFILING OF CULTURED CELL SAMPLES

A STR DNA profile was constructed as in section 2.2.2.9. The AMG loci showed that the HUVEC cells came from a female donor and that the HMEC-1 cells came from a male donor (figure 2.18). Another cell-lines routinely used in this laboratory, HaCat, a keratinocyte cell-line were also profiled and none matched the HMEC-1 cell-line indicating that there has been no cross contamination of cells.

Sample	AMG	D16	D18	D19	D2	D21	D3	D8	FGA	TH01	vWA
HaCat	X	9, 12	12	13, 14	17, 25	28, 30.2	16	14	24	9.3	16, 17
HUVEC	X	12, 13	14, 15	10, 15	17, 20	30, 30.2	15	10, 12	21, 24	9.3	16, 18
HMEC-1	X,Y	11, 12	17, 21	12, 17.2	19, 25	29, 30	16, 17	11, 14	21, 22	7	15, 17

Figure 2.18: STR Profiling of HUVEC and HMEC-1 (p27) cells. HUVEC and HaCat are isolated from a female and the HMEC-1 cell-line from a male (AMG loci). Whilst there are some loci where the number of repeat sequences tallied between the cell-lines, HMEC-1, HUVEC and HaCat were all shown to have a different profile of 11 loci studied.

2.4

DISCUSSION

Two endothelial cell-lines were evaluated for their suitability to be used to study macromolecular permeability; ECV304 and HMEC-1. When designing cell culture experiments it is important to be aware of the growth rate of the cultures used (Freshney, 1994). There was no significant difference between the growth rates of the ECV304 and HMEC-1 cell-lines. As the time taken for both cell-lines to reach confluence was similar, a direct comparison of the results in the subsequent experiments was feasible.

Burke-Gaffney and Keenan (1995) demonstrated that the seeding density of human endothelial cells onto porous membranes is an important determinant to consider when setting up an *in-vitro* model of endothelial permeability. In addition to the effects seeding density had on the basal permeability of their system, they also showed that certain cytokines, which increased permeability, did so in a reduced manner in monolayers derived from sub-optimum seeding densities. The ECV304 cells were evaluated initially. Seeding them onto the Anopore inserts at 5×10^5 cells ml^{-1} gave the tightest barrier to FD70 after 72hr. of growth and so was used in subsequent experiments. Interestingly the FD70 flux increased significantly from 5×10^5 cells ml^{-1} ($p < 0.05$) when the inserts were seeded at a high density of 5×10^6 cells ml^{-1} . This may result from the seeding density producing an over confluent monolayer. This is in agreement with work by Schaeffer *et al.* (1992) who reported that bovine pulmonary artery endothelial cells (BPAEC) seeded at supraconfluent densities exhibited higher basal permeability than those seeded at a confluent density, and Burke-Gaffney and Keenan (1995) who showed similar observations with

HUVEC. Weinbaum *et al.* (1985) suggested that in monolayers formed from high cell densities there is a high turnover rate. Enhanced cell turnover has been associated with endothelial cell regeneration and poorly formed intercellular junctions *in vivo* (Spagnoli *et al.*, 1982; Weinbaum *et al.*, 1985) and that may contribute to the observed permeability increase. Low basal permeability was achieved when cells were allowed to grow to confluency from a lower seeding density (Casnocha *et al.*, 1989). In these studies the cells were cultured for up to 15 days, before permeability was assessed. The 3 day culture period employed in this study enabled the assay to be completed within one week, keeping the number of plates in culture at any one time low, reducing the potential risk of contamination.

The effect of well-known modulators of permeability (IL-1 α , A23187, TNF α and PMA) was measured on the flux of FD70 across the ECV304 monolayer. All four modulators increased the permeability of the cultures. The size of response to the concentrations of IL-1 α used did not concur with the literature. Burke-Gaffney and Keenan (1995), following 20hr exposure to IL-1 α at 20U ml⁻¹ in HUVEC cultures, showed a 2.1 fold increase in the percentage clearance of BSA. The data in this study showed a 1.2 fold increase in percentage clearance at 0.5ng ml⁻¹. This is roughly equivalent to 80U ml⁻¹, indicating that IL-1 α does not elicit the same magnitude of response in the ECV304 cell-line as is reported for HUVEC cultures. This could be due to the difference in exposure time; 4hr exposure in this study compared with 20 hrs in the Burke-Gaffney and Keenan (1995) study. However, Marcus *et al.* (1996) observed an approximate 10-fold increase in permeability in HUVECs exposed to 10 pg ml⁻¹ (approximately 0.2 U ml⁻¹) IL-1 for 4hrs. This indicated that 4hrs

exposure should be sufficient for endothelial cells to respond. Introna *et al.* (1994) stated that the *in-vitro* passage of primary endothelial cells resulted in the refractiveness to activation by exogenous IL-1. Thus, the studies using HUVEC cultures may have used cells that were further along the route to senescence than the ECV304 cells were at the time of immortalisation. Another possible reason could be that the ECV304 cells exhibited a lower basal percentage clearance of $0.96 \pm 0.02\%$ than their HUVEC cultures (2.3 - 4.2 %) and this 'tighter' cell monolayer responded in a diminished fashion to the IL-1 α .

At 1000mg ml^{-1} A23187 (containing 10% DMSO) compromised the integrity of the monolayer. The increase in permeability seen at this concentration was not purely due to the action of the compound, but to a combination of damage to the cells by A23187, followed by perturbation of the layer through the mechanics of the assay (washing etc.). Data for this concentration was, therefore, not used in the determination of the R^2 value.

The effect of TNF- α concurs partially with reports from Langelier *et al.* (1991) who showed an increase in human umbilical artery endothelial cell monolayer permeability following 24hr. exposure to 500U ml^{-1} , but not at lower concentrations. Additionally Partridge *et al.* (1992) showed an increase in the permeability of bovine pulmonary microvascular endothelial monolayers exposed to 100U ml^{-1} TNF- α for 24hr.

The ECV304 cell monolayer response to PMA was consistent with the literature; Liu and Sundqvist (1995), showed an increase in endothelial permeability following $30\mu\text{g ml}^{-1}$ PMA for 6hrs and Nagpala *et al.* (1996),

observed permeability increases at lower concentrations of approximately $0.01\mu\text{g ml}^{-1}$.

The variety of mechanisms by which these four agents increased permeability indicated that the ECV304 cell-line had the capability of responding to stimulation via diverse signaling pathways. Based on these data studies, the ECV304 cell-line was progressed.

Although the Anopore membrane lent itself to the study of permeability in this system, they could not be used for TEM due to their aluminium oxide membranes which could not be cut. The most promising insert available at the time was the CM insert; however this required coating with components of the ECM in order to support cell growth. Collagen-coating of the CM inserts appeared to support the production of a stable monolayer of ECV304 cells and, therefore, it was deemed appropriate to use in further studies. The HMEC-1 cells formed a stable monolayer with a low permeability on both collagen- and laminin-coated CM inserts, so collagen was chosen as the ECM coating of choice for these studies. The optimum seeding density of the HMEC-1 cells on the collagen-coated CM inserts was $5 \times 10^5 \text{ cells ml}^{-1}$, the same as the ECV304 cell-line, again enabling a tight comparison of the two cell-lines.

An integral part of any study on vascular permeability should include the investigation of the pertinent molecules known to be involved in the regulation of endothelial permeability. There was a marked contrast in the expression of adhesion molecules between the HMEC-I and the HUVEC on the one hand and the ECV304 cells on the other. The ECV304 cell-line did not express PECAM-1 or VE-cadherin that are part of the cell machinery necessary to regulate endothelial permeability. The decision was made, therefore, to

discontinue the use of the ECV304 cell-line. This is significant in that it has now become apparent that the ECV304 cells are “contaminated” with the tumourigenic bladder epithelioid cell-line, T24. Hence, in the light of recent information from the ECACC it is clear that the ECV304 cells are not comparable to either the HMEC-1 or HUVEC cells; they have therefore acted as suitable negative controls for VE-cadherin, PECAM-1 and vWF in this research project. However, the observed response of the ECV304 cell-line to cytokines tested was to be expected, given that epithelial cells employ similar mechanisms to endothelial cells in the regulation of paracellular permeability, albeit with adhesion molecules from the same superfamily.

Tandemly repeated DNA sequences are widespread throughout the human genome and show sufficient variability among individuals in a population that they have become important in several fields including genetic mapping, linkage analysis, and human identity testing. The variety of alleles present in a population is such that a high degree of discrimination among individuals in the population may be obtained when multiple STR loci are examined. The authenticity of the HMEC-1 cells was confirmed, showing a different pattern of loci to HUVEC or HaCat, a well-used keratinocyte cell-line in this laboratory. These data implied that the HMEC-1 could be a useful tool for investigating the molecular regulation of endothelial permeability, and therefore was further evaluated.

CHAPTER 3

EVALUATION OF METHODS FOR

STUDYING ENDOTHELIAL

PERMEABILITY IN-VITRO.

CHAPTER 3

EVALUATION OF METHODS FOR STUDYING ENDOTHELIAL PERMEABILITY IN VITRO.

3.1

INTRODUCTION

The studies of vascular permeability *in-vivo*, apply modifications of the classical Miles and Miles (1952) permeability assay. The vascular leakage of an intra-venous injected marker, from the plasma into the skin of challenged areas is measured. Other *in-vivo/ex-vivo* systems use the mesenteric or hamster cheek pouch microcirculation (Grega and Adamski, 1991; Rumbaut *et al.*, 1999) or isolated perfused organs of interest (Leach *et al.*, 1995). With the development of techniques to isolate and culture endothelial cells *in-vitro*, more direct methods have been introduced to study vascular permeability. A commonly used system employs endothelial cells grown to confluence on a porous surface, an insert with particular pore sizes. The surface separates two compartments and allows measurement of macromolecules permeation (e.g., labelled albumin, dextran or enzymes, such as horseradish peroxidase) from one compartment to the other. The confluent monolayer of endothelial cells acts to restrict the flux of these macromolecules until stimulated with compounds that affect the barrier function of the monolayer.

3.1.1

FACTORS AFFECTING CAPILLARY PERMEABILITY

3.1.1.1

GENERAL FACTORS

The primary forces producing movement of water and solutes across the capillary wall are diffusion, solvent drag, filtration, osmosis, active transport, and the processes of exocytosis and endocytosis. It should be noted that next to biological membranes *in-vivo* there is a layer of relatively unstirred fluid. Solutes cross this unstirred layer by diffusion.

Diffusion

Diffusion is the process by which a substance in solution expands, because of the motion of its particles, to fill all of the available space. There is a net flux of particles from areas of high to areas of low concentration. The time required for equilibrium to occur is proportional to the square of the diffusion distance. The magnitude of this flux is directly related to the cross-sectional area available for the diffusion, the concentration gradient (Fick's law of diffusion).

Solvent Drag

When there is net solvent flow in one direction (bulk flow), the solvent tends to drag along some molecules of the solute. This force is called solvent drag. In most *in-vivo* situations its effects are very small.

Filtration

Filtration is the process by which fluid is forced through a barrier because of a difference in pressure on the two sides. The amount of fluid filtered per unit time is proportional to the difference in pressure, the surface area available and

the permeability of the barrier. Molecules that are smaller in diameter than the pores of the barrier pass through with the fluid, and larger molecules are retained.

Osmosis

The diffusion of solvent molecules across a barrier into a region in which there is a higher concentration of solute to which the barrier is impermeable is called osmosis. This can be prevented by the application of pressure to the more concentrated solution. The pressure necessary to prevent solvent migration is called the osmotic pressure of the solution. Osmotic pressure depends upon the number rather than the type of particles in the solution. In an 'ideal solution' it is related to temperature and volume. If temperature is constant then the osmotic pressure is proportionate to the number of particles in solution per unit volume of solution. If the solute is a non-ionising compound such as glucose, the osmotic pressure is a function of the number of glucose molecules present. If the solute ionises, each ion is an osmotically active particle. It should be noted that although a homogeneous solution contains osmotically active particles and can be said to have an osmotic pressure, it could only exert the said pressure when in contact with another solution across a barrier that is permeable to the solvent but NOT the solute.

3.1.1.2

HYDROSTATIC AND OSMOTIC PRESSURE ACROSS A CAPILLARY WALL

The structure of the capillary wall varies from one vascular bed to another (Stevens & Lowe, 1999). However, in many organs water and relatively small

solutes are the only substances that cross the wall with ease. Small molecules diffuse through the capillary walls and, therefore, should achieve equal concentrations on both sides and make no contribution to the effective osmotic pressure. Plasma proteins with M_r greater than 40,000 cannot cross the capillary wall and thus cause an effective capillary pressure. Plasma proteins amount to approximately 1 mmol l^{-1} of plasma and, as a simplification there are almost no proteins in the interstitial fluid. The difference between the plasma colloid concentration between the blood and the interstitial fluid causes an effective osmotic pressure of 16mmHg. These proteins are negatively charged and attract diffusible cations and repel diffusible anions. This leads to an uneven distribution of small ions with a small excess inside the capillary. This contributes a further 9mmHg giving a total osmotic pressure of 25mmHg. The Starling Equilibrium describes the control of circulating blood and changes in capillary blood pressure affecting the redistribution of fluid between the blood and the interstitial fluid (figure 3.1). The blood pressure (hydrostatic pressure) at the arteriolar end of a capillary is about 32 mmHg and at the venular end about 15 mmHg. The hydrostatic pressure of interstitial fluid is on average -2. The net hydrostatic pressure forces fluid out of the capillaries by ultra filtration. This ultra filtration is opposed by osmosis returning fluid into the capillaries, the osmotic force being the difference between the osmotic pressure of the plasma and interstitial fluid. At the arteriolar end the net balance of these pressures results in ultra filtration, with reabsorption at the venular end. In some capillary beds, blood perfusion is intermittent and ultra filtration, when blood pressure is high, is balanced by osmosis when blood pressure is low. This scenario differs according to the organ involved. For example in the

kidney blood pressure is high and ultra filtration is favoured, in the lung blood pressure is low and osmotic pressure is negative preventing liquid accumulating in the alveolae. At rest the difference in the hydrostatic pressure between the blood and the interstitial fluid is virtually balanced by the osmotic pressure (Bray *et al.*, 1989).

3.1.2

THE USE OF *IN-VITRO* TECHNIQUES TO STUDY ENDOTHELIAL PERMEABILITY

The advent of cell culture in the 1970's enabled endothelial cells to be isolated and grown *in-vitro*, leading to the development of *in-vitro* methods to study the role of the endothelium in the regulation of vascular permeability. One of the commonest methods for investigation is the growth of endothelial cells on porous filters to form a confluent layer, modelling the endothelial lining of the blood vessels. The cultured cells represent an effective model of an intact endothelium and can be analysed for changes in permeability.

There are some major limitations to the use of monolayer cultures for modelling vascular permeability. The most widely used solute, serum albumin, has given diffusional permeability values (P_d) in the range of $10^{-6} \text{ cm s}^{-1}$ (Albelda *et al.*, 1988). This is two orders of magnitude greater than estimates based on the flux of albumin through the walls of intact microvessels (Michel and Curry, 1999). The reflection coefficients of monolayers to macromolecules are too low for plasma proteins to exert a significant osmotic pressure across them (Turner, 1992).

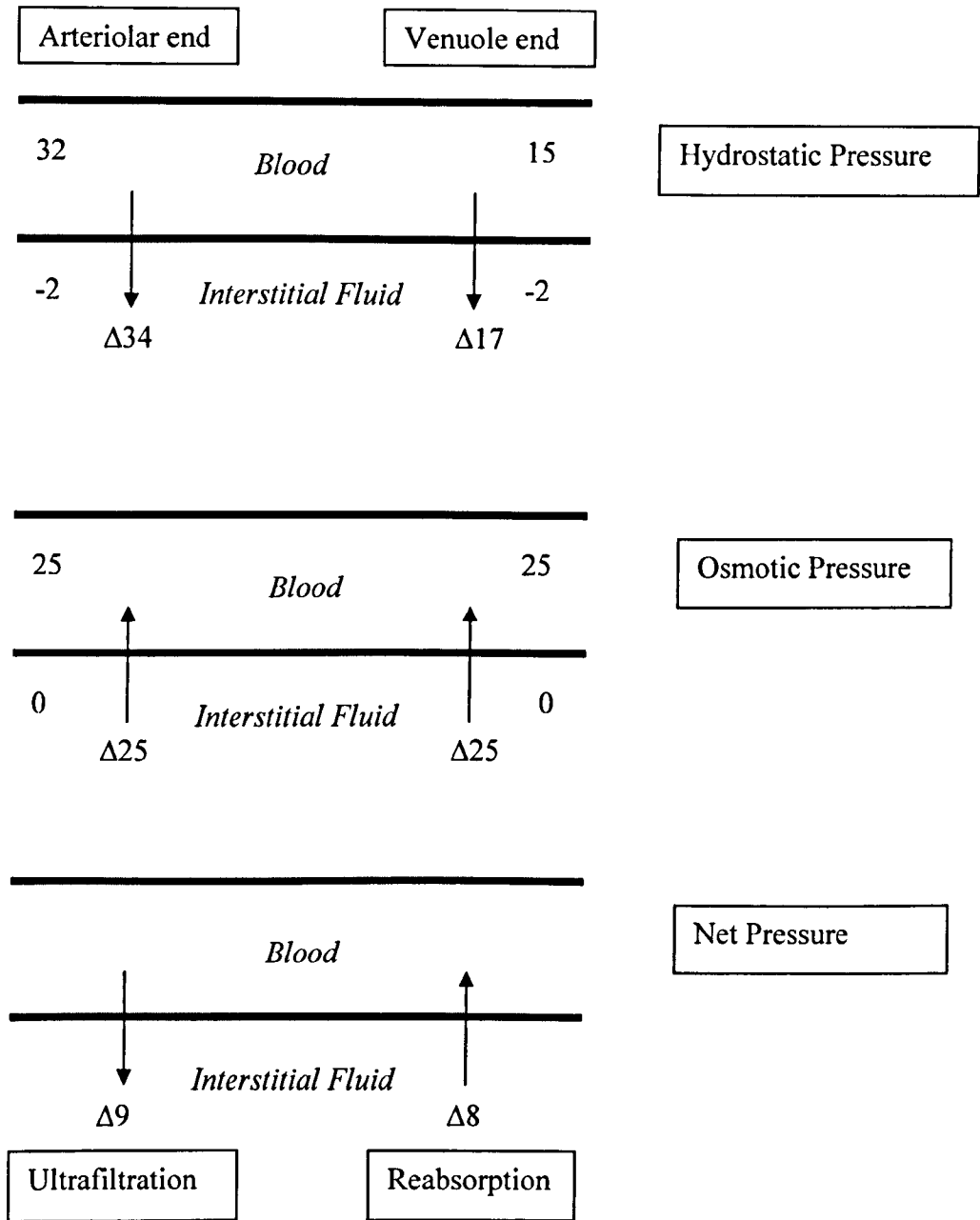


Figure 3.1: Hydrostatic, osmotic and combinatorial pressures across the capillary wall.
(Derived from Bray *et al.*, 1989).

It has been suggested that cultured monolayers of endothelial cells do not reflect the permeability characteristics of the endothelium *in-vivo*. Nevertheless, the *in vitro* approach remains a useful method by which many substances of physiological and pathological interest have been studied. Cultured endothelial cells using permeability models have given evidence that alterations in endothelial cell-cell adhesion with or without contractile events may be involved in the endothelial barrier functions observed. For example both histamine and α -thrombin increase the permeability of cultured endothelial cell monolayers in a time- and dose-dependent fashion and alter endothelial cell morphology in a manner suggestive of activation of the contractile apparatus (Alexander *et al.*, 2000). They also cause a rearrangement of intercellular junction molecules (Leach *et al.*, 1995; Tsukita *et al.*, 1992). The mechanism by which increased paracellular permeability occurs has been hypothesised as the disruption of interendothelial junctions concomitantly with cell contraction and the formation of intercellular gaps (Carson *et al.*, 1989; Majno and Palade, 1961; Stasek *et al.*, 1992).

In addition to the functional assessment of molecular passage, the structural integrity of tight junctions can be monitored electrophysiologically (Madara and Hecht, 1989). Trans-endothelial electrical resistance (TEER) employs an electrical circuit with the endothelium positioned as the variable resistor. In practise the endothelial monolayer is placed between an apical and a basal electrode whilst both analytic and reference currents are pulsed across the cells. The difference between the analytic and reference current is understood to be the resistivity of the endothelial monolayer. Although the kinetics of endothelial permeability can be accurately assessed using TEER, the main

disadvantage is the inherently low electrical values in endothelium in comparison to epithelial cells (Albelda *et al.*, 1988).

3.1.3

VARIATIONS IN THE *IN-VITRO* METHOD

The method of growing endothelial cells on porous membranes to measure the flux of a variety of molecules across the monolayer has become the tool of choice for many *in vitro* investigators. Even with this simple method, many variations have been employed.

There is a wide range of tissue culture inserts (figure 3.2) that vary in porosity, pore size, area, chemical nature/structure and filtration rates. Studies with different insert types have also shown that, for epithelial cells, the nature of the membrane can affect the permeability response following chemical exposure (Ward *et al.*, 1997). Villars *et al.*, (1996) examined the suitability of a variety of tissue culture inserts for their ability to support the growth of HUVEC cultures. Thus there is a possibility that the type of insert chosen could also affect the barrier function of endothelial cells in a similar fashion. There is also a choice of markers to demonstrate the leakage capacity of endothelial and epithelial cells, to distinguish the paracellular route from the cellular route.

The aims of these studies were to determine if the method/s chosen (Chapter 2) could not only determine the leakage characteristics of the cell lines, but also link these to the expression and location of specific key adhesion molecules (Chapters 5 & 6).

The dyes chosen were to be of different molecular sizes, and easily detectable via spectrofluorimetry. Thus the non-ionising molecules were chosen which

would not affect the osmotic pressure significantly by entering the cells. Dextran was chosen, with sodium fluorescein being employed in Chapter 6. Sodium fluorescein has been employed with epithelial cells to determine the chemical modulation of tight-junctions (Shaw *et al.*, 1990; Shaw *et al.*, 1991; Tchao, 1989).

Figure 3.2. Details of Commercially Available Inserts

Insert Name	Transwell-COL and Transwell	Cyclopore	Cellagen	Anopore	Millicell-HA	Millicell-CM
Manufacturer	Costar	Falcon	ICN	Nunc	Millipore	Millipore
Membrane Type	Polycarbonate	Polyethylene Terephthalate	Collagen	Aluminium Oxide	Esters of Cellulose	Cellulose Nitrate
Pore Size (μm)	0.4	0.45	0.45	0.02 / 0.2	0.45	0.45
Additional Coating	Types I and III collagen precoated onto Transwell-COL	Feasible	Feasible	Feasible	Unspecified	Obligatory
Porosity	Approx 30%	Approx 30%	unknown	50 %	unknown	unknown

3.2

MATERIALS AND METHODS

3.2.1

MATERIALS

3.2.1.1

Chemical Reagents

Rhodamine B isothiocyanate (TRITC) labelled 40-kDa dextran (TD40) and non-labelled 70-kDa dextran were purchased from Sigma, Poole, UK. These were used in addition to those employed in the experiments outlined in chapter 2 (2.2.1.1)

3.2.2

METHODS

ECV304 cells were seeded in Anopore inserts and the monolayer permeability to FD70 determined as in section 2.2.2.6 with the following modifications:

3.2.2.1

Effect of hydrostatic pressure on the flux of 70kDa-dextran

To investigate the effects of the absence of, or a very low, hydrostatic pressure, 200µl of FD70 were placed into the insert and 700ul of DMEM/FCS were placed in the well during the permeability measurement.

3.2.2.2

Effect of osmotic pressure on the flux of 70kDa-dextran.

The addition of 50 μ M non-labelled 70-kDa dextran into the abluminal chamber during the permeability measurement was undertaken to negate any osmotic pressure due to the dextran.

3.2.2.3

Effect of removal of a small volume of liquid from the abluminal compartment on the flux of 70-kDa dextran

During the permeability assay 20 μ l aliquots were removed from the abluminal compartment after 20, 40, 60 minutes leakage time. The fluorescence of the FD70 left in the well at the end of the 2hour leakage period was measured.

3.2.2.4

Effect of medium used in permeability assay on the flux of 70-kDa dextran

DMEM/FCS or M199 + 10% FCS were used as the media in the permeability assay.

3.2.2.5

Assessment of measuring the flux of two dextrans of differing molecular weights simultaneously

The leakage assay was performed on blank Anopore inserts only. The leakage of 50 μ M FD70 alone across 3 no-cell inserts was assessed as usual. Extra triplicate inserts were used to measure the leakage of 50 μ M TD40 alone and the combination of 50 μ M of both FD70 and TD40. The fluorescence of FD70

was measured at 485/530 (ex/em) as stated previously and the fluorescence of TD40 was measured at 530/590 (ex/em).

3.3

RESULTS

The following experiments investigated alteration in the method of macromolecular permeability assessment used in chapter 2. Some of these experiments were undertaken using the ECV304 cell-line prior to the knowledge that it did not express the marker endothelial molecule, vWF or the molecules thought to regulate permeability, VE-cadherin and PECAM-1. Even without the expression of these important molecules vasoactive agents caused a predictive increase in the monolayer permeability of these cells to FD70. The following experiments use the ECV304 cells as a restrictive monolayer and were, therefore, adequate to investigate the effects of the proposed changes in the basic methodology.

3.3.1

EFFECT OF HYDROSTATIC PRESSURE ON THE FLUX OF 70-KDa DEXTRAN

In chapter 2 the method used incorporated a hydrostatic pressure from the head of liquid applied to the luminal compartment at the beginning of the assay. It was desirable to limit the forces affecting the flux of FD70 across the cell monolayer in order to reveal the role that the monolayer itself had in permeability alteration. The processes of solvent drag and ultra filtration could occur when the level of liquid above the cell monolayer induces a hydrostatic pressure. The assay was changed such that the resultant model had approximately equal levels of liquid inside and outside the insert. As less overall FD70 was added into the insert, the total amount of dextran available

for transfer across the insert was decreased. As the molarity of the solution was the same and since the diffusion of the dextran across the insert never reached equilibrium during the 2 hours leakage time, it was assumed that the rate of flux would not be affected by this factor. After 2 hours the leakage of FD70 through the insert was still linear (see chapter 2, section 2.3.1).

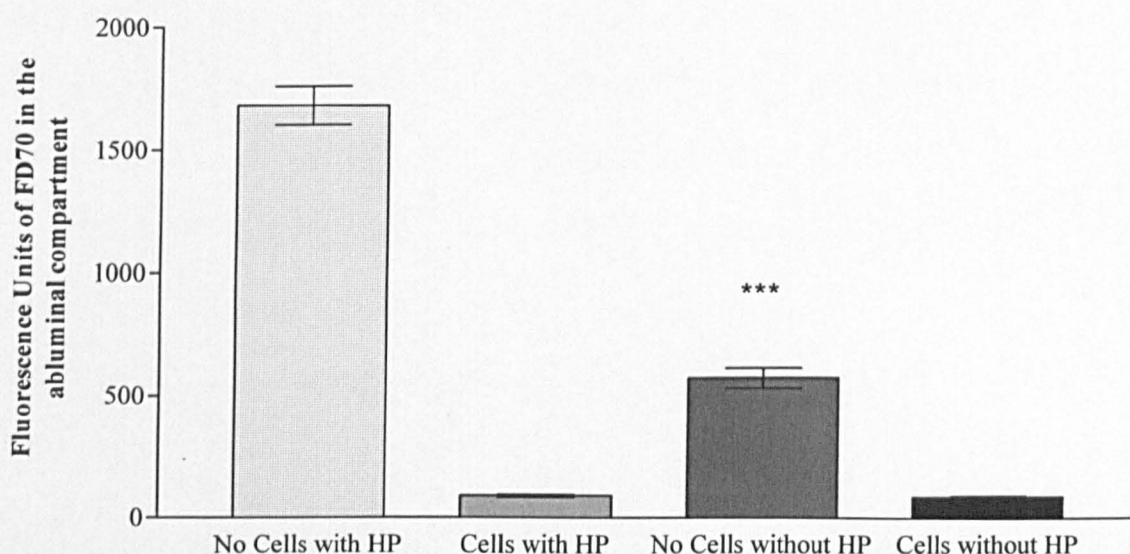


Figure 3.3: Effect of hydrostatic pressure on the flux of 70-kDa dextran. When the FD70 leakage was assessed under conditions where the hydrostatic pressure (HP) was removed, the flux was significantly reduced (***) = $p < 0.001$, compared to no cell with HP). However when the cells were present this hydrostatic pressure did not affect the flux. Figure shows mean values from triplicate inserts for each variable, error bars show standard error of the mean, (n=4).

The leakage of FD70 through the blank insert in the presence of a hydrostatic pressure was significantly higher ($p < 0.001$) than if that pressure was not present (figure 3.3). The leakage through the monolayer of cells, however, showed no difference between the two groups. The cell monolayers were

significantly lower than either no cell insert (significance markers not shown). Using a method without hydrostatic pressure would, therefore, significantly alter the percentage leakage values. For example, data from this experiment would lead to a percentage leakage of 5.4% for the assay performed under hydrostatic pressure, whilst a value of 15.2% would be obtained when no hydrostatic pressure was present. As the actual fluorescent units of FD70 that had crossed the cell monolayer were no different in the presence or absence of the hydrostatic pressure (figure 3.3) it was deemed that the hydrostatic pressure had no effect upon the passage of the FD70 between the cells. Possibly the use of a hydrostatic pressure within the assay would amplify any increase in permeability that was induced by a chemical exposure, as the area for flux would increase as the intercellular clefts open.

3.3.2

EFFECT OF OSMOTIC PRESSURE ON FLUX OF 70-KDa DEXTRAN

In chapter 2 the assay was performed in the presence of 10% FCS above and below the insert, but dextran was only placed in the luminal compartment. This could have produced an osmotic pressure of dextran that could have affected the flux of FD70 across the insert. Hence this needs to be taken into account if permeability in the absence of a pressure is required.

The addition of dextran to equate the osmotic pressure above and below the endothelial monolayer did not significantly alter the flux of the FD70 through either the blank insert or the cell monolayer (figure 3.4).

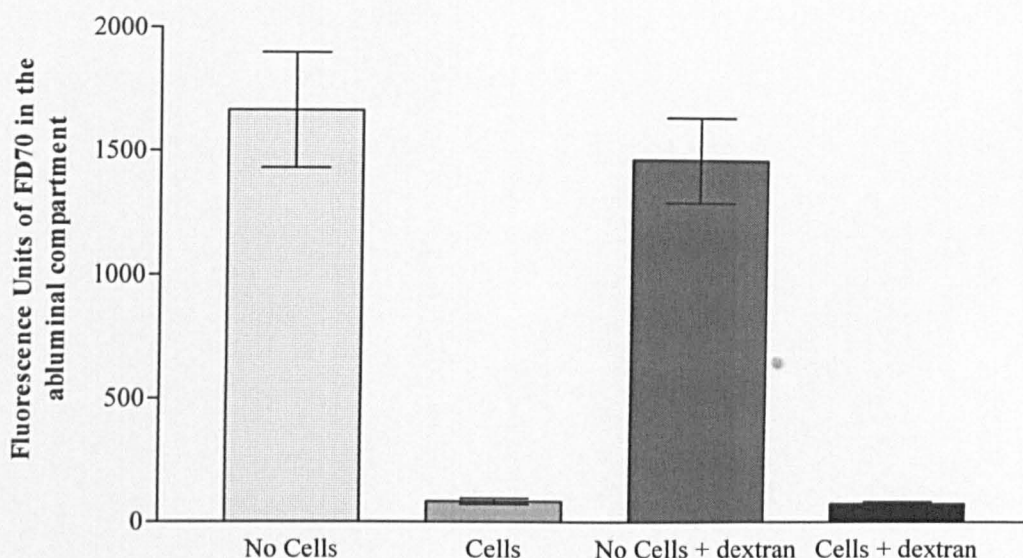


Figure 3.4: Effect of osmotic pressure on flux of 70-kDa dextran. The addition of 50 μ M unlabeled dextran into the abluminal compartment did not significantly change the flux of FD70 through either no-cell inserts or ECV304 monolayers. Figure shows mean results from triplicate inserts for each variable, error bars show standard error of the mean, (n=3).

3.3.3

EFFECT OF REMOVAL OF A SMALL VOLUME OF LIQUID FROM THE ABLUMINAL COMPARTMENT ON THE FLUX OF 70-KDa DEXTRAN

The method employed for chapter 2 involved measuring the flux of FD70 over 2 hours and gave one cumulative reading at the end of that time. In order to more accurately investigate the kinetics of endothelial permeability, it was deemed useful to be able to measure the flux at several time points throughout the total time course of the assay. This would give more information as to the leakage profile and thus any permeability changes that occurred over time. To achieve this it was decided to remove small aliquots from the abluminal compartment over time. The removal of several of these small volumes could

lead to changes in the hydrostatic pressure or dextran concentration that could change the diffusional flow rate of the FD70.

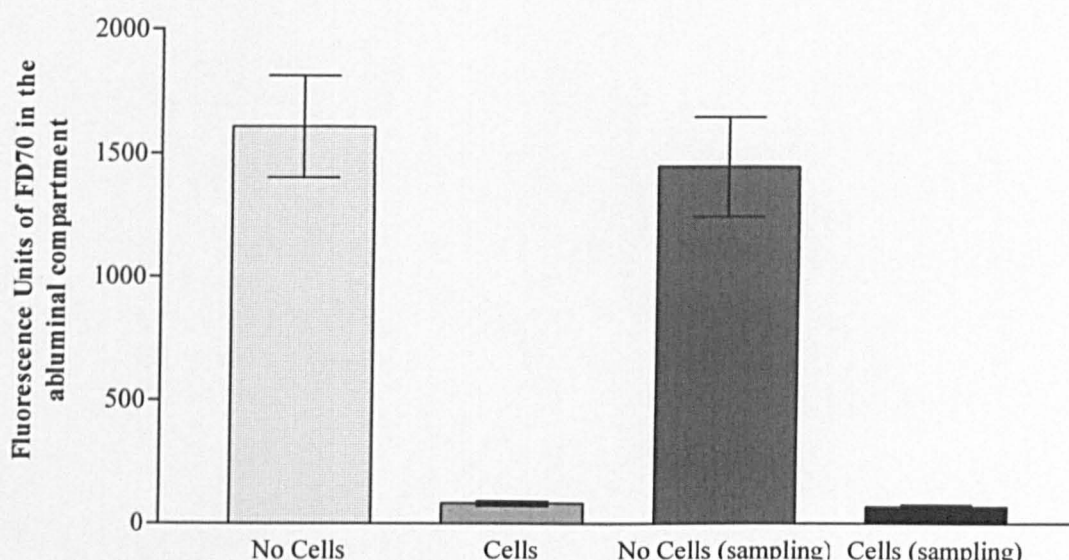


Figure 3.5: Effect of removing a small volume from the abluminal compartment on the flux of 70-kDa dextran. Sampling a total of 60 μ l from the Abluminal compartment had no significant effect on the flux of FD70 through either the no-cell insert or the ECV304 cell monolayer. Figure shows mean results from triplicate inserts for each variable, error bars show standard error of the mean, (n=3).

There were no significant differences between the flux of FD70 through either a blank insert or monolayer when 20 μ l was removed from under the insert at several time points throughout the assay (figure 3.5). The removal of aliquots up to 60 μ l from the abluminal compartment, containing 700 μ l, could be undertaken without modifying the leakage of FD70 across either the blank insert or the cell monolayer.

3.3.4

EFFECT OF MEDIUM USED IN PERMEABILITY ASSAY ON FLUX OF 70-KDa DEXTRAN

Hashida *et al.*, (1986) used DMEM in their assessment of endothelial permeability, and this method was used for the experiments in Chapter 2. However, evidence has suggested that it would be more suitable to keep the cells in tissue culture media used for culturing endothelial cells. Although MCDB 131 was used for the culture of the HMEC-1 cell-line, it was important to obtain medium that did not contain phenol red that would have interfered with detection of the fluorescence. MCDB 131 could not be obtained free from phenol red. Phenol red free Medium 199 (M199) was readily available.

When the assay was performed in DMEM, the fluorescence units (FU) of FD70, which had diffused across the inserts, were 1506 ± 189 and 91 ± 25 for the blank insert and the cell monolayer respectively. For M199 the corresponding fluorescence units were 1979 ± 222 and 108 ± 27 (figure 3.6). This represents 6% and 5.5% respectively that gives no significant difference between the fluxes of FD70 through the monolayer on the inserts regardless of the medium used.

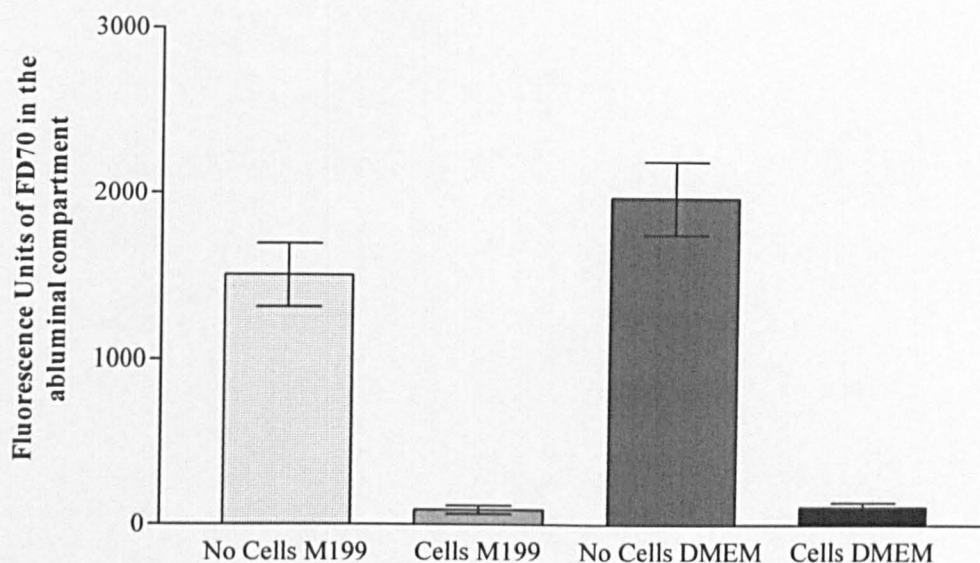


Figure 3.6: Effect of M199 on flux of 70-kDa dextran across insert and cell monolayer. Undertaking the permeability assay using M199 did not significantly alter the leakage of FD70 through either the no-cell inserts or the ECV304 cell monolayers. Figure shows mean results from triplicate inserts, error bars show standard error of the mean, (n=3).

3.3.5

ASSESSMENT OF MEASURING THE FLUX OF TWO DEXTRANS OF DIFFERING MOLECULAR WEIGHTS SIMULTANEOUSLY

Work reported in chapter 2 suggested that Anopore inserts should be ruled out for further use in studying endothelial barrier function. Collagen coated Millicell-CM seemed to be able to support the production of a stable monolayer of endothelial cells. Villars *et al.*, (1996) examined the suitability of a variety of tissue culture inserts for their ability to support the growth of HUVEC and for their ease in handling. They concluded that Transwell-Col inserts gave one of the best substrates, whilst the Anopore and the Millicell-CM inserts were not deemed to be as favourable for cell attachment, adhesion

and proliferation of these cells. Additionally the membrane supports used most frequently in studies on the involvement of interendothelial junctions were polycarbonate. Thus it was decided to use polycarbonate Transwell™ inserts for our future investigations to enhance direct comparisons with published literature, since porosity can be variable (figure 3.2). It was assumed that there were no properties of the Transwell inserts that would cause the conclusions from the above studies in this chapter to differ from those obtained with the Anopore inserts.

To increase the amount of data collected in one experiment, the simultaneous exposure of differentially labelled dextrans was attempted. This would have also allowed the same monolayer of cells to be used to assess permeability of two or more markers. The largest molecule that can cross the endothelium has a MW of approximately 40 kDa, e.g. HRP (44 kDa). FITC-labelled 70-kDa dextran was employed as previously and a 40-kDa dextran labelled with TRITC (TD40) was also added in this permeability assay.

The FITC fluorescence (485/530nm (ex/em)) in the abluminal compartment after 60 minutes leakage of FD70 or FD70 combined with TD40, showed that the presence of TD40 did not significantly alter the fluorescence of the FD70 (figure 3.7 a). However, the combined fluorescence of TD40 with FD70 gave an increased fluorescence at 530/590 (ex/em) ($P < 0.01$), even in the presence of the relatively small amount FD70 (figure 3.7 b). The excitation and emission spectra of the two fluorophores were so close that interference could have occurred. Other molecules labelled with different fluorophores were investigated for use but proved to be too expensive to use on a regular basis for

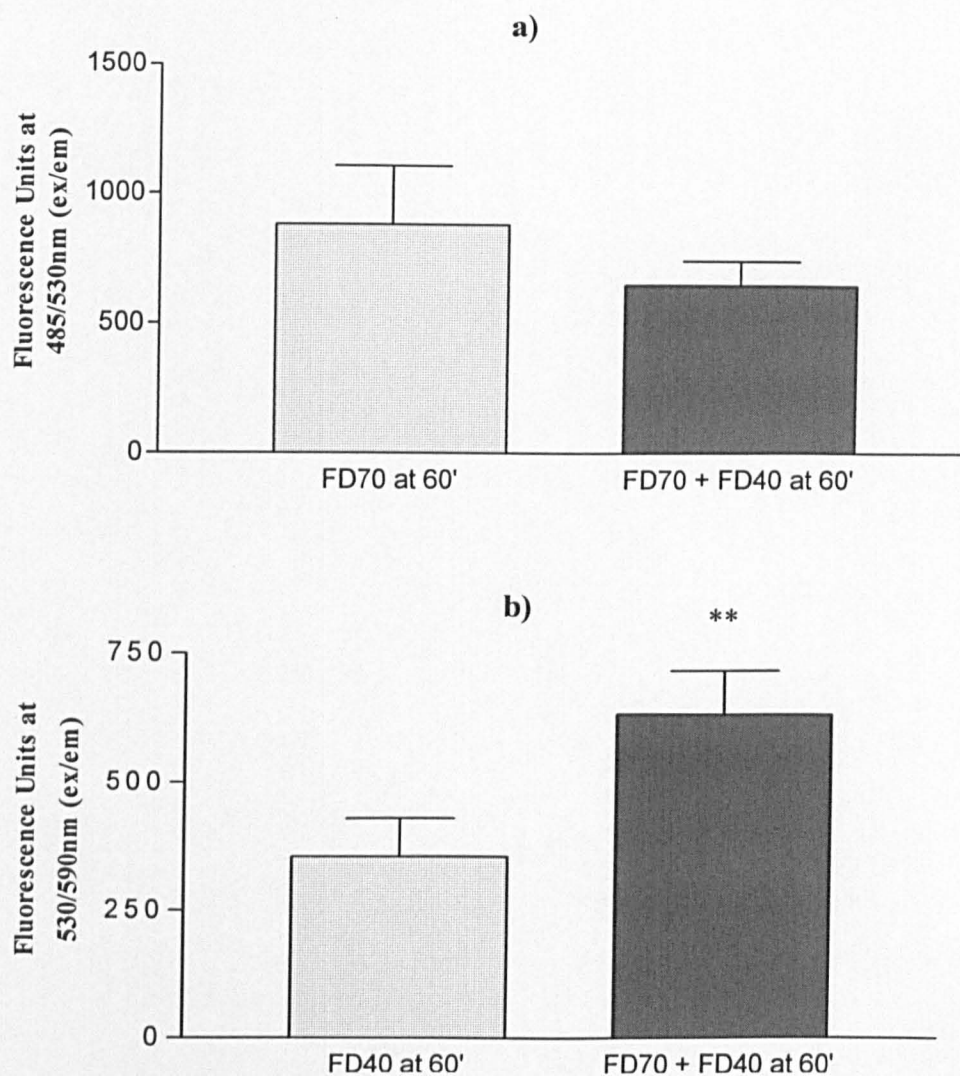


Figure 3.7: Measuring the flux of two dextrans of differing molecular weights simultaneously. A) shows fluorescence at 485/530nm (ex/em), b) shows fluorescence at 530/590nm (ex/em). The presence of TD40 in the solution did not significantly alter the fluorescence at the FITC detection wavelength. However FD70 significantly increased the fluorescence at the TRITC detection wavelength (** = $p < 0.01$, compared to FD40 at 530/590 (ex/em)). Figure shows mean results from triplicate inserts, error bars show standard error of the mean, (n=3).

these studies and so dual flux measurements of two markers simultaneously was not pursued.

3.4

DISCUSSION

The method adapted from Hashida *et al.*, (1986) in Chapter 2 incorporated a hydrostatic pressure in the luminal compartment of the system. On removing this pressure a significant reduction in the leakage of FD70 across no-cell inserts was observed. This was in agreement with Schaeffer and colleagues (1992b) who studied the size-selective transport characteristics of polycarbonate filters. The leakage across intact ECV304 monolayers however did not alter with this reduction in hydrostatic pressure. Dull *et al.*, (1991) showed that a hydrostatic pressure of 10cm of water across BPAEC caused a 3.7- fold increase in albumin permeability. In our study the hydrostatic pressure from 500µl of media would have been extremely small and thus possibly not significant across an effective barrier such as the ECV304 monolayer. Taking small samples from the abluminal chamber over the course of the assay did not significantly affect the total amount of dextran (FU) in the abluminal chamber after a 2 hour leakage period. This was a surprise as the total amount taken was 60µl, 8.6% of the total volume available. However this amount was not taken all at once, but over 2 hours, making the effect this had on the dynamics of FD70 flux difficult to interpret. Initial experiments closely followed the permeability method by Hashida *et al.*, (1986), who used DMEM in their assay. It was considered beneficial to keep the endothelial cells in a media commonly used in their culture rather than continuing to use DMEM. M199 was used for the culture of HUVEC and ECV304 and could be obtained phenol red-free, which was required as phenol red interferes with the fluorometric assays. M199 media did not affect the end-point of the leakage

assay either with no-cell inserts or ECV304 monolayers. Schaeffer *et al.*, (1992a) had observed that changing their media from DMEM to M199 gave a rise in permeability of bovine pulmonary artery endothelial cells. He suggested that the 0.2 mg l^{-1} ATP that M199 contains could have stimulated the cells via the P_{2y} purinergic receptor. Given this fact, it would have been prudent to test the HMEC-1 cells as well. Attempts to develop the assay to measure the flux of two dextrans simultaneously proved unsuccessful. This was due to interference from the TRITC-labelled dextran when measuring the fluorescence from FITC-labelled dextran. It would be worthwhile to investigate the use of different fluorophores with which to label the dextrans. The savings in time and money from the reduced number of experiments would weigh favourably against the additional cost of some of these fluorophores. From these studies the basic method was altered so that there was no deliberate hydrostatic pressure across the insert; 200:700 μl , the media used was changed to M199 – phenol red free and sampling from the abluminal compartment was introduced in an attempt to measure the dynamics within the system.

CHAPTER 4

MODULATION OF PERMEABILITY AND
MOLECULES OF THE INTERCELLULAR
JUNCTIONS IN THE HMEC-1
CELL-LINE.

CHAPTER 4

MODULATION OF PERMEABILITY AND MOLECULES OF THE INTERCELLULAR JUNCTIONS IN THE HMEC-1 CELL-LINE.

4.1

INTRODUCTION

The main aim of this research was to define a permeability model to be used, alongside a variety of other *in-vitro* assays, to predict the cytotoxic effects of unknown compounds on microvascular functionality. Following oral administration, absorption results in the drug being present in the blood. The vascular endothelium, by virtue of its location, is not only a direct target tissue for toxicity, but has a control over the drug's delivery to the body's organs. Endothelial damage leads to the loss of various regulatory functions such as prostacyclin synthesis and release of prothrombotic substances into the circulation (Vane *et al.*, 1990). An *in-vitro* model of the vascular endothelium could be used to obtain information on the mechanisms by which toxic substances or drugs induce vascular alterations (Chappey *et al.*, 1995). Direct damage to the endothelium and inflammatory effects of mediators released from other damaged cells in the vicinity can contribute to the vascular response. In the skin, for example, mediators released after contact with an irritant attract and activate other cells such as neutrophils and macrophages (Laskin and Pendino, 1995). These then release further mediators and active components leading to a cascade that amplifies the inflammatory response of the endothelium. The use of a two-cell system to assess the toxicity of skin irritants could use keratinocytes as the initial cell exposed to the irritant,

followed by the application of the conditioned medium, from these keratinocytes, to cultures of endothelial cells, evaluating the effects on their functions. This has the added benefit that each mediator influencing the endothelial cells would not need to be identified and there would be a more natural balance between pro-inflammatory mediators and natural cellular inhibitors (Parish, 1990). Such an approach has been successfully employed with irritant-exposed human keratinocytes, with the conditioned medium (containing mediators) affecting macrophage release of nitric oxide (Ward *et al.*, 1998). More recently the electrical stimulation of dermal fibroblasts to produce TGF- β 1 was evaluated (Todd *et al.*, 2001).

Before the assessment of the HMEC-1 monolayer in a two-cell system could be undertaken, the response of the HMEC-1 cells to a set of compounds known to alter permeability, via different mechanisms, was undertaken. In the HUVEC endothelium, during the establishment of confluency, first VE-cadherin with α - and β -catenin are organised at junctions without apparent linkage with the actin cytoskeleton. Only at later stages do plakoglobin and actin microfilaments get associated to these structures (Lampugnani, 1995). Various vasoactive mediators including thrombin, elastase and inflammatory cytokines have been shown to change VE-cadherin distribution at junctions in parallel with increased permeability (Lampugnani *et al.*, 1992). Additionally alterations in endothelial permeability have been strongly linked with an alteration in the expression of the F-actin cytoskeleton (Yu and Gotlieb, 1992). Therefore, in addition to measuring the permeability of the HMEC-1 monolayer following exposure to the chosen chemicals, the effects on VE-cadherin and F-actin was also investigated. The aim was to provide evidence to link permeability

changes in HMEC-1 cells with regulation by molecules of the adherens junction. From this data a clear decision could be made on the suitability of the HMEC-1 cell-line for further study as a model of *in-vivo* vascular beds. Adherens and tight junctions act as resistance in a series to the transport of hydrophilic molecules. Therefore the presence of tight junctions in the HMEC-1 cell-line was investigated using TEM and immunocytochemistry.

Compounds chosen were the calcium chelator, ethyleneglycol-bis (β -aminoethylether)-N, N'-tetraacetic acid (EGTA), the calcium ionophore A23187, the mild amphoteric surfactant, cocamido-propylbetaine (CAPB), and the tumour promotor phorbol myrisate -13 - acetylester (PMA). EGTA and A23187 were chosen as calcium is a key element in maintaining functionality of the cadherins. CAPB was chosen, since it has been shown *in-vitro* to cause damage to epithelial cell junctions, followed by reversal of these effects (Clothier and Sansom, 1998). PMA, a known tumour promoter, is well known to activate PKC, which in turn affects cell-to-cell contacts and endothelial permeability (Lynch *et al.*, 1990; Van Nieuw *et al.*, 1998).

4.2

MATERIALS AND METHODS

4.2.1

MATERIALS

4.2.1.1

Chemicals and Reagents

Ethylene glycol-bis (beta-aminoethyl ether)-N, N, N', N'-tetraacetic acid (EGTA); FITC labelled 40 and 150-kDa dextrans (FD40 and FD150) and FITC conjugated phalloidin were purchased from Sigma, Poole, UK. Alamar Blue™ was obtained from Serotec Ltd, Kidlington, UK, and used in accordance with the manufacturers instructions. Vectorshield with propidium iodide was purchased from Vector Laboratories, Peterborough, UK. Cocamidopropylbetaine was a gift from Boots Contract Manufacturing, Nottingham, UK. Transmit™ resin was obtained from TAAB Laboratories Equipment Ltd., Bershire, UK.

4.2.1.2

Antibodies

Rabbit polyclonal anti-occludin and rabbit polyclonal anti-ZO-1 were purchased from Zymed, USA. Both anti-occludin and anti-ZO-1 were dispensed into aliquots and stored at -80°C. Anti-occludin was used at 50µg ml⁻¹ and anti-ZO-1 was used at 20µg ml⁻¹.

4.2.2

METHODS

4.2.2.1

Leakage of macromolecules through HMEC-1 monolayers.

The basic assay protocol to assess endothelial permeability (section 2.2.2.6) was modified as follows. Transwell inserts were pre-coated with fibronectin. To achieve this 200µl of a 25µg.ml⁻¹ solution of human plasma fibronectin in serum-free medium was placed into the insert and incubated for 3hrs at room temperature under sterile conditions. The inserts were then washed in serum-free medium and used immediately. HMEC-1 cells were seeded into the fibronectin-coated Transwell inserts at 5 x 10⁵ cells ml⁻¹ in 200µl of medium, i.e. 1 x 10⁵ cells per insert. Three inserts received 200µl of medium alone and were referred to as the no-cell control inserts. The inserts were placed into 12-well culture plates containing 700µl of medium in the wells. Cultures were maintained at 37°C, 5% (v/v) CO₂ in air. A confluent monolayer, visible through the inserts, usually formed within 48hrs. At all times the inserts were handled in a sterile fashion. After 72 hrs in culture and following any exposure to chemicals of interest, the leakage of fluorescein isothiocyanate labelled dextrans (40, 70 or 150kDa) was determined. The cells were washed with 500µl of HBSS and the inserts transferred into fresh wells containing 700µl medium 199 (phenol red-free) with 10% FCS (199/FCS). 200µl of the marker of interest at 50µM was applied to the luminal compartment, above the cells. Plates were incubated for a total of 2hrs, alternating placing them at 37°C, 5% (v/v) CO₂ in air or at room temperature on an orbital shaker for 20 minutes at a

time. This was undertaken to encourage even mixing of the labelled dextran and avoid a concentration gradient across the insert. 10µl aliquots were removed, from the basal compartment, at various time intervals, over the 2 hour period. 90µl of 199/FCS was added to the 10µl aliquots and the amount of fluorescence measured on the Cytofluor fluorescent plate reader at an excitation wavelength of 485/20nm and an emission wavelength of 530/25nm. Converting the fluorescence of the marker to moles facilitated the comparison of leakage of the different markers.

4.2.2.2

Alamar Blue™ / Resazurin assay.

The Alamar Blue™ assay was marketed as a method to quantitatively measure the proliferation of various human and animal cell lines, bacteria and fungi. It was also suggested to be of use in the evaluation of relative cytotoxicity of agents within various chemical classes. The solution incorporates a fluorometric/colourimetric growth indicator based on detection of metabolic activity within the cells. The active compound in Alamar Blue™ is resazurin an oxidised form of resorufin, the former being blue and non-fluorescent the latter fluoresces and is a pink colour (Rassmusen, 1999; O'Brien *et al.*, 2000). Cells rapidly take in the Alamar Blue (resazurin), reduce it to resorufin and export it in to the surrounding medium (Garside *et al.*, 1997).

HMEC-1 cells were seeded into 24-well plates at 1×10^5 cells ml⁻¹ in 400µl of medium and grown at 37°C, 5% (v/v) CO₂ in air for 72 hrs. Wells containing medium alone were also prepared. Following exposure to the chemical, of interest, for the required time, the confluent monolayers were washed in HBSS.

500µl of a 1:10 dilution of Alamar Blue™ in HBSS was then added to all wells and the cells incubated at 37°C, 5% (v/v) CO₂ in air for 1 hour. The resultant conversion of the Alamar Blue, to the fluorescent product resorufin, by the cells was measured on the Cytofluor fluorescent plate reader at an excitation wavelength of 530/25nm with an emission wavelength of 590/35nm. Data was expressed as fluorescent units, unless otherwise stated.

4.2.2.3

Treatment of confluent HMEC-1 monolayers with chemicals.

The concentration of chemicals exposed to HMEC-1 cells, the diluent used and the period of exposure is summarised in figure 4.1. Cells were seeded into Transwell™ inserts as in section 4.2.21. and incubated for 72hrs at 37°C, 5% (v/v) CO₂ in air. Media was removed from the cells and the 200µl of chemical dilution added. Following the appropriate exposure time the chemical was washed from the cells with 200µl of HBSS and the leakage assay immediately undertaken (as described in section 4.2.2.1). It should, therefore, be noted that in the following data the leakage time refers to the time that the dextran has been in contact with the monolayer only. Treatment of the HMEC-1 cells with PMA, however, was different. When confluent at 72 hr, leakage of FD70 was assessed up to collection of the 20 minute aliquot. At this point 2µl of medium alone or PMA in medium was added to control cells and inserts with no cells. The final concentration of PMA in the luminal chamber was 1×10^{-7} or 1×10^{-8} M respectively. The leakage assay was allowed to proceed for the remaining 30 minutes, with aliquots retrieved at 15 minutes intervals. Therefore, for the

PMA data, the leakage time refers to the time that the PMA and the dextran have been in contact with the monolayer.

4.2.2.4

Immunocytochemistry for VE-cadherin, Occludin and ZO-1.

Chamber slides were pre-coated with fibronectin. 150µl of a 25µg.ml⁻¹ solution of human plasma fibronectin in serum-free medium was placed into each well of a chamber slide and incubated for 3hrs at room temperature under sterile conditions. The wells were then washed in serum-free medium and used immediately. HMEC-1 cells were seeded at a density of 1.5 x 10⁵ cells per well, in 300µl of medium. Cultures were allowed to attach and grow to confluence at 37⁰C, 5% (v/v) CO₂ in air for 72hr after which time they were fixed in 300µl of 4% paraformaldehyde at room temperature for 30 minutes. The fixed cells were washed once for 10 min with 300µl of 0.1%BSA in PBS (PBS/BSA) and blocked in 5% goat serum in PBS for 30 min at room temperature. 200µl of anti-human VE-cadherin, diluted in PBS/BSA, was exposed to the cells overnight at 4⁰C in a humidified environment. Anti-VE-Cadherin was used at 10µg ml⁻¹. Occludin and ZO-1 were used at 50µg ml⁻¹ and 20µg ml⁻¹ respectively. Cultures were washed three times for 10 minutes each time, with 300µl of PBS/BSA. Cells were then exposed to 200µl of anti-mouse IgG FITC-tagged secondary antibody for 1hr at room temperature in the dark. Secondary antibody was used at 5µg ml⁻¹. Following removal of the wells and glue from the slides, they were mounted in Vectorshield (containing propidium iodide to visualise the nuclei when necessary). The cells were examined using a Leica TCS 4D confocal laser-scanning microscope. When

required, cultures were double labelled against VE-cadherin and F-actin. When this was undertaken the FITC-conjugated phalloidin (section 4.2.2.5) was exposed to the cultures at the same time as the secondary antibody, ensuring that the final concentrations were still $5\mu\text{g ml}^{-1}$ for F-actin and $5\mu\text{g ml}^{-1}$ for the secondary antibody.

4.2.2.5

Phalloidin staining for F-actin

Cells were seeded and fixed as described in section 4.2.2.4. They were then washed in 0.1% BSA/PBS and permeabilised in 1% Triton X-100 in PBS for 5 minutes. Following two more washes the cells were exposed to $5\mu\text{g ml}^{-1}$ of FITC-conjugated phalloidin in PBS at 37°C for 1 hour. The cells were washed three times in 0.1%BSA/PBS and 2 x 10 minute washes in distilled water to remove unbound dye. The slides were mounted in Vectashield and visualised using a Nikon fluorescence microscope, with a fluorescence filter of 490nm excitation / 550nm emission. In addition, when necessary, cells were observed using a Leica TCS 4D confocal laser-scanning microscope.

4.2.2.6

Transmission Electron Microscopy

All steps were carried out in a fume cupboard.

Endothelial cells were grown to confluence on collagen-coated CM inserts as in section 2.3.4.1. They were fixed by immersion in 3% (v/v) glutaraldehyde in 0.1M phosphate buffer (pH 7.2) for 30 minutes at RT. The inserts were washed three times in 0.1M phosphate buffer and stored in 6% sucrose in 0.1M

phosphate buffer at 4°C. This fixation does not add electron opacity to the cells, so staining and post-fixation in osmium tetroxide (OsO₄), uranyl acetate and lead citrate are required when ultrathin sections are to be examined. The preparations were exposed to 1% OsO₄ in Millonig's buffer for 1 hour. The inserts were washed five times in distilled water before immersion in a 2% (w/v) solution of uranyl acetate in distilled water for 30 minutes protected from light. The fixed cells were then dehydrated through a series of alcohols before infiltration with resin. During these dehydration steps the CM membrane was removed from the polystyrene casing of the tissue culture insert and further processing carried out on the cells attached to the membrane alone. TransmitTM, a low viscosity, low toxicity resin was used for these delicate samples. Once the samples were infiltrated with the resin/hardener/accelerator mixture, the blocks were moved to an oven and polymerised overnight at 70°C. Sections of 1µm were taken to orientate the blocks for ultrathin sections of a suitable portion of the monolayer. Ultrathin sections (70-90 nm) were cut on a Reichert Ultracut E microtome, placed onto copper grids and contrasted with Reynolds lead citrate. Samples were then viewed in a Phillips 410 Transmission Electron Microscope operated at 80kV. The department's EM technician, Mr Barry Shaw, undertook the cutting of the ultrathin sections.

	EGTA	A23187	CAPB	PMA ¹
Concentration of chemical tested	0.5 and 5mM	100 μ g.ml ⁻¹	1 and 2mg.ml ⁻¹	10 ⁻⁷ and 10 ⁻⁶ M
Diluent Used	HBSS	HMEC-1 medium containing 1% DMSO	HBSS	199/FCS
Period of Exposure	5 minutes	15 minutes	20 minutes	30 minutes

Figure 4.1: Treatment protocol of confluent layers of HMEC-1 cells.

1. Note that the exposure method used for PMA differs from the other chemicals, refer to section 4.2.2.3.

4.3

RESULTS

4.3.1

OBSERVATION OF JUNCTION ULTRASTRUCTURE AND MOLECULES IN HMEC-1 CULTURES ON COLLAGEN-COATED CM INSERTS

Having concluded that the HMEC-1 cell-line was the most appropriate cell-line to use for these studies, the presence of tight junctions in the HMEC-1 cell-line was examined. This was conducted both by ultrastructural study of the paracellular clefts between the cells (observation of adherens junctions was carried out at the same time) and detection of tight junction molecules occludin and ZO-1 (as described in Chapter 1) by immunocytochemistry.

4.3.1.1

ULTRASTRUCTURE OF HMEC-1 PARACELLULAR CLEFT

Cells were seeded and processed for TEM as in section 4.2.2.6.

The HMEC-1 cells exhibited regions of extensive overlap between cells of an elongated phenotype (figure 4.2a) similar to that seen in the microcirculation *in situ*. The paracellular cleft was long and convoluted (figure 4.2b, arrow indicates cleft). Areas of granulofibrilla cytoplasmic plaques, characteristic of zonula adherentes were present (figure 4.2c brackets). Additionally there were regions where the adjacent cell membranes appeared to converge, but not fuse, denoting 'tight-junction like' areas (figure 4.2c*).

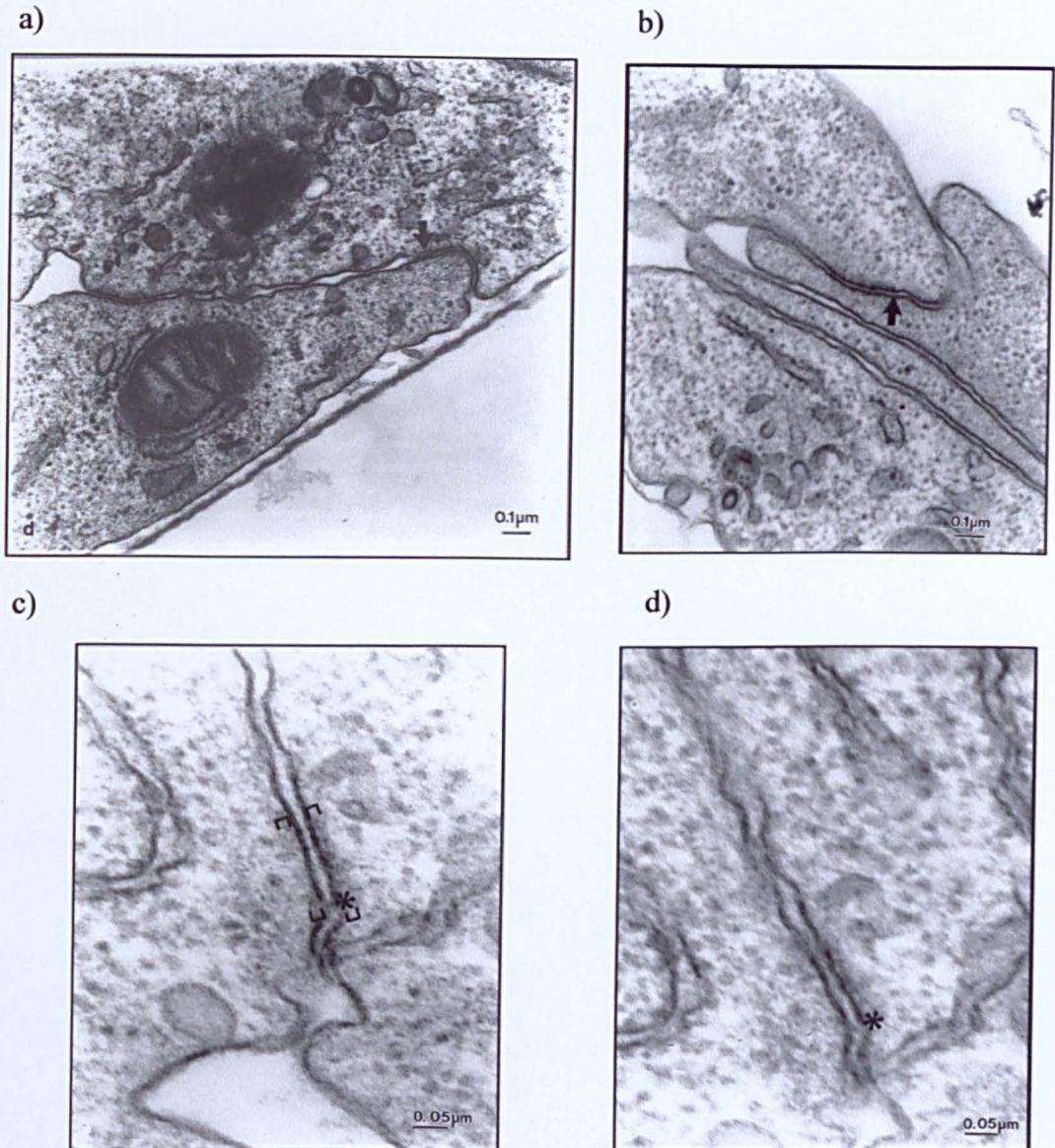


Figure 4.2: Electron micrographs concerning the paracellular clefts of HMEC-1 cells. The cells show extensive overlap (a), with convoluted paracellular clefts (b). Characteristic granulo-fibrillar cytoplasmic plaque associated with adherens junctions are present (c, brackets). Membrane convergence in places suggests tight junctions (c*), however on observation of the same area several sections further into the sample, the membranes are not fused (d*). Figures show representative images. Magnification: a) 37,780, b) 39,890, c) 100,500, d) x 100,500.

Observation of this same junctional region several sections further into the sample shows that this 'tight-junction like' area was not continuous throughout the cleft (figure 4.2d*). Higher magnification analysis showed that the separation between adjoining cell membranes at these regions were greater than the 4nm gap reported for all non-CNS microvessel tight junctions (Firth *et al.*, 1983; Leach *et al.*, 1992; Ward *et al.*, 1988)

4.3.1.2

THE DETECTION OF TIGHT JUNCTION MOLECULES IN THE HMEC-1 CELL-LINE

Cells were seeded and processed as described in section 4.2.2.4, to detect occludin and ZO-1. Occludin was detected in HMEC-1 monolayers (figure 4.3a), however it was not localised to the cell-cell contacts, but generally expressed throughout the cytoplasm. There was a dense band of occludin around the nucleus of most cells. Some cells expressed higher levels of fluorescence than others (figure 4.3a, arrow), possibly indicating heterogeneity in the expression of occludin. Expression of ZO-1 was distributed in a similar way, with staining seen throughout the cytoplasm, but not at cell-cell contacts (figure 4.3c).

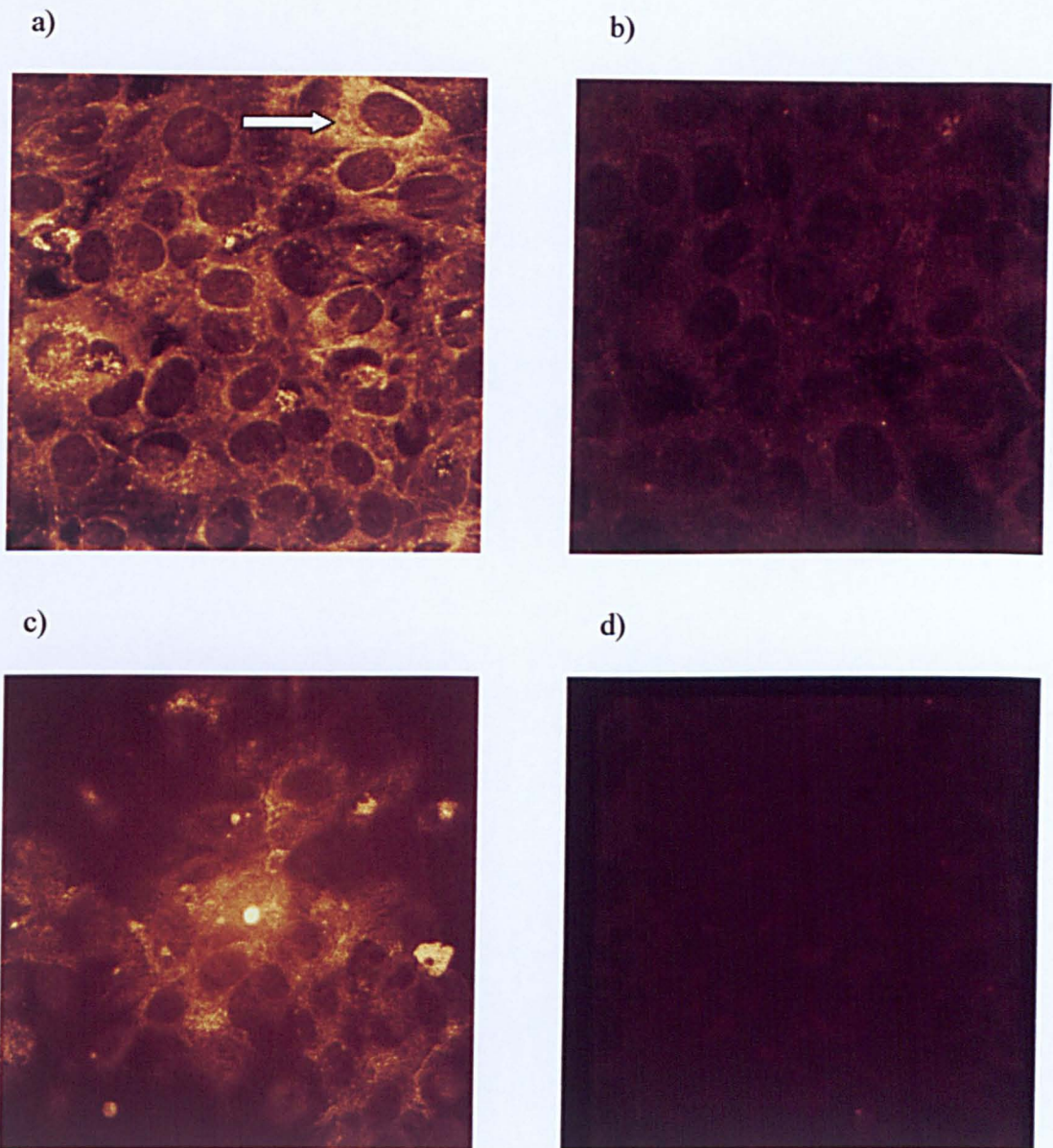


Figure 4.4: Immuno-reactivity against tight junction molecules in HMEC-1. Occludin was positively expressed in the cytoplasm (a), control (b) received rabbit serum diluted 1:100 in PBS/BSA instead of the primary antibody. HMEC-1 positively expressed ZO-1 throughout the cell cytoplasm (c). Control (d) received PBS instead of the primary antibody. Figure shows representative images. Magnification x850.

4.3.2

PERMEABILITY OF HMEC-1 CELL-LINE TO DEXTRANS OF 40, 70 AND 150-kDa.

Previously the permeability of the endothelial monolayers was assessed using a 70kDa dextran (See Chapter 2). In order to ensure that the HMEC-1 monolayer acted in a size selective manner, the baseline permeability profile of the HMEC-1 monolayers to dextran of 40, 70 and 150kDa was undertaken. Leakage of the markers was undertaken as in section 4.2.2.1.

To compare the data from the different dextrans, standard curves were constructed so that the dextran leakage could be presented as a concentration instead of fluorescence units or percent leakage. This was undertaken as the number of FITC moles per mole of dextran differed for each molecular weight dextran. Expression of the leakage results as fluorescence units would have resulted in an inaccurate comparison between the dextrans. However, conversion of fluorescence to concentration of dextran negates this source of variation. A typical standard curve from a single experiment for 40kDa dextran (figure 4.4) demonstrates the linearity of the curve between 0 and 300nM. An R^2 value of 0.9986 indicated that the fluorescence of the dextran had a linear relationship to its concentration, allowing the equation of a straight line to be used to determine unknown concentrations of the dextrans. This relationship was consistent for each dextran and was also maintained through higher concentrations. This was observed up to 23 μ M, 13 μ M and 4 μ M for FD40, 70 and 150 respectively. These concentrations were substantially below those which actually passed across the inserts, with or without cells, during the maximum time/duration of the assay (figure 4.5 and 4.6).

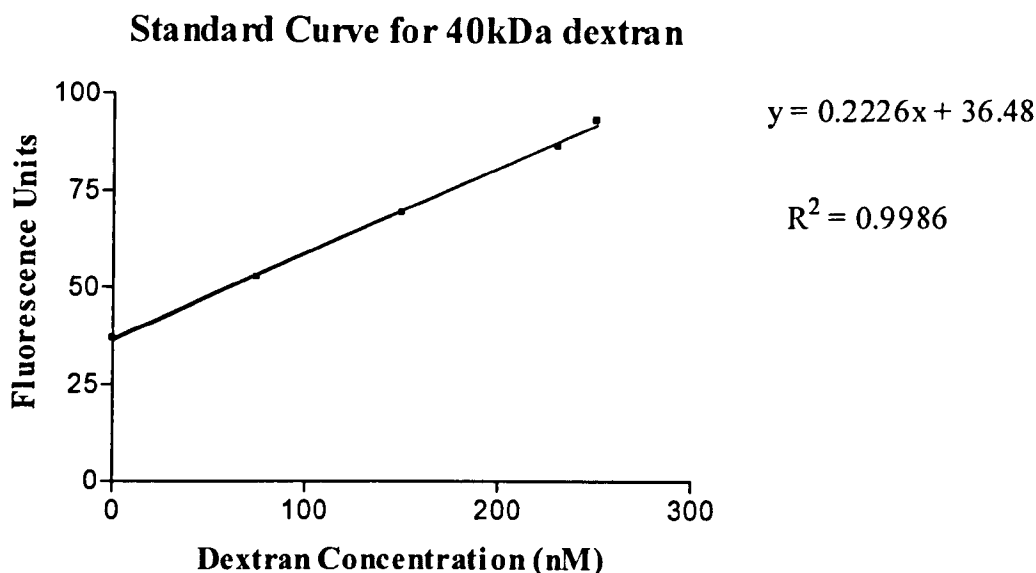


Figure 4.4: Standard curve from 0 - 250nM of 40kDa dextran. The relationship between dextran concentration and fluorescence was linear between these concentrations. Mean \pm SEM of triplicate wells from one experiment.

The amount of each dextran that crossed the Transwell inserts alone significantly increased as the leakage time increased (figure 4.5). Additionally the rate of leakage (flux) was related to the size of the dextran molecule examined, with the smaller dextran moving across the insert faster than the larger molecules (figure 4.7). The ratio of molecular weights for FD40: FD70: FD150 were 1: 1.75: 3.75 with respect to the FD40. The ratios of the respective leakage rates (when expressed as 1/leakage rate) were very similar at 1: 1.79: 3.27. This indicated that the leakage rates were indirectly proportional to the molecular weight/size of the dextran molecule examined.

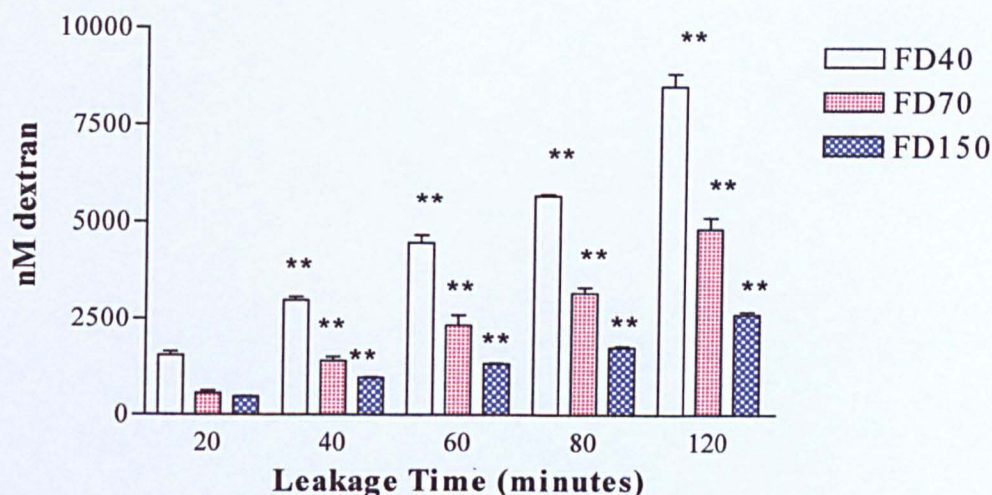


Figure 4.5: Basal leakage of 40, 70 and 150kDa dextran through fibronectin-coated Transwell inserts alone over time. The amount of dextran that crossed the insert over the 120 min leakage time increased significantly (** = $p < 0.01$ with respect to 20 min time point). Mean \pm SEM from triplicate inserts for each variable, ($n=3$).

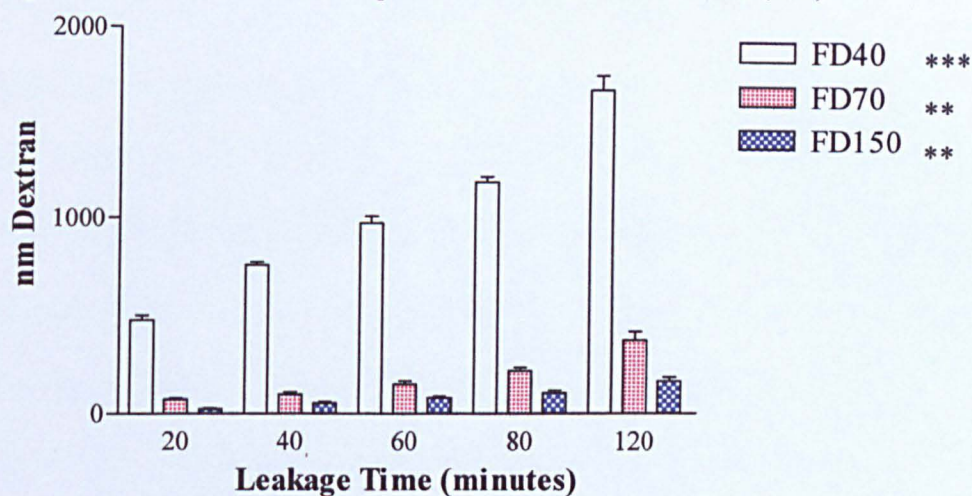


Figure 4.6: Basal leakage of 40, 70 and 150kDa dextran through HMEC-1 cells on inserts over time. The amount of dextran that crossed the insert over 120 min leakage time increased significantly (*** = $p < 0.001$, ** = $p < 0.01$, compared to 20 min time point cultures). Mean \pm SEM from triplicate inserts for each variable, ($n=3$).

	Dextran Empirical Flux Rates (nM min ⁻¹) ± S.E.M (n=3)		
	FD40	FD70	FD150
No Cells	71.2 ± 2.7	40.3 ± 2.4	21.8 ± 0.61
monolayer	13.9 ± 0.64 (***)	3.12 ± 0.38 (***)	1.39 ± 0.18 (***)

Figure 4.7: Empirical flux rates of 40, 70 and 150kDa dextrans through no cell insert or HMEC-1 monolayer. Data shown taken from the slope of the data used to construct figures 4.5 and 4.6. The flux rate was related to dextran size, the smallest molecule crossing fastest. The flux rates through the HMEC-1 monolayer for each dextran was significantly lower than for the insert alone (no cell) (***) = $p < 0.001$, unpaired t-tests)

The presence of the HMEC-1 cell monolayer significantly impeded the movement of the dextrans into the basal compartment (figures 4.6 and 4.7). However, there was still a significant increase in flux over the 120 minutes for each dextran (figure 4.6). The percentage of dextran in the basal compartment, following 120 minutes of leakage, in relation to the originally applied 50 μ M, indicated that the majority of each dextran was still present in the upper compartment (figure 4.8). Thus equilibrium of the dextrans was not achieved even for leak times of up to 2 hrs (figures 4.5 and 4.6). The flow of the dextrans across the cell monolayer was significantly lower for each dextran than through the insert alone (figure 4.7). Additionally examination of the ratios between the leakage rates, in terms of the rate through the cells for FD40, gave values of 1: 4.46: 10 for the FD40: FD70: FD150 respectively which does not correspond with the ratios between the molecular weights/size, or rates of leakage through the inserts alone.

	Percent of dextran in the basal compartment after 120 mins		
	± SEM		
	FD40	FD70	FD150
No Cells	17.1 ± 0.63	9.7 ± 0.58	5.2 ± 0.17
monolayer	3.3 ± 0.14*	0.75 ± 0.09*	0.33 ± 0.05*

Figure 4.8: Percent of the originally applied 50 μ M 40, 70 and 150kDa dextrans that were detected in the basal compartment. The majority of each dextran remained in the upper compartment during the assay. The presence of the HMEC-1 monolayer significantly lowered the percentage which moved across the insert (* = $p < 0.05$, compared to No Cell insert, unpaired t-test).

Expression of the data as percentage leakage, i.e. the amount of dextran which had crossed the monolayer in relation to that which had crossed an insert with no cells, enabled the assessment of the consistency of this relationship over the leakage time to be determined (figure 4.9). The percentage leakage of FD40 and 70 after 20 minutes differed significantly from any of the subsequent values ($P < 0.001$). This was also noted with FD40 between the percentages at 60 minutes and 120 minutes ($P < 0.01$). There was no significant difference between 80 and 120 minute time points.

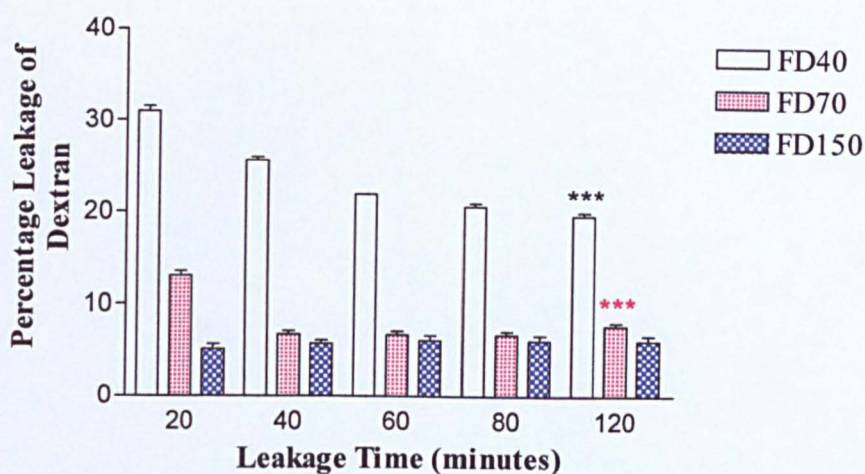


Figure 4.9: Percent Leakage of 40, 70 and 150kDa dextran over 120 minutes. The percentage leakage of FD40 and FD70 significantly decreased over 120 min leakage time (***/** = $p < 0.001$, compared to 20 min time point cultures). Mean \pm SEM from triplicate inserts for each variable, ($n=3$).

With FD70, at 40 minutes and above, and for all FD150 time points, no significant differences were observed between the percentages. These changes in percentage leakage over time occurred because the flux rate of the dextrans differed between the no-cell insert and that supporting a monolayer of HMEC-1 cells. So over time these two flux rates moved further apart, changing the relationship between them. The rate of flux of the FD150 through the insert with no cells and that with cells remained constant over time. It was decided, based on these data, that there was no need to go beyond 60 min leakage time to get a consistent leakage for each dextran for the following experiments. It should be noted that statistical analysis was performed on this and future percentage data only after it had been subjected to an Arcsine conversion. This is an angular transformation that stretches out both tails of a distribution and compresses the middle, approximating the data to a more normal distribution.

4.3.3

PERMEABILITY OF THE HMEC-1 CELL-LINE TO KNOWN VASO-ACTIVE AGENTS WHICH ACT VIA A VARIETY OF MECHANISMS

In Chapter 2, the ECV304 endothelial cell-line was investigated for its ability to respond to a variety of vaso-active agents, so a similar question was posed regarding the HMEC-1 cell-line. The chemicals were chosen to represent effects from a variety of signaling pathways known to be involved in the regulation of endothelial permeability.

HMEC-1 cells were seeded and grown to confluence over 72 hrs. The compound of interest was then exposed to the cells, for the required time (section 4.2.2.3), and the leakage of dextran was determined (section 4.2.2.3). Data was expressed as percent leakage of the dextran.

4.3.3.1

EFFECT OF EGTA ON THE PERMEABILITY AND ADHERENS JUNCTION MOLECULES OF HMEC-1 CELLS

EGTA and EDTA have been used extensively to investigate the importance of extracellular calcium in controlling endothelial permeability both *in-vivo* (Kern and Malik, 1985) and *in-vitro* (Shasby and Shasby, 1986). Shasby and Shasby (1986) reported that depletion of extracellular calcium by EGTA caused retraction of porcine pulmonary artery endothelial cells and a centripetal retraction of the peripheral band of actin in individual cells. These effects resulted in an increase in albumin permeability and were reversible once calcium was returned to the cultures. For these studies EGTA was used, as it is a competent calcium chelator in the presence of magnesium, and studies by

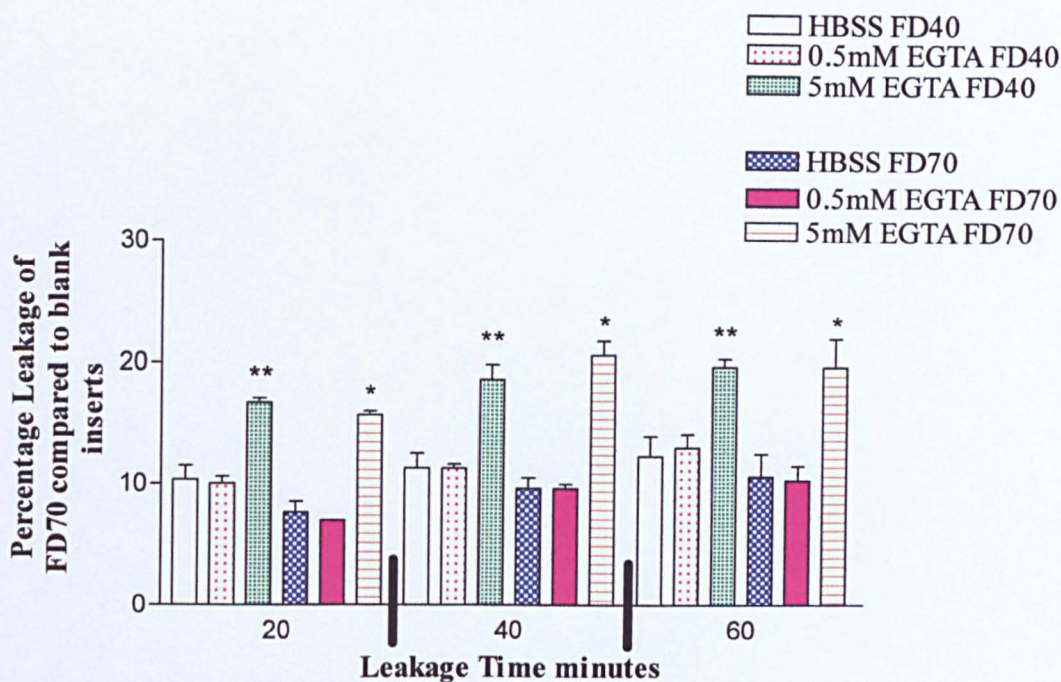


Figure 4.10: Effect of EGTA on monolayer permeability of HMEC-1 cells.

Percentage leakage of both FD40 and FD70 significantly increased following exposure to 5mM EGTA (** = $p < 0.01$, * = $p < 0.05$, compared to HBSS control for each dextran at each time point). Mean \pm SEM from triplicate inserts for each variable, ($n=3$).

Lampugnani *et al.*, (1992) showed that it strongly affected the expression of VE-cadherin in HUVEC.

At 5mM, EGTA caused a significant increase in the percentage leakage of both FD40 and 70 when compared to the relevant HBSS controls throughout the leakage time (figure 4.10). EGTA, at either 0.5 or 5mM, had no effect on the metabolic capacity of the cells to reduce Alamar BlueTM (figure 4.11), indicating that the alteration in permeability was not due to a significant cytotoxic effect on the cells.

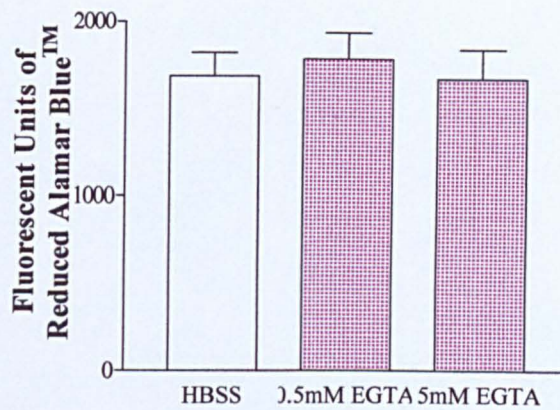


Figure 4.11: Effect of EGTA on ability of HMEC-1 cells to metabolise Alamar Blue™. EGTA had no effect on the cells' ability to metabolise Alamar Blue™ at either concentration investigated. Figure shows mean values from triplicate inserts for each variable, error bars show standard error of the mean, (n=3).

Control cultures of HMEC-1 exhibited a population of essentially uniformly sized, tightly packed polygonal or spindle-shaped cells (figure 4.12a). No gaps were observed between the cells. The addition of 0.5 or 5mM EGTA had little effect on the cells' morphology (figure 4.12b and c), confirming that there was no cell loss following exposure. VE-cadherin immunocytochemistry was performed separately to F-actin staining for this experiment and, therefore, the nuclei were visualised using propidium iodide. The expression and localisation of VE-cadherin in control cultures was localised to cell-cell borders as a continuous or discontinuous fluorescence (figure 4.13a). Exposure to 0.5mM EGTA did not affect VE-cadherin expression or localisation (figure 4.13c). However, 5mM EGTA completely obliterated VE-cadherin expression (figure 4.13b). The integrity of the endothelial monolayer was maintained with no intercellular gaps formed.

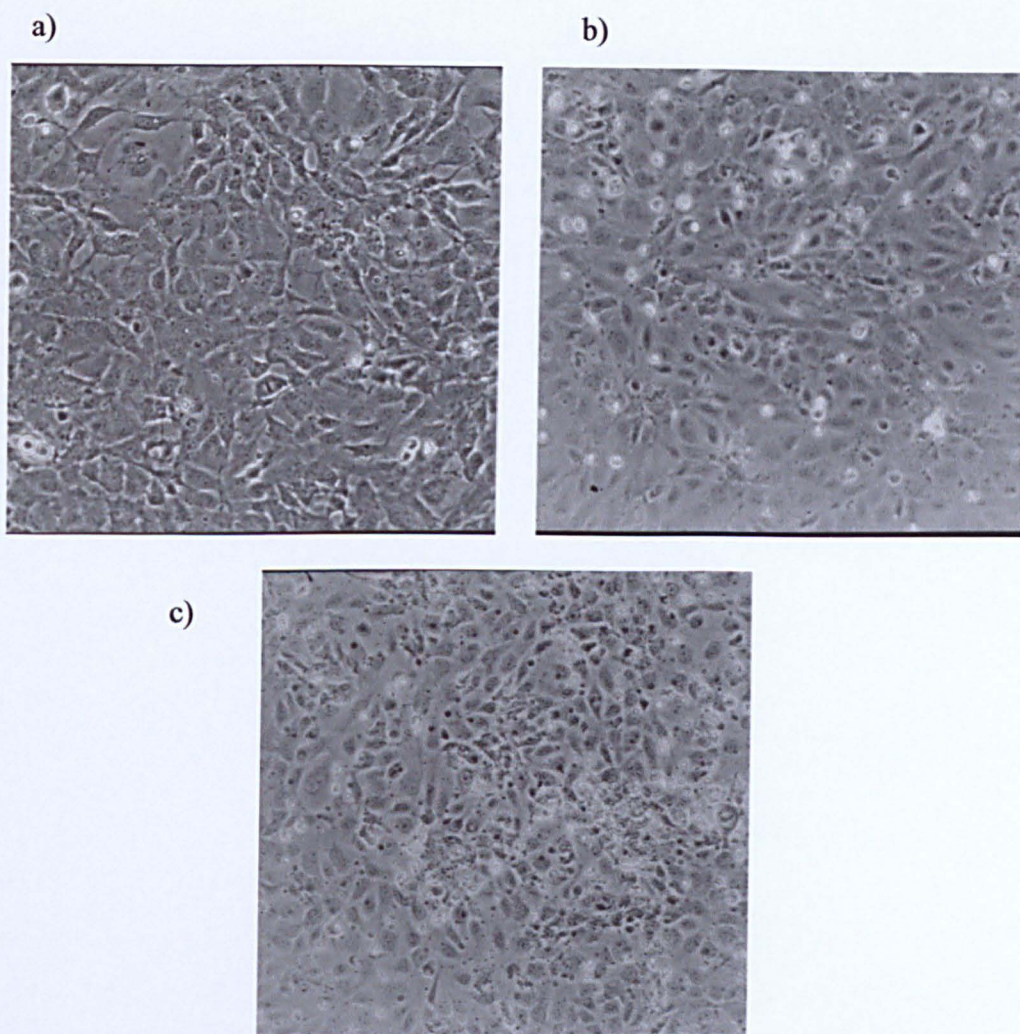


Figure 4.12: Phase-contrast micrograph of HMEC-1 cells exposed to either HBSS alone (a), 0.5mM (b) or 5mM EGTA in HBSS (c). Exposure to EGTA did not cause any discernible changes in the cells' morphology and left the monolayer intact. Magnification x250.

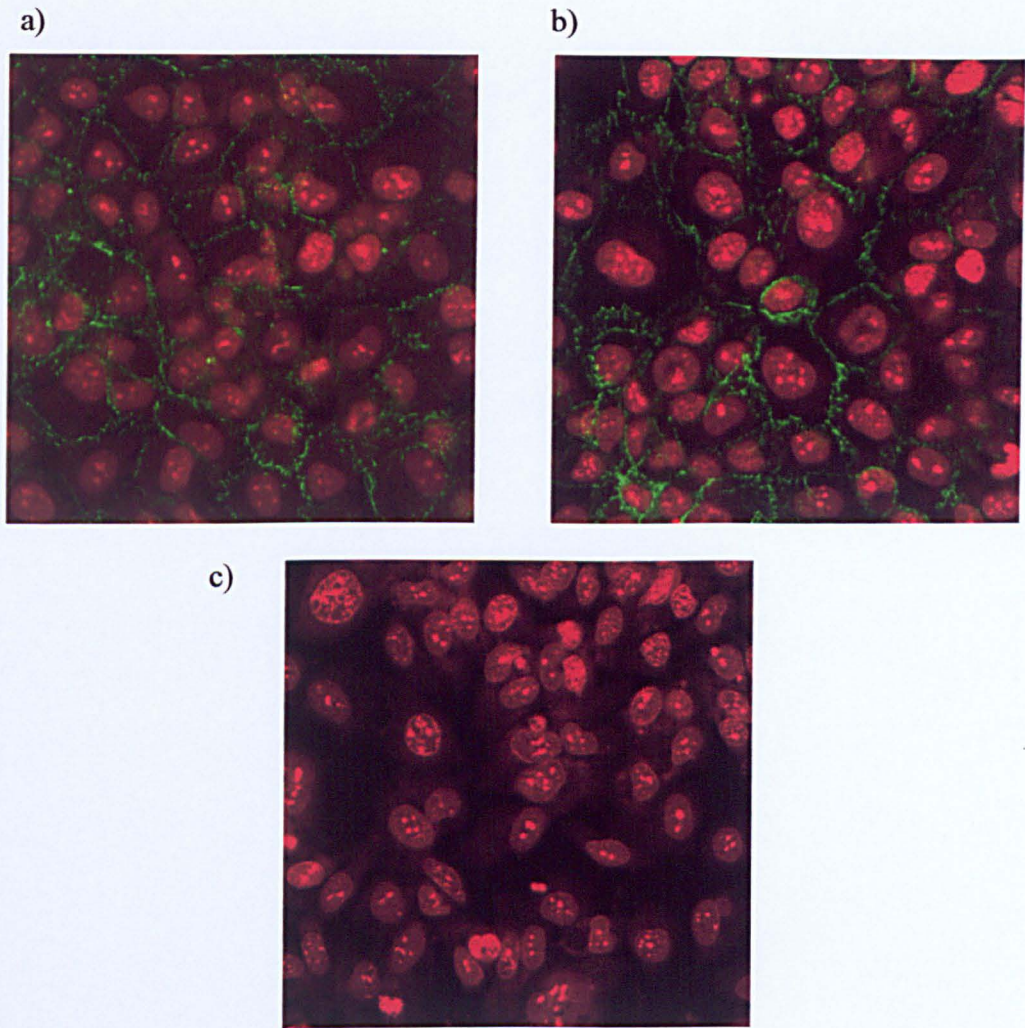


Figure 4.13. Confocal scanning micrograph of HMEC-1 cells immunostained for VE-cadherin (green) and nuclei counter-stained with propidium iodide (red). Cells were exposed to either HBSS alone (a), 0.5mM (b) or 5mM EGTA in HBSS (c). At 5mM, EGTA completely obliterated the expression of VE-cadherin. Magnification x 850.

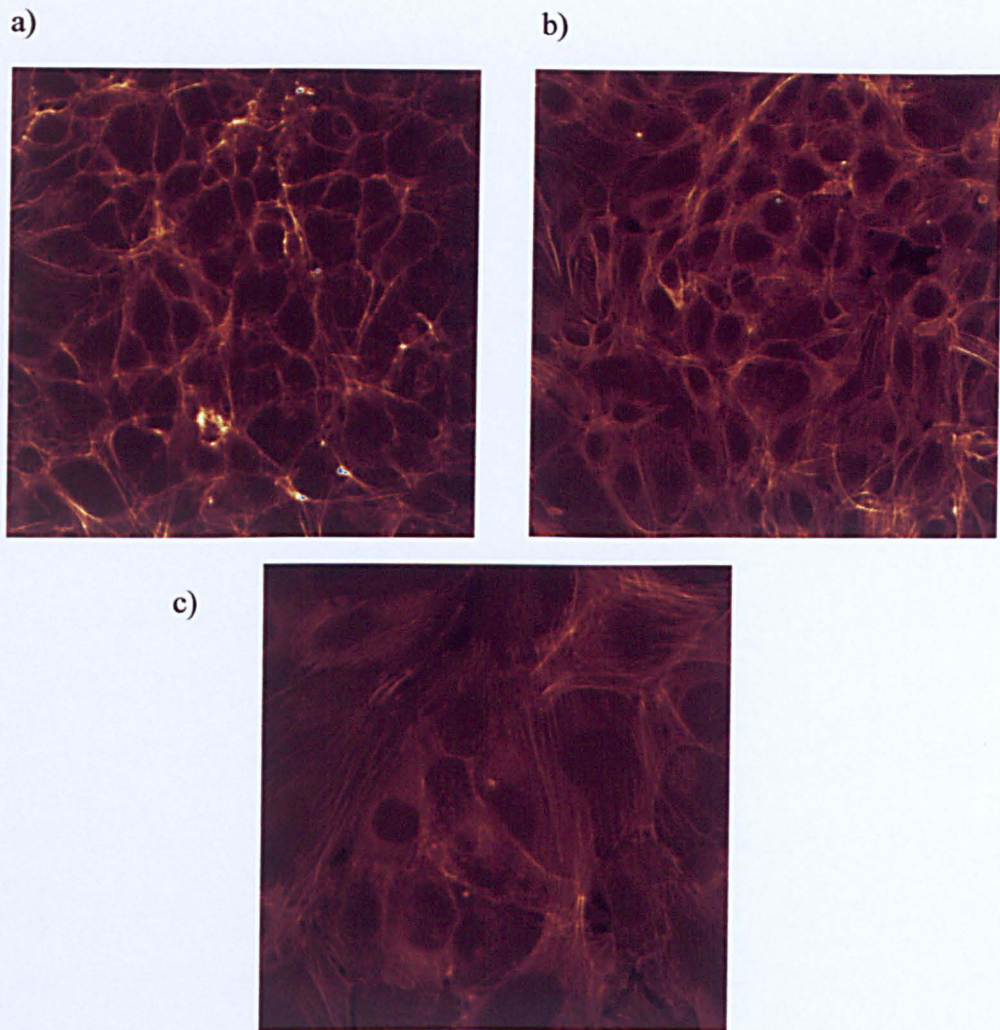


Figure 4.14. Confocal scanning micrograph of HMEC-1 cells FITC-phalloidin-stained for F-actin. Cells were exposed to either HBSS alone (a), 0.5mM (b) or 5mM EGTA in HBSS (c). HBSS control cultures and those exposed to 0.5mM EGTA did not differ in their expression and localisation of F-actin (b). At 5mM EGTA caused the loss of the dense peripheral band of F-actin, with the increased stress fibres (c). Magnification x 850.

Actin filaments in the control cultures of HMEC-1 were arranged as thin, dense peripheral bands, with some linear stress fibres in the cytoplasm along the cells' axes (figure 4.14a). The dense peripheral bands were closely apposed to each other, possibly overlapping. EGTA at 0.5mM did not alter F-actin expression (figure 4.14b), whilst at 5mM the dense peripheral band had disappeared and the stress fibres within the cells increased in frequency.

4.3.3.2

EFFECTS OF A23187 ON THE PERMEABILITY AND ADHERENS JUNCTION MOLECULES OF HMEC-1 CELLS

In addition to the role of external calcium, the importance of intracellular calcium levels was shown by Shasby *et al.* (1985), who reported that the calcium ionophore A23197 increased endothelial albumin leakage. Ionophores are small hydrophobic molecules that dissolve in the lipid bilayer of cell membranes, increasing their calcium ion permeability. A23187 is a mobile ion carrier, shielding the charge of the transported ion so that it can traverse the cell membrane (Alberts *et al.*, 1989). It is commonly used to increase intracellular calcium levels in intact cells. Many well-known vaso-active mediators regulate endothelial permeability by increasing intracellular calcium levels, e.g. histamine, bradykinin and thrombin (Curry, 1992). There is also some evidence that the ionophore may work by promoting the release of nitric oxide (NO) from the endothelial cells (Boulanger *et al.*, 1990). A23187 has been shown to act both *in-vivo* (Neal and Michel, 1995) and *in-vitro* (Haselton, 1992) to increase vascular and endothelial permeability respectively.

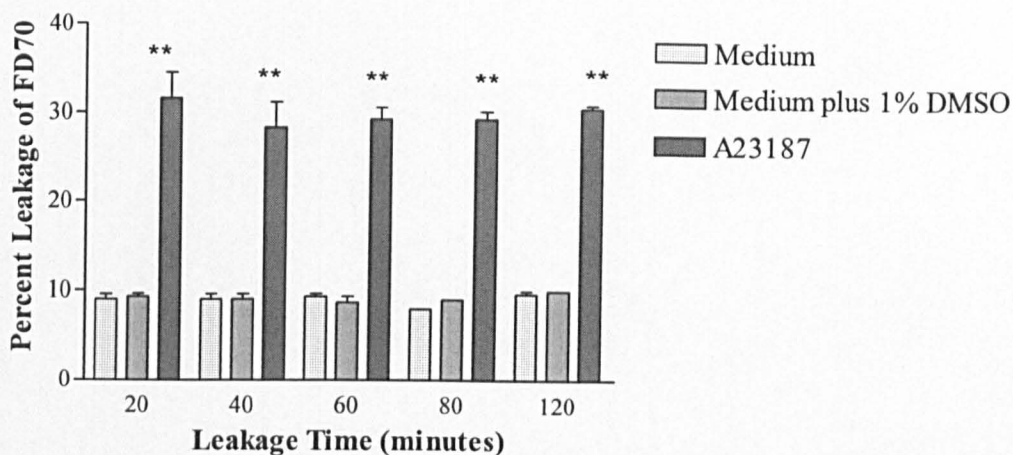


Figure 4.15: Effect of A23187 on monolayer permeability of HMEC-1 cells. Percentage leakage was significantly higher in cultures exposed to $100\mu\text{g ml}^{-1}$ A23197 (** = $p < 0.01$, compared control cultures). 1% DMSO did not affect the leakage. Mean \pm SEM from triplicate inserts for each variable, (n=3).

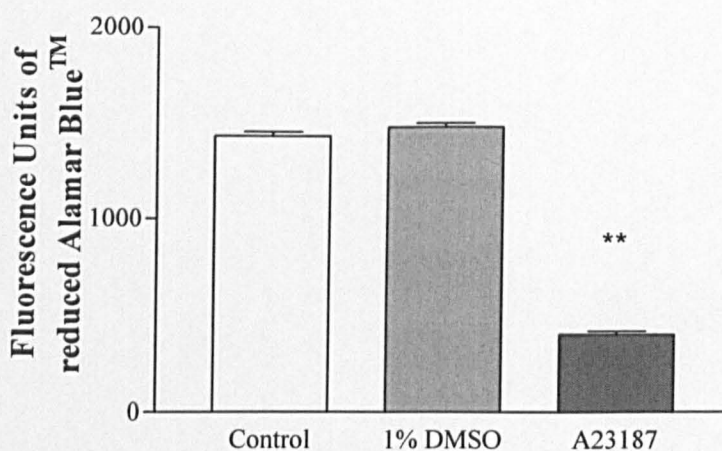


Figure 4.16: Effect of A23187 and DMSO on the ability of HMEC-1 cells to metabolise Alamar Blue™. 0.1% DMSO had no effect on the levels of reduced Alamar Blue™. A23187, however significantly lowered the amount of reduced Alamar Blue™ produced (** = $p < 0.01$, compared to control cultures). Mean \pm SEM from triplicate inserts for each variable, (n=3).

Exposure to $100\mu\text{g ml}^{-1}$ of A23187 significantly raised the permeability of the HMEC-1 monolayer to FD70 at all time points measured (figure 4.15). The leakage for A23187-treated cells remained significantly higher over the 120 minutes. The leakage remained at the same ratio, between the A23187-treated HMEC-1 monolayer and the blank insert, throughout the whole time course of the experiment even though the chemical itself was not present. This indicated that the changes in the monolayer resulting in elevated leakage occurred early, at or before 20 minutes, and remained constant; hence the percentage of the control remained constant. The dose chosen was based on the results with the ECV304 cell-line (section 2.3.3.2) where higher doses were cytotoxic; damaging the membrane and lower doses had no detectable effects on permeability. However, $100\mu\text{g ml}^{-1}$ of A23187 caused a significant decrease on the reduction of Alamar BlueTM ($p<0.01$, figure 4.16). A solvent control of 1% DMSO was used as A23187 was initially dissolved in DMSO at 10mg ml^{-1} ; this did not significantly affect FD70 permeability.

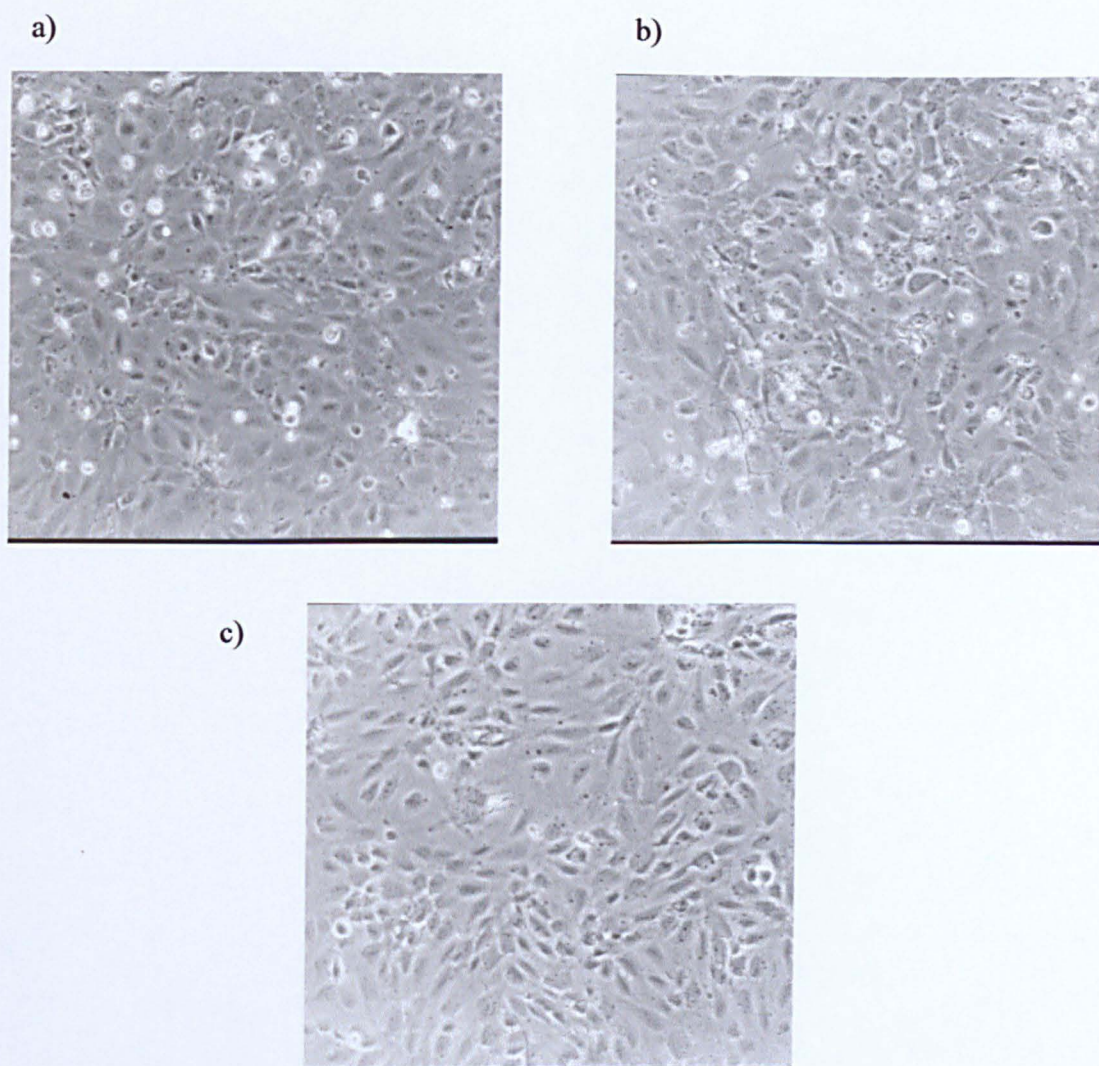


Figure 4.17: Phase-contrast micrograph of HMEC-1 cells exposed to either medium alone (a), medium containing 1% DMSO (b) or $100\mu\text{g.ml}^{-1}$ A23187 solution (c). Upon exposure to A23187, the HMEC-1 cultures appeared less densely packed, indicating a rearrangement in monolayer morphology. 1% DMSO did not appear to affect the cells' morphology. Magnification x 250.

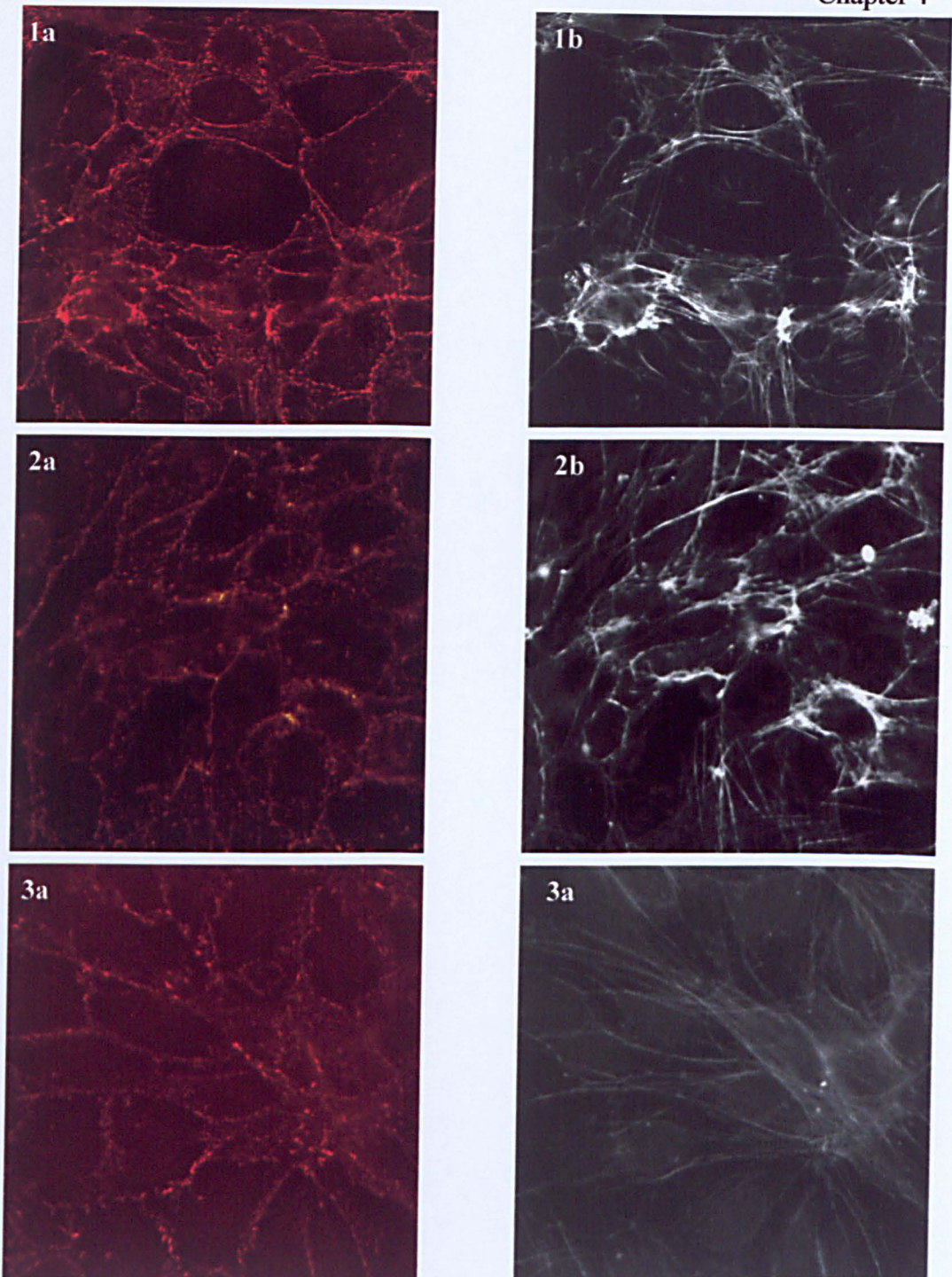


Figure 4.18. Confocal scanning micrograph of HMEC-1 cells immunostained for VE-cadherin (red) and F-actin (black and white). Cells were exposed to either medium alone (1a and b), medium containing 1% DMSO (2a and b) or $100\mu\text{g.ml}^{-1}$ A23187 solution (3a and b). 1% DMSO did not affect the expression or localisation of either VE-cadherin or F-actin. A23187 ($100\mu\text{g ml}^{-1}$) exposure resulted in a jagged, thicker VE-cadherin labelling at the cell edges, a diminishment of F-actin peripheral band intensity and an increases in the cytoplasmic FITC-phalloidin staining. Magnification x 850

The addition of $100\mu\text{g ml}^{-1}$ A23187 affected the cells' morphology (figure 4.17c). Whilst the monolayer appeared intact, the cells appeared less densely packed, indicating a rearrangement in monolayer morphology, either by cells loss or by a change in the previously observed tendency towards cell overlap and multilayering. The cultures exposed to 1% DMSO were not different to control cells (figure 4.17a and b). A23187 appeared to alter the expression of VE-cadherin, with a jagged staining pattern observed, and the area that contained staining at the cell edges appeared thicker (figure 4.18, 3a). However this was difficult to ascertain and may not be subjective as the control cultures expressed VE-cadherin in a heterogeneous pattern (figure 4.18, 1a) F-actin expression appeared less dramatic than in control cultures (figure 4.18, 1b and 3b), with a fainter dense peripheral band and an increase in the general cytoplasmic glow within the cell. Stress fibres were less distinct. DMSO at 1% did not affect the VE-cadherin or F-actin expression or localisation (figure 4.18, 2a and 2b).

4.3.3.3

EFFECT OF COCAMIDO-PROPYLBETAINE (CAPB) ON THE PERMEABILITY AND ADHERENS JUNCTION MOLECULES OF HMEC-1 CELLS

CAPB is a mild, amphoteric surfactant. Clothier and Samson (1996) evaluated its effects on cell junctions in epithelial cells and showed that exposure to 1 or 2 mg ml^{-1} for 1 minute caused damage to the junctional components observed via TEM (Starzec *et al.*, 1999) and permeability to sodium fluorescein which returned to control levels within 24 hours.

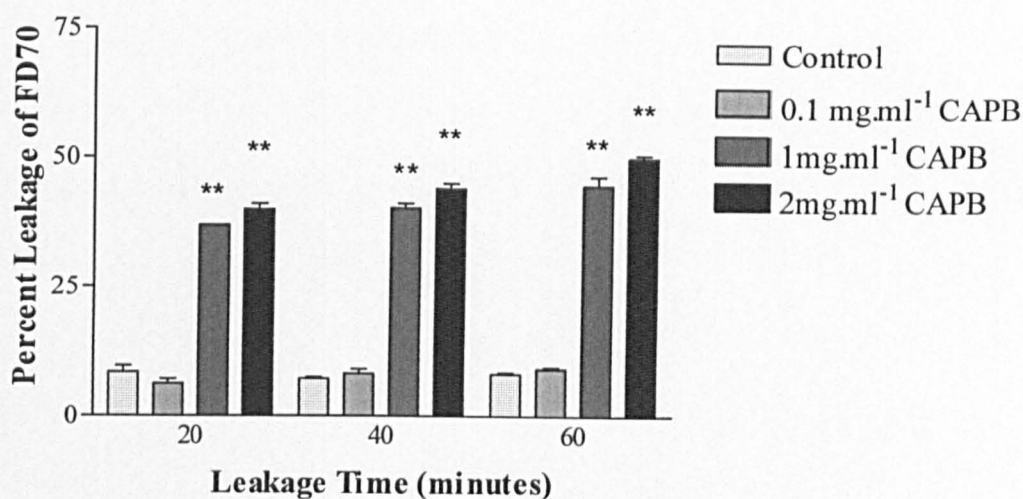


Figure 4.19: Effect of CAPB on monolayer permeability of HMEC-1 cells. CAPB at 1 and 2 mg ml⁻¹ significantly increased percentage leakage (** = $p < 0.01$, compared to control cultures at each time point). Mean \pm SEM from triplicate inserts for each variable, (n=3).

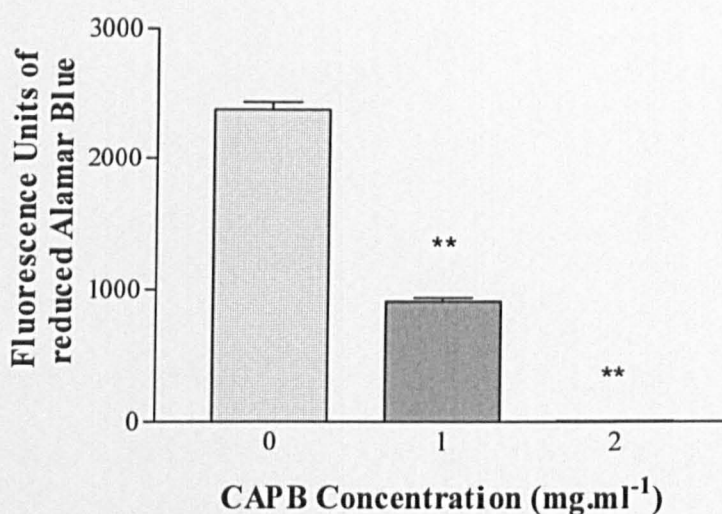


Figure 4.20: Effect of CAPB on ability of HMEC-1 cells to metabolise Alamar BlueTM. CAPB at 1 and 2 mg ml⁻¹ significantly decreased the amount of reduced Alamar BlueTM formed (** = $p < 0.01$, compared to control cultures). Mean \pm SEM from triplicate inserts for each variable, (n=3).

Exposure to CAPB at 1 and 2mg ml⁻¹ significantly increased the leakage of FD70 through the HMEC-1 monolayer ($p<0.01$), an effect that remained for up to 60 minutes following the removal of the surfactant (figure 4.19). This was linked to a reduction in Alamar Blue reduction of around 50% following exposure to 1mg ml⁻¹ CAPB, but a complete abolishment of the cells' reductive capacity when exposed to 2mg.ml⁻¹ CAPB (figure 4.20). Indeed after exposure to 2mg.ml⁻¹ CAPB, the morphology of the cells changed drastically (figure 4.21, c). The nuclei appeared less dense, picnotic, whilst after exposure to 1mg ml⁻¹, the monolayer exhibited intercellular gaps and some cellular damage. Expression of VE-cadherin following exposure to 1 and 2mg.ml⁻¹ CAPB changed from that seen in controls. 1mg ml⁻¹ caused a slight disruption in the continuity of VE-cadherin; however, it was still present at all cell-cell contacts (figure 4.22, 2a). This also shows that the monolayer remained intact. Two mg ml⁻¹ CAPB caused drastic changes in the cells which caused the disruption as revealed by the immunofluorescence staining (figure 4.22, 3a). Areas of the cells which remained intact, still expressed VE-cadherin in a similar pattern to control cultures. F-actin distribution was markedly affected, with a loss of the cell membrane-associated DPB (figure 4.22, 1b) at 1mg/ml (figure 4.22, 2b). Upon exposure 2mg ml⁻¹ CAPB the F-actin staining was present only as a general cytoplasmic glow that was more intense in the nuclear region (figure 4.22, 3b).

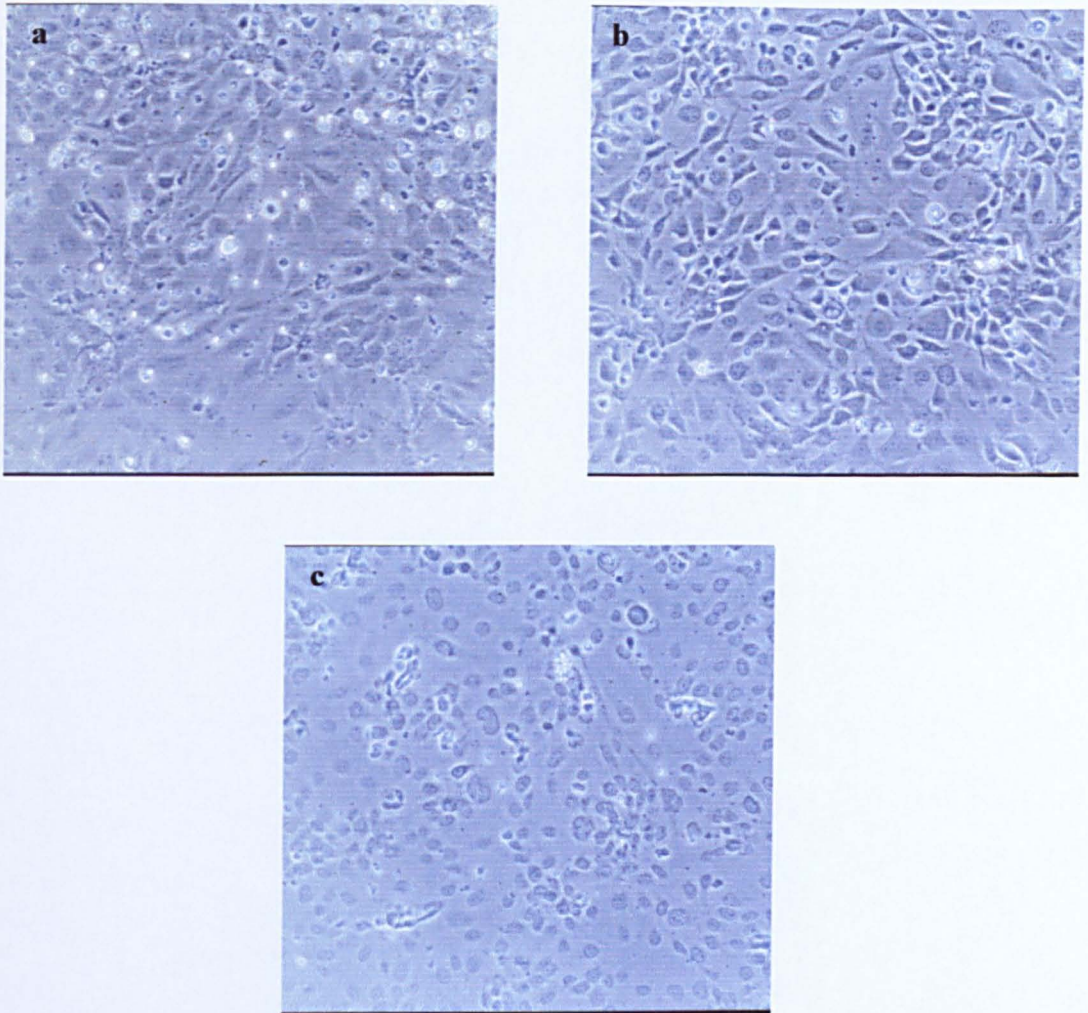


Figure 4.21: Phase-contrast micrograph of HMEC-1 cells exposed to HBSS alone (a), 1mg.ml^{-1} CAPB (b) or 2mg.ml^{-1} CAPB (c). Upon exposure to 1mg ml^{-1} CAPB intercellular gaps appeared in the monolayer (arrow), whilst at 2mg ml^{-1} the HMEC-1 cultures were drastically affected with picnotic nuclei. Magnification x 250.

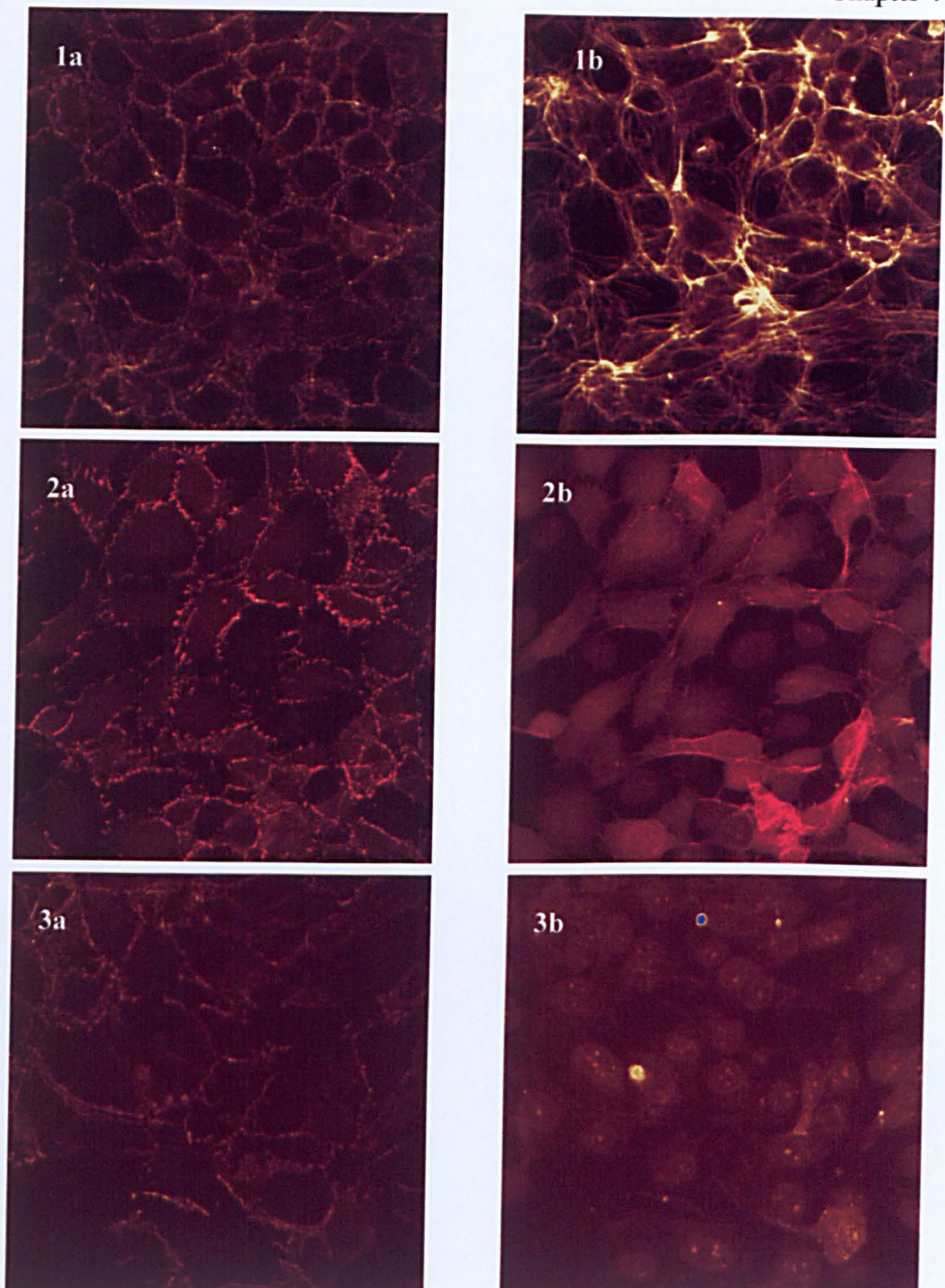


Figure 4.22. Confocal scanning micrograph of HMEC-1 cells immunostained for VE-cadherin (1a, 2a, 3a) and F-actin (1b, 2b, 3b). Cells were exposed to either HBSS alone (1a and b), 1mg.ml⁻¹ CAPB in HBSS (2a and b) or 2mg.ml⁻¹ CAPB in HBSS (3a and b). 1mg ml⁻¹ CAPB resulted in disruption of the continuity of VE-cadherin expression (2a) and a loss of the F-actin DPB (2b). At 2mg ml⁻¹, where the monolayer was still intact, VE-cadherin staining was still present, but disrupted (3a), whilst F-actin appeared as a general cytoplasmic glow, concentrated in the nuclear region (3b). Magnification x 850.

4.3.3.4

EFFECT OF PHORBOL MYRISATE-13-ACETYLESTER (PMA) ON THE PERMEABILITY OF THE HMEC-1 CELLS

It has been reported that the permeability of pulmonary artery endothelial cells was increased by the stimulation of protein kinase C (PKC), using phorbol-12, 13-dibutyrate (Shasby *et al.*, 1988), hydrogen peroxide (Johnson *et al.*, 1989), or thrombin (Lynch *et al.*, 1989). PMA was used as a diacylglycerol (DAG) mimic to stimulate the PKC second messenger system within the cells.

Exposure to PMA at both 10^{-6} and 10^{-7} M gave a significant increase in the leakage of FD70 after 50 minutes (i.e. 30 minutes exposure time), although no effect was observed following 35 minutes of leakage (i.e. 15 min exposure time, figure 4.23). The percentage leakage for 10^{-6} M PMA, compared to the control cultures, approximately doubled after 30 minutes in contact with the HMEC-1 cells. No effect of PMA on the reduction of Alamar Blue TM was observed (figure 4.24). PMA, at both concentrations tested, caused a disruption in VE-cadherin staining, showing discontinuous staining and free cell edges, devoid of fluorescence (figure 4.25, 2a and 3a). Additionally there was a dramatic reduction in the DPB of F-actin (figure 4.25, 2b and 3b) with punctate staining present in the cytoplasm of some cells (figure 4.25, 2b and 3b, arrows).

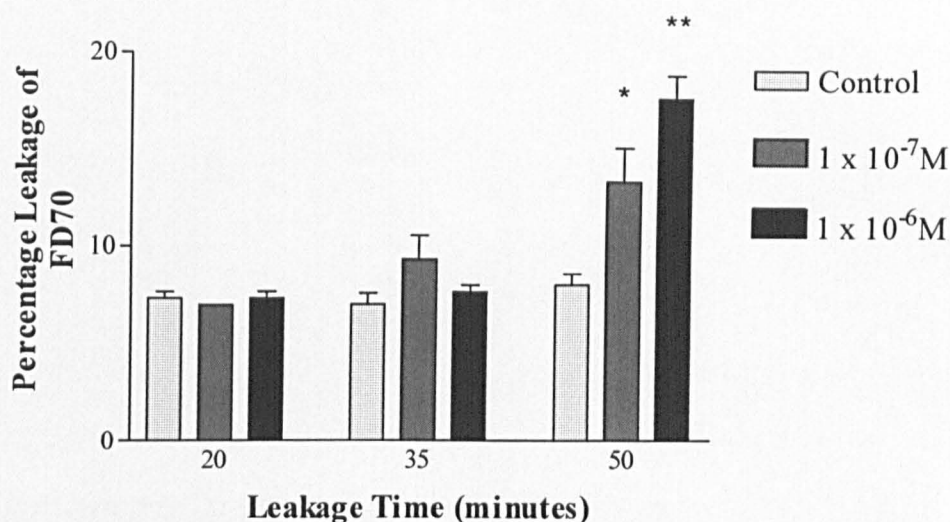


Figure 4.23: Effect of PMA on monolayer permeability of HMEC-1 cells. Both 10^{-6} M and 10^{-7} M significantly increased the percentage leakage of FD70 (* = $p < 0.05$, ** = $p < 0.01$ compared to control cultures. Mean \pm SEM from triplicate inserts for each variable, (n=3).

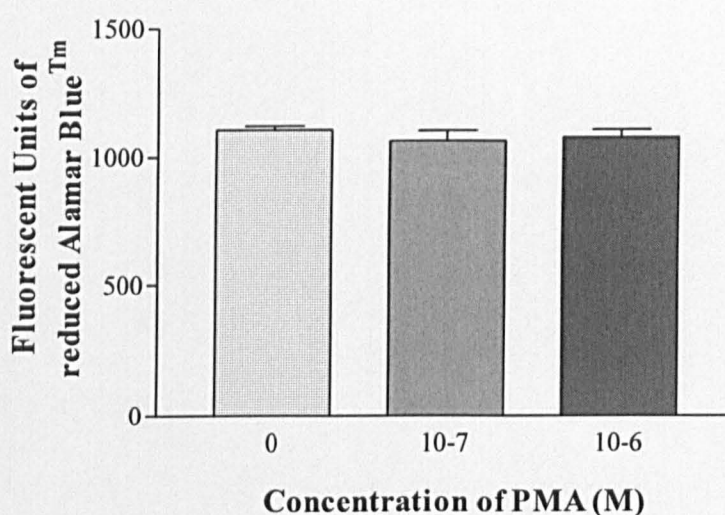


Figure 4.24: Effect of PMA on ability of HMEC-1 cells to metabolise Alamar Blue™. At the concentrations used, PMA did not significantly affect the metabolism of Alamar Blue™. Mean \pm SEM from triplicate inserts for each variable, (n=3).

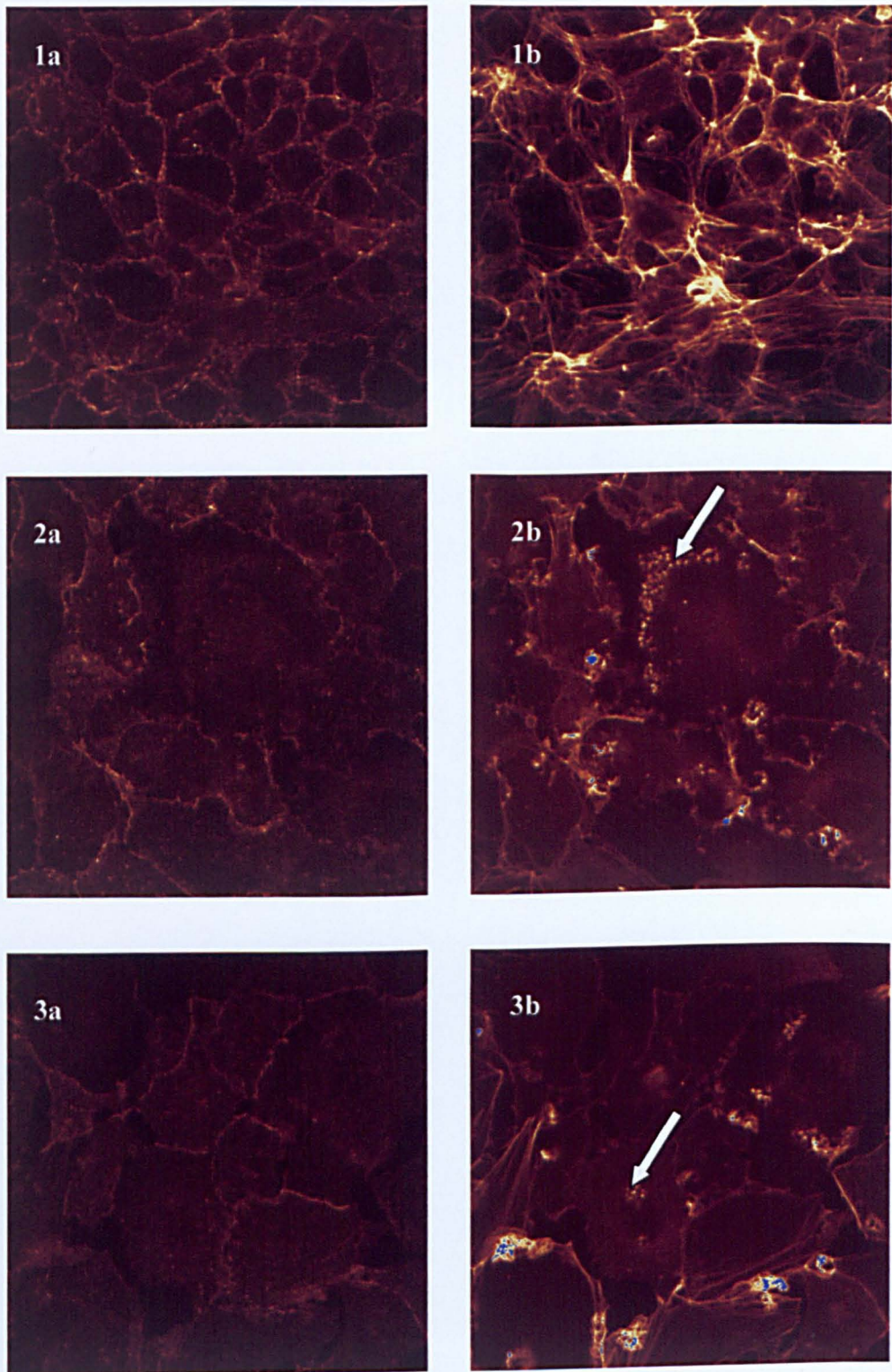


Figure 4.25: Confocal scanning micrograph of HMEC-1 cells immunostained for VE-cadherin (1a, 2a, 3a) and F-actin (1b, 2b, 3b). Cells were exposed to HBSS alone (1a and b), 10^{-7} PMA in 199/FCS (2a and b) or 10^{-6} PMA in 199/FCS (3a and b). PMA (at both concentrations) caused a disruption of the VE-cadherin expression, showing discontinuous staining and free cell edges (2a and 3a) and a reduction of the F-actin DPB (2b and 3b) with punctate staining observed in the cytoplasm of some cells (arrows). Magnification x 850.

Chemical	Concentration	Percentage FD70 Leakage (at 60 min)	Alamar blue reduction	VE-Cadherin	F-actin
None		$9.8 \pm 0.1\%$	Normal	Localised at cell-cell contacts.	Thin dense peripheral band + stress fibres
EGTA	0.5mM	$10.1 \pm 0.15\%$	Normal	As control expression	As control expression
	5mM	$19.3 \pm 0.09\%$	Normal	Loss of staining	DPB lost, with increased stress fibres
A23187	$100\mu\text{g.ml}^{-1}$	$29.3 \pm 0.02\%$	28% of control value	Less continual fluorescence at cell-cell contacts	DPB reduced and increased general cytoplasmic glow
DMSO	1% v/v	9.3 ± 0.3	Normal	As control expression	As control expression

Figure 4.26a: Effect of EGTA, A23187 and DMSO on VE-cadherin and F-actin of HMEC-1 cells and related to the monolayer permeability of 70 kDa dextran.

Chemical	Concentration	Percentage FD70 Leakage (at 60 min)	Alamar blue reduction	VE-Cadherin	F-actin
CAPB	0.1mg.ml ⁻¹	9.0 ± 0.01%	Normal	N/A	N/A
	1mg.ml ⁻¹	44.7 ± 0.04%	38% of control value.	Less continual	No DPB.
	2mg.ml ⁻¹	50 ± 0.01%	0% of control value.	fluorescence at cell-cell contacts	No DPB with a general cytoplasmic glow, concentrated at the nuclear region
PMA	10 ⁻⁷ M	13.2 ± 0.07%	Normal	Less continual	Reduction of DPB with
	10 ⁻⁶ M	17.6 ± 0.02%	Normal	fluorescence at cell-cell contacts, with free cell edges	occasional punctate cytoplasmic expression

Figure 4.26b: Effect of CAPB and PMA on VE-cadherin and F-actin of HMEC-1 cells and related to the monolayer permeability of 70 kDa dextran.

4.3.3.5

CONCLUSION OF THE PERMEABILITY STUDIES

In relation to the leakage of FD70, the individual controls for each chemical were not significantly different from one another, providing evidence that the HMEC-1 monolayer acted consistently as a barrier against this macromolecule. The average percentage leakage was $8.9 \pm 0.5\%$. The maximum percentage leakage through the HMEC-1 monolayer, $45 \pm 2\%$, occurred following exposure to 1mg ml^{-1} of the surfactant CAPB (2mg ml^{-1} was not considered due to its deleterious effect on the cultures). This was significantly higher than EGTA, A23187 and PMA (figure 4.27). As a surfactant, the direct effects on cell membranes were expected. The chemical that caused the second highest change in percentage leakage was $100\mu\text{g.ml}^{-1}$ of the calcium ionophore A23187, known to generically raise levels of intracellular calcium. Again this percentage leakage of $29.3 \pm 1.3\%$ was significantly higher than that of each of the other chemicals except for CAPB. EGTA gave a percentage leakage of $19.3 \pm 2.4\%$ which was significantly different to the leakage of A23187 and CAPB but not to PMA, which had a mean leakage of $17.7 \pm 1.2\%$. The chemicals themselves had no effects on the leakage of FD70 through a fibronectin-coated insert (data not shown). Therefore the effects noted are a direct result on the cellular layer and its barrier function. The initial experiments on the basal flow of dextrans through the HMEC-1 monolayer indicated that the basal percent leakage of FD70 was affected by the duration of the leakage time. With this group of experiments, however, no such change in percent leakage was observed over time in the control group, i.e. this was consistent over the longest time examined.

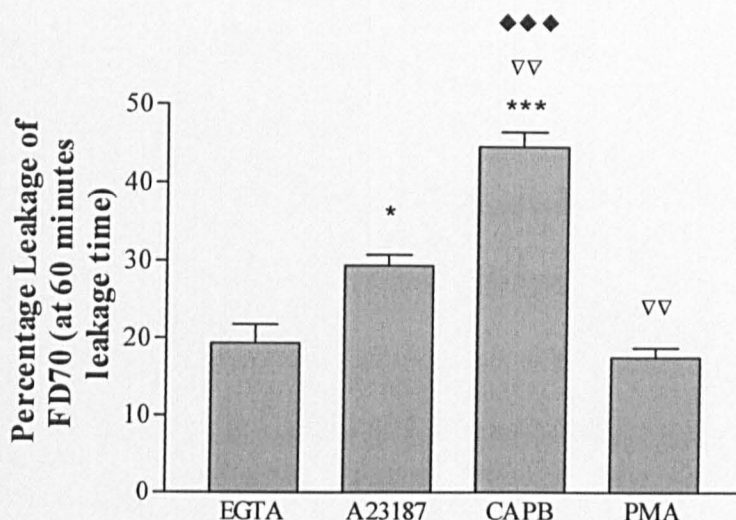


Figure 4.27: Percentage Leakage for FD70: a comparison between chemicals. Data taken as percentage leakage after exposure to chemical and 60 minutes leakage time. The dose of each chemical chosen was that which gave the highest percentage leakage but retained reasonable morphology of the HMEC-1 monolayer. Mean \pm SEM from triplicate inserts for each variable, (n=3). * - significantly different from EGTA, ∇ - significantly different to A23187, \blacklozenge - significantly different to PMA.

Thus the change in concentration of FD70 as the leakage continued was not great enough to alter the leakage rate. Similarly, the effects of exposure to 5mM EGTA and 100 $\mu\text{g}.\text{ml}^{-1}$ A23187 on dextran flux resulted in percent leakages that were constant over the entire leakage time. CAPB on the other hand gave a significant rise in percent leakage between 20 and 60 minutes ($p < 0.01$ for 1 $\text{mg}.\text{ml}^{-1}$ and $p < 0.001$ for 2 $\text{mg}.\text{ml}^{-1}$). Also PMA which, due to the modification of the method, had only 30 minutes leakage time, gave an increase in the percent leakage between 15 and 30 minutes (i.e. 35 and 50 minutes after the commencement of the experimental exposure to the PMA at

10^{-6} M ($p < 0.001$), whilst 10^{-7} M did not change significantly between these two time points.

4.4

DISCUSSION

Monolayers of HMEC-1 cell-line exhibited extensive regions of cell overlap with tortuous paracellular clefts, which is in agreement with *in-vivo* studies of the microvascular endothelium. This contrasts to large vessel endothelial cells where a more abut morphology is common with a much shorter region of cell-cell contact. Tight junctions could not be found ultrastructurally, and whilst pertinent TJ molecules, occludin and ZO-1 were expressed, they were not targeted to the cell-cell contacts. This indicated that, in this cell-line, only the adherens junctions were available for permeability regulation. Whilst not in agreement with the normal *in-vivo* scenario, this gave rise to a valuable cellular tool with which to observe the adherens junction in isolation.

The amount of dextran that crossed the confluent endothelial cell monolayer on the insert was much smaller than that which crossed the insert alone, indicating that the confluent endothelial monolayer functioned as an effective barrier to all the dextrans, i.e. those of 40, 70 and 150kDa. Ideally the permeability profile of the HMEC-1 cell layer should be as close to that observed normal *in-vivo* situation as possible. The flux of the dextrans across the cell monolayer was not directly proportional to the molecular weight of the dextrans, as the inserts alone had been. The flux of the 40 kDa dextran was much greater than that of either the 70 or 150kDa dextrans. Thus the monolayer was acting as a heteroporous system, discriminating between greater than and less than 40 kDa sizes as described for the *in-vivo* situation (Malik *et al.*, 1989). The barrier was less effective to FD40 with a 20% leakage of dextran through the confluent HMEC-1 layer while the rate for the FD70 and FD150 is 7.7% and 6.4%

respectively. The initial decline seen in percentage leakage indicated that the leakage was faster at first through the confluent cell monolayer, than through the no-cells insert. The precise reason for this phenomenon is not clear, but could be that the change in medium, that is part of the permeability assay, caused a transitory disruption of the barrier function. This possible disruption was enough to facilitate passage of the lower molecular weight dextrans FD40 and FD70, but not large enough to allow molecules as large as FD150. Hence, this could be an important influence if early and transitory modulation of permeability upon chemical exposure was to be investigated.

The HMEC-1 monolayer permeability was raised to varying degrees, following exposure to each of the chemicals investigated. Yamada *et al.*, (1990) showed a 2.7 times increase in albumin permeability in HUVEC cultures, following 60 minutes exposure to 2mM EGTA. With the HMEC-1 cultures, 5mM resulted only in a 2-fold increase of FD70, additionally the HMEC-1 cells showed no response to 0.5mM EGTA. In contrast, Yamada *et al.*, (1990) showed a 2-fold increase in permeability at this lower concentration with HUVEC. These cell-based differences could relate to the relative expression of VE-cadherin in the two cell-types. In chapter 2, data was presented showing that in HUVEC cultures the continuity of VE-cadherin was greater than that observed in the HMEC-1 cells. Thus the strength of the adherens junctions, between the cells, is likely to be stronger in HUVEC cultures. Indeed Lampugnani *et al.* (1995) showed that in HUVEC monolayers, junction maturity was related to a continuous pattern of VE-cadherin. EGTA is known to directly affect the binding of calcium to VE-cadherin that would lead to conformational changes in structure and the

weakening of homophilic bonds between cells (Ozawa *et al.*, 1990). If the bonds were already weaker in the HMEC-1 cells, then 0.5mM calcium may not have affected the already raised permeability. Langelier and van Hinsburgh (1988), exposed human umbilical artery endothelial cells to 5mM EGTA and this gave a 1 – 2 fold increase in horse radish peroxidase permeability (HRP). This supports the hypothesis of weak bonds between the HMEC-1 cells as the same fold increase in a 70 kDa molecule was observed in this project as that seen by Langelier and van Hinsburgh with the smaller 44kDa molecule (HRP). In Yamada *et al.*'s (1990) study, the basal percentage leakage of albumin across the HUVEC monolayer as a percentage of the no-cell insert (they used collagen-coated Transwell inserts, 0.4µm pore size) was comparable to the HMEC-1 cultures, namely approximately 10%. This contradicts our theory suggesting that the basal tightness of the junction is not the explanation. However Andriopoulou *et al.*, (1999) suggested that in endothelial monolayers with mature adherens junctions, the increase in permeability following histamine exposure was greater than in monolayers with immature junction. Alternatively the discrepancy could be related to the use of albumin to measure paracellular permeability. Albumin transfer is active as well as passive, but to negate this in the method most investigators flood the system with cold albumin prior to the experiment. It may be that external Ca^{2+} effects macromolecular transport across the endothelium in ways other than via the intercellular junctions, which may also be reliant upon the sub-type of endothelium studied.

Yamada *et al.* (1990) showed a doubling in albumin permeability following exposure to 10^{-5}M A23187 (60') using HUVECs. In this study, $100\mu\text{g.ml}^{-1}$ (2

$\times 10^{-4}\text{M}$) increased the leakage of the similar sized FD70 approximately three times, which would be in line with Yamada's data, were it to be extrapolated. PMA activates PKC, substituting for the endogenous messenger diacylglycerol, one of the products of phospholipid breakdown (Castagna *et al.*, 1982). Yamada *et al.* (1990), also used this to activate PKC, but, in contradiction to our results with HMEC-1 cells, they saw a decrease in the permeability rate of albumin following exposure of HUVEC to PMA for 60 minutes, from $46\mu\text{g}\cdot\text{ml}^{-1}$ to approximately $10\mu\text{g}\cdot\text{ml}^{-1}$. This again reveals a sensitivity of the HUVEC cells not noted with the HMEC-1's. Therefore, the observations presented in this study may be relevant to human microvascular endothelial cells only. Indeed Nagpala *et al.* (1996) showed that in the HMEC-1 cell-line PMA at 10^{-8}M for 30 minutes gave approximately a 7-fold increase in albumin permeability. Additionally Vuong *et al.* (1998) showed that at $2 \times 10^{-9}\text{M}$ PMA resulted in a 3-fold increase in HMEC-1 monolayers. Whilst this confirms our results that PMA causes increased endothelial permeability in the HMEC-1 cell-line, the magnitude of the increase was greatly muted in our cells, only showing a 2-fold increase at 10^{-6}M . These discrepancies could be partially explained by method variation. The inserts they used had pores of $0.8\mu\text{m}$, compared to $0.4\mu\text{m}$ with our system. A greater pore size could allow more albumin from luminal to abluminal compartment, however relating the flux to the control cultures should negate this. The volumes of media used in their permeability assay were $500\mu\text{l}$ in the insert and 25ml in the well, this could affect albumin flux, and indeed our data suggests (Chapter 3) that the presence of a hydrostatic pressure in the luminal compartment significantly enhanced

FD70 flux. However, whether an increased volume in the abluminal compartment would affect flux has not been confirmed.

No research investigating the effect of CAPB on the endothelial permeability or junctions has been published; however Clothier and Samson (1996) evaluated its effects on cell junctions in epithelial cells. They showed that permeability to sodium fluorescein increased following exposure to 1 or 2mg ml⁻¹ for 1 minute which returned to control values within 24 hours. Our data are in general agreement with this showing a significant increase in FD70 leakage after 20 minutes exposure to 1 or 2mg ml⁻¹ CAPB, whilst 0.1mg ml⁻¹ had no affect.

Both VE-cadherin and F-actin, molecules of the HMEC-1 intercellular adherens junctions responded to these chemicals in a variety of ways, decisively linking a change in permeability with altered expression and location of these molecules in the cells. A summary of results from all experiments in section 4.3.3 is tabulated in figures 4.26, a and b. EGTA (5mM) caused a complete loss of immunoreactive fluorescence of VE-cadherin, in agreement with studies on HUVEC by Lampugnani *et al.* (1992). The F-actin dense peripheral band (DPB) was lost, with an increase in stress fibres. Lampugnani *et al.* (1992) showed that EGTA caused the F-actin staining to diminish in intensity overall with greatly reduced DPB and the formation of stress fibres.

Exposure to A23187 resulted in more subtle changes in the VE-cadherin, causing slight disruption of the regions of continuous fluorescence, so that the majority of the membranes exhibited more discontinuous staining. Detection of this change however was considered to be potentially subjective

due to the heterogeneous nature of VE-cadherin staining in control cultures. F-actin expression altered such that the DPB was reduced in intensity, but was still visible. There appeared to be an overall fluorescent glow in the cells' cytoplasm, but stress fibres did not appear significantly different to control cultures. This correlates with a study by Piper *et al.* (1992) who showed that A23187 (10^{-5}M) caused the disintegration of F-actin fibres throughout porcine aorta endothelial cells.

CAPB caused similar, but clearer changes to the VE-cadherin expression as A23187, with a change to a fragmented expression at cell-cell contacts. The DPB of F-actin was abolished, along with (at 2mg ml^{-1} only) an increase in the general fluorescence of the cytoplasm. Whilst there are no published studies on the endothelial junctions or permeability and CAPB, it has been shown to cause damage to the junctional components of epithelial cells observed via TEM (Starzec *et al.*, 1999). This could indicate a common mode of action in the two cell types.

PMA caused VE-cadherin expression to change drastically, exhibiting, along with an increase in discontinuous staining, the detection of free cell edges. This possibly indicated a loss of cell-cell contact in these areas. Again the DPB of F-actin was reduced in intensity as reported by Wong and Gotlieb (1990); however PMA also caused F-actin to accumulate punctate regions of staining in the nucleus. Wong and Gotlieb (1990) reported elongation of the cells. Unfortunately phase images of HMEC-1 following PMA exposure were not collected in this study. The general cytoplasmic fluorescence seen in some of culture stained for F-actin could indicate that the alteration in expression is combined with an internalisation of the actin rather than degradation.

The results of this study verify that calcium (both internal and external) and protein kinase C play important roles in the regulation of permeability in the HMEC-1 cell-line, in a similar way to other endothelial cell-lines studied (Morel *et al.*, 1994; Rabiet *et al.*, 1996; Yu and Gotlieb, 1992). There is clear evidence to link alterations in the molecular architecture of the adherens junction with regulation of paracellular permeability in these cells. This cell-line was, therefore, deemed suitable to further investigate the role that the junctional molecules, especially VE-cadherin, play in permeability changes. Further, the development of an *in-vitro* model for the prediction of potential changes in the macromolecular permeability of the microvascular endothelium based on these cells could be feasible.

CHAPTER 5

ACTION OF HISTAMINE ON
PERMEABILITY AND ADHERENS
JUNCTION COMPONENTS OF THE
HMEC-1 CELL-LINE.

CHAPTER 5**ACTION OF HISTAMINE ON PERMEABILITY AND ADHERENS
JUNCTION COMPONENTS OF THE HMEC-1 CELL-LINE****5.1****INTRODUCTION**

In the previous chapters it has been shown that the endothelial cell barrier of HMEC-1 is permeable to fluorescently tagged dextrans of 40 to 150 KD in size. This permeability is low, representing only 1-2% of the total dextrans added, in a two hour period. In this chapter the effect of the well-known vaso-active mediator histamine on macromolecular permeability and the arrangement of VE-cadherin and F-actin in HMEC-1 cells were studied.

5.1.1**HISTAMINE**

Histamine and its actions were first described in 1910 by British physiologist Henry Dale (Dale and Laidlaw, 1910). Histamine is a potent mediator that serves

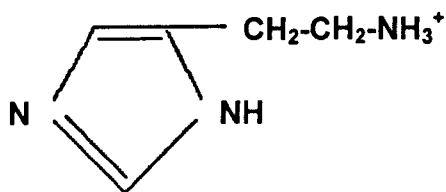


Figure 5.1: Histamine (amine-2-(4-imidazolyl)-ethylamine)

an important physiologic and pathophysiologic role in many diverse processes: allergies, vasoconstriction and dilatation, uterine contraction, gastric acid secretion, neurotransmission and immunoregulation (Hill, 1990). It is a basic amine – 2-(4-imidazolyl)–ethylamine (figure 5.1), formed from the amino acid histidine by histidine decarboxylase. It is found in most tissues of the body but in higher levels in the lungs, skin and GI tract. At the cellular level it is found in high concentrations in mast cells and basophils where it is held in intracellular granules. Other cell types can synthesise it, e.g. keratinocytes (Koizumi and Ohkawara, 1999). It is metabolised to N-methylhistamine by an N-methyl-transferase or to imidazole acetic acid by diamine oxidase. The N-methylhistamine can be further metabolized to N-methyl-imidazole acetic acid by monoamine oxidase.

5.1.2

HISTAMINE RECEPTORS

Histamine-mediated effects are mediated through four pharmacologically distinct subtypes of receptors, i.e., the H₁R, H₂R, H₃R and H₄R receptors, which are all members of the G-protein coupled receptor family. Histamine receptors display 7 transmembrane domains, an extracellular N-terminus, and a cytoplasmic C-terminus of variable length.

H₁R is distributed in the brain, most smooth muscle cells, cardiovascular system, adrenal medulla, gastrointestinal tract, genitourinary system, endothelial cells and lymphocytes (Hill, 1990). H₁ receptor plays roles in smooth muscle contraction, stimulation of nitric oxide formation, endothelial cell contraction, and increasing

vascular permeability (Barnes, 2001; Majno and Palade, 1961), all of which have close relationships with allergic conditions.

H₂R has been localised on vascular smooth muscle cells, neutrophils, CNS, heart and uterus of the rat (Hill, 1997). This subtype is chiefly linked to stimulation of adenylyl cyclase activity, and in the stomach leads to release of acid into the gastric lumen. When histamine binds this receptor it leads to smooth muscle relaxation, inhibition of lymphocyte function and alteration of gastric acid secretion.

H₃R, the third subtype of histamine receptor, is primarily expressed in the brain. They exist in histaminergic neuronal pathways in the brain and periphery and function to limit histamine synthesis and release and also to modulate the release of other important transmitter amines. Several studies using H₃ selective agonists revealed that H₃ receptor couples to pertussis toxin-sensitive Gi/o protein causing a decrease in the cellular levels of cAMP (Schneider *et al.*, 2002).

H₄R is the most recently discovered histamine receptor. A novel orphan G-protein coupled receptor, it has been cloned and characterized and is most closely related to H₃R (~37% homology). Unlike H₃R, H₄R has a distinct tissue distribution and it is localized in the peripheral blood leukocytes, spleen, thymus and colon. Mammalian cells expressing H₄R were demonstrated to bind and respond to histamine in a concentration-dependent manner. In functional assays, an H₃ receptor agonist, R-(a)-methylhistamine, but also a H₃ receptor antagonist, clobenpropit, and a neuroleptic, clozapine, activated H₄R-expressing cells (Schneider *et al.*, 2002).

5.1.3

ACTION OF HISTAMINE ON THE ENDOTHELIUM

The endothelium of vessels is one of the primary tissues affected by histamine, producing a marked increase in vascular permeability (particularly in postcapillary venules). Additional cellular responses include prostacyclin synthesis and synthesis of platelet activating factor, (Hill, 1997).

The oedema caused by histamine is associated with the separation of adjacent endothelial cells from one another (Majno and Palade, 1961). This mechanism of cell separation remains incompletely understood. Agents that disrupt actin filaments or that disrupt calcium-dependent cell-cell adhesion cause oedema through separation of adjacent endothelial cells. One hypothesis is that the loss of tethering between cells unbalances the opposing relationship between the constitutive centripetal intracellular cytoskeletal tension and the cell-cell tethering (Moy *et al*, 2002). Alternatively others (Schnittler *et al.*, 1990) have suggested that the separation involves an active contraction by actin and myosin. When histamine binds to an H₁ receptor on an endothelial cell it initiates a signal transduction cascade that results in an increase in cell calcium and diacylglycerol (DAG) (Carson *et al.*, 1989). This could lead to the phosphorylation of the 20-kD myosin light chain (MLC₂₀) by myosin light chain kinase (calcium dependent) or by PKC (calcium and DAG dependent). This acute increase in light chain phosphorylation could then increase actomyosin contraction and centripetal tension. Indeed Carson *et al* (1999) showed that histamine does increase the phosphorylation of MLC₂₀. Calcium binds to calmodulin inducing activation of

calcium/calmodulin dependent MLCK. This then promotes actin-myosin interaction by phosphorylation of MLC_{20} . Calcium signalling could also regulate VE-cadherin function, therefore mediating permeability by interfering with VE-cadherin interactions (Corada *et al.*, 1999; Rabiet *et al.*, 1996; Vouret-Craviar *et al.*, 1998). Alternatively the signalling cascade initiated by histamine may lead directly to phosphorylation of junctional adhesion molecules. This has subsequently been shown to occur in the HMEC-1 cell-line (Andripoulou *et al.*, 1999) at the same time as we were just finishing off the work in this chapter. However the dynamics and percentage changes in VE-cadherin expression reported here are novel.

Following the confirmation that the HMEC-1 cells could respond to a range of chemicals known to effect endothelial permeability, the aim of this chapter was to investigate the response to the well-known inflammatory mediator histamine. In terms of an *in-vitro* model this would then act as a positive control in future experiments with unknown chemicals or conditioned media.

5.2

MATERIALS AND METHODS

5.2.1

MATERIALS

5.2.1.1

Chemicals and Reagents

Histamine dihydrochloride and Neutral Red were purchased from Sigma, Poole, UK. Other chemicals and reagents are as for pervious chapters.

5.2.2

METHODS

5.2.2.1

Histamine exposure – Original permeability method.

HMEC-1 cells were seeded in TranswellTM inserts as in section 4.2.2.1. Following 72hrs, media was removed and 200µl of a 10⁻⁵M histamine dihydrochloride solution in culture medium was applied to the luminal compartment for 10 minutes at 37°C. The agonist-containing medium was removed, the monolayer washed with 500µl of HBSS and its permeability determined with FD40, FD70 and FD150 as in section 4.2.2.1.

5.2.2.2

METHOD VARIATIONS TO MEASURE THE EFFECT OF HISTAMINE ON HMEC-1 MONOLAYER PERMEABILITY

5.2.2.2.1

'Above and Below' permeability method.

Using treatment both above and below the monolayer ensured that histamine would be available, wherever histamine receptors are located.

Cells were seeded and grown to confluence as in section 4.2.2.1. The exposure to histamine was undertaken as in section 5.2.1 with the following modification. The media was removed from the basolateral compartment and 700µl of 10^{-5} M histamine solution was added for 10 minutes at 37°C. The agonist-containing medium was removed, the monolayer washed with 500µl of HBSS and its permeability determined with FD40, FD70 and FD150 as in section 4.2.2.1.

5.2.2.2.2

'Bolus' permeability method

The bolus method ensured that the barrier function of the confluent monolayer, measured as leakage of the dextran could be observed during, rather than after, the exposure time of the histamine.

Cells were seeded and grown to confluence (section 4.2.2.1). The cells were washed with 500µl of HBSS and the inserts transferred into fresh wells containing 700µl of medium 199 (phenol red-free) with 10% FCS (199/FCS). 200µl of FD70

at 50 μ M was applied to the luminal compartment, above the cells. After 20 minutes at room temperature (approximately 23°C) a 10 μ l sample was removed from the basolateral compartment under each insert. This was to give an indication of the initial level of leakage, and thus confirm the confluence of the layer prior to histamine exposure. After a subsequent 10 min, (30 min total leakage time) 2 μ l of a 10⁻³M solution of histamine in media was added to the insert (final concentration 10⁻⁵M) and further 10 μ l samples were taken at 35, 40, 60, 80 and 120 minutes, i.e. 5, 10, 20, 40 and 90 minutes after the addition of histamine. 90 μ l of 199/FCS was added to the 10 μ l aliquots and the amount of fluorescence measured on the Cytofluor fluorescent plate reader at an excitation wavelength of 485/20nm and an emission wavelength of 530/25nm. 100 μ l of 199/FCS was also measured as the blank. During the assay, plates were alternately incubated at 37°C, 5% (v/v) CO₂ in air and at room temperature on an orbital shaker for 20 minutes at a time.

5.2.2.3

Histamine exposure for immunofluorescence studies

HMEC-1 cells were seeded onto 8-well chamber slides at 1.7 x 10⁵ cells ml⁻¹ (300 μ l/well) and incubated at 37°C in 5% CO for 72 hours. The chamber slides were pre-coated with 25 μ g/cm² of fibronectin as in section 4.2.2.4. Confluent cultures were exposed to 10⁻⁵M or 10⁻⁴M histamine dihydrochloride in culture medium for 1, 5, 10 or 15 minutes at room temperature. Two wells only on one chamber slide were used for each experimental condition (n=4). The agonist-containing medium was removed and the cells were stained for F-actin as

described in section 4.2.2.5 or immuno-labelled for VE-cadherin as in section 4.2.2.4.

5.2.2.4

Reversal of histamine effects for F-actin studies.

The cells were grown as described in section 5.2.1.3 and exposed to 10^{-5} M histamine in culture medium for 1 minute. The histamine was then removed and the cells washed briefly in 0.1% PBS/BSA. Agonist-free culture medium was then placed onto the cells for 4, 9 or 14 minutes after which time they were fixed as for 30 min in 1% paraformaldehyde at room temperature. Staining for F-actin was carried out as in section 4.2.2.5.

5.2.2.5

Counting method for quantifying the number of rounded cells.

To quantify the responses seen the numbers of rounded up cells were counted from phase contrast micrographs and expressed as a percentage of the numbers of cells observed. Twelve micrographs were used, taken at each time point, for the 10^{-5} M histamine exposure experiments, whilst seven micrographs were used from each time point in the 10^{-4} M histamine exposure experiments. Eight micrographs per time point were used in the recovery studies.

5.2.2.6

Counting method for quantifying VE-cadherin immunolabelling

In order to quantitate the localisation of VE-cadherin following histamine challenge at minimum of 9 images were taken from each permutation, using a random sampling method. Briefly the well was placed so that the top left corner could be viewed. A number was picked, blind, from 1-10, and the sample moved that number of fields of view (fov) over to the right. This randomly chose the starting point. An image was collected at x63 magnification. Micrographs were then taken every 6 fov across. When the side of the well was reached, the sample was moved 4 fov down and the procedure continued. The images were displayed on a 17 inch computer screen with a 10x10 grid placed over it. Where the VE-cadherin staining crossed a grid line the type of expression was noted. This could be either a) continuous, b) discontinuous or c) stitch (figure 5.4). These numbers were converted into a percentage of the total number of staining types counted. In addition the number of free cell edges observed, in the entire micrograph, were counted and expressed as a percentage of the number of cells (indicated by the number of nuclei).

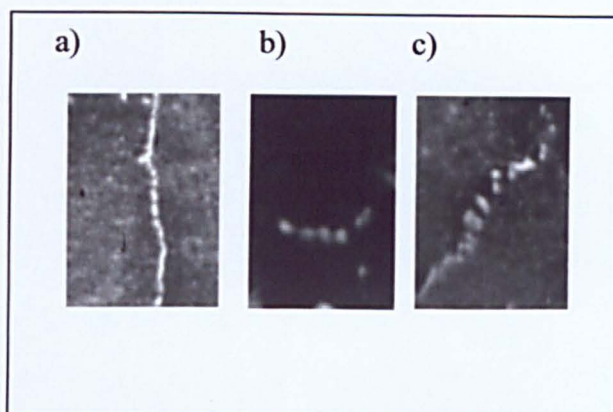


Figure 5.2: Types of VE-cadherin labelling in HMEC-1 cells. The staining appears either continuous along the cell-cell junction (a), more broken up, in a discontinuous manner (b), or appears as small lines of staining perpendicular to the cell membranes, termed ‘stitch’ (c).

5.2.2.7

Neutral red uptake (NRU) assay.

Endothelial cells were seeded into 96-well plates at 1.7×10^5 cells /ml (235 μ l) and incubated at 37°C in 5% CO for 72 hours. Cells were exposed to 10^{-5} M and 100^{-4} M histamine as described in section 5.2.1.3 and the agonist removed. Assessment of neutral red uptake was undertaken using a modification (Riddell *et al.*, 1986) of the method according to Borenfreund and Puerner (1985). Briefly, cells were incubated in 50 μ g ml $^{-1}$ of neutral red for 45 minutes. Following washes and solubilisation of the dye taken up by the cells, the solution was read on an Anthos Labtec spectrophotometric plate reader at 540nm with a reference filter of 405nm.

5.3

RESULTS

5.3.1

EFFECT OF HISTAMINE ON 40, 70 AND 150-kDa DEXTRAN LEAKAGE – ORIGINAL METHOD

The flux of the fluorescein dextrans, increased significantly over time across both control and histamine-treated cells (figure 5.3). Thus there is a continuous and reproducible leakage of these large molecules across the monolayers. The addition of 10^{-5} M histamine to the HMEC-1 monolayer did not alter the flux of either FD40, 70 or 150 compared with the control monolayers for any of the time points, i.e. up to 2hours leakage.

It was noticeable that the number of fluorescent units that leaked across the monolayer was greater for the FD150 than the FD40 and FD70. However, the level of binding of the fluorescent dye was not the same for each of the dextrans.

5.3.2

EFFECT OF HISTAMINE ON FD70 LEAKAGE – ‘ABOVE AND BELOW’ METHOD

Histamine did not elicit a response in the permeability profile of the HMEC-1 cells when applied to the luminal compartment of the TranswellTM inserts. It was considered possible that the histamine applied could swiftly diffuse through the cell layer and into the basal compartment of the system thus reducing the amount

of histamine available for interaction with its receptors. Therefore, the method was changed so that 10^{-5}M histamine was exposed to both the luminal and basal compartments. FD70 alone was investigated with this method and the flux of both medium control and histamine-exposed cells were not significantly different to that obtained using the original method (graphs not shown).

5.3.3

EFFECT OF HISTAMINE ON FD70 LEAKAGE – ‘BOLUS’ METHOD

Due to the transient nature of the action of histamine (Beynon *et al.*, 1993), it was considered important to assess the constant contact of histamine with the HMEC-1 monolayer throughout the measurement of permeability, to maximise the possible effects. With this in mind a small ‘bolus’ of histamine, 100x more concentrated than required was added to the luminal chamber of the Transwell™ insert during the leakage of FD70, i.e. in the presence of the FD70. The application of the bolus significantly raised the amount of FD70 that crossed the cell layer by 120min, total leakage time ($p < 0.01$). The difference although indicated was not shown to be significant prior to this time point (figure 5.4a). It is unlikely that the addition of a $2\mu\text{l}$ bolus to the $200\mu\text{l}$ FD70 solution would give rise to a significant change in the hydrostatic pressure. Also while the addition of a bolus did increase the leakage, when only medium was added, this disturbance of the monolayer did not account for the histamine effect since there was a further enhanced leakage when the bolus contained the histamine (figure 5.4b). Using this method to detect the effects from histamine exposure on the barrier function, gave a significant difference at 120

min total leakage time (figure 5.4b, $p < 0.05$). This was equivalent to a 90 min exposure to the histamine, as it was added after 30 min leakage time had already passed.

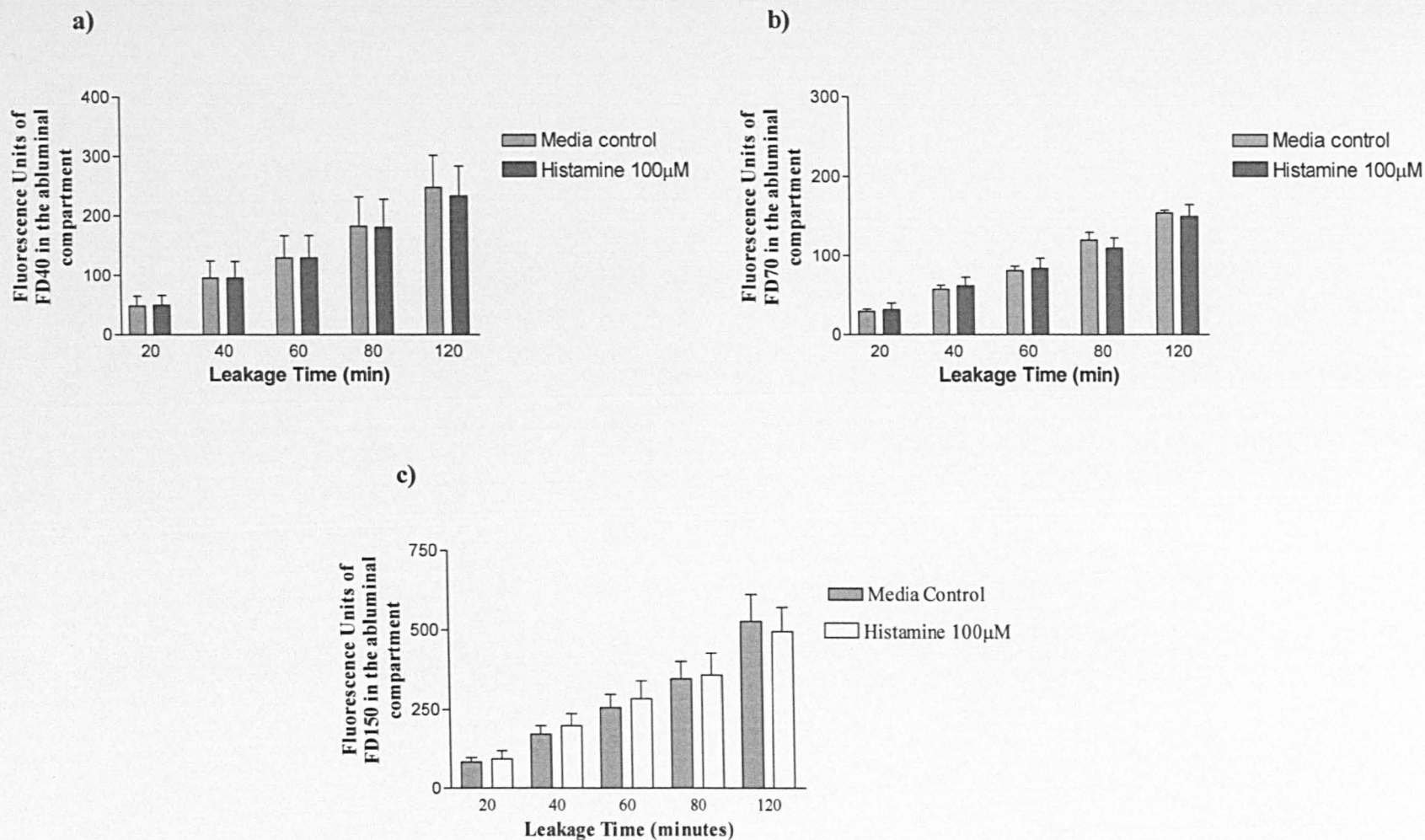


Figure 5.3: Effect of histamine on leakage of dextrans through HMEC-1 monolayer – ‘original method’. Leakage of a) FD40, b) FD70 and c) FD150. Histamine (10^{-5} M) did not significantly affect the flux of any of the molecules. Mean \pm SEM from triplicate inserts for each variable, (n=3).

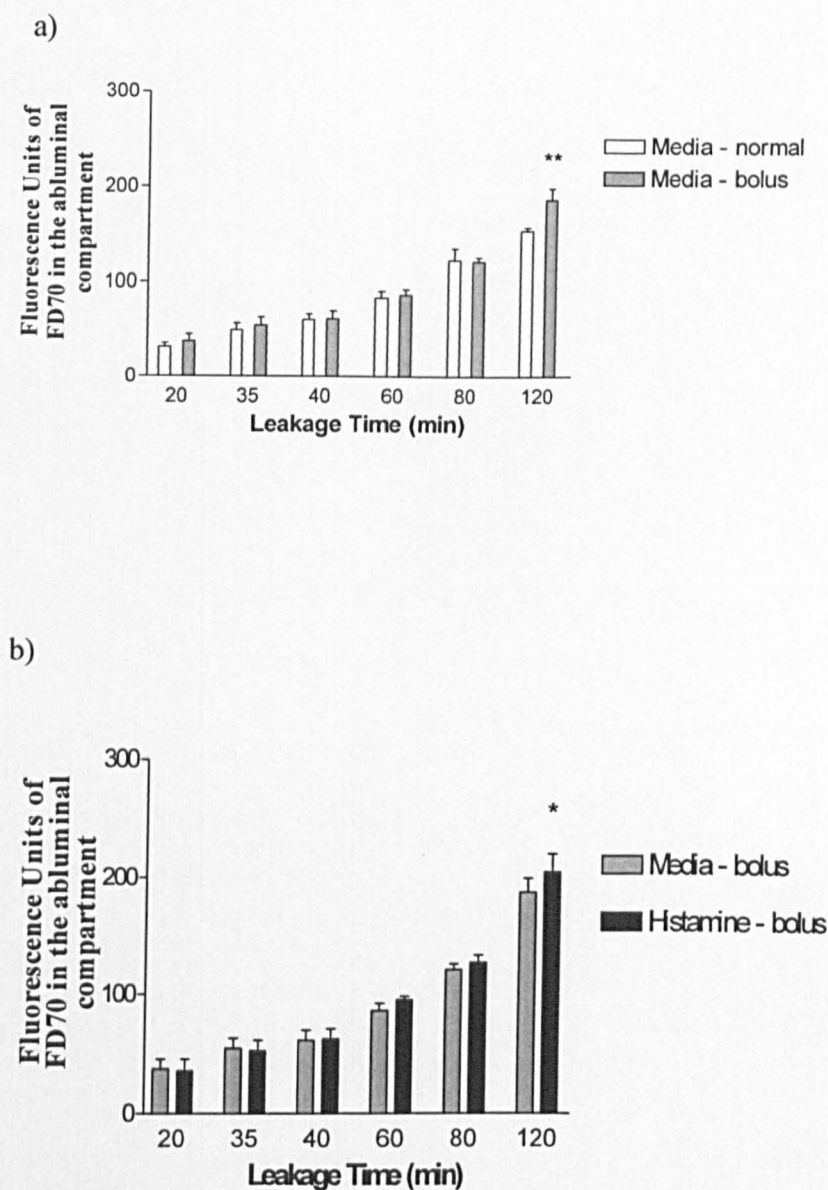


Figure 5.4: Permeability of the HMEC-1 monolayer to FD70 following application of the 'bolus' method without (a) or with (b) 10^{-5} M histamine. Whilst the bolus method did significantly increase the flux of FD70 after 120 min (** = $p < 0.01$, compared to timed control cultures), the addition of histamine (10^{-5}) using this method increased the flux still further (* = $p < 0.05$, compared to control cultures where the 'bolus' method was undertaken). Mean \pm SEM from triplicate inserts for each variable, (n=3).

5.3.4

EFFECT OF HISTAMINE ON HMEC-1 MORPHOLOGY AND F-ACTIN DISTRIBUTION

The HMEC-1 cells exhibited a polygonal morphology under the *in vitro* control conditions employed. F-actin was localised at cell margins (figure 5.5a). Fine filaments emanated from these peripheral bands and traversed the cells. After exposure to both 10^{-5} M and 10^{-4} M histamine, the percentage of rounded cells in the cultures increased linearly with exposure time (figure 5.6 & 5.5c). There were no significant differences between the effects of the two histamine concentrations used. Following 1 minute exposure to histamine the cells became more elongated than in control cultures. The dense peripheral band (DPB) of F-actin disappeared from the majority of the cells (figure 5.5b). The pattern of stress fibres changed dramatically, becoming less distinct. After 5 min exposure over 20% of the cells exhibited a rounded morphology (figure 5.6) and large gaps developed between cells as their morphology altered. In the rounded cells F-actin had a perinuclear localisation and a punctate appearance (figure 5.4b & 5.5c). Stress fibres were still observed in these rounded cells emanating from the perinuclear band. 10 minutes of histamine exposure resulted in cells of a similar appearance as that of the 5 minute exposure cultures.

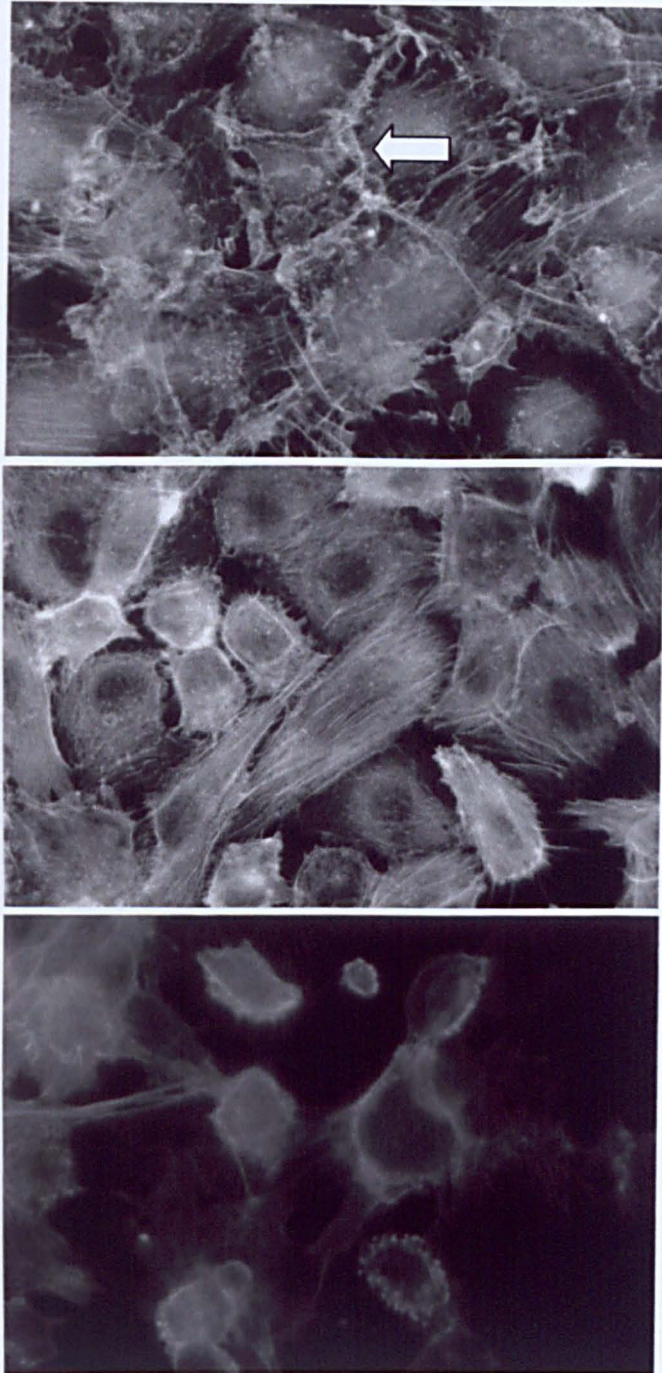


Figure 5.5: Fluorescein-phalloidin staining of F-actin in HMEC-1 monolayers: effects of histamine exposure. In control cultures (a) a peripheral band of F-actin (arrow) was observed at cell-cell contacts. 1 min of exposure to 10^{-5} M histamine (b) caused the cells to become elongated and gaps to appear in the monolayer. The majority of peripheral F-actin disappeared from the culture. After 15 min of exposure to histamine (c) many cells had a rounded morphology with perinuclear F-actin, some of which had a punctate appearance. No peripheral actin was present in these cultures. (Magnification x60, n=3)

Following 15 minutes in the presence of histamine, over 40% of the cells in the culture exhibited a rounded morphology (figure 5.6), displaying perinuclear F-actin (figure 5.5c). Few stress fibres and cell-cell contacts were evident. No DPB were present in the cells.

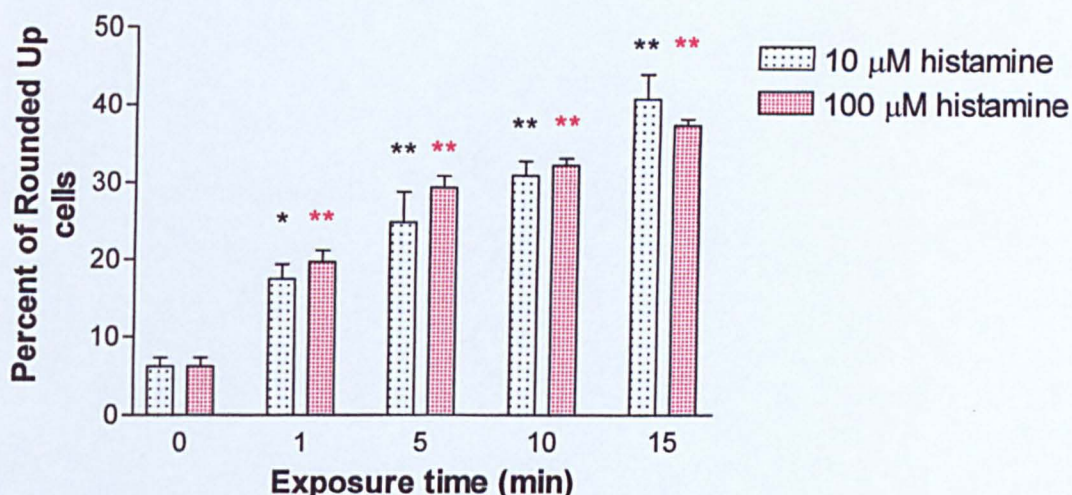


Figure 5.6: HMEC-1 response to histamine exposure. Cells were exposed to 10^{-5} M (black and white bars) and 100μM (green bars) histamine for 1, 5, 10 and 15 min. Effect on cell shape was determined by calculating the percentage of rounded cells in the cultures. The percentage of rounded cells significantly increased with the length of histamine exposure time with both histamine concentrations (* = $p < 0.05$ and **/** = $p < 0.01$, with respect to control cultures). No significant differences were observed between the effects of the two histamine concentrations. (Mean \pm SEM, $n=3$).

5.3.5

TOXICITY OF HISTAMINE

In order to ensure that these effects were not a toxic response to histamine the Neutral Red Uptake assay was undertaken (5.2.2.4). There were no significant differences between the control cultures and those cultures exposed to 10^{-5} M and 10^{-4} M histamine in their ability to take up this vital dye (figure 5.7).

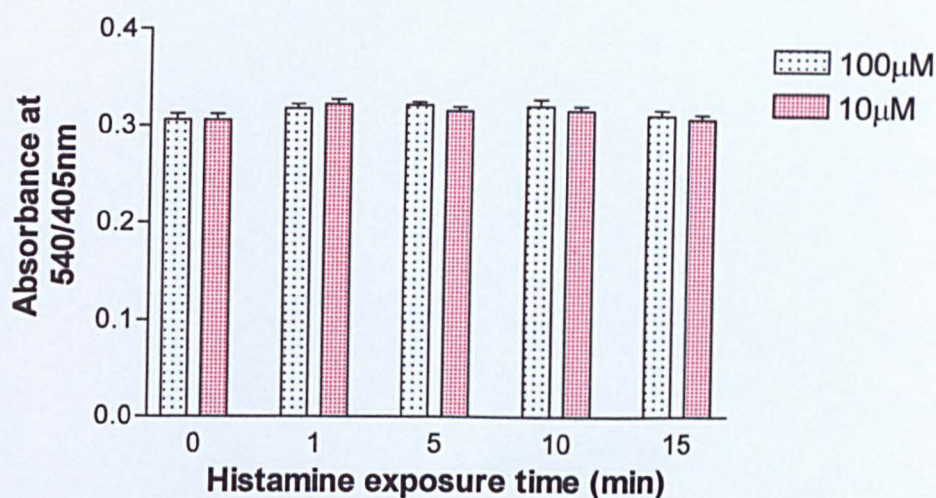


Figure 5.7: Effect of histamine on the uptake of the vital dye, neutral red in HMEC-1 cultures. There were no significant differences following histamine exposure at either 10^{-5} M or 10^{-4} M, (with respect to control cultures). Figure shows mean results from triplicate wells for each concentration and exposure time, error bars show standard error of the mean, (n=3).

5.3.6

RECOVERY OF HMEC-1 F-ACTIN ARRANGEMENT FOLLOWING HISTAMINE EXPOSURE

To assess the potential of the HMEC-1 cells to recover their normal F-actin arrangement, cells were exposed to 10^{-5} M histamine for 1 minute then normal media was replaced for a further 4, 9 or 14 min as in section 5.2.2.4. After 4 minutes in normal media the morphology and F-actin distribution in the culture was very similar to that after 1 minute exposure to histamine (figure 5.8a).

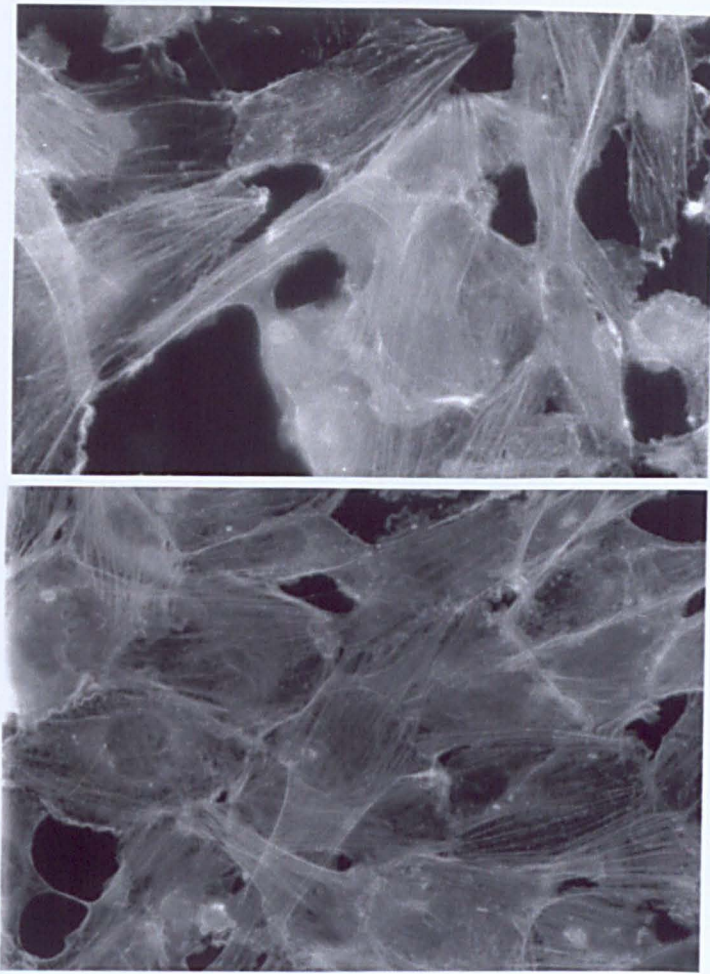


Figure 5.8: Fluorescein-phalloidin staining of F-actin in HMEC-1 monolayers: recovery of cells following histamine exposure. HMEC-1 cells were exposed to 10^{-5} M histamine for 1 min followed by 4, 9 or 14 min in agonist-free media. After 4 min in normal media (a) the cells' appearance was similar to cultures exposed to histamine for 1 min only. However after 14 min in agonist-free media (b) the cells had returned to a polygonal shape. Peripheral F-actin was present again in the majority of cells. (Magnification x60, n=3).

After 9 minutes in normal media the HMEC-1 cells showed signs of recovery. The cells remained elongated with gaps still present between cells. However, more peripheral actin was present than in the 1 minute histamine exposed cultures. After 14 minutes in normal media the cells' returned to a polygonal shape and peripheral F-actin distribution returned to normal (figure 5.8b), with the exception of a few cells where gaps were still evident. The percentage of completely rounded cells in the cultures decreased significantly after 9 minutes in agonist-free media ($p < 0.01$), (figure 5.9).

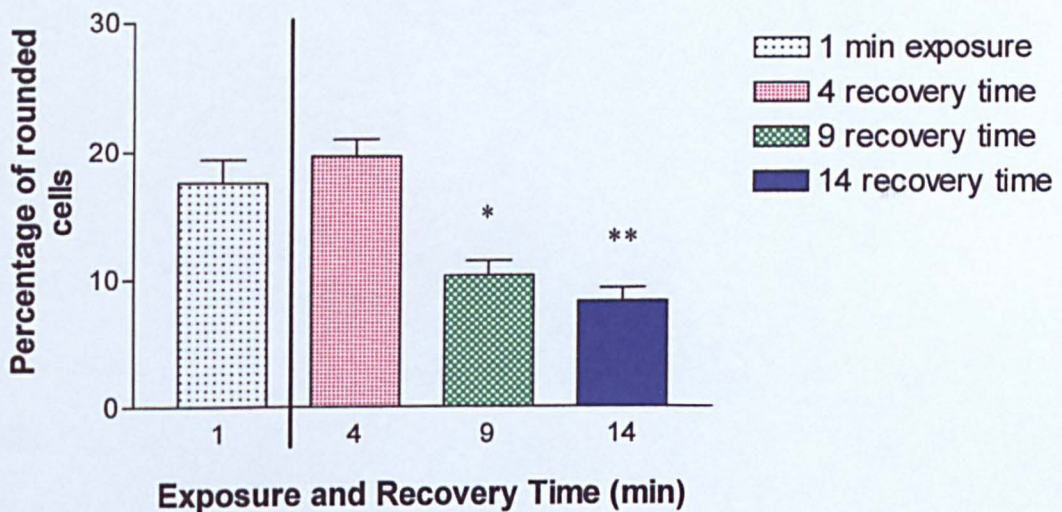


Figure 5.9: HMEC-1 recovery from histamine exposure. Cells were exposed to 10^{-5} M histamine for 1 min (black and white bar) and then placed into agonist free medium for 4, 9 or 14 min. Effect on cell shape was determined by calculating the percentage of rounded cells in the cultures. Removal of histamine significantly decreased the number of rounded cells after 9 min. (* = $p < 0.05$, ** = $p < 0.01$, with respect to 1 min exposure cultures). (Mean \pm SEM. $n=3$).

5.3.7

EFFECT OF HISTAMINE ON THE EXPRESSION AND LOCALISATION OF VE-CADHERIN

The examination of F-actin and histamine in the HMEC-1 cells was conducted initially. These experiments were repeated observing the expression of VE-cadherin with exposure continued up to 30 min, therefore the response of F-actin was evaluated concomitantly to incorporate the extra exposure time. The changes in F-actin up to 10 min were as reported above (figure 5.5 and associated text). At 20 and 30 min exposure to histamine the DPB returned, however the increase in the expression of stress fibre appeared to remain until 30 min (figure 5.11d & e). Histamine appeared to cause more discontinuities in VE-cadherin staining over the course of the experiment, with an increase in free-cell edges (figure 5.10). These alterations in VE-cadherin, as seen in chapter 4, were again subjective, therefore an attempt was made to quantify any possible changes following the method described in section 5.2.2.6.

5.3.8

QUANTITATION OF VE-CADHERIN LOCALISATION

Histamine had a significant effect on the localisation of VE-cadherin immunolabeling in the HMEC-1 cultures (figure 5.12). The percentage of the cell membrane that exhibited a continuous staining decreased steadily and significantly (**, $p < 0.01$, compared to control cultures) with increasing exposure time up to 15 min, after which it began to increase again (figure 5.12a). It did not however return to control values within 30 min. The percentage of the membrane that exhibited a 'stitch' staining significantly

increased from 5min exposure and then decreased again after 10min, however was still significantly raised from control values after 30min histamine exposure (*= $p<0.05$, ** = $p<0.01$, compared to control cultures). The remaining membrane staining was expressed as a discontinuous expression and increased significantly from control cultures (* = $p<0.05$, ** = $p<0.01$, compared to control cultures), however there did not seem to be a relationship with the exposure time.

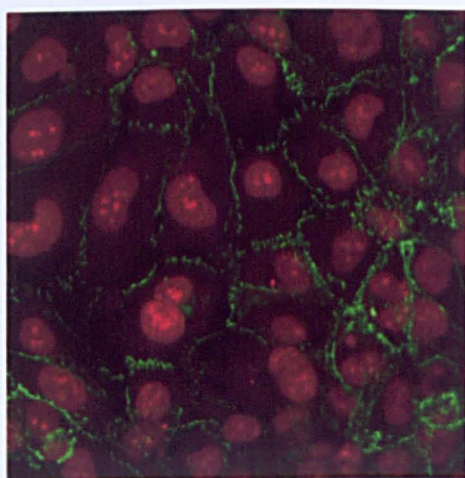
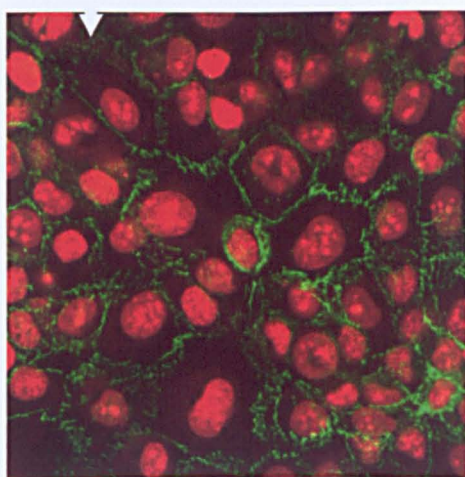
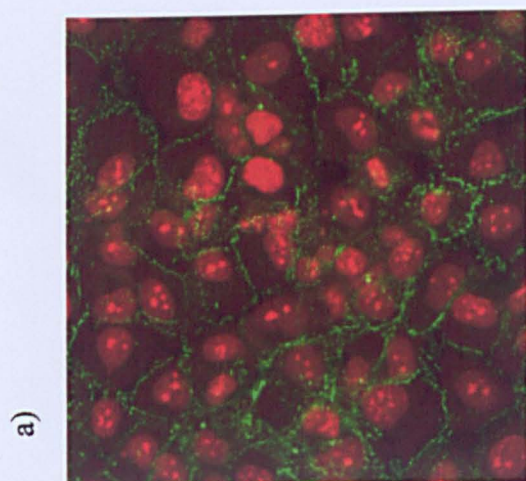
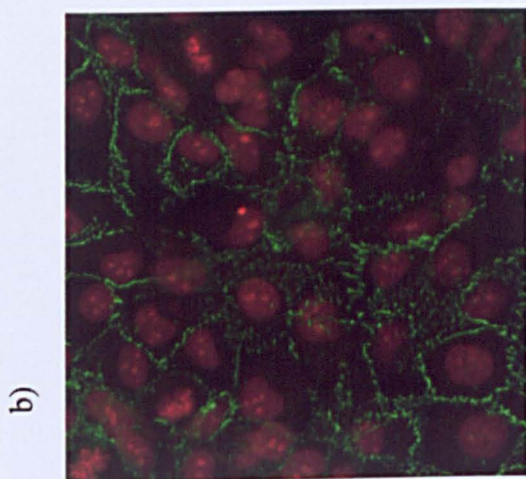
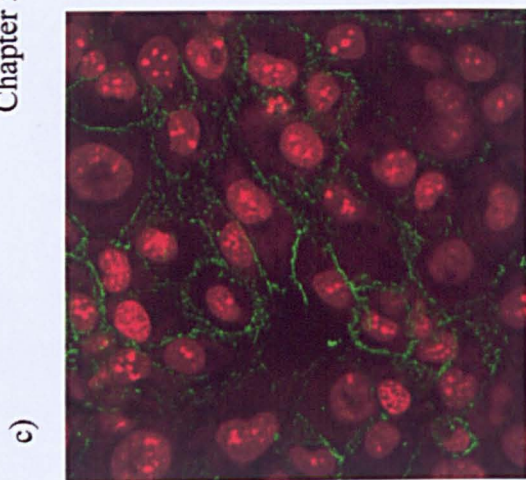
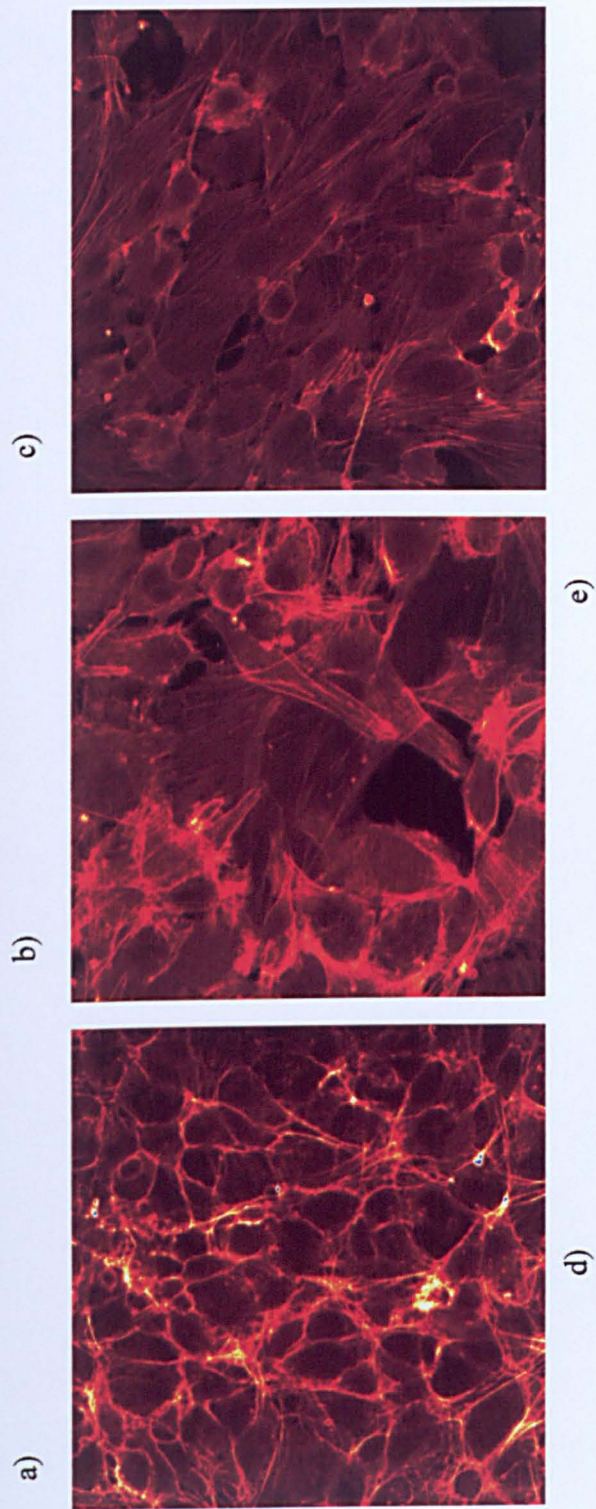


Figure 5.10 - previous page: The effect of histamine (10^{-5} M) on the expression and localisation of VE-cadherin (green), nuclei counter-stained with propidium iodide. Control cultures (a) exhibited a heterogeneous expression of VE-cadherin at cell-cell contacts, including mainly continuous but some discontinuous staining. Histamine was exposed for 1, 10, 20 and 30min (b, c, d, e respectively). There appeared to be an increase in discontinuous staining with some free-cell edges observed at 10 and 20 min (arrows). At 30 min the expression appears more continuous in nature, similar to control cultures.

Figure 5.11 – next page: The effect of histamine (10^{-5} M) on the expression and localisation of F-actin. Control cultures (a) exhibited a dense peripheral band (DPB) of F-actin with some stress fibres. Histamine was exposed for 1, 10, 20 and 30min (b, c, d, e respectively). The DPB disappeared after 1 min (b) and 10 min (c). Its presence was detected again, i.e. recovery after 20 min exposure (d), although did not appear to return to the thick DPB seen in control cultures. Concomitant with the re-appearance of the DPB, the level of stress fibres within the cells dropped back down to control levels by 30 min.



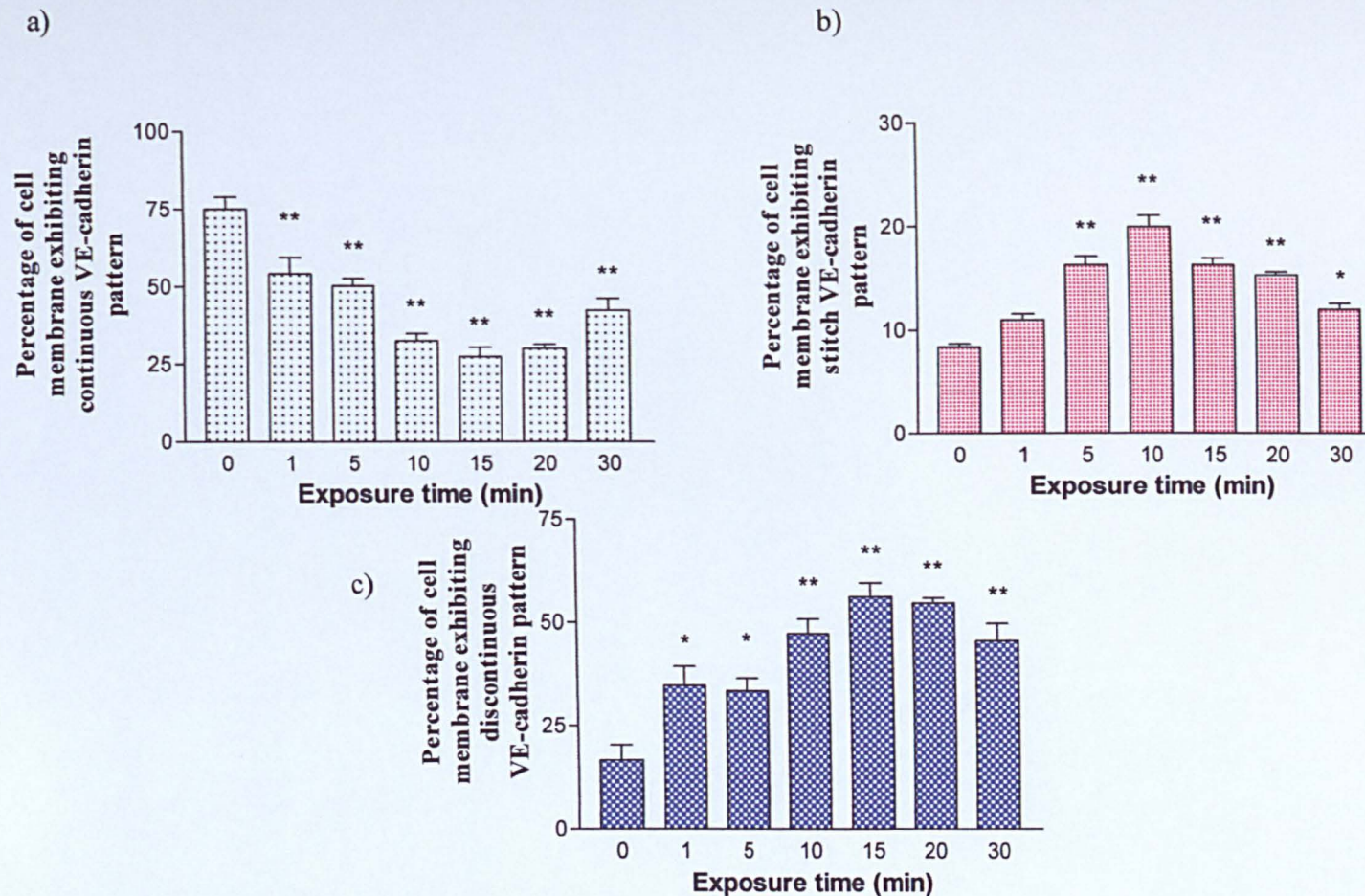


Figure 5.12: Effect of histamine on the pattern of VE-cadherin expression; continuous (a), stitch (b), or discontinuous (c). The percentage of continuous VE-cadherin significantly decreased 1 min after exposure to histamine and remained significantly different throughout the experiment. The lowest level of continuous staining was seen at 15 min, after which it rose back towards control levels. Mean \pm SEM, $n=3$. (**= $p<0.01$ compared to control cultures)

5.4

DISCUSSION

In-vivo studies have shown that exposure of endothelia to histamine leads to a dose-dependent transient increase in permeability (Wu and Baldwin, 1992; Leach *et al.*, 1995; Baldwin and Thurston, 1995). This is accompanied by the formation of intercellular gaps (Majno and Palade, 1961; Leach *et al.*, 1995). In this study histamine caused a significant increase in the permeability of the monolayer of HMEC-1 cells ($p < 0.05$) only when using the 'Bolus' method described in section 5.2.1.2. The significant difference occurred only after 120 min leakage time (90 min histamine exposure). It was expected that histamine would act with the first 1 – 20 min of exposure to the endothelial cells. It could be that the change was marginal and took time to be revealed using this method. As was discussed in Chapter 4 when two flux rates differ they will gradually move further apart, changing the relationship between them. Therefore the method may not have been able to detect the permeability change when it happened, but only after an increased leakage time. Beynon *et al.*, (1993) showed that histamine gave a dose dependent increase in endothelial monolayer permeability at 1h. This was reversible after a 4h wash out period and could be antagonised by incubation with H1 antagonist, chlorpheniramine.

Histamine has been shown to cause conformational change in F-actin involving a reduction in peripheral banding and an increase in central stress fibres and perinuclear actin (Budworth *et al.*, 1999; Niimi *et al.*, 1992). The peripheral bands are the predominant actin filaments seen *in-vivo* (Rungger-Brändle and Gabbiani, 1983) and are thought to play a role in intercellular adherence *in-vitro* (Tsukita *et*

al., 1992) due to its association with tight and adherens junctions. It is clear that histamine exposure (1-15 minutes) induced alterations in cell shape and F-actin arrangement in HMEC-1 cells. This response was related to the length of histamine exposure and was a reversible phenomenon. Similar changes have been reported in rat mesentery (Thurston and Baldwin, 1995) and in HUVEC cells (Ehringer *et al.*, 1996, Niimi *et al.*, 1992). The *in-vitro* phenomenon of cell rounding in response to histamine exposure could occur for a variety of reasons. During the process of cell death the cells detach and become rounded. We investigated this possibility by analysing the cells' ability to absorb the vital dye neutral red. Our results suggest that 10^{-5}M and 10^{-4}M histamine had no toxic effect on the viability of HMEC-1 cells for the exposure times used in this study. Cell division is also characterised by cell rounding but no evidence of cells in mid mitosis was observed. It is most likely that the cell rounding observed here was due to the physiological effect of histamine on the HMEC-1 cells. The mechanism by which histamine produces these morphological alterations and rearrangement of F-actin is not clear. However studies have implicated roles for a number of second messengers including calcium (Rotosen and Gallin, 1986), cAMP (Takeda *et al.*, 1992) and phosphoinositides (Carson *et al.*, 1989). It is clear that the stark effects on HMEC-1 cells observed after five minutes or longer histamine exposure do not represent a physiological state. Such effect would have disastrous results on vascular integrity. Rather the appearance of HMEC-1 following one minute exposure is more likely to represent the *in-vivo* situation. The first event on exposure to histamine appears to be the disappearance of the dense peripheral band of F-actin. This supports the hypothesis by Langille *et al.* (1991) that peripheral

actin plays a role in regulating permeability. The reversal studies reported here clarifies that receptor occupancy was a requirement for the extensive rounding up of cells observed after fifteen minutes exposure to histamine. No desensitisation was observed within the time course of our experiments. The rapid reversibility of HMEC-1 phenotype reported here provides further evidence for the plasticity of the F-actin cytoskeleton and its role in modulating endothelial cell shape and permeability.

PECAM-1 and VE-cadherin showed an altered pattern of staining and redistribution following cell exposure to histamine (Leach *et al.*, 1995). In agreement histamine did seem to effect the expression and localisation of VE-cadherin in HMEC-1 cells, reducing the brightness and changing its localisation after 10 and 20 min exposure. However, it was not objective enough and a method was required to attempt to quantify the localisation (section 5.2.2.6). From this method it became clear that histamine did indeed effect the localisation of VE-cadherin in HMEC-1 cultures in a time-dependent manner. There was an indication that, in this study, part of the response was an increase in the relative amount of 'stitch-like' membrane pattern and a concomitant decrease in continuous membrane pattern. This is broadly in agreement with recent work (Andriopoulou *et al.*, 1999). Disruption of VE-cadherin is a common response following exposure to other inflammatory mediators (Dejana, 1995; Esser *et al.*, 1998; Lampugnani *et al.*, 1992).

In conclusion we have elucidated the response of HMEC-1 cell junctional molecules to histamine exposure and the reversibility of these observations. The changes in F-actin and VE-cadherin arrangement might contribute to the transient

increase in vascular permeability observed both *in vivo* and *in-vitro*. The muted response to histamine in the permeability studies, linked with the cell-line's unusual intercellular junction components (AJ, but not TJ components present) suggests that external regulation of junctional maturity may be beneficial to acquiring a useable *in-vitro* model of the endothelium in general.

CHAPTER 6

EFFECT OF CYCLIC AMP ON THE
EXPRESSION AND LOCALISATION OF
JUNCTIONAL MOLECULES AND
PERMEABILITY OF HMEC-1
CELLS.

CHAPTER 6**EFFECT OF CYCLIC AMP ON THE EXPRESSION AND
LOCALISATION OF JUNCTIONAL MOLECULES PERMEABILITY OF
HMEC-1 CELLS.****6.1****INTRODUCTION**

The HMEC-1 cell-line expresses VE-cadherin at cell-cell contacts in confluent cultures (See chapter 2). Under the influence of histamine the positive actin staining in the cortical regions of control cultures disappeared, and the pattern of VE-cadherin immunolocalisation changed significantly to a more discontinuous one with an increase in the regions of 'stitch' or 'zig zag' fluorescence (see chapter 5). Both of these results suggest that the HMEC-1 cells are able to respond to histamine. However, as described in chapter 5, histamine did not evoke a rapid change in the permeability profiles of these cells. This lack of detection of early permeability changes could be due to a cell monolayer that is initially extremely 'leaky'.

The VE-cadherin immunolocalisation in control cultures was heterogeneous in nature, with some cells showing strong, continuous VE-cadherin isolated at cell-cell borders, (figure 6.1, arrow); whilst in other areas the expression was more discontinuous and fragmented (figure 6.1, asterisk). From these observations we hypothesised that the junctions being formed by these cells were not mature, possibly lacking the correct molecular composition required for effective barrier function.

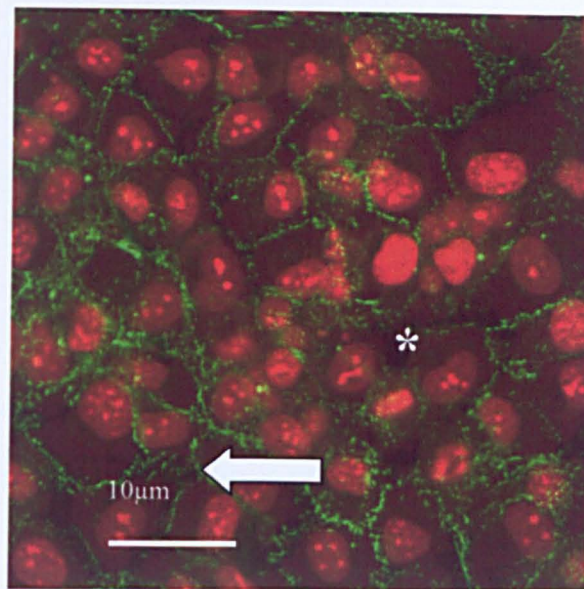


Figure 6.1: Expression of VE-cadherin in HMEC-1 cells, from chapter 5.

VE-cadherin (green) was expressed at cell-cell contacts (arrow); however there were some regions that displayed a more discontinuous, fragmented pattern of staining.

6.1.1

ROLE OF CYCLIC AMP IN CELL-CELL ADHESION.

Cyclic Adenosine 3', 5' -Monophosphate (cAMP) has been shown to affect microvascular permeability, e.g. increased cAMP prevents or reverses permeability-induced pulmonary oedema in nearly every animal species studied (Moore *et al.*, 1998). Other reports indicate that intracellular cAMP induces decreased paracellular permeability *in-vitro* and *in-vivo* (Langeler and van Hinsburgh, 1991; Rubin *et al.*, 1991; Stelzner *et al.*, 1989; Suttorp *et al.*, 1993) and this may be correlated with an increase in tight junction number or complexity (Adamson *et al.*, 1998; Duffey *et al.*, 1981; Wolburg *et al.*, 1994). Previous studies have found that increased intracellular cAMP can block the inflammatory response in a variety of experimental models, both *in vivo* and *in*

vitro. Carson *et al.*, (1989) were able to demonstrate that increasing the cyclic AMP levels in HUVEC cells did not result in a histamine-induced increase in albumin flux across the monolayer to the same amounts as observed in control cultures. However, the histamine-induced flux was increased in comparison to the baseline permeability of the cells with raised levels of cAMP. Therefore, the histamine may have still modulated the permeability of the HUVEC monolayer.

One suggested mechanism for cyclic AMP's ability to decrease permeability is through its action, via protein kinase A (PKA), on myosin light chain kinase (MLCK). It has been proposed by Wyslmerski and Lagunoff (1991) that gap formation occurs following an actin/myosin dependent increase in cell tension, producing a centripetal force on the cells' cytoskeleton and drawing the peripheral regions away from bordering cells. Cyclic AMP-dependent PKA phosphorylation of MLCK is thought to regulate this tension development as it reduces the activity of the MLCK. The subsequent decrease in tension development could aid the stability of intercellular junctions.

6.1.2

AIMS

Identify key molecules in the HMEC-1 junctional complexes that were sensitive to regulation by cAMP levels. The monolayer permeability was also investigated. Additionally the effect of histamine exposure on the barrier function of these cAMP-stimulated cells was investigated.

6.2

MATERIALS AND METHODS

6.2.1

MATERIALS

6.2.1.1

Chemicals and Reagents

Morpholinoethanesulfonic acid (MES); magnesium chloride; forskolin; isobutylmethyl xanthine; cholera toxin; sodium fluorescein (NaFl); sodium dodecyl sulphate (SDS), Tris, glycerol, Triton X-100 and Tween 20 were purchased from Sigma, Poole, UK. Enhanced chemiluminescence was purchased from Amersham Life Science, Buckinghamshire, UK.

6.2.1.2

Antibodies

Rabbit polyclonal anti- α -catenin ($2\mu\text{g ml}^{-1}$) and rabbit polyclonal anti- β -catenin ($2\mu\text{g ml}^{-1}$) were obtained from Sigma, Poole, UK. Rabbit polyclonal anti-plakoglobin ($50\mu\text{g ml}^{-1}$) was obtained from Biodesign International, USA. Horse radish peroxidase – labelled polyclonal goat anti rabbit antibody was obtained from Dakocytomation, Cambridge, UK.

6.2.1.3

Preparation of solutions and cell culture media

For cAMP raising medium, (cAMP medium) MCDB 131 was supplemented with 10% (v/v) FCS, forskolin ($50\mu\text{g ml}^{-1}$), isobutyl-methyl xanthine (IBMX, $200\mu\text{M}$), cholera toxin ($0.01\mu\text{g ml}^{-1}$), penicillin (100 Units ml^{-1}), streptomycin ($100\mu\text{g ml}^{-1}$) and amphotericin B ($1\mu\text{g ml}^{-1}$).

Extraction Buffer was prepared at 5x concentrated and diluted to 1x in distilled water prior to use. To sterile distilled H_2O the following was added: 250mM morpholinoethanesulfuric acid (MES), 125mM EGTA, 25mM magnesium chloride and 2.5% triton X-100. The pH was adjusted to 6.8 prior to the addition of the EGTA to prevent precipitation.

SDS-lysis buffer was prepared at 2x concentrate and diluted to 1x in distilled H_2O prior to use. SDS-lysis 2x buffer consisted of 200mM tris.Cl (pH 6.8), 4% w/v SDS, 20% v/v glycerol, 33.3mM β -mercaptoethanol and 0.2% bromophenol blue in distilled H_2O .

PBST was prepared by adding 0.03% (v/v) Tween 20 to PBS.

6.2.2

METHODS

6.2.2.1

Cyclic AMP treatment

HMEC-1 cells were seeded onto fibronectin-coated Transwell inserts as previously described (section 4.2.2.1). 1×10^5 cells were placed into the insert in 200 μl of media (from a 5×10^5 cells ml^{-1} stock), and 700 μl of media alone

was placed outside the insert in the well. This ensured that the medium level in the insert and outside the insert were the same. Cells were cultured at 37°C/5% CO₂ for 48hrs. The cells' media was then changed for either 200µl of normal medium or cAMP-raising medium and the cells cultured for a further 24 hrs.

6.2.2.2

Leakage of macromolecules and sodium fluorescein through HMEC-1 monolayers

This was undertaken as in section 4.2.2.1 with the following alterations. In addition to measuring the flux of FD70, separate experiments were undertaken to measure any changes in flux of FD40 or 50µM sodium fluorescein (NaFl). To measure the effect of histamine on the cells grown in cAMP media the cells were grown as in section 6.2.2.1, and then the leakage of FD40, 70 and NaFl as in section 5.2.2.2.2.

6.2.2.3

Measurement of triton-soluble and triton-insoluble α -catenin by western blot

HMEC-1 cells were seeded at 2×10^6 cells ml⁻¹ into 75cm² cell-culture flasks. Following growth and exposure to cAMP-raising media as in section 6.2.2.1 the triton-soluble and triton-insoluble components of the cells were separated by the following method: Cells were washed briefly with HBSS. One ml of extraction buffer (EB) was added to the cells for 5 minutes at room temperature and then collected. This was defined as the triton-soluble fraction. Another 1ml of EB was added to the flask and the cells scraped off and centrifuged for 2 min at 1200 rcf. The pellet was resuspended in 2ml of fresh EB. This was

defined as the triton-insoluble fraction and included the cytoskeletal fibres and associated proteins. 2ml of SDS-lysis buffer was added to both fractions. These were heated to 95°C, for 3 min, in a thermblock and pulsed for 10 seconds in a mini centrifuge to ensure adequate breakdown of the proteins.

Fifteen µl of each sample was loaded into wells of an agarose gel and run at 3mA, constant current for 1hr. The gel was electroblotted onto nitro-cellulose membrane using standard procedures. The membrane was blocked in 8% (w/v) milk protein (Marvel) for 1hr at room temperature followed by an overnight incubation at 4°C with anti α -catenin antibody (1/500) in 8% (w/v) milk protein in PBS. Following three 10 min. washings with PBST, immunoreactive bands were visualised after 1hr incubation at room temperature with horse radish peroxidase – labelled anti rabbit antibody (1/5000). The membrane was given three 10 min washes in PBST and followed by enhanced chemiluminescence exposure to a Fuji film intelligent dark box.

6.3

RESULTS

6.3.1

EFFECT OF CYCLIC AMP MEDIA ON LEAKAGE OF FD40, 70 AND SODIUM FLUORESECIN THROUGH THE HMEC-1 MONOLAYER

Cyclic AMP raising media reduced the macro-molecular permeability to FD70 and 40, but not small molecule permeability to NaFl, in HMEC-1 cells (figure 6.2).

By 20 minutes an apparent decrease in permeability of those cells where cAMP had been induced was observed, with FD40 and FD70 (Figure 6.2 a and b). The effect lasted for the whole 60 min assay time. For the smaller NaFl, not only was there no difference in the leakage, but the concentration that did leak through was over twice that for the FD40 or FD70 (Figure 6.2 c). Thus there was a differential leakage of the molecules as had been seen in HMEC-1 cultures in chapter 4. Within the hour, 0.75 μ M of the 50 μ M NaFl added to the inserts, had leaked across, i.e. 1.5% compared to 0.63% of the FD40 and 0.54% of the FD70 had leaked across the monolayer. Following 60 minutes 314nM of FD40 had leaked through the control monolayer of cells whilst only 214nM had passed through the cells treated to induce cAMP production. FD70 behaved in a similar, but slightly more restrictive, manner with 272nM moving through the control monolayer reducing to 177nM through the cAMP-induced cells.

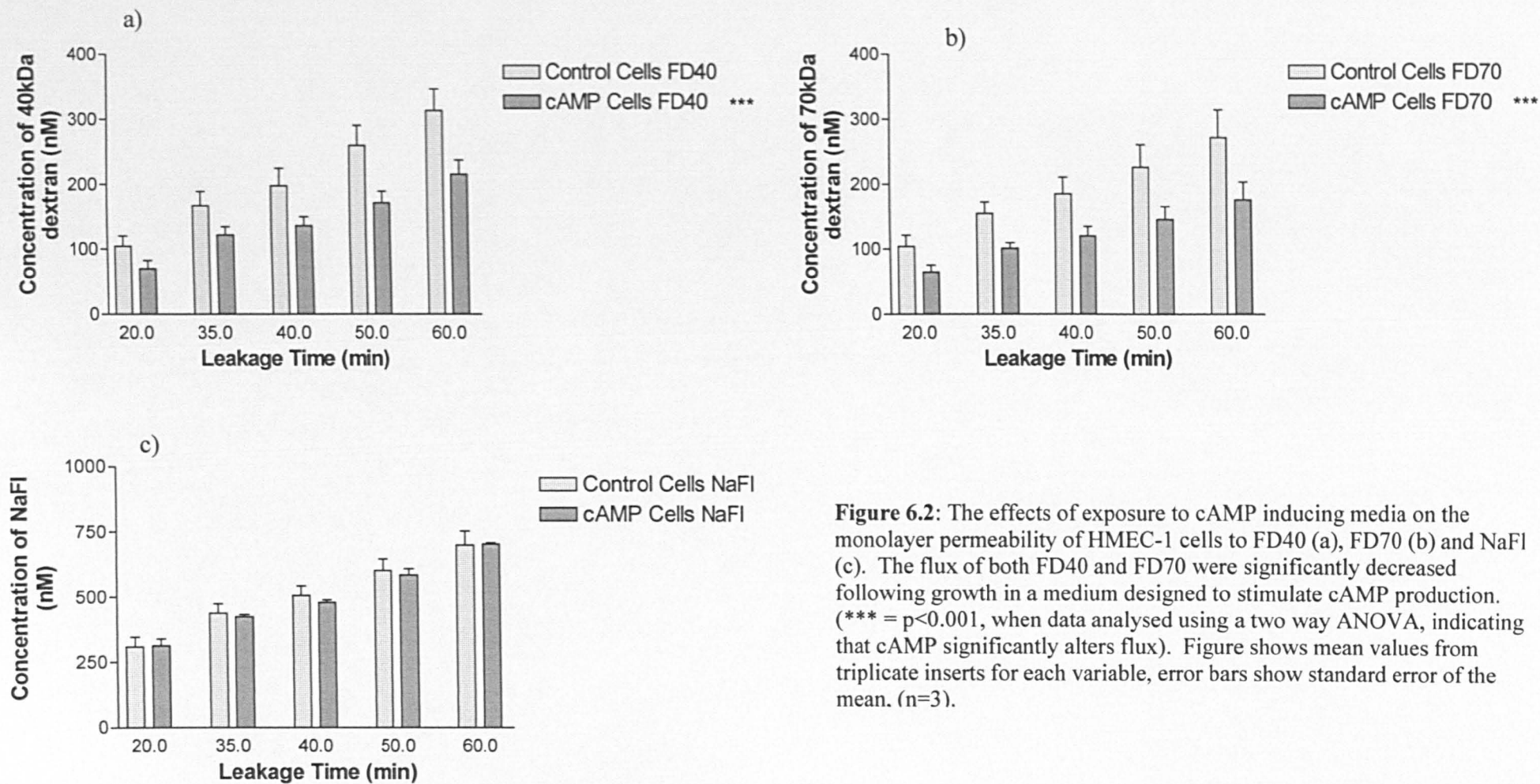


Figure 6.2: The effects of exposure to cAMP inducing media on the monolayer permeability of HMEC-1 cells to FD40 (a), FD70 (b) and NaFI (c). The flux of both FD40 and FD70 were significantly decreased following growth in a medium designed to stimulate cAMP production. (***) = $p < 0.001$, when data analysed using a two way ANOVA, indicating that cAMP significantly alters flux). Figure shows mean values from triplicate inserts for each variable, error bars show standard error of the mean. (n=3).

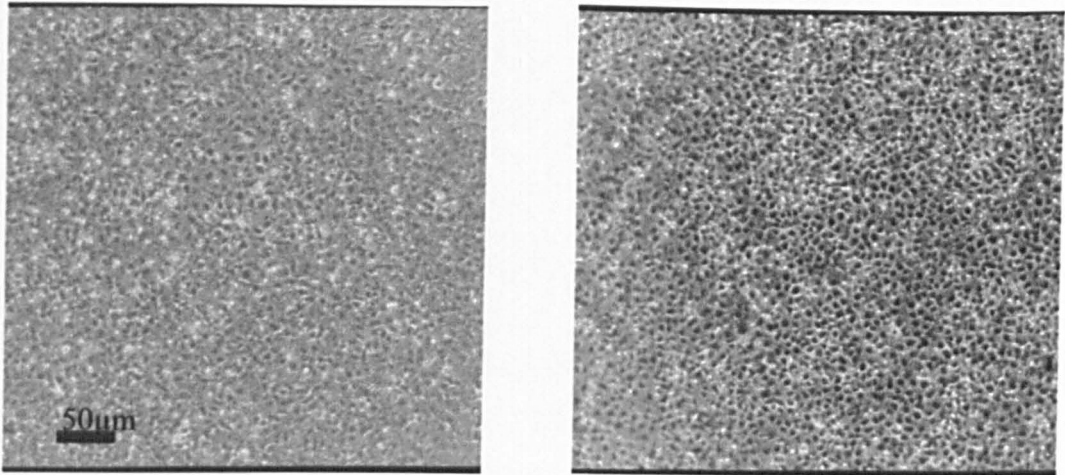


Figure 6.3: Phase-contrast micrograph of HMEC-1 cells exposed to either normal media alone (a), or cAMP media (b). Culturing the cells in cAMP media caused them to exhibit a more tightly packed, cobblestone appearance. Bars = 50 μ m

6.3.2

EFFECT OF CYCLIC AMP MEDIA ON MORPHOLOGY AND JUNCTION COMPONENTS OF THE HMEC-1 CELL-LINE

The morphology of the HMEC-1 cells appeared more cobblestone when grown in the cAMP media (figure 6.3). Upon detection of the junctional molecules a number of differences were noted (figures 6.4 – 6.6). The cortical F-actin staining of cells exposed to cAMP media appeared thicker than control cultures and the number and intensity of stress fibres were drastically reduced (figure 6.4 a and b). VE-cadherin was associated with inter-endothelial contacts in both control and cAMP cells; however, in the latter there was a greater continuity of staining along the cells membranes, than in control cultures (figure 6.4 c and d). Staining with the anti β -catenin antibody was positive under both culture conditions (figure 6.5 a and b), however the cAMP media

cultures appeared to exhibit less general cytoplasmic staining, seemingly enhancing the cell membrane immunofluorescence (figure 6.5b). In control cultures α -catenin was expressed throughout the cell, with the exception of the nuclear area (figure 6.5 c). Cyclic AMP media caused an increase in the intensity of staining observed at cell-cell contacts, while maintaining a general cytoplasmic presence (figure 6.5 d). In control cultures γ -catenin (plakoglobin) was expressed throughout the cells (figure 6.6a), however the cAMP media caused an increase in the protein localised at cell-cell contacts, whilst maintaining a cytoplasmic presence (figure 6.6 b). Occludin was present in low amounts in the cytoplasm (figure 6.6 c) as had been shown in chapter 4, but cAMP media did not appear to significantly affect its expression (figure 6.6 d).

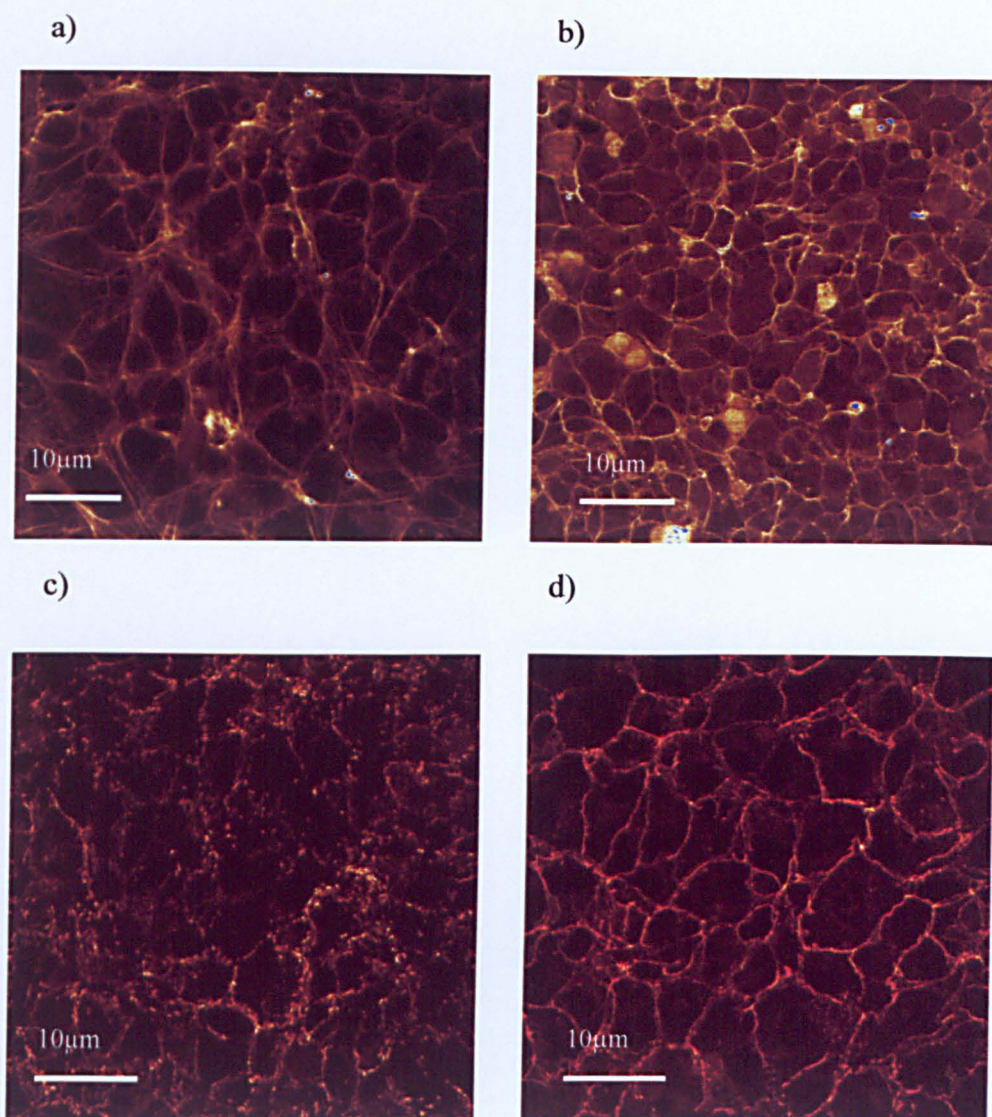


Figure 6.4: Fluorescence micrograph of HMEC-1 cells exposed to either normal media alone (a and c), or cAMP media (b and d). Cyclic AMP media caused the thickening in the cortical F-actin to thicken, along with a reduction in the number and intensity of stress fibres with the cell (b). VE-cadherin staining exhibited a more continuous pattern of expression than control cultures (c and d). It was still localised at the cell-cell contacts, no free cell edges were observed (d). Bars = 10 μm .

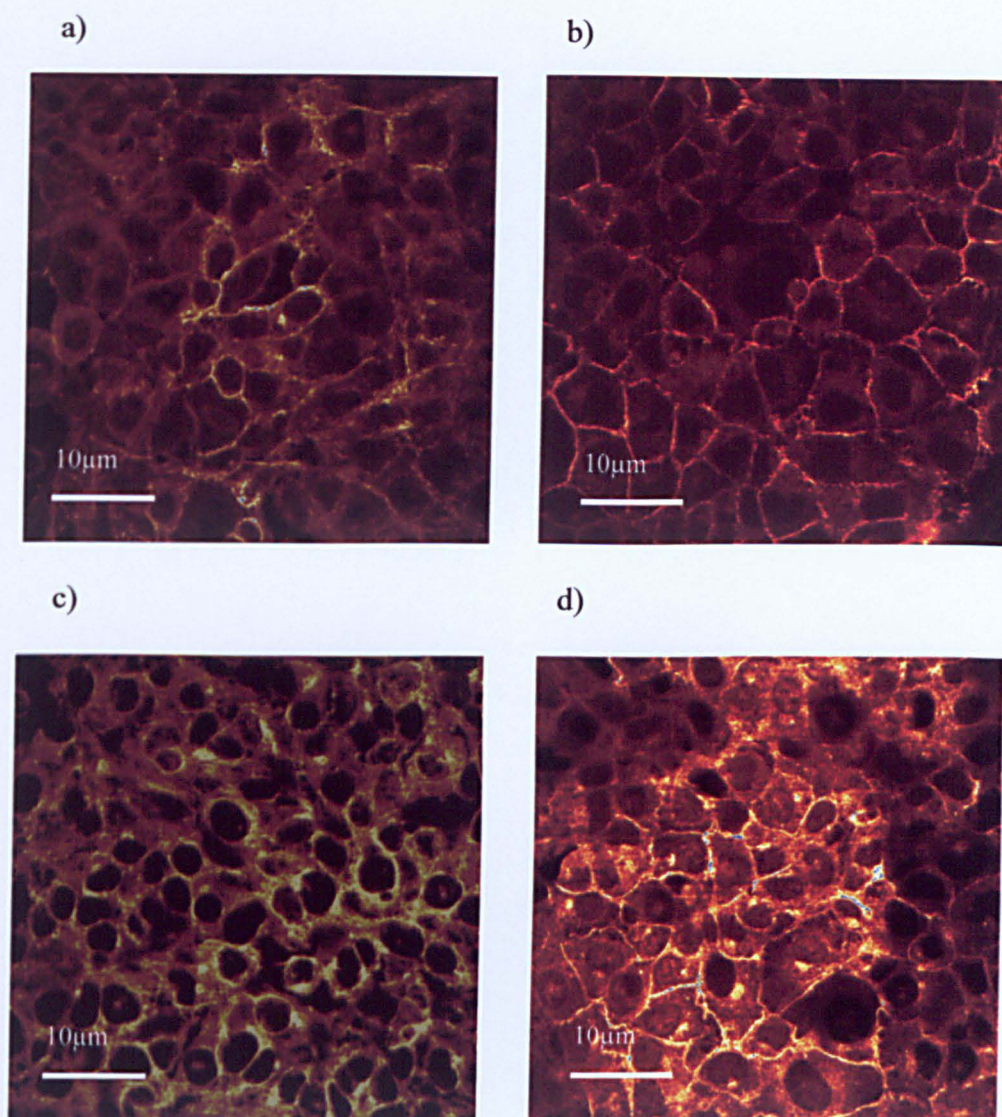


Figure 6.5: Fluorescence micrograph of HMEC-1 cells exposed to either normal media alone (a and c), or cAMP media (b and d). β -catenin was expressed in cells under both culture conditions (a and b), however the cAMP media cultures appeared to exhibit less general cytoplasmic staining, seemingly enhancing the cell membrane immunofluorescence (b). In control cultures α -catenin was expressed throughout the cell, with the exception of the nuclear area (c). Cyclic AMP media caused an increase in the intensity of staining observed at cell-cell contacts, while maintaining a general cytoplasmic presence (d). Bars = 10µm

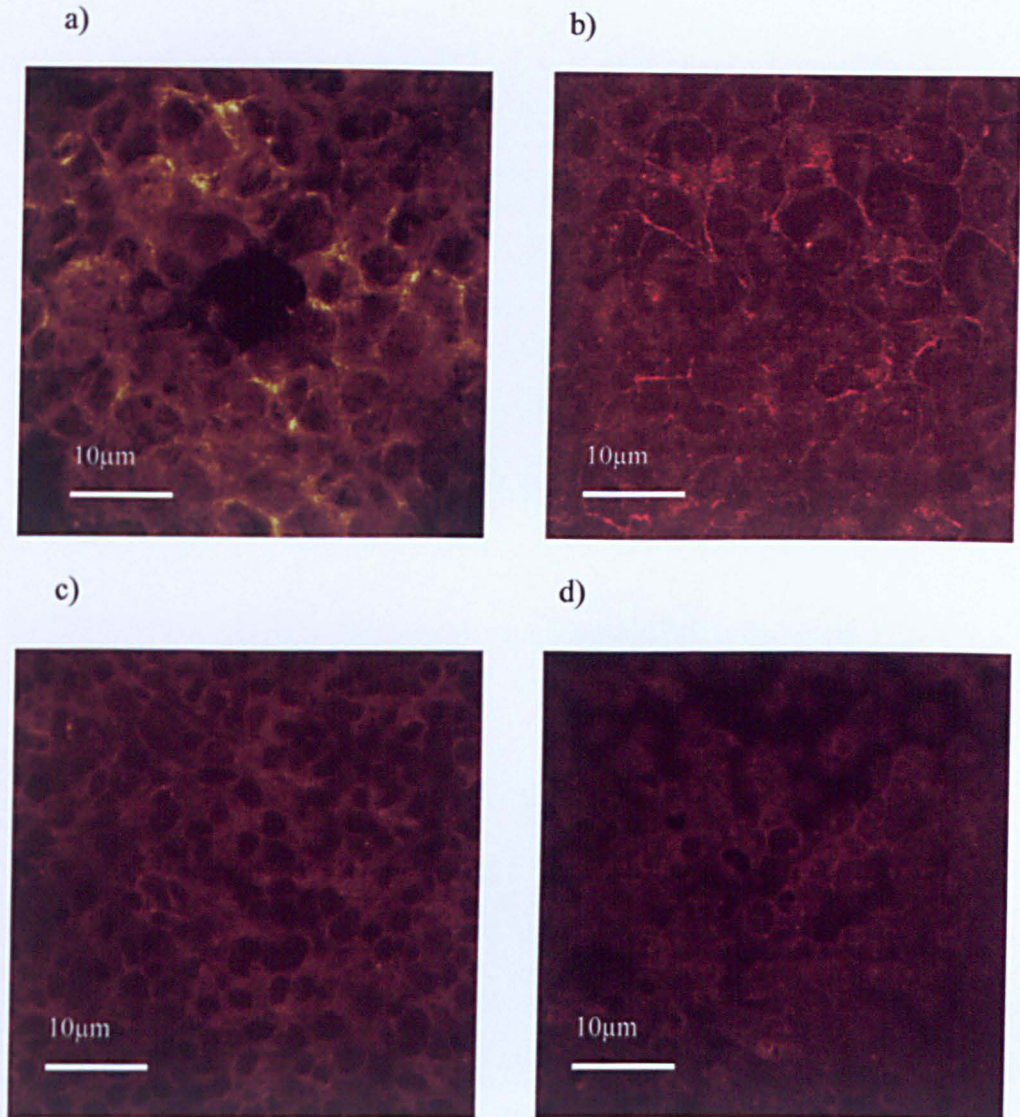


Figure 6.6: Fluorescence micrograph of HMEC-1 cells exposed to either normal media alone (a and c), or cAMP media (b and d). In control cultures γ -catenin (plakoglobin) was expressed throughout the cells (a), however the cAMP media caused an increase in the protein localised at cell-cell contacts, whilst maintaining a cytoplasmic presence (b). Occludin was non-reactive under both culture conditions (c and d). Bars = 10 μ m

6.3.3

EFFECT OF CYCLIC AMP MEDIA ON THE LEVELS OF α -CATENIN PROTEIN IN TRITON-SOLUBLE AND -INSOLUBLE CELL FRACTIONS

Antibody binding indicated that cAMP up regulation resulted in α -catenin and plakoglobin localisation directed to the cell-cell junctions. This was further studied by examining the triton-soluble and insoluble fractions of the cells by western blotting and using antibodies to α -catenin. Only α -catenin was chosen due to its more dramatic apparent move to the cell-cell contacts. Separation of the cells constituents on the basis of triton solubility is a well-known method. Triton-insolubility is commonly interpreted as an indicator for cytoskeletal association (McNeill *et al.*, 1993). Therefore junctionally-linked molecules should be in the triton-insoluble fraction.

A band of approximately 100 - 110kDa reacted with the anti- α -catenin antibody (figure 6.8). In control cultures a band that reacted with anti- α -catenin was observed in the triton-soluble fraction (lane A). There was a down regulation of the α -catenin band in triton-soluble fraction when the cells were grown in cAMP media (lane B). Control cultures exhibited substantial amounts of α -catenin in the triton-insoluble fraction (lane C). Cyclic AMP media caused an increase in the intensity of α -catenin found in the triton-insoluble fraction, which included proteins of mature cellular junctions (lane D).

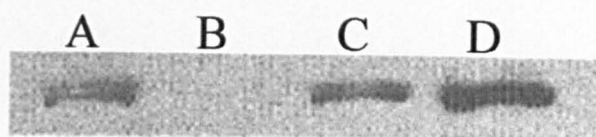


Figure 6.8: Western blot of HMEC-1 cell extracts, control (lanes A and C) and exposed to cAMP media (lanes B and D). In control cultures a band that reacted with anti- α -catenin at approximately 100kDa was observed in the triton-soluble fraction (lane A). This band disappeared when the cells were grown in cAMP media (lane B). Control cultures exhibited substantial amounts of α -catenin in the triton-insoluble fraction (lane C). It appeared that cAMP media caused an increase in the amount of α -catenin found in the triton-insoluble fraction (lane D).

6.3.4

EFFECT OF CYCLIC AMP ON HMEC-1 PERMEABILITY RESPONSE TO HISTAMINE

The upregulation of the monolayer barrier function observed with the induction of cAMP was not compromised by the addition of 10 μ M histamine over 30 min (figure 6.7). This was true with both the FD40 and FD70 dextrans (figure 6.7 a and b). Additionally the NaFl leakage was also unaffected by the exposure to 10 μ M histamine (Figure 6.7 c).

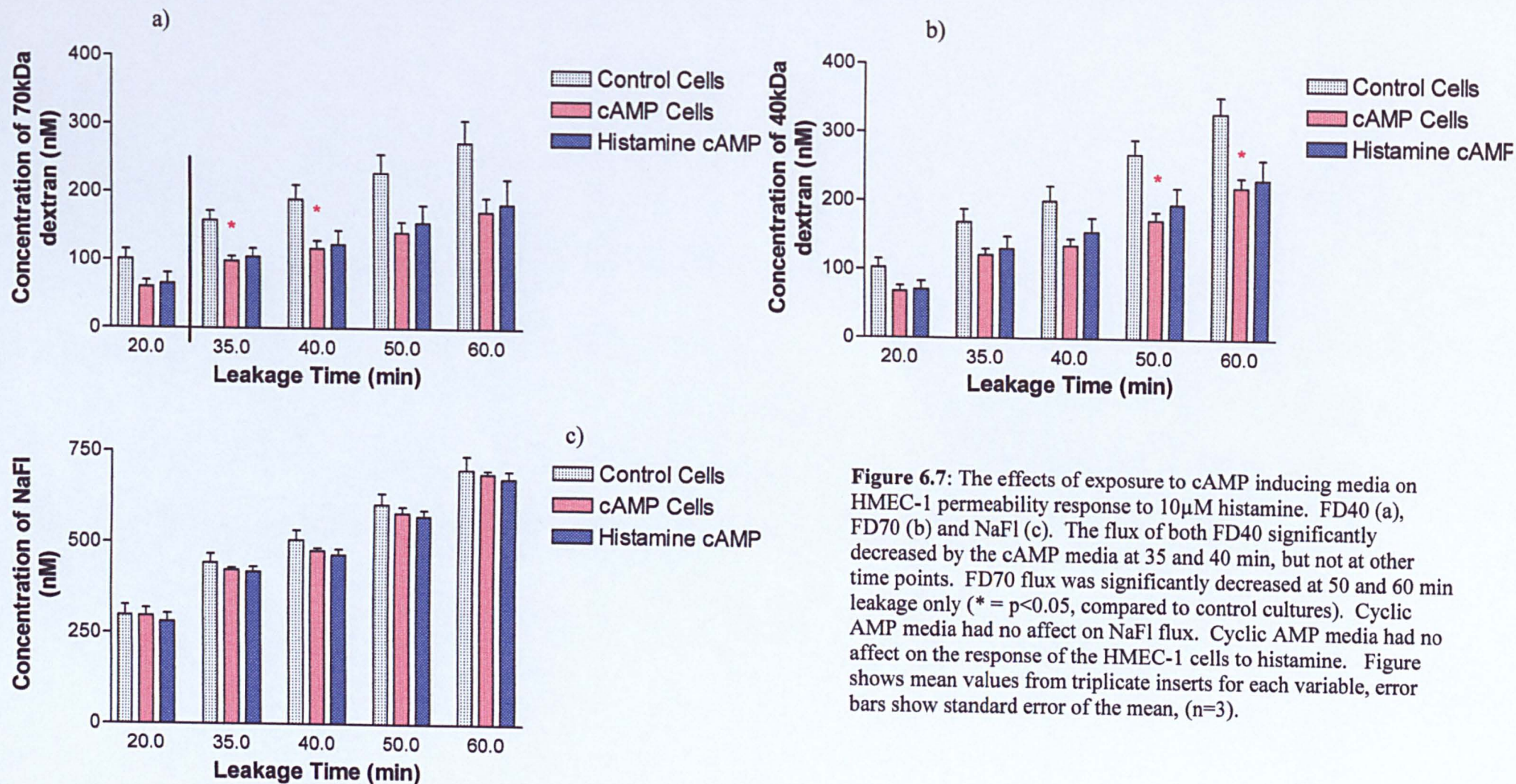


Figure 6.7: The effects of exposure to cAMP inducing media on HMEC-1 permeability response to 10 μ M histamine. FD40 (a), FD70 (b) and NaFI (c). The flux of both FD40 significantly decreased by the cAMP media at 35 and 40 min, but not at other time points. FD70 flux was significantly decreased at 50 and 60 min leakage only (* = $p < 0.05$, compared to control cultures). Cyclic AMP media had no affect on NaFI flux. Cyclic AMP media had no affect on the response of the HMEC-1 cells to histamine. Figure shows mean values from triplicate inserts for each variable, error bars show standard error of the mean, ($n=3$).

6.4

DISCUSSION

Exposure of HMEC-1 cells to a media formulated to increase the levels of cyclic AMP within the cells had a large effect on both the monolayer permeability and the expression and localisation of adherens junction molecules. Cyclic AMP media decreased the leakage of the macromolecules FD40 and FD70. However the flux of the small molecule NaFl did not alter when cells were grown in cAMP media. This, linked with that fact that the expression of occludin was not affected, indicated that the decrease in macromolecule permeability was probably not due to the involvement of tight junctions. Following the exposure to cAMP-media, VE-cadherin, α - and γ -catenin appeared more profusely at junctional regions with less staining seen in the cytoplasm. F-actin exhibited more dense cortical bands and the general level of β -catenin within the cell appeared to diminish, however these images were difficult to interpret. Beta-catenin down-regulation is linked with a more mature junction phenotype (Lampugnani *et al.*, 1995) as is plakoglobin upregulation. This suggests that cAMP in our system is promoting the formation of more mature junctions. Increasing the levels of cAMP in the HMEC-1 cells led not only to an increase in the junctional expression of α -catenin (as observed by immunofluorescence) but western blots of triton-extracted cell fractions confirmed that the α -catenin levels dropped in the triton-soluble fraction while concomitantly rising in the triton-insoluble/junction containing fraction. This lead to a hypothesis that α -catenin moved from the triton-soluble fraction to the junction-containing fraction, becoming incorporated into the junctions. Dye *et al.* (2001) are the only other

researchers to have looked at the effect of cAMP on interendothelial junction molecules and reported an upregulation of VE-cadherin, plakoglobin at the cell-cell contacts, in agreement with the study here. However they also showed an upregulation of occludin and ZO-1 in their system. They used placental microvascular endothelial cells which already expressed the tight junction molecules at cell-cell contacts whilst HMEC-1 cells expressed these molecules in the cytoplasm. No relocalisation of occludin was observed in our study.

Agents that increase cAMP in endothelial cells are known to prevent the increase in permeability that follows histamine exposure both *in-vivo* (Carson *et al.*, 1989) and *in-vitro* Langelier and van Hinsburgh, 1991). In agreement with this the permeability profile of the HMEC-1 cell-line also showed no change upon exposure to 10^{-5} M histamine for up to 30 minutes. However, as histamine did not cause any permeability increases initially within 60 min (Chapter 5), there may be some doubt as to the mode of action of the cAMP media on the cells' response to histamine.

CHAPTER 7

GENERAL DISCUSSION.

CHAPTER 7**GENERAL DISCUSSION.**

The primary aim of this thesis was to develop an *in-vitro* assay with which to investigate endothelial barrier properties following exposure to known inflammatory mediators. This model could then be used to examine, *in-vitro*, the effect of unknown cocktails of cytokines and mediators found in conditioned media, to further skin irritation toxicology studies. Furthermore, the study aimed to understand the role of the paracellular cleft in permeability regulation, specifically that of the adherens junctions and its molecules.

The emphasis at the beginning of the work was to examine two immortalised endothelial cell-lines, ECV304 and HMEC-1 for their potential value in permeability research (Chapter 2). Both cell-lines had been used extensively in endothelial cell research in general (recent examples include: Liu *et al.*, 2000; Maxwell and Davies, 2000; Moreno, 2001), with a small number of studies on permeability regulation published for both (recent examples include: Hirase *et al.*, 2001; Venkiteswaran *et al.*, 2002). The use of porous membrane supports in the study of permeability across cell monolayers has become second nature within cell biology. The seeding density required to form a monolayer restrictive to the molecules of choice, in a time frame considered usable is most important. Indeed Burke-Gaffney and Keenan (1995) showed that monolayers derived from HUVEC seeded at a sub-optimum density responded to cytokines in a diminished fashion. The seeding density which resulted in the most restrictive monolayer to 70 kDa

dextran after 72 hrs in culture was 5×10^5 cells ml^{-1} for both the ECV304 and HMEC-1 cell-lines. In immortalised cell-lines certain functions may be lost at the time of the immortalisation procedure or with increasing passage number. If this loss of specific functions does not affect cell growth it may not be identified when the immortalised cells are initially characterised. With this in mind, the response of the cell-lines to chemicals known to affect endothelial permeability both in-vivo and in-vitro was prudent. The ECV304 cells were investigated for their response to IL-1 α , TNF α , PMA and A23187 and responded by increasing monolayer permeability to FD70. Only PMA gave comparable levels of permeability with the literature. As the ECV304 cell-line claimed to be immortalised from HUVEC cultures it may be expected that it would respond in a similar fashion to previous HUVEC reports, however this was not the case. The discrepancy was partly explained when the use of immunocytochemistry against VE-cadherin, PECAM-1 and vWF was performed. We were among the first to show that the ECV304 cell-line did not express any of these common endothelial molecules (Hughes, 1996; Budworth *et al.*, 1997b). Of prime importance was VE-cadherin as studies have suggested that it may be a regulator of endothelial permeability (Lampugnani *et al.*, 1992). However PECAM-1, whilst not part of intercellular junctional machinery, has been shown to play a role in the trafficking of β - and γ -catenin, important players in the regulation of junctional integrity (Ilan *et al.*, 2000). Therefore the decision was made to stop further research on this cell-line. In 2000, it was found that the ECV304 cell-line had been contaminated by the T24 cell-line (Brown *et al.*, 2000). This cell-line is derived from human urinary bladder

carcinoma, and therefore would not necessarily be expected to express endothelial specific markers. However Suda *et al.* (2001) indicated that, despite identical genotypes, ECV304 cells differ to T24 in a variety of criteria, e.g. growth behaviour, and express several endothelial markers (Kießling *et al.*, 1999) that the T24 cells did not.

The studies investigating the growth of the two cell-lines on various ECM was undertaken to distinguish the best matrix for stable adhesion and confluence of cells prior to permeability measurement. However, it also highlights some basic differences in the interactions between the cell-lines and the ECM proteins. This is probably due to a differential expression of integrins. In endothelial cells integrin expression is heterogeneous, dependent upon culture conditions, animal species and vascular bed of origin (Bazzoni *et al.*, 1999).

Variations in the methodology used to measure endothelial permeability *in-vitro* can make comparisons of data difficult, if not impossible. In Chapter 3 certain common variations were investigated to evaluate the effect they may have upon the leakage of FD70 through a restrictive monolayer of cells (the ECV304 cell-line were used). The changes made to the basic method in order to equalise hydrostatic and osmotic pressure, ensure use of an endothelial medium and optimise the data from one experiment by sampling flux over time can be used collectively in the method to measure the permeability of endothelial monolayers. The only change that caused a significant difference to the leakage of FD70 was reducing the hydrostatic pressure across the no-cell insert. Additionally the potential to

measure the leakage of two dextrans simultaneously was not realised in this project due to interference between the two fluorophores chosen.

Regulation of vascular permeability is one of the most important functions of the endothelium; interference with which may promote pathological changes in the vascular wall and play a major role in the development of an inflammatory reaction. In Chapter 4 the HMEC-1 immortalised cell line, derived from human dermal microvascular endothelial cells, was investigated for its potential to respond to known vaso-active compounds, via measurement of paracellular permeability and by observation of the adherens junction molecules; VE-cadherin and F-actin. The *in-vitro* system described here is a simple model of the microvasculature in which the cellular regulatory mechanisms of endothelial permeability were directly investigated. Monolayers of HMEC-1 cells exhibited extensive regions of cell overlap with tortuous paracellular clefts, which is in agreement with *in-vivo* studies of the microvascular endothelium (Leach and Firth, 1992). This contrasts to large vessel endothelial cells where the paracellular clefts are more abutting with a much shorter region of cell-cell contact. Tight junctions could not be found ultrastructurally; indeed pertinent TJ molecules, occludin and ZO-1 were not located at cell-cell contacts. This indicated that, in this cell-line, only the adherens junctions are available for permeability regulation. The important TJ family of molecules, the claudins, were not studied in this project. They have been shown to be expressed in endothelial cells (Morita *et al.*, 1999), linking intracellularly with ZO-1, ZO-2, and ZO-3 (Itoh *et al.*, 1999). As the HMEC-1 cell-line does not target ZO-1 to the junctional regions it is likely that

they do not express any of the claudin family. Whilst not in agreement with the *in-vivo* scenario, the lack of TJs in this cell-line gave rise to a valuable cellular tool with which to observe the adherens junction in isolation. The basal permeability of the HMEC-1 cell-line to dextrans of 40-, 70- and 150-kDa and sodium fluorescein (346 Da) was restrictive in a size-selective manner. Thus the monolayer was acting as a heteroporous system, discriminating between greater than and less than 40 kDa, as described *in-vivo* (Malik *et al.*, 1989). A common means to refer to the permeability of the endothelium is Permeability Coefficient (PC). Albelda *et al.*, (1989) compared the PC of albumin (66kDa) from various endothelial cell-filter systems. PC ranged from $4.8 - 7.7 \times 10^{-6} \text{ cm s}^{-1}$ over a variety of endothelial cell subtypes. Upon conversion of our data to PC using a linear approximation of Fick's first law of diffusion (described in Kazakoff *et al.*, 1995), it is apparent that the HMEC-1 monolayer gives a low PC for FD70 - $2.47 \times 10^{-6} \text{ cm s}^{-1}$ (figure 7.1). The PC values of FD40, 70, 150 and NaFl were all significantly different from one another ($p < 0.001$), with the exception of FD70 compared with FD150. This indicates that the basal permeability of the HMEC-1 cell-line is consistent for macromolecules between 70 and 150 kDa. The low PC of the albumin-sized molecule FD70, compared to many other endothelial cells, was not expected given the lack of tight junctions in this cell-line. This suggests that the adherens junction alone may be the key junction involved in regulation of macromolecular permeability (70 kDa).

The HMEC-1 cell-line responded predictably to the vasoactive compounds A23187, EGTA, PMA and CAPB. However it appeared that response to EGTA (FD70) was more likened to that observed by Langelier and van Hinsburg (1988)

who investigated the flux of HRP, a molecule of around 40kDa. This supported our theory that the junctions of the HMEC-1 cell-line may be immature in their permeability response to certain compounds.

Marker Molecule	Molecular Weight	Permeability Coefficient for Marker Molecule, $\text{cm s}^{-1} \times 10^{-6}$
Sodium Fluorescein	346 Da	16.8 ± 0.59
FD40	40 kDa	11.5 ± 0.41
FD70	70 kDa	2.5 ± 0.24
FD150	150 kDa	0.99 ± 0.12

Figure 7.1: Permeability Coefficients (PC) of the Molecules used to study Endothelial Permeability in this Study. PC is related to the molecular weight of the molecule investigated. All PC values are significantly different from each other (***) = $p < 0.001$) with the exception of FD70 and FD150, where no significant difference was demonstrated. Mean \pm SEM from triplicate inserts for each variable, (n=3).

Also the response of our HMEC-1 cell-line to PMA was significantly muted in comparison with similar studies also using the HMEC-1 cell-line (Nagpala *et al.*, 1996; Vuong *et al.*, 1998). However our data is in agreement with Stasek *et al.*, (1992) who also showed a significant increase in albumin clearance at 10^{-6}M using BPAEC cells. There does appear to be some controversy over the action of PMA on endothelial permeability *in-vitro*. Aschner *et al.* (1997) showed that exposure to 10^{-8}M PMA for 20hr did not affect albumin clearance in BPAEC cells. Whilst Yamada *et al.* (1990) saw a decrease in the permeability rate of albumin following exposure to 10^{-8} and 10^{-7}M for 60 minutes. Evidence that the divergence of affects

may be related to the species of the endothelial cells was provided by Yamada and Yokota (1996) who showed that PMA decreased albumin permeability in human aortic endothelial cells and increased it in bovine aortic endothelial cells.

Whilst all four compounds increased the monolayer permeability to FD70 in the HMEC-1 cell-line, the affect they had on the expression and localisation of VE-cadherin and F-actin varied. The relationships between the maximum permeability responses of the compounds were such that CAPB>A23187>PMA>EGTA. Whilst alteration of permeability was linked positively with rearrangement of VE-cadherin and F-actin, it did not appear to agree with the order stated above. It was not possible to clearly distinguish between the affects that PMA, CAPB and A23187 had on these molecules, however it was clear that EGTA completely abolished VE-cadherin immunoreactivity. The lowest permeability increase was observed following EGTA exposure indicating that, whilst VE-cadherin expression appeared to be abolished the barrier function was still somewhat intact. For A23187, PMA and CAPB, exposure resulted in a higher increase in permeability. This may have been due to both the junctional and the transcellular pathway being affected. Alternatively increases in percentage leakage over around 20% may be considered non-physiological, with responses of this magnitude not regularly seen in normal inflammatory reactions *in-vivo* without pathology.

Chapter 5 investigated the response of HMEC-1 cell to histamine. Its affect on permeability to FD70 and expression of VE-cadherin and F-actin were studied. Histamine gave a muted, delayed increase in permeability to FD70 compared with

previously described (Wu and Baldwin, 1992; Yuan *et al.*, 1993). However Ehringer *et al.* (1996) showed that, in HUVEC, the histamine-induced increase in albumin permeability (expressed as PC) remained elevated until 120 min. Additionally Ikeda *et al.*, 1999 showed that the response to histamine (as PMA, discussed earlier) is significantly linked to endothelial species- and site-of origin. In their studies (using FD70) they demonstrated that histamine (10^{-5} M) only caused an increase in permeability in HUVEC. They saw no response in human aortic endothelial cells or bovine post caval vein endothelial cells, and a decrease in permeability in bovine aortic endothelial cells. These studies illustrate that histamine, generally considered to be predictable in its affect on endothelial permeability, is still a molecule where active research is needed in this field. Whilst it is easy to criticize the in-vitro systems, in-vivo studies that have investigated histamine have tendered to use albumin as the marker molecule (Baldwin and Thurston, 1995; Svensjo *et al.*, 1999; Yuan *et al.*, 1993). Predescu *et al.*, (2002) have shown that when nitric oxide (NO) is released in the body any available albumin may become nitrosated on tyrosine residues. And this form of albumin can itself actively open endothelial junctions and increase permeability, even when pre-perfused with native albumin. Data such as this additionally brings the in-vivo data into question

Changes in permeability have been associated with a distinct reorganisation of F-actin within the cells. In normal, confluent endothelial cells there is a dense peripheral band of F-actin and a few fibres running longitudinally across the central region (Niimi *et al.*, 1992). Upon exposure to histamine there is a disruption of the peripheral band, an increase in the density of the central stress

fibres and an increase in diffuse actin present throughout the cytosol (Niimi *et al.*, 1992; Baldwin and Thurston, 1995). The relationship between inflammatory stimuli, actin reorganisation and loss of functional cell-cell contact is still not fully understood. In confluent monolayers of HMEC-1 the F-actin was present in two areas of the cell – at the cell periphery as a thin dense band, and more centrally in longitudinal stress fibres. This is in agreement with work carried out in cultured endothelial cells of both animal (Haugland *et al.*, 1994, Ayalon and Geiger, 1997) and human (Niimi *et al.*, 1992, Ehringer *et al.*, 1996) origin, although these studies reported a much more obvious and thicker peripheral band. The bands may be thicker in these studies since the cells were of large vessel origin where the endothelium is subject to greater haemodynamic stress than in microvessels. A study of rat mesentery microvasculature under physiological conditions (Thurston and Baldwin, 1994) observed that endothelium from mid-sized arterioles and venules displayed a thin peripheral rim of actin and occasional short central fibres. Capillary endothelium contained few actin fibres but displayed a diffuse staining with phalloidin. The HMEC-1 results indicate similarities with the results from these arterioles and venules. Histamine (1-5 min) strongly affected the cell shape and F-actin arrangement in the HMEC-1 cells. This response was related to the length of histamine exposure and was a reversible phenomenon. Similar changes have been reported previously (Niimi *et al.*, 1992; Thurston and Baldwin, 1995). Stasek *et al* (1992) suggested that intracellular phosphorylation does not occur until five to ten minutes after exposure of endothelial cells to thrombin. This led to the hypothesis that only a brief challenge is required to initiate an intracellular cascade of events, including protein phosphorylation, leading to extensive cell

rounding. Our F-actin studies agree with this, however the percentage of cells rounding up increased with continuing presence of histamine. The dissociation of F-actin from the membrane (loss of the DPB) may allow a degree of intercellular junction disorganisation. Loss of anchorage of transmembrane adhesion molecules, such as VE-cadherin, to the F-actin cytoskeleton is thought to coincide with redistribution of these molecules to non-junctional regions and lead to disruption of junctions (Tsukita *et al.*, 1992, Leach *et al.*, 1995). This would facilitate gap formation and increase permeability.

VE-cadherin expression in HMEC-1 cells following histamine exposure appeared less continuous, with observation of free cell edges at 10 and 20 min exposure. It was realised, however, that these changes were not clear and a way of quantifying the expression was attempted. The knowledge that alteration of VE-cadherin clustering within the paracellular cleft leads to a disruption in monolayer integrity and that intact VE-cadherin is necessary for normal homotypic cell-cell binding shows that examination of VE-cadherin staining patterns following histamine exposure may provide useful information as to the role of VE-cadherin in endothelial permeability (Navarro *et al.*, 1998; Gulino *et al.*, 1998). This project achieved this by examining the change in immunofluorescent pattern of VE-cadherin in response to histamine exposure of different times furthering recent work published on basic VE-cadherin dynamics (Andriopoulou *et al.*, 1999).

In-vitro studies have described a transformation from continuous immunofluorescent staining to discontinuous 'zig-zag' or 'stitch-like' pattern (Andriopoulou *et al.*, 1999; Budworth *et al.*, 1999). There was an indication from this study that 'stitch-like' and continuous VE-cadherin staining were linked, i.e.

the more membrane that exhibited a 'stitch-like' pattern the less was available to be continuous in nature. It is interesting to note that the relative level of discontinuous immunolabeling of VE-cadherin did not appear to show any consistent trends (possibly explaining the results in Chapter 4). This suggests that the discontinuous pattern (as defined in this project) is not a reaction of the VE-cadherin to histamine exposure – rather it is a constant feature of confluent HMEC-1 cells grown *in-vitro*. In conjunction with this the increase in 'stitch-like' and the decrease in continuous staining pattern would appear to be central to the histamine-induced VE-cadherin reaction. Using this deduction, it can be inferred that the 'stitch-like' pattern is related to modulation of the adherens junction. Indeed it is possible that the VE-cadherin is reorganising in a similar fashion as is seen in cells whose intercellular connections are being weakened. Reinforcing this theory is the presence of the 'stitch-like' pattern of VE-cadherin in the control cultures; they may be associated with the dynamic nature of the cell-cell interactions – connections between cells are constantly changing in strength and positioning in response to prevailing environmental conditions. This aspect of cells in culture is often ignored by many researchers. A similar change is seen with other inflammatory mediators, including VEGF, TNF α and thrombin and is correlated with increased permeability (Dejana, 1995; Esser *et al.*, 1998; Lampugnani *et al.*, 1992). This increases the possibility of a common pathway for endothelial permeability induction.

Analysis of the VE-cadherin arrangement was expected to give an indication of the level of involvement of VE-cadherin in endothelial permeability changes. Interpretation of the images was an important part as it was to be the basis upon

which conclusions were to be made. The method allowed a qualitative and quantitative analysis of VE-cadherin localisation following histamine exposure. The definition of each category – continuous, stitch-like and discontinuous is clear. However, when examining images, there was not always a clear distinction between categories. This introduced subjective interpretation, but the blinding of the images pre-analysis controlled for this. Further work to elucidate additional information upon the roles of VE-cadherin in the process of inflammation could use histamine antagonists, inhibitors of tyrosine kinases. Additionally reversal studies, like those done in chapter 5 with F-actin could be repeated analysing VE-cadherin to further link the two molecules. No quantitative estimation of total VE-cadherin at the membrane contact area was attempted. This could have been achieved used Western Blotting, Additionally the visualisation of VE-cadherin movement in live cells would give useful information during the rearrangement observed in this project and may be attempted by tagging it with GFP. Alexander *et al.* (2000) showed, via ELISA, that 10^{-4} M histamine decreased the total amount of VE-cadherin expressed on the surface of HUVEC to 62% of control values within 15 min, and returned to control levels by 60 min. However they indicate that these changes in surface VE-cadherin levels were not linked to an alteration in junctional location of the molecule.

Chapter 6 attempted to modulate the HMEC-1 junctions using cyclic AMP. Lampugnani *et al.* (1995) showed that in recently confluent cultures of HUVEC, where the adherens junction was proposed to be immature, the pattern of VE-cadherin staining was a fine, segmented line along the cell margins. In long

confluent HUVEC, VE-cadherin was a thick belt along cell contact area presenting a complex pattern. In these cultures the area occupied by a single cell declined and the actin DPB increased, whilst axial stress fibres were more common in recently confluent cells. In our HMEC-1 cultures the actin DPB was thin and VE-cadherin staining segmented in places. This, along with the muted permeability response the cells gave to histamine, led us to attempt to mature their junctions. An increase in intracellular cAMP has been shown to decrease paracellular permeability *in-vitro* and *in-vivo* (Langelier and van Hinsburgh, 1991; Rubin *et al.*, 1991, Stelzner *et al.*, 1989; Suttorp *et al.*, 1993) and this may be correlated with an increase in tight junction number or complexity (Adamson *et al.*, 1998; Duffey *et al.*, 1981; Wolburg *et al.*, 1994). We therefore added a cocktail of cAMP inducing agents to the media and observed the cell's basal and post-histamine permeability and the expression of junctional components. In agreement with Dye *et al.* (2001), increasing cAMP caused an upregulation in the expression intensity and localisation of the adherens junction molecules; VE-cadherin, α -catenin, plakoglobin (γ -catenin) and cortical F-actin. This indicated that cAMP affected the localisation of the AJs in the HMEC-1 cells. This together with the apparent decrease in junctional staining of β -catenin indicated that cAMP altered the cadherin-catenin complex, as in long-confluent HUVEC cultures (Andriopoulou *et al.*, 1999; Lampugnani *et al.*, 1995). Furthermore, analysis of the distribution of α -catenin between the triton-soluble and the triton-insoluble (purported to contain the intercellular junctions) fractions of the cells showed that cAMP caused an elimination of the catenin in the triton-soluble fraction, whilst there appeared to be

an increase in the catenin levels in the triton-insoluble fraction. This suggests that cAMP caused the redirection of α -catenin to the junctional regions of the cells. Further molecular biology work would be required to verify this observation. In HMEC-1 cells pre-exposed to cAMP media, exposure to histamine did not result in an increase in permeability to FD70. This was in agreement with a number of researchers (Carson *et al.*, 1989; Langeler and van Hinsburgh, 1991) who indicated that the histamine-related increase in permeability they observed was attenuated by pre-exposure to cAMP raising agents.

In conclusion this study has identified that the HMEC-1 cell-line possess pertinent components of the adherens junction, but not the tight junction. Non-physiological compounds that affect Ca^{2+} signalling and a surfactant, known to target cell-cell junctions in epithelial cells were shown to increase HMEC-1 permeability and disrupt VE-cadherin and F-actin. The physiologically relevant molecule histamine also caused an increase in permeability and a rearrangement of VE-cadherin and F-actin. Here the dynamics of VE-cadherin staining were quantified and found to correlate to histamine exposure time. Finally the HMEC-1 cells responded to cAMP media by decreasing the permeability and up-regulating junctional molecules. Many questions about the mechanisms that regulate paracellular permeability remain to be answered. It may be that each junctional component plays a particular role in the maintenance of endothelial barrier function.

The central hypothesis of this dissertation has been proven.

Future Work:

Much remains to be elucidated about the mechanisms that regulate endothelial permeability *in-vitro* or *in-vivo*. Some ideas for future research that may bring one closer to understanding the key mechanisms are discussed below.

1. The hypothesis tested in this project is that disruption of endothelial junctions causes increased transport of tracers through paracellular clefts. The alternative hypothesis to this states that increases in vascular permeability occurs via the formation of transient transcellular channels by fusion of caveolae or vesicles (Dvorak *et al.*, 1996; Michel and Neal, 1999). Preliminary work was undertaken in this laboratory using confocal microscopy, optical sectioning and tilting of sections at the z axis, in order to observe the position of FD70 as it passed through the cell monolayer. No free FD70 was visible within the cells indicating that in HMEC-1, FD70 does not cross through cells thus providing support to the paracellular transport route. However, this work needs to be confirmed with the use of transmission electron microscopy and electron dense tracers to observe whether transendothelial channels are indeed induced in the HMEC-1 cells following challenge with histamine. It is likely however that the actual scenario may well be a combination of the two hypothesis.

2. The work investigating the effect of increased cAMP on the molecular structure of the AJ requires furthering. This thesis concentrated on the changes that

occurred with α -catenin, tracking the localisation of the catenin via western blotting. The location of the subcellular pools of β - and γ -catenin and VE-cadherin should be investigated in a similar manner. The hypothesis by Lampugnani *et al.* (1995) states that in matures, restrictive junctions γ -catenin replaces β -catenin in the AJ. This thesis supports this observation with qualitative evidence; western blots of the cytosolic and cytoskeletal fragments of the cells would confirm whether cAMP also returns γ -catenin to the adherens junction, thus strengthening the present consensus of opinion. The dramatic effect that histamine had on the rearrangement of VE-cadherin in the cells should be supported by further experiments where cells are stimulated with histamine, in the presence of histamine receptor antagonists. If this inhibits the perturbation of VE-cadherin, then the proposed link between histamine signalling and VE-cadherin alterations would be strengthened. Furthermore, the use of neutralising anti-VE-cadherin antibodies should also be used to verify whether it is VE-cadherin itself or its sister molecules which are responsible for the junctional disruption seen in the presence of histamine. Additionally the reversal of the histamine-induced VE-cadherin changes following removal of the agonist could show the plasticity of VE-cadherin in this response.

3. The phosphorylation status of the VE-cadherin, and the other AJ molecules, after inflammatory insult would be an interesting avenue to pursue. This would confirm the mechanism behind the molecular movement seen. Immunocytochemistry could be used to investigate the expression of

phosphorylated tyrosine residues throughout the cells, with expression expected to have a greater intensity at cell-cell contacts in immature/disrupted junction (Dye *et al.*, 2001). Further, western blotting could be used to indicate the levels of phosphorylation of the junctional molecules of interest. This was undertaken by Andriopoulou *et al.* (1999), however the strain of HMEC-1 cell used by these authors appeared to be different from the HMEC-1 used in this project. Their HMEC-1 cells responded with increased permeability to FD70 following brief histamine challenge, a response not echoed in our system. To follow on from this the use of tyrosine kinase, serine/threonine protein kinases and PKC inhibitors and tyrosine phosphatases could help dissect out the signalling pathway that histamine is evoking in this cell line.

4. The HMEC-1 cell line does not express TJs, which has given us an exciting tool with which to study the roles of the TJ and AJ in the endothelium separately. Of prime interest would be to investigate the effect of transfecting these cells with occludin or ZO-1 and test their effect on basal permeability, molecular occupancy and ultrastructure of the junctions. The importance of tight junctions in regulating permeability in non-brain endothelial cells would be elucidated with this type of study.

5. Finally, real time visualisation of VE-cadherin movement in live cells would be the ultimate evidence for our hypothesis. This may be attempted by tagging VE-cadherin with Green Fluorescent Protein, transfecting cells with this tagged protein, and then stimulating the cells with histamine. Tracking the movement of

VE-cadherin would allow one to gain information as to how soon histamine affects VE-cadherin, as well as the ultimate fate of the perturbed molecule. Whether VE-cadherin moves away from junctional regions but remains in the plasma membrane, or whether internalisation and degradation occurs remain to be resolved.

As always science stays dormant for no one, there are always questions to be answered, and the field of endothelial permeability is no exception.

REFERENCES.

Adamson RH. (1990). Permeability of frog mesenteric capillaries after partial pronase digestion of the endothelial glycocalyx. *Journal of Physiology (London)*. 428. 1-13.

Adamson RH and Clough G. (1992). Plasma proteins modify the endothelial cell glycocalyx of frog mesenteric microvessels. *Journal of Physiology (London)*. 445. 473-486.

Adamson RH and Michel CC. (1993). Pathways through the intercellular clefts of frog mesenteric capillaries. *Journal of Physiology (London)*. 466. 303-327.

Adamson RH, Liu B, Fry GN, Rubin LL and Curry FE. (1998). Microvascular permeability and number of tight junctions are modulated by cAMP. *American Journal of Physiology*. 274. H1885-94.

Ades EW, Candal FJ, Swerlick RA, George VG, Summers S, Bosse DC and Lawley TJ. (1992). HMEC-1: establishment of an immortalized human microvascular endothelial cell line. *Journal of Investigative Dermatology*. 99. 683-690.

Albelda SM, Sampson PM, Haselton FR, McNiff JM, Mueller SN, Williams SK, Fishman AP and Levine EM. (1988). Permeability characteristics of cultured endothelial cell monolayers. *Journal of Applied Physiology*. 64. 308-322.

Albelda SM, Muller WA, Buck CA and Newman PJ. (1991). Molecular and cellular properties of PECAM-1 (endoCAM/CD31): A novel vascular cell-cell adhesion molecule. *Journal of Cell Biology*. **114**. 1059-1068.

Alberts B, Bray D, Lewis J, Raff M, Roberts K and Watson JD. (1989). Chapter 6. The Plasma Membrane. In *"Molecular Biology of the Cell"*. 322-323. Published by Garland Publishing, Inc. New York.

Alexander JS, Alexander BC, Eppihimer LA, Goodyear N, Haque R, Davis CP, Kalogeris TJ, Carden DL, Zhu Y and Nevil CG. (2000). Inflammatory mediators incude sequestration of VE-cadherin in cultured human endothelial cells. *Inflammation*. **24**. 99 – 113.

Ali J, Liao F, Martens E and Muller W. (1997). Vascular endothelial cadherin (VE-cadherin): Cloning and role in endothelial cell-cell adhesion. *Microcirculation*. **4**. 267-277.

Anderson JM, Balda MS and Fanning AS. (1993). The structure and regulation of tight junctions. *Current Opinions in Cell Biology*. **5**. 772-778.

- Andriopoulou P, Navarro P, Zanetti A, Lampugnani MG and Dejana E. (1999). Histamine induces tyrosine phosphorylation of endothelial cell-to-cell adherens junctions. *Arteriosclerosis Thrombosis and Vascular Biology*. **19**. 2286-2297.
- Aschner JL, Lum H, Fletcher PW and Malik AB. (1997). Bradykinin- and thrombin-induced increases in endothelial permeability occur independently of phospholipase C but require protein kinase C activation. *Journal of Cellular Physiology*. **173**. 387-396.
- Auerbach R, Alby L, Morrissey L W, Tu M and Joseph J. (1985). Expression of organ-specific antigens on capillary endothelial cells. *Microvascular Research*. **29**. 401-411.
- Ayalon O. and Geiger B. (1997). Cyclic changes in the organisation of cell adhesions and associated cytoskeleton, induced by stimulation of tyrosine phosphorylation in bovine aortic endothelial cells. *Journal of Cell Science*. **110**. 547-556.
- Balda MS, Whitney JA, Flores C, Gonzaliz S, Cereijido M and Matter K. (1996). Functional dissociation of paracellular permeability and transepithelial electrical-resistance and disruption of the apical-basolateral intramembrane diffusion barrier by expression of a mutant tight junction membrane-protein. *Journal of Cell Biology*. **134**. 1031-1049.

Baldwin AL and Thurston G. (1995). Changes in endothelial actin cytoskeleton in venules with time after histamine treatment. *American Journal of Physiology*. **269**. H1528-1537.

Balls M and Karcher S. (1995). The validation of alternative test methods. *ATLA*. **23**. 884-886.

Barnes PJ. (2001). Histamine and serotonin. *Pulmonary Pharmacology & Therapeutics*. **14**. 329 – 339.

Bates DO, Lodwick D and Williams B. (1999). Vascular endothelial growth factor and microvascular permeability. *Microcirculation*. **6**. 83-96.

Bazzoni G, Dejana E and Lampugnani MG. (1999). Endothelial adhesion molecules in the development of the vascular tree: the garden of forking paths. *Current Opinion in Cell Biology*. **11**. 573-581.

Beynon HLC, Haskard DO, Davies KA, Haroutunian R and Walport MJ. (1993). Combinations of low concentrations of cytokines and acute agonists synergize in increasing the permeability of endothelial monolayers. *Clinical and Experimental Immunology*. **91**. 314-319.

Boller K, Vestweber D and Kemler R. (1985). Cell-adhesion molecule uvomorulin is localized in the intermediate junctions of adult intestinal epithelial cells. *Journal of Cell Biology*. **100**. 327-332.

Borenfreund E and Puerner JA. (1985). Toxicity determined in vitro by morphological alterations and neutral red absorption. *Toxicology Letters*. **24**. 119-124.

Boulanger C, Schini VB, Moncada S and Vanhoutte PM. (1990). Stimulation of cyclic GMP production in cultured endothelial cells of the pig by bradykinin, adenosine diphosphate, calcium ionophore A23187 and nitric oxide. *British Journal of Pharmacology*. **101**. 152-156.

Braverman IM and Keh-Yen A. (1986). Three-dimensional reconstruction of endothelial cell gaps in psoriatic vessels and their morphologic identity with gaps produced by the intradermal injection of histamine. *Journal of Investigative Dermatology*. **86**. 577-581.

Bray JJ, Cragg PA, Macknight ADC, Mills RG and Taylor DW. (1989). Chapter 1. Introduction to Physiology. In '*Lecture Notes on Human Physiology*'. 1-33. Published by Blackwell Scientific Publications. Oxford.

Brevario F, Caveda L, Corada M, Martin-Padura I, Navarro P, Golay J, Introna M, Gulino D, Lampugnani MG and Dejana E. (1995). Functional properties of human vascular endothelial cadherin (7B4/cadherin-5), an endothelium-specific cadherin. *Arteriosclerosis, Thrombosis and Vascular Biology*. **15**. 1229-1239.

Brown J, Reading SJ, Jones S, Fitchett CJ, Howl J, Martin A, Longland, CL, Michelangeli F, Dubrova YE and Brown CA. (2000). Critical evaluation of ECV304 as a human endothelial cell model defined by genetic analysis and functional responses: a comparison with the human bladder cancer derived epithelial cell line T24/83. *Laboratory Investigation*. **80**. 37-45.

Brown Z and Neild GH. (1987). Cyclosporine inhibits prostacyclin production by cultured human endothelial cells. *Transplantation Proceedings*. **19**. 1178-1180.

Budworth RA, Clothier RH and Leach L. (1997a). Characterisation of two human endothelial cell-lines for use in *in-vitro* paracellular permeability studies. *International Journal of Microcirculation*. **17**. 210.

Budworth RA, Anderson M, Clothier RH and Leach L. (1997b). The interendothelial junctions of the human endothelial cell-line, HMEC-1. *Journal of Anatomy*. **192**. 463-464.

Budworth RA, Anderson M, Clothier RN and Leach L. (1999). Histamine-induced changes in the actin cytoskeleton of the human microvascular endothelial cell line HMEC-1. *Toxicology In Vitro*. **13**. 789-795.

Burke-Gaffney A and Keenan AK. (1995). Assessment of human endothelial permeability *in vitro*: The importance of cell seeding density. *Endothelium* **3**. 75-79.

Carmeliet P, Lampugnani MG, Moons L, Breviario F, Bono F, Balconi G, Compernelle V, Spagnuolo R, Dewerchin M, Zanetti A, Oosthuysen B, Angelillo A, Nuyens D, Clotman F, de Ruiter MC, Gittenberger-de Groot A, Herbert JM, Lupu F, Collen D and Dejana E. (1999). Targeted deficiency or cytosolic truncation of the VE-cadherin gene in mice impairs VEGF-mediated endothelial survival and angiogenesis. *Cell*. **98**. 147-157.

Carson MR, Shasby SS and Shasby DM. (1989). Histamine and inositol phosphate accumulation in endothelium: cAMP and a G protein. *American Journal of Physiology*. **257**. L259-L264.

Casnocha S A, Eskin S G, Hail E R and McIntire L V. (1989). Permeability of human endothelial monolayers: Effects of vasoactive agonists and cAMP. *Journal of Applied Physiology*. **67**. 1997-2005.

Castagna M, Takai Y, Kaibuchi K, Sano K, Kikkawa U and Nishizuka Y. (1982). Direct activation of calcium-activated, phospholipid-dependent protein kinase by tumor-promoting phorbol esters. *Journal of Biological Chemistry*. **257**. 7847 – 7851.

Caveda L, Martin-Padura I, Navarro P, Brevario F, Corada M, Gulino D, Lampugnani MG and Dejana E. (1996). Inhibition of cultured cell growth by vascular endothelial cadherin (cadherin-5/VE-cadherin). *Journal of Clinical Investigation*. **98**. 886-893.

Chappey O, Wautier MP and Wautier JL. (1995). Endothelial cells in culture: a model to study *in vitro* vascular toxicity. *Toxicology In Vitro*. **9**(4). 411-419.

Cines DB, Pollak ES, Buck CA, Loscalzo J, Zimmerman GA, McEver RP, Poer JS, Wick TM, Konkle BA, Schwartz GA, Barnathan ES, McCrae KR, Hug BA, Schmidt A, Stern DM. (1998). Endothelial cells in physiology and pathophysiology of vascular disorders. *Blood*. **91**. 3527-3561.

Clough G. (1991). Relationship between microvascular permeability and ultrastructure. *Progress in Biophysics and Molecular Biology*. **55**. 47-69.

Cohen AW, Carbajal JM and Schaeffer RC. (1999). VEGF stimulates tyrosine phosphorylation of β -catenin and small-pore endothelial barrier dysfunction. *American Journal of Physiology*. 277. H2038-H2049.

Collares-Buzato CB, Jepson MA, Simmons NL and Hirst BH. (1998). Increased tyrosine phosphorylation causes redistribution of adherens junction and tight junction proteins and perturbs paracellular barrier function in MDCK epithelia. *European Journal of Cell Biology*. 76. 85-92.

Corada M, Marriotti M, Thurston G, Smith K, Kunkel R, Brockhaus M, Lampugnani MG, Martin-Padura I, Stoppacciaro A, Ruco L, McDonald DM, Ward PA and Dejana E. (1999). Vascular-endothelial cadherin is an important determinant of microvascular integrity *in-vivo*. *Proceedings of the National Academy of Science, USA*. 96. 9815-9820.

Curren RD, Southey JA, Spielmann H, Liebsch M, Fentem JH & Balls M. (1995). The role of prevalidation in the development, validation and acceptance of alternative methods. ECVAM prevalidation task force report 1. *ATLA*. 23. 211-217.

Curry FE and Michel CC. (1980). A fiber matrix model of capillary permeability. *Microvascular Research*. 20. 96-99.

- Curry FE. (1992). Modulation of venular microvessel permeability by calcium influx into endothelial cells. *FASEB Journal*. **6**. 2456-2466.
- Dale HH and Laidlaw PP. (1910). The physiological action of β -imidazolyethylamine. *Journal of Physiology (London)*. **41**. 318 – 344.
- Davies MG and Hagen PO. (1993). The vascular endothelium: A new horizon. *Annals of Surgery*. **218**. 593-609.
- Dejana E, Corada M and Lampugnani MG. (1995). Endothelial cell-cell junctions. *FASEB Journal*. **9**. 910-918.
- Dejana E. (1996). Cell adhesion in vascular biology: Endothelial adherens junctions: Implications in the control of vascular permeability and angiogenesis. *Journal of Clinical Investigation*. **98**. 1949-1952.
- Dull RO, Jo H, Sill H, Hollis TM and Tarbell JM. (1991). The effect of varying albumin concentration and hydrostatic pressure on hydraulic conductivity and albumin permeability of cultured endothelial monolayers. *Microvascular Research*. **41**. 390-407.
- Duffey ME, Hainau B, Ho SS, Bentzel CJ. (1981). Regulation of epithelial tight junction permeability by cyclic AMP. *Nature*. **294**. 451-453.

Dvorak AM, Kohn S, Morgan ES, Fox P, Nagy JA and Dvorak HF. (1996). The vesiculo-vacuolar organelle (VVO): A distinct endothelial cell structure that provides a transcellular pathways for macromolecular extravasation. *Journal of Leukocyte Biology*. **59**. 495-509.

Dye JF, Clark P, Leach L and Firth JA. (1998). Modulation of cell-cell contacts in human microvascular endothelial cells *in-vitro*: distinct effects of cAMP and growth factors. *Journal of Vascular Research*. **35**. 20.

Dye JF, Jablenska R, Donnelly JL, Lawrence L, Leach L, Clark P and Firth JA. (2001). Phenotype of the endothelium in the human term placenta. *Placenta*. **22**. 32-43.

Ehringer WD, Edwards MJ and Miller FN. (1996). Mechanisms of α -thrombin, histamine and bradykinin induced endothelial permeability. *Journal of Cellular Physiology*. **167**. 562-569.

Esser S, Lampugnani MG, Corada M, Dejana E and Risau W. (1998). Vascular endothelial growth factor induces VE-cadherin tyrosine phosphorylation in endothelial cells. *Journal of Cell Biology*. **111**. 1853-1865.

Farquhar M and Palade G. (1963). Junctional complexes in various epithelia. *Journal of Cell Biology*. **17**. 375-412.

Firth JA, Bauman KF and Sibley CP. (1983). The intercellular junctions of guinea-pig placental capillaries: a possible structural basis for endothelial solute permeability. *Journal of Ultrastructural Research*. **85**. 45-57.

Franke WW, Cowin P, Grund C, Kuhn C and Kapprell HP. (1988). The endothelial junction. The plaque and its components. In *"Endothelial Cell Biology In Health and Disease"* (Eds. N Simionescu and M Simionescu). 147-166. Plenum Publishing Corporation, New York.

Franke WW, Kich PJ, Schäfer S, Heid HW, Troyanovsky SM, Moll I and Moll R. (1994). The desmosome and the syndesmos: cell junctions in normal development and in malignancy. *Princess Takamatsu Symposium*. **24**. 14-27.

Freshney R I, (1994). Chapter 18. Quantitation and Experimental Design. In *"Culture of Animal Cells: A manual of Basic Technique"*. 3rd Edition. 267-286. Published by Wiley-Liss, Inc. New York.

Furuse M, Hirase T, Itoh M, Nagafuchi A, Yonemura S, Tsukita S and Tsukita S (1993). Occludin – A novel integral membrane-protein localizing at tight junctions. *Journal of Cell Biology*. **123**. 1777-1788.

Furuse M, Itoh M, Hirase T, Nagafuchi A, Yonemura S, Tsukita S and Tsukita S. (1994). Direct association of occludin with ZO-1 and its possible involvement in the localization of occludin at tight junctions. *Journal of Cell Biology*. **127**. 1617-1626.

Galyani M, Ikrenyi C, Fekrete J, Ikrenyi K and Kovach GB. (1988). Ion concentrations in subcutaneous interstitial fluid: measured versus expected values. *American Journal of Physiology*. **24**. F513 – 519.

Gao X, Koulis P, Xu N, Minshall RD, Sandoval R, Vogel SM, and Malik AB. (2000). Reversibility of increased microvessel permeability in response to VE-cadherin disassembly. *American Journal of Physiology*. **279**. L1218-L1225.

Garcia JGN, Davis HW and Patterson CE. (1995). Regulation of endothelial cell gap formation and barrier dysfunction: Role of myosin light chain phosphorylation. *Journal of Cellular Physiology*. **163**. 510-522.

Garside J, Clothier RH, Somekh M and See CW. (1998). The use of simultaneous fluorescence and differential phase confocal microscopy to study Alamar Blue reduction in an epithelial cell line. *ATLA*. **26**. 505-522.

Geiger B and Ginsburg D. (1991). The cytoplasmic domain of adherens-type junctions. *Cell Motility and the Cytoskeleton*. **20**. 1-6.

Geiger B. (1989). Cytoskeleton-associated cell contacts. *Current Opinion in Cell Biology*. **1**. 103-109.

Geiger B, Ginsburg D, Salomon D, Volberg T. (1990). The molecular basis for the assembly and modulation of adherens-type junctions. *Cellular Differentiation and Development*. **32**. 343-354.

Gilbert-McClain LI, Verin AD, Shi S, Irwin RP and Garcia JGN. (1998). Regulation of endothelial cell myosin light chain phosphorylation and permeability by vanadate. *Journal of Cellular Biochemistry*. **70**. 141-155.

Gillies MC, Su T, Naidoo D. (1995). Electrical resistance and macromolecule permeability of retinal capillary endothelial cells *in-vitro*. *Current Eye Research*. **14**. 435-442.

Gimbrone Jr, MA. (1986). Vascular endothelium: Nature's blood container. In "*Vascular Endothelium in Haemostasis and Thrombosis*". Published by Churchill Livingstone, London.

Glynn PA, Picot J and Evans TJ. (2001). Coexpressed nitric oxide synthase and apical beta (1) integrins influence tubule cell adhesion after cytokine-induced injury. *Journal of the American Society of Nephrology*. **12**. 2370-2383.

Goebeler M, Yoshimura T, Toksoy A, Ritter U, Brücker E and Gillitzer R. (1997). The chemokine repertoire of human dermal microvascular endothelial cells and its regulation by inflammatory cytokines. *Journal of Investigative Dermatology*. **108**. 445-451.

Gotlieb AI, Langille BL, Wong MKK and Kim DW. (1991). Biology of disease: structure and function of the endothelial cytoskeleton. *Laboratory Investigations*. **65**. 123-137.

Grant DS, Kinsella JL, Kibbey MC, LaFlamme S, Burbelo PD, Goldstein AL and Kleinman HK. (1995). Matrigel induces thymosin β 4 gene in differentiating endothelial cells. *Journal of Cell Science*. **108**. 3685-3694.

Grega GJ and Adamski SW. (1991). Effect of local mast cell degranulation on vascular permeability to macromolecules. *Microcirculation, Endothelium and Lymphatics*. **7**. 267-291.

Gullino D, Delachanal E, Concord E, Genoux Y, Morand B, Valiron BM, Sulpice E, Scaife R, Alemany M and Vernet T. (1998). Alteration of endothelial cell

monolayer integrity triggers resynthesis of vascular endothelial cadherin. *Journal of Biological Chemistry*. **273**. 29786-29793.

Hall A. (1994). Small GTP-binding proteins and the regulation of the actin cytoskeleton. *Annual Reviews in Cellular Biology*. **10**. 31-54.

Haselton FR, Alexander JS, Mueller SN and Fishman AP. (1992). Chapter 6. Modulation of endothelial paracellular permeability: A mechanistic approach. In *"Endothelial Cell Dysfunctions"* (eds. N Simionescu and M Simionescu). 103-126. Published by Plenum Press. New York.

Hashida R, Anamizu C, Yagyu-Mizuno Y, Ohkuma S and Takano T. (1986) Transcellular Transport of Fluorescein Dextran through an Arterial Endothelial Cell Monolayer. *Cell Structure and Function*. **11**. 343-349.

Haugland RP, You W, Paragas K, Wells S and DuBose DA. (1994). Simultaneous visualisation of G- and F-actin in endothelial cells. *The Journal of Histochemistry and Cytochemistry*. **42**. 345-350.

Heimark RL, Degner M and Schwartz SM. (1990). Identification of a calcium-dependent cell-cell adhesion molecule in endothelial cells. *Journal of Cell Biology*. **110**. 1745-1756.

Hill SJ. (1990). Distribution, properties, and functional characteristics of three classes of histamine receptor. *Pharmacological Reviews*. **42**. 45-83.

Hill SJ. (1997). International Union of Pharmacology. XIII. Classification of histamine receptors. *Pharmacological Reviews*. **49**. 253 – 278.

Hirano S, Kimoto N, Shimovama Y, Hirohashi S and Takeichi M. (1992). Identification of a neural alpha-catenin as a key regulator of cadherin function and multicellular organization. *Cell*. **70**. 293-301.

Hirase T, Kawashima S, Wong EY, Ueyama T, Rititake Y, Tsyukita S, Yokoyama M and Staddon JM. (2001). Regulation of tight junction permeability and occludin phosphorylation by Rhoa-p160ROCK-dependent and -independent mechanisms. *Journal of Biological Chemistry*. **276**. 10423-10431.

Hirohashi S. (1998). Inactivation of the E-cadherin-mediated cell adhesion system in human cancers. *American Journal of Pathology*. **153**. 333-339.

Holbrook KA. (1994). The Ultrastructure of the Epidermis. In *“Keratinocyte Handbook”* (Eds. Leigh I, Watt F, Lane B). 3-39. Cambridge University Press, Cambridge.

Hordijk PL, Anthony E, Mul FPJ, Rientsma R, Oomen CJM and Roos D. (1999). Vascular-endothelial Cadherin modulates endothelial monolayer permeability. *Journal of Cell Science*. **112**. 1915-1923.

Hoschuetzky H, Aberle H and Kemler R. (1994). Beta-catenin mediates the interaction of the cadherin-catenin complex with epidermal growth factor receptor. *Journal of Cell Biology*. **127**. 1375-1380.

Ikeda K, Utoguchi N, Makimoto H, Mizuguchi H, Nakagawa S and Mayumi T. (1999). Different reactions of aortic and venular endothelial cell monolayers to histamine on macromolecular permeability: role of cAMP, cytosolic Ca²⁺ and F-actin. *Inflammation*. **23**. 87-97.

Ilan N, Cheung L, Pinter E and Madri JA. (2000). Platelet-endothelial cell adhesion molecule-1 (CD31), a scaffolding molecule for selected catenin family members whose binding is mediated by different tyrosine and serine/threonine phosphorylation. *Journal of Biological Chemistry*. **275**. 21435-21443.

Introna M, Colotta F, Sozzani S, Dejana E and Mantovani A. (1994). Pro- and anti-inflammatory cytokines: Interactions with vascular endothelium. *Clinical and Experimental Rheumatology*. **12**. S19-S23.

- Itoh M, Furuse M, Morita K, Kubota K, Saitou M and Tsukita S. (1999). Direct Binding of Three Tight Junction-associated MAGUKs, ZO-1, ZO-2, and ZO-3, with the COOH Termini of Claudins. *Journal of Cell Biology*. 147. 1351-1363.
- Jaffe EA, Nachman RL, Becker CG and Minick CR. (1973). Culture of human endothelial cells derived from umbilical veins. Identification by morphologic and immunologic criteria. *Journal of Clinical Investigations*. 52. 2745-2756.
- Jaffe EA. (1987). Cell biology of endothelial cells. *Human Pathology*. 18. 234-239.
- Janssens B, Goossens S, Staes K, Gilbert B, van Hengel J, Colpaert C, Bruzneeel E, Marel M and van Roy F. (2001). Alpha T-catenin; a novel tissue-specific beta-catenin-binding protein mediating strong cell-cell adhesion. *Journal of Cell Science*. 114. 3177-3188.
- Johnson A, Phillips P, Hocking D, Tsan MF and Ferro T. (1989). Protein kinase C inhibitor prevents pulmonary edema in response to H₂O₂. *American Journal of Physiology*. 256. H1012 – H1022.
- Kazakoff PW, McGuire TR, Hole EB, Gano M and Inersen PL. (1995). An in vitro model for endothelial permeability : Assessment of monolayer integrity. *In-Vitro Cellular and Developmental Biology – Animal*. 31. 846-852.

Kemler R. 1993. From cadherins to catenins: cytoplasmic protein interactions and regulation of cell adhesion. *Trends in Genetics*. **9**. 317 - 321.

Kern DF and Malik AB. (1985). Microvascular albumin permeability in isolated perfused lung: effects of EDTA. *Journal of Applied Physiology*. **58**. 372-375.

Kiessling F, Kartenbeck J and Haller C. (1999). Cell-cell contacts in the human cell-line ECV304 exhibit both endothelial and epithelial characteristics. *Cell and Tissue Research*. **297**. 131-140.

Killackey JJF, Johnston MG and Movat HZ. (1984). An in vitro system for the study of vascular permeability using endothelial cells cultured on collagen-coated microcarriers. *Federation Proceedings*. **43**. 4014.

Kimura M, Sawada N, Kimura H, Isomura H, Kirata K and Mori M. (1996). Comparison between the distribution of 7H6 tight junction associated antigen and occludin during the development of chick interline. *Cell Structure And Function* **22**. 91-96.

Knudsen KA, Soler AP, Johnson KR and Wheeler MJ. (1995). Interactions of α -actinin with the cadherin catenin cell-cell adhesion complex via α -catenin. *Journal of Cell Biology*. **130**.

Kodama A, Matozak M, Shinohara M, Fukuhara A, Tachibana K, Ichihashi M, Nakanishi H and Takai Y. (2001). Regulation of Ras and Rho small G proteins by SHP-2. *Genes Cells*. **6**. 869-876.

Koizumi H and Ohkawaara A. (1999). H₂ histamine receptor-mediated increase in intracellular Ca²⁺ in cultured human keratinocytes. *Journal of Dermatological Science*. **21**. 127-132.

Lampugnani MG, Resnati M, Dejana E and Marchisio PC. (1991). The role of integrins in the maintenance of endothelial monolayer integrity. *Journal of Cell Biology*. **112**. 479-490.

Lampugnani MG, Resnati M, Raiteri M, Pigott R, Pisacane A, Houen G, Ruco LP, Dejana E. (1992). A novel endothelial specific membrane protein is a marker of cell-cell contacts. *Journal of Cell Biology*. **118**. 1511 - 1522.

Lampugnani MG, Corada M, Caveda L, Breviario F, Ayalon O, Geiger B, Dejana E. (1995). The molecular organisation of endothelial cell-to-cell junctions: differential association of plakoglobin, β -catenin and α -catenin with vascular endothelial cadherin. *Journal of Cell Biology*. **129**. 203 - 217.

- Lampugnani MG and Dejana E. (1997). Interendothelial junctions: structure, signalling and functional roles. *Current Opinion in Cell Biology*. **9**. 674-682.
- Langelier EG, Fiers W and van Hinsbergh VWM. (1991). Effects of tumor necrosis factor on prostacyclin production and the barrier function of human endothelial cell monolayers. *Arteriosclerosis and Thrombosis*. **11**. 872-881.
- Langelier EG and van Hinsburgh VWM. (1988). Characterisation of an in-vitro model to study the permeability of a human arterial endothelial cell monolayer. *Thrombosis and Haemostasis*. **60**. 240-246.
- Langelier EG and van Hinsburgh VWM. (1991). Norepinephrine and iloprost improve barrier function of human endothelial cell monolayers: Role of cAMP. *American Journal of Physiology*. **260**. C1052-C1059.
- Langille BL, Graham JJK, Kim D and Gotlieb AI. (1991). Dynamics of shear-induced redistribution of F-actin in endothelial cells *in vitro*. *Arteriosclerosis and Thrombosis*. **11**. 1814-1820.
- Laskin DL and Pendino KJ. (1995). Macophages and Inflammatory mediators in tissue injury. *Annual Reviews in Pharmacology and Toxicology*. **35**. 655-677.

Lau DCW, Wong KL and Hwang WS. (1989). Cyclosporine toxicity on cultured rat microvascular endothelial cells. *Kidney International*. **35**. 604-613.

Lawley TJ and Kubota Y. (1989). Induction of morphologic differentiation of endothelial cells in culture. *Journal of Investigative Dermatology*. **93**. 59S-61S.

Leach L and Firth JA. (1992). Fine structure of the paracellular junctions of terminal villous capillaries in the perfuse human placenta. *Cell and Tissue Research*. **268**. 447-452.

Leach L and Firth JA. (1995). Advances in understanding permeability in fetal capillaries of the human placenta: A review of the organisation of the endothelial paracellular clefts and their junctional complexes. *Reproduction, Fertility and Development*. **7**. 1451-1456.

Leach L, Eaton BM, Westcott EDA and Firth JA. (1995). Effect of histamine on endothelial permeability and structure and adhesion molecules of the paracellular junctions of perfused human placental microvessels. *Microvascular Research*. **50**. 323-337.

Leach L, Lammiman MJ, Babawale MO, Hobson SA, Bromilou B, Lovat S and Simmonds MJR. (2000). Molecular organisation of tight and adherens junction in the human placental vascular tree. *Placenta*. **21**. 547-557.

Li JM, Mullen AM and Shah AM. (2001). Phenotypic properties and characteristics of superoxide production by mouse coronary microvascular endothelial cells. *Journal of Molecular and Cellular Cardiology*. **33**. 1119-1131.

Liaw CW, Cannon C, Power MD, Kiboneka PK and Rubin LL. (1990). Identification and cloning of two species of cadherins in bovine endothelial cells. *EMBO Journal*. **9**. 2701-2708.

Liu L, Gao B, Mirshahi F, Sanval AJ, Khanolkar AD, Makriyannis A and Kunos G. (2000). Functional CB1 cannabinoid receptors in human vascular endothelial cells. *Biochemistry Journal*. **346**. 835-840.

Liu L, Li H, Underwood T, Lloyd M, David M, Speri G, Pamukcu R and Thompson WJ. (2001). Cyclic GMP-dependent protein kinase activation and induction by exisulind and CP461 in colon tumor cells. *Journal of Pharmacology and Experimental Therapeutics*. **299**. 583-589.

Liu SM and Sundqvist T. (1995). Involvement of nitric oxide in permeability alteration and F-actin redistribution induced by phorbol myristate acetate in endothelial cells. *Experimental Cell Research*. **221**. 289-293

Lum SM and Malik AB. (1996). Mechanisms of increased endothelial permeability. *Canadian Journal of Physiology and Pharmacology*. **74**. 787-800.

Lynch JJ, Ferro TJ, Brockenauer AM and Malik AB. (1989). Thrombin-mediated increases in endothelial permeability: roles of protein kinase C activation. *American Reviews in Respiratory Disorders*. **139**. A425.

Lynch JJ, Blumenstock FA, Brockenauer AM and Malik AB. (1990). Increased endothelial albumin permeability mediated by protein kinase C activation. *Journal of Clinical Investigation*. **85**. 1991-1998.

Madar JL, Hecht G. (1989). In *"Tight (Occluding) Junctions in Cultured (and Native) Epithelial Cells"* 131-163. Published by Alan Liss, Inc. New York

Madri JA, Williams SK, Wyatt T and Mezzio C. (1983). Capillary endothelial cultures: Phenotypic modulation by matrix components. *Journal of Cell Biology*. **97**. 153-165.

Malik AB, Lynch JJ and Cooper JA. (1989). Endothelial barrier function. *Journal of Investigative Dermatology*. **93**. 62S – 67S.

- Majno G and Palade G. (1961). Studies on Inflammation. 1. Effect of histamine and serotonin on vascular permeability: an electron microscopic study. *Journal of Biophysics, Biochemistry and Cytology*. **11**. 571 – 605.
- Mantovani A and Dejana E. (1989). Cytokines as communication signals between leukocytes and endothelial cells. *Immunology Today*. **10**. 370-375.
- Marcus BC, Wyble CW, Hynes KL and Gewertz BL. (1996). Cytokine-induced increases in endothelial permeability occur after adhesion molecule expression. *Surgery*. **120**. 411-417.
- Maruo N, Morita I, Shirao M. and Murota S. (1992). IL-6 increases endothelial permeability *in-vitro*. *Endocrinology*. **131**. 710-714.
- Maurer P, Hohenester E and Engel J. (1996). Extracellular calcium-binding proteins. *Current Opinion in Cell Biology*. **8**. 609 – 617.
- Mauro L, Bartucci M, Morelli C, Ando S and Surmacz E. (2001). IGF-1 receptor induced cell-cell adhesion of MCF-7 breast cancer cells requires the expression of junction protein ZO-1. *Journal of Biological Chemistry*. **276**. 39892-39897.

- Maxwell SA and Davies GE. (2000). Biological and molecular characteristics of an ECV-304-derived cell-line resistant to p53-mediated apoptosis. *Apoptosis*. **5**. 277-290.
- McDonald DM, Thruston G and Baluk P. (1999). Endothelial gaps as sites for plasma leakage in inflammation. *Microcirculation*. **6**. 7-22.
- McNeill H, Ryan TA, Smith SJ and Nelson WJ. (1993). Spatial and temporal dissection of intermediate and early events following cadherin-mediated epithelial cell adhesion. *Journal of Cell Biology*. **120**. 1217-1226.
- Mehta D, Rahman A and Malik AB. (2001). Protein kinase C- α signals Rho-guanine nucleotide dissociation inhibitor phosphorylation and Rho activation and regulates the endothelial barrier function. *Journal of Biological Chemistry*. **276**. 22614-22620.
- Menon GK, Elias PM and Feingold KR. (1994). Integrity of the permeability barrier is crucial for maintenance of the epidermal Ca^{2+} gradient. *British Journal of Dermatology*. **130**. 139 – 147.
- Michel CC and Curry FE. (1999). Microvascular permeability. *Physiological Reviews*. **79**. 703-761.

- Michel CC and Neal CR. (1999). Openings through endothelial cells associated with increased microvascular permeability. *Microcirculation*. **6**. 45-54.
- Miles AA and Miles EM. (1952). Vascular reaction to histamine, histamine liberator and leukotaxyne in the skin of guinea pigs. *Journal of Physiology*. **118**. 228-257.
- Morel NM. (1994). An Inflammatory stimulus induces rapid changes in wheat germ agglutination binding to cultured microvascular endothelial cells. *Endothelium*. **2**. 255 – 264.
- Morita K, Sasaki H, Furuse M and Tsukita S. (1999). Endothelial Claudin: Claudin-5/TMVCF Constitutes Tight Junction Strands in Endothelial Cells. *Journal of Cell Biology*. **147**. 185-194.
- Moreno JJ. (2001). Antiflammin-2 prevents HL-60 adhesion to endothelial cells and prostanoid production induced by lipopolysaccharides. *Journal of Pharmacology and Experimental Therapeutics*. **296**. 884-889.
- Moy AB, Blackwell K and Kamath A. (2002). Differential effects of histamine and thrombin on endothelial barrier function and actin-myosin tension. *Amercian Journal of Physiology*. **282**. H21-H29.

- Muller WA, Ratti CM, McDonnell SL and Cohn ZA. (1989). A human endothelial cell-restricted, externally disposed plasmalemmal protein enriched in intercellular junctions. *Journal of Experimental Medicine*. **170**. 399-414.
- Nagpala PG, Malik AB, Vuong PT and Lum H. (1996). Protein kinase C β_1 overexpression augments phorbol ester-induced increase in endothelial permeability. *Journal of Cellular Physiology*. **166**. 249-255.
- Narumiya S, Ishizaki T and Watanabe N. (1997). Rho effectors and reorganisation of actin cytoskeleton. *FEBS Letters*. **410**. 68-72.
- Navarro P, Caveda L, Brevario F, Mandoteanu , Lampugnani MG and Dejana E. (1995). Catenin-dependent and -independent functions of vascular endothelial cadherin. *Journal of Biological Chemistry*. **270**. 30965-30972.
- Neal CR and Michel CC. (1995). Transcellular gaps in microvascular walls of frog and rat when permeability is increased by perfusion with the ionophore A23187. *Journal of Physiology*. **488**. 427-437.
- Niimi N, Noso N. and Yamamoto S. (1992). The effect of histamine on cultured endothelial cells. A study of the mechanism of increased vascular permeability. *European Journal of Pharmacology*. **221**. 325-331.

O'Brien J, Wilson I, Orton T and Pognan F. (2000). Investigation of the Alamar Blue (Resazurin) fluorescent dye for the assessment of mammalian cell cytotoxicity. *European Journal of Biochemistry*. **267**. 5421-5436.

Odland, G.F. (1983). Structure of the skin. In "*Biochemistry and Physiology of the skin*". (Ed. L.A. Goldsmith). Oxford University Press, New York.

Ozawa M, Engel J and Kemler R. (1990). Single amino acid substitutions in one Ca^{2+} binding site of uvomorulin abolish the adhesive function. *Cell*. **63**. 1033-1038.

Palacio S, Schmitt D and Viac J. (1997). Contact allergens and sodium lauryl sulphate upregulates vascular endothelial growth factor in normal keratinocytes. *British Journal of Dermatitis*. **137**. 540-544.

Palade GE. (1960). Transport in quanta across the endothelium of blood capillaries. *Anatomy Records*. **116**. 254.

Pappenheimer JR, Renkin EM and Borrero JM. (1951). Filtration, diffusion and molecular sieving through peripheral capillary membranes. A contribution to the pore theory of capillary permeability. *American Journal of Physiology*. **167**. 13-46.

Parish WE. (1990). Inflammatory mediators applied to *in vitro* toxicology: Studies on mediator release and two-cell systems. *Toxicology In Vitro*. **4**. 231-241.

Park JH, Okayama N, Gute D, Krsmanovic A, Battarbee H and Alexander JS. (1999). Hypoxia/aglycemia increases endothelial permeability: Role of second messengers and cytoskeleton. *American Journal of Physiology*. **277**. C1066-C1074.

Partridge CA, Horvath CJ, Del Vecchio PJ, Phillips PG and Mailk AB. (1992). Influence of extracellular matrix in tumor necrosis factor-induced increase in endothelial permeability. *American Journal of Physiology*. **263**. L627 - L633.

Patterson CE, Davis HW, Schaphorst KL and Garcia JGN. (1994). Mechanisms of cholera toxin prevention of thrombin and PMA-induced endothelial barrier dysfunction. *Microvascular Research*. **48**. 212-235.

Pearson JD. (1991). Endothelial cell biology. *Radiology*. **179**. 9-14.

Pokutta S, Herrenknecht K, Kemler R, Engel J. (1994). Conformational changes of the recombinant extracellular domain of E-cadherin upon Ca^{2+} binding. *European Journal of Biochemistry*. **223**. 1019 – 1026.

Predescu D, Predescu S and Mailk AB. (2002). Transport of nitrated albumin across continuous vascular endothelium. *Proceedings of the National Academy of Science, USA*. 99. 13932-13937.

Rabiet MJ, Plantier JL, Rival Y, Genoux Y, Lampugnani MG and Dejana E. (1996). Thrombin-induced increase in endothelial permeability is associated with changes in cell-to-cell junction organisation. *Arteriosclerosis, Thrombosis and Vascular Biology*. 16. 488-496.

Rasmussen E.S. (1999). Use of fluorescent redox indicators to evaluate cell proliferation and viability. In *"Alternatives 53; in vitro Molecular Toxicology*. 12. 47-58. Edited by A Goldberg. Published by Mary Ann Liebert, Inc. New York.

Ratcliffe MJ, Smales C and Staddon JM. (1999). Dephosphorylation of the catenins p120 and p100 in endothelial cells in response to inflammatory stimuli. *Biochemistry Journal*. 338. 471-478.

Renkin EM. (1994). Cellular aspects of transvascular exchange: a 40-year perspective. *Microcirculation*. 1. 157-167.

Rimm DL and Morrow JS. (1994). Molecular cloning of human E-cadherin suggests a novel subdivision of the cadherin superfamily. *Biochemical and Biophysical Research Communications*. **200**. 1754 – 1761.

Rotrosen D. and Gallin JI. (1986). Histamine type-1 receptor occupancy increases endothelial cytosolic calcium, reduces F-actin, and promotes albumin diffusion across cultured endothelial monolayers. *Journal of Cell Biology*. **103**. 2379-2387.

Rubin LL, Hall DE, Porter S, Barbu K, Cannon C, Horner HC, Janatpour M, Liaw CW, Manning K, Morales J, Tanner LI, Tomaselli KJ and Bard F. (1991). A cell culture model of the blood-brain barrier. *Journal of Cell Biology*. **115**. 1725-1735.

Rubin LL. (1992). Endothelial cells: adhesion and tight junctions. *Current Opinions in Cell Biology*. **4**. 830 - 833.

Rumbaut RE, Harris NR, Sial AJ, Huxley VH and Granger N. (1999). Leakage responses to L-NAME differ with the fluorescent dye used to label albumin. *American Journal of Physiology*. **276**. H333-H339.

- Rungger-Brändle E. and Gabbiani G. (1983). The role of cytoskeletal and cytocontractile elements in pathologic processes. *American Journal of Pathology*. **110**. 361-392.
- Salomon D, Ayalon O, Patel-King R, Hynes RO, Geiger B. (1992). Extrajunctional distribution of N-cadherin in cultured endothelial cells. *Journal of Cell Science*. **102**. 1 - 11.
- Schaeffer RC, Bitrick MS, Holberg WC and Katz MA. (1992a). Macromolecular transport across endothelial monolayers. *International Journal of Microcirculation, Clinical and Experimental*. **11**. 181-201.
- Schaeffer R C Jr., Gorg F, and Bitrick M S Jr. (1992b). Restricted diffusion of macromolecules by endothelial monolayers and small-pore filters. *American Journal of Physiology*. **263**. L27-36.
- Schmelz M, Schmid VJ and Parrish AR. (2001). Selective disruption of cadherin/catenin complexes by oxidative stress in precision-cut mouse liver slices. *Toxicological Sciences*. **61**. 389-394.
- Schneeberger EE and Hamelin M. (1984). Interaction of serum proteins with lung endothelial glycocalyx: Its effect on endothelial permeability. *American Journal of Physiology*. **247**. H206-H217.

Schneider E, Rolli-Derkinderen M, Arock M and Dy M. (2002). Trends in histamine research: new functions during immune responses and haematopoiesis. *Trends in Immunology*. **23**. 255-263.

Schnittler H, Wilke A, Gress T, Suttorp N and Drenckhahn D. (1990). Role of actin and myosin in the control of paracellular permeability in pig, rat and human vascular endothelium. *Journal of Physiology (London)*. **431**. 379-401.

Schulze C and Firth JA. (1992). The interendothelial junction in myocardial capillaries: Evidence for the existence of regularly spaced cleft-spanning structures. *Journal of Cell Science*. **101**. 647-655.

Scism JL, Laska DA, Horn JW, Gimple JL, Pratt SE, Shepard RL, Dantzig AH and Wrighton SA. (1999). Evaluation of an in vitro coculture model for the blood-brain barrier: comparison of human umbilical vein endothelial cells (ECV304) and rat glioma cells (C6) from two commercial sources. *In Vitro Cellular and Developmental Biology – Animal*. **35**. 580-592.

Shasby DM, Shasby SS, Sullivan JM and Peach MJ. (1982). Role of endothelial cell cytoskeleton in control of endothelial permeability. *Circulation Research*. **51**. 657-661.

Shasby DM, Lind SE, Shasby SS, Goldsmith JC, Hunninghake GW. (1985). Reversible oxidant-induced increases in albumin transfer across cultured endothelium: Alterations in cell shape and calcium homeostasis. *Blood*. **65**. 605-614.

Shasby DM and Shasby SS. (1986). Effects of calcium on transendothelial albumin transfer and electrical resistance. *Journal of Applied Physiology*. **60**. 71-79.

Shasby DM, Yorek M and Shasby SS. (1988). Exogenous oxidants initiate hydrolysis of endothelial cell inositol phospholipids. *Blood*. **72**. 491 – 499.

Shaw AJ, Clothier RH and Balls M. (1990). Loss of trans-epithelial impermeability of a confluent monolayer of madin darby canine kidney cells as a determinant of ocular irritancy potential. *ATLA*. **18**. 145-151.

Shaw AJ, Balls M and Clothier RH. (1991). Predicting ocular irritancy and recovery from injury using madin darby canine kidney cells. *Toxicology In Vitro*. **5**. 569-571.

Simionescu M. (1988). Receptor mediated transcytosis of plasma molecules by vascular endothelium. In *“Endothelial Cell Biology in Health and Disease”* (eds. N Simionescu and M Simionescu). 69-109. Published by Plenum Press. London.

Simionescu N and Simionescu M. (1988). Chapter 1. In *"Endothelial Cell Biology"* 1-120. Published by Plenum Press. New York.

Simionescu N and Simionescu M. (1991). Endothelial transport of macromolecules: transcytosis and endocytosis. *Cell Biology Reviews*. **25**. 5-80.

Spagnoli LG, Pietra GG, Villaschi S and Johns LW. (1982). Morphometric analysis of gap junctions in regenerating arterial endothelium. *Laboratory Investigation*. **46**. 139-148.

Starcevic SL, Bortolin S, Woodcroft KJ and Novak RF. (2001). Kepone (Chlordecone) disrupts adherens junctions in human breast epithelial cells cultured in Matrigel. *In vivo*. **15**. 289-294.

Stasek JE, Patterson CE and Garcia JGN. (1992). Protein kinase C phosphorylates caldesmon₇₇ and vimentin and enhances albumin permeability across cultured bovine pulmonary artery endothelial cell monolayers. *Journal of Cellular Physiology*. **153**. 62-75.

Starzec, G, Owen M, Stipho S, and Clothier RH. (1999). Morphological changes in two epithelial cell lines upon exposure to a surfactant. *ATLA*. **27**. 331.

Stelzner TJ, Weil JV and O'Brien RF. (1989). Role of cAMP in the induction of endothelial barrier function. *Journal of Cellular Physiology*. **139**. 157-166.

Stevens A and Lowe JS. (1999). Histology. Gower Medical Publishing, London.

Stockinger et al. (2001). Calcium signalling and PKC α activate increased endothelial permeability by disassembly of VE-cadherin junctions. *Journal of Cell Biology*. **154**. 1185-1196.

Stuart RO and Nigam SK. (1995). Regulated assembly of tight junctions by protein-kinase-C. *Proceedings of the National Academy of Sciences of the United States of America*. **92**. 6072-6076.

Stylianou E and Saklatvala J. (1998). Interleukin-1. *The International Journal of Biochemistry and Cell Biology*. **30**. 1075 – 1079.

Suda K, Rothen-Rutishauser B, Gunthert M and Wunderlie-Allenspach H. (2001). Phenotypic characterization of human umbilical vein endothelial (ECV304) and urinary carcinoma (T24) cells: endothelial versus epithelial features. *In Vitro Cellular and Development Biology – Animal*. **37**. 505-514.

- Suttorp N, Weber U, Welsch T and Schudt C. (1993). Role of phosphodiesterases in the regulation of endothelial permeability in vitro. *Journal of Clinical Investigation*. **91**. 1421-1428.
- Suzuki S, Sano K, Tanihara H. (1991). Diversity of the cadherin family: evidence for eight new cadherins in nervous tissue. *Cell Regulation*. **2**. 261 - 270.
- Svensjo E. (1978). The hamster cheek pouch preparation as a model for studies of macromolecular permeability of the microvasculature. *Upsala Journal of Medical Sciences*. **83**. 71-79.
- Svensjo E, Cyrino F, Michoud E, Ruggiero D, Bouskela E and Wiernsperger N. (1999). Vascular permeability increase as induced by histamine or bradykinin is enhanced by advanced glycation endproducts (AGEs). *Journal of Diabetes and Its Complications*. **13**. 187-190.
- Swerlick RA. and Lawley TJ. (1993). Role of microvascular endothelial cells in inflammation. *Journal of Investigative Dermatology*. **100**. 111S-115S.
- Takahashi K, Sawasaki Y, Hata J, Mukai K and Goto T. (1990). Spontaneous transformation and immortalisation of human endothelial cells. *In Vitro Cellular and Developmental Biology*. **25**. 265-274.

- Takeda T, Yamashita Y, Shimazaki S and Mitsui Y. (1992). Histamine decreases the permeability of an endothelial cell monolayer by stimulating cAMP production through the H₂-receptor. *Journal of Cell Science*. **101**. 745-750.
- Takeichi M. (1991). Cadherin cell adhesion receptors as a morphogenic regulator. *Science*. **251**. 1451 – 1455.
- Tchao R. (1988). Trans-epithelial permeability of fluorescein *in-vitro* as an assay to determine eye irritants. In “*Alternative Methods in Toxicology, Progress in In Vitro Toxicology. Vol. 6*” (Ed. Goldberg AM). Mary Ann Liebert Inc., New York. 271.
- Thurston G. and Baldwin AI. (1994). Endothelial actin cytoskeleton in rat mesentery microvasculature. *American Journal of Physiology*. **266**. H1896-1909.
- Thurston G. and Baldwin AI. (1995). Changes in endothelial actin cytoskeleton at leakage sites in the rat mesenteric microvasculature. *American Journal of Physiology*. **266**. H316-H329.
- Todd I, Clothier RH, Huggins M, Patel N, Searle C, Jeyarajah S, Pradel L, and Lacey KL. (2001). Electrical stimulation of transforming growth factor- β 1 secreted by human dermal fibroblasts and the U937 human monocyte cell line. *ATLA*. **29**. 693-702.

- Tomschy A, Fauser C, Landwehr R and Engel J. (1996). Homophilic adhesion of E-cadherin occurs by a co-operative two step interaction of the N-terminal domains. *EMBO Journal*. **15** 3507 – 3514.
- Torres M, Stovkova A, Huber O, Chowdhury K, Bonaldo P, Mansouri A, Butz S, Kemler S and Gruss P. (1997). An alpha-E-catenin gene trap mutation defines its function in preimplantation development. *PNAS USA*. **94**. 901-906.
- Tsukita S, Tsukita S, Nagafuchi A, Yonemura S. (1992). Molecular linkage between cadherins and actin filaments in cell-cell adherens junctions. *Current Opinions in Cell Biology*. **4**. 834 - 839.
- Tu AT. (1992). Natural protein toxins affecting cutaneous microvascular permeability. *Journal of Toxicology - Toxin Reviews*. **1**. 193-239.
- Turner M. (1992). Effects of proteins on the permeability of monolayers of cultured bovine arterial endothelium. *Journal of Physiology (London)*. **449**. 21-35.
- Van Nieuw Amerongen GP, Draijer R, Vermeer AM and Van Hinsbergh VWM. (1998). Transient and prolonged increase in endothelial permeability induced by

histamine and thrombin: role of protein kinases, calcium and RhoA. *Circulation Research*. **83**. 1115-1123.

Vane JR, Anggard EE and Bottingh RM. (1990). Regulatory functions of the vascular endothelium. *New England Journal of Medicine*. **323**. 27-36.

Venkiteswaran K, Xiao K, Summers S, Calkins C, Vincent PA, Pumiglia K and Kowalczyk AP. (2002). Regulation of endothelial barrier function and growth by VE-cadherin, plakoglobin, and beta-catenin. *American Journal of Physiology*. **283**. C811-C821.

Verin AD, Patterson CE, Day MA and Garcia JG. (1995). Regulation of endothelial cell gap formation and barrier function by myosin-associated phosphatase activities. *American Journal of Physiology*. **269**. L99-L108.

Villars F, Conrad V, Rouais F, Lefebvre F, Amédée J and Bordenave L. (1996). Ability of various inserts to promote endothelium cell culture for the establishment of coculture models. *Cellular and Biological Toxicology*. **12**. 207-214.

Volberg T, Zick Y, Dror R, Sabanay I, Gilon C, Levitzki A and Geiger B. (1992). The effect of tyrosine-specific protein phosphorylation on the assembly of adherens-type junctions. *EMBO Journal*. **11**. 1733-1742.

Volk T, Geiger B and Raz A. (1984). Motility and adhesive properties of high- and low-metastatic murine neoplastic cells. *Cancer Research*. **44**. 811-824.

Volk T and Geiger B. (1986a). A-CAM: a 135kD receptor of the intercellular adherens junctions. I Immunoelectron microscopic localization and biochemical studies. *Journal of Cell Biology*. **103**. 1441 – 1450.

Volk T and Geiger B. (1986b). A-CAM: a 135kD receptor of the intercellular adherens junctions. II Antibody-mediated modulation of junction formation. *Journal of Cell Biology*. **103**. 1451 – 1464.

Vuong PT, Malik AB, Nagpala PG and Lum H. (1998). Protein kinase C β modulates thrombin-induced Ca^{2+} signalling and endothelial permeability increase. *Journal of Cellular Physiology*. **175**. 379-387.

Ward BJ, Bauman KF and Firth JA. (1988). Interendothelial junctions of cardiac capillaries in rats: Their structure and permeability Properties. *Cell and Tissue Research*. **252**. 57-66.

Ward RW and Clothier RH. (1996). Assessment of surfactants using an in vitro human epidermal equivalent. *ATLA*. **24**. 297.

- Ward RW, Carter J and Clothier RH. (1996). Insert pore size effects on epithelial cell responses to detergents. In *"Alternatives to Animal Testing"* (eds. SG Liansky, R Macmillan and J Dupuis). 376- 377. CLP Press. United Kingdom.
- Ward RW, Hubbard AW, Sulley H, Garle MJ and Clothier RH. (1998). Human keratinocyte cultures in an *in vitro* approach for the assessment of surfactant-induced irritation. *Toxicology in Vitro*. **12**. 163-173.
- Ward RW, Mungall S, Carter J and Clothier RH. (1997). Evaluation of tissue culture insert membranes compatibility in the fluorescein leakage assay. *Toxicology In Vitro*. **11**. 761 - 768.
- Watabe M, Nagafuchi A, Tsukita S and Tackeichi M. (1994). Induction of polarized cell-cell association and retardation of growth by activation of the E-cadherin-catenin adhesion system in a dispersed carcinoma line. *Journal of Cell Biology*. **127**. 247-256.
- Weinbaum S, Tzeghai G, Ganatos P, Pfeffer R and Chien S. (1985). Effect of cell turnover and leaky junctions on arterial macromolecular transport. *American Journal of Physiology*. **248**. H945-960.

- Weiske J, Schoneberg T, Schroder W, Hatzfeld M, Tauber R & Huber O. (2001). The fate of desmosomal proteins in apoptotic cells. *Journal of Biological Chemistry*. **276**. 41175-41181.
- Wójciak-Stothard B, Entwistle A, Garg R and Ridley AJ. (1998). Regulation of TNF- α -induced reorganisation of the actin cytoskeleton and cell-cell junctions by Rho, Rac and Cdc42 in human endothelial cells. *Journal of Cellular Physiology*. **176**. 150-165.
- Wolburg H, Neuhaus J, Kniesel U, Krauss B, Schmid E-M, Ocalan M, Farrell C and Risau W. (1994). Modulation of tight junction structure in blood-brain barrier endothelial cells: Effects of tissue culture, second messengers and cocultured astrocytes. *Journal of Cell Science*. **107**. 1347-1357.
- Wolinsky H. (1980). A proposal linking clearing of circulating lipoproteins to tissue metabolic activity as a basis for understanding atherogenesis. *Circulation Research*. **47**. 301.
- Wong and Gotlieb. (1990). Endothelial monolayer integrity. Perturbation of F-actin filaments and the dense peripheral band-vinculin network. *Arteriosclerosis*. **10**. 76-84.

- Wong EYM, Morgan L, Smales C, Lang P, Gubby SE and Staddon JM. (2000). Vascular endothelial growth factor stimulates dephosphorylation of the catenins p120 and p100 in endothelial cells. *Biochemistry Journal*. **346**. 209-216
- Worth AP and Balls M. (2001). The importance of the prediction model in the validation of alternative tests. *ATLA*. **29**. 135-143.
- Wu NZ and Baldwin AL. (1992). Transient venular permeability and endothelial gap formation induced by histamine. *American Journal of Physiology*. **262**. H1238-1247.
- Wysolmerski RB and Lagunoff D. (1990). Involvement of myosin light-chain kinase in endothelial cell retraction. *Proceedings of the National Academy of Sciences of the United States of America*. **87**. 16-20.
- Xu Y, Swerlick R, Sepp N, Bosse D, Ades EW and Lawley TJ. (1994). Characterisation of expression and modulation of cell adhesion molecules on an immortalised human dermal microvascular endothelial cell line (HMEC-1). *Journal of Investigative Dermatology*. **102**. 833-837.
- Yamada Y, Furumuchi T, Furui H, Yokoi T, Ito T, Yamauchi K, Yokata M, Hayashi H and Saito H. (1990). Roles of calcium, cyclic nucleotides and protein kinase C in regulation of endothelial permeability. *Arteriosclerosis*. **10**. 410-420.

- Yap AS, Niessen CM and Gumbiner BM. (1998). The juxtamembrane region of the cadherin cytoplasmic tail supports lateral clustering, adhesive strengthening and interaction with p120_{cas}. *Journal of Cell Biology*. **141**. 779-789.
- Yu JCM and Gotlieb AI. (1992). Disruption of endothelial actin microfilaments by protein kinase C Inhibitors. *Microvascular Research*. **43**. 100-111.
- Yuan Y, Granger HJ, Zawieja D, DeFily D and Chilian W. (1993). Histamine induces venular permeability via a phospholipase C-NO synthase-guanylate cyclase cascade. *American Journal of Physiology*. **264**. H1734-H1739.